

Characterization of the role of
the NLR proteins NLRC5 and NLRP11
in the immune response

Dissertation zur Erlangung des Doktorgrades
der Naturwissenschaften (Dr. rer. nat.)

Fakultät Naturwissenschaften
Universität Hohenheim

Institut für Ernährungsmedizin,
Fachgebiet Immunologie

Vorgelegt von:

Ioannis Kienēs

aus: München

2021

Dekan:	Prof. Dr. rer. nat. Uwe Beifuss
1. berichtende Person:	Prof. Dr. rer. nat. Thomas Kufer
2. berichtende Person:	Prof. Dr. med. Dr. rer. nat. Sascha Venturelli
Mündliche Prüfung am:	1.12.2021

Table of content

Abbreviations	VI
Abstract	VIII
Zusammenfassung.....	X
1 Introduction	1
1.1 Recognition of pathogen associated molecular patterns is a prerequisite for innate immune responses	1
1.2 NOD-like receptors	2
1.2.1 NOD-like receptors as master regulators of antigen presentation	4
1.2.2 CIITA - the master regulator of major histocompatibility complex class II expression .	5
1.3 The role of NLRC5 in major histocompatibility complex class I expression	6
1.3.1 Histone deacetylases – Sin3A	10
1.3.2 The negative elongation factor complex	11
1.4 NOD-like receptors as inhibitors of type I interferon responses	13
1.4.1 Functions of NLRP11	15
1.4.2 DDX3X	16
1.5 Aim of the study	18
2 Material and Methods.....	20
2.1 Materials.....	20
2.1.1 Cell lines and bacteria	20
2.1.2 Chemicals and reagents	23
2.1.3 Kits	24
2.1.4 Plasmids.....	24
2.1.5 Oligonucleotides.....	27
2.1.6 siRNAs	30
2.1.7 Antibodies	30
2.1.8 Instruments.....	31
2.1.9 Software.....	31
2.2 Methods.....	32

2.2.1	Cell biological methods.....	32
2.2.2	Molecular methods	35
2.2.3	Biochemical methods	38
2.2.4	Bioinformatic methods	42
2.2.5	Yeast two-hybrid screening.....	42
3	Results	43
3.1	NLRC5	43
3.1.1	Identification of NLRC5 interaction partners by co-immunoprecipitation following fractionation.....	43
3.1.2	Establishment of a proximity biotin ligation system (BioID2) for identification of further NLRC5 interaction partners	46
3.1.3	Sin3A interacts with NLRC5 at the Death Domain and inhibits major histocompatibility complex transcription	49
3.1.4	NELFB interacts with NLRC5 via its Death Domain and inhibits major histocompatibility complex transcription.....	52
3.1.5	Structural analysis of NLRC5	55
3.2	DDX3X links NLRP11 to the regulation of type I interferon responses and NLRP3 inflammasome activation.....	60
3.2.1	Identification of novel NLRP11 interaction partners	60
3.2.2	Functional characterization of the interplay between NLRP11 and DDX3X	64
4	Discussion	72
4.1.1	Proximity ligation – a promising approach for the identification of novel interaction partners	73
4.1.2	Sin3A and NELFB do not determine MHC class I specificity of NLRC5.....	74
4.1.3	Recombinant expression of NLRC5.....	76
4.1.4	The role of NLRP11 as a negative regulator of innate immune responses.....	77
4.1.5	The interaction between NLRs and DExD-box helicases is an emerging synergistical pattern.....	77
4.1.6	Role of the NLRP11-DDX3X complex in antiviral type I interferon response	78
4.1.7	Inhibition of the NLRP3 inflammasome by NLRP11	81

4.1.8	The physiological role of the NLRP11-DDX3X interaction.....	82
	References	85
	Supplement.....	102
	Eidesstattliche Versicherung	121
	Danksagung.....	122
	Publikationen.....	123
	Curriculum Vitae.....	124

Abbreviations

Abbreviations

°C	<i>Degree Celsius</i>
AIF	<i>Apoptosis inducing factor</i>
ASC	<i>Apoptosis-associated speck-like protein containing a CARD</i>
BioID2	<i>Bifunctional ligase/repressor BirA R40G</i>
BLS	<i>Bare lymphocyte syndrome</i>
CARD	<i>Caspase activation and recruitment domain</i>
AD	<i>Transcriptional activation domain</i>
cDNA	<i>Complementary DNA</i>
cGAS	<i>cyclic GMP-AMP synthase</i>
CHX	<i>Cycloheximide</i>
CIITA	<i>MHC class II transcriptional activator</i>
CRM1	<i>Exportin 1</i>
C-terminus	<i>Carboxyl-terminus</i>
DD	<i>Death domain-like fold</i>
DMEM	<i>Dulbecco's modified Eagle's medium</i>
DNA	<i>Desoxyribonucleic acid</i>
Dox	<i>Doxycycline</i>
dsRNA	<i>double stranded RNA</i>
EDTA	<i>Ethylenediaminetetraacetic acid</i>
ELISA	<i>Enzyme-linked immunosorbent assay</i>
ER	<i>Endoplasmic reticulum</i>
<i>et al.</i>	<i>et alii; and others</i>
FL	<i>Full-length</i>
FlpIn	<i>Flp-FRT recombination system</i>
GAPDH	<i>Glycerinaldehyd-3-phosphat-dehydrogenase</i>
h	<i>Hours</i>
HAU	<i>Hemagglutination units</i>
HDAC	<i>Histone deacetylase</i>
HEK	<i>Human embryonic kidney cells</i>
HEK293T	<i>Human embryonic kidney 293T cells</i>
HLA	<i>Human leukocyte antigen</i>
HRP	<i>Horseraddish peroxidase</i>
IF	<i>Indirect immunofluorescence</i>
IKK ϵ	<i>Inhibitor of nuclear factor kappa B kinase subunit epsilon</i>
IMAC	<i>Immobilized metal affinity chromatography</i>
IP	<i>Immunoprecipitation</i>
IPTG	<i>Isopropyl-β-D-thiogalactopyranosid</i>
ISRE	<i>Interferon-sensitive response element</i>
kbp	<i>Kilobase pairs</i>
kDa	<i>Kilodalton</i>
LB	<i>Lysogeny broth</i>
LB-Amp	<i>LB medium containing 100 μg/ml ampicillin</i>
LPS	<i>Lipopolysaccharide</i>
LRRs	<i>Leucine-rich repeats</i>
M	<i>Molar</i>
MAVS	<i>Mitochondrial antiviral signaling protein</i>
mg	<i>Milligram</i>
MHC I	<i>Major histocompatibility complex class I</i>
MHC II	<i>Major histocompatibility complex class II</i>
min	<i>Minutes</i>
ml	<i>Milliliter</i>
mM	<i>Millimolar</i>

Abbreviations

<i>mRNA</i>	<i>Messenger RNA</i>
<i>NACHT</i>	<i>Nucleotide binding and oligomerization domain</i>
<i>NELF</i>	<i>Negative elongation factor</i>
<i>NF-κB</i>	<i>Nuclear factor 'kappa-light-chain-enhancer' of activated B cells</i>
<i>ng</i>	<i>Nanogram</i>
<i>NLR</i>	<i>Nucleotide-binding domain and leucine-rich repeat containing protein</i>
<i>nM</i>	<i>Nanomolar</i>
<i>nRLU</i>	<i>Normalized relative light units</i>
<i>N-terminus</i>	<i>Amino-terminus</i>
<i>ONPG</i>	<i>o-Nitrophenyl-β-D-galactopyranoside</i>
<i>PAMP</i>	<i>Pathogen associated molecular pattern</i>
<i>PBS</i>	<i>Phosphate-buffered saline</i>
<i>PCR</i>	<i>Polymerase chain reaction</i>
<i>Pen/Strep</i>	<i>Penicillin and streptomycin</i>
<i>PFA</i>	<i>Paraformaldehyde</i>
<i>PMA</i>	<i>Phorbol 12-myristate 13-acetate</i>
<i>Pol II</i>	<i>RNA Polymerase II</i>
<i>PRR</i>	<i>Pattern recognition receptor</i>
<i>PTM</i>	<i>Post-translational modification</i>
<i>PYD</i>	<i>Pyrin domain</i>
<i>qRT-PCR</i>	<i>Quantitative reverse transcription polymerase chain reaction</i>
<i>RIG-I</i>	<i>Retinoic acid-inducible gene I protein</i>
<i>RLRs</i>	<i>RIG-I-like receptors</i>
<i>RLU</i>	<i>Relative light units</i>
<i>RNA</i>	<i>Ribonucleic acid</i>
<i>rpm</i>	<i>Rounds per minute</i>
<i>RPMI 164</i>	<i>Roswell Park Memorial Institute 1640 medium</i>
<i>RT</i>	<i>Room temperature</i>
<i>SD</i>	<i>Standard deviation</i>
<i>SDS</i>	<i>Sodium dodecyl sulfate</i>
<i>SDS-PAGE</i>	<i>Sodium dodecyl sulfate polyacrylamide gel electrophoresis</i>
<i>SEAP</i>	<i>Secreted embryonic alkaline phosphatase</i>
<i>sec</i>	<i>Seconds</i>
<i>SEM</i>	<i>Standard error of means</i>
<i>SeV</i>	<i>Sendai Virus</i>
<i>shRNA</i>	<i>Short hairpin RNA</i>
<i>siRNA</i>	<i>Small interfering RNA</i>
<i>TAE</i>	<i>Tris-Acetic acid-EDTA</i>
<i>TAP</i>	<i>Transporter associated with antigen processing</i>
<i>TBK1</i>	<i>TANK-binding kinase 1</i>
<i>TEV</i>	<i>Tobacco etch virus</i>
<i>TLR</i>	<i>Toll-like receptor</i>
<i>T-REx</i>	<i>Tetracycline-regulated mammalian expression system</i>
<i>Tris</i>	<i>Tris(hydroxymethyl)aminomethane</i>
<i>Triton-X100</i>	<i>Polyethylene glycol p-(1,1,3,3-tetramethylbutyl)-phenyl ether</i>
<i>TrxA</i>	<i>Thioredoxin I</i>
<i>Tween-20</i>	<i>Polyoxyethylene (20) sorbitan monolaurate</i>
<i>U</i>	<i>Units</i>
<i>WT</i>	<i>Wildtype</i>
Δ	<i>Deletion of</i>
μ g	<i>Microgram</i>
μ l	<i>Microliter</i>
μ M	<i>Micromolar</i>

Abstract

Recognition of conserved microbial molecular patterns by pattern recognition receptors (PRRs) is crucial for the initiation of an innate immune response. Within this group of PRRs, the NOD-like receptor (NLR) family, a group of 22 cytosolic proteins in humans, have been shown to function as PRRs of the innate immune system and as regulators of adaptive immune responses. However, it has become evident, that several NLR proteins also function as regulators of innate immune responses. In this thesis the function of the human NLR proteins NLRC5 and NLRP11 in immune responses was further characterized.

NLRC5 and major histocompatibility complex (MHC) class II transcriptional activator (CIITA) are the master regulators of MHC class I and II transcription, respectively. Both NLR proteins can translocate into the nucleus, where they induce transcription of MHC class I and class II, respectively. As NLRC5 and CIITA do not possess intrinsic DNA binding capacities, they are recruited to MHC promotor elements by binding to a common multiprotein complex, termed MHC enhanceosome. Although the MHC enhanceosome components are, as known thus far, identical, NLRC5 and CIITA are specific for their respective transcriptional targets. In this work we employed multiple techniques to identify novel interaction partners of NLRC5 to understand the mechanisms behind this specificity. As it has been shown that the N-terminal domain death-domain like fold (DD) of NLRC5 is involved in conferring specificity, we adapted a protocol for a proximity ligation assay by fusion of the NLRC5 DD to the modified biotin ligase from *Aquifex aeolicus* (BioID2) to unravel the interactome of this NLRC5 domain. By enrichment of biotinylated proteins through streptavidin-biotin precipitation and analysis of the proteins by LC-MS/MS, we identified novel putative interactors. This approach was complemented by a yeast two-hybrid screen, using the NLRC5 DD as bait and screening a cDNA library from human CD4⁺ and CD8⁺ T cells for the identification of novel interaction partners. This led to the identification of the paired amphipathic helix protein Sin3A (Sin3A) and the negative elongation factor B (NELFB) as interactors of NLRC5 DD. Characterization of their role in transcriptional regulation of MHC class I revealed an inhibitory role of both proteins. However, as we also observed repression of CIITA-mediated MHC class II transcription, both proteins are likely not involved in determination of target-specificity of NLRC5.

Translocation of NLRC5 into the nucleus is essential for the induction of MHC class I transcription but forced nuclear localization of NLRC5 strongly diminishes its activity as a transcriptional activator. In order to understand the reason for this, we employed co-immunoprecipitation assays of differentially localized NLRC5 constructs to identify cytosolic interaction partners which might be involved in post-translational regulation of NLRC5 to enable its transcriptional activation.

Abstract

Furthermore, to advance our understanding of the NLRC5 DD, a protocol for large-scale recombinant expression and purification of the NLRC5 DD was established for subsequent structural analysis of NLRC5.

The second part of this thesis was focused on NLRP11, that was not functionally characterized at the beginning of this work. During this work, NLRP11 was then reported to regulate type I interferon (IFN) and other pro-inflammatory responses. Type I IFNs are critical cytokines in antiviral defense and upon binding to their receptor, induce a multitude of antiviral interferon-stimulated genes. Tight regulation of inflammatory cytokine and IFN production in innate immunity is pivotal for the control of pathogens and avoidance of immunopathology. To gain a deeper understanding of the function of NLRP11 in this pathway, we screened for novel NLRP11 interactors using cell lines with inducible expression of NLRP11-eGFP. We identified the ATP-dependent RNA helicase DDX3X as a novel binding partner of NLRP11 by co-immunoprecipitation and LC-MS/MS. DDX3X is known to enhance type I IFN responses and NLRP3 inflammasome activation. We demonstrate that NLRP11 could abolish IKK ϵ -mediated phosphorylation of DDX3X, resulting in lower type I IFN induction upon viral infection. These effects were dependent on the leucine-rich repeat (LRR) domain of NLRP11 that we mapped as the interaction domain for DDX3X. In addition, NLRP11 also suppressed NLRP3-mediated caspase-1 activation in an LRR domain-dependent manner, suggesting, that NLRP11 might sequester DDX3X and prevent it from promoting NLRP3-induced inflammasome activation. Taken together, this data revealed DDX3X as a central target of NLRP11, which can mediate the effects of NLRP11 on type I IFN induction, as well as NLRP3 inflammasome activation. This expands our knowledge of the molecular mechanisms underlying NLRP11 function in innate immunity and suggests that both NLRP11 and DDX3X might be promising targets for modulation of innate immune responses.

Zusammenfassung

Die Erkennung konservierter mikrobieller molekularer Muster durch Mustererkennungsrezeptoren ist von grundlegender Bedeutung für die Einleitung einer angeborenen Immunreaktion. Innerhalb der Gruppe der Mustererkennungsrezeptoren stellen die NOD-like Rezeptoren (NLRs) im Menschen eine Gruppe von 22 cytosolischen Proteinen dar, welche Funktionen als Mustererkennungsrezeptoren, sowie in der Regulation der adaptiven Immunantwort besitzen. Es konnte allerdings gezeigt werden, dass einige NLR Proteine auch als Regulatoren angeborener Immunreaktionen wirken. In dieser Arbeit wurde die Rolle der humanen NLR Proteine NLRC5 und NLRP11 in der Immunantwort weiterführend charakterisiert.

NLRC5 und der major histocompatibility complex class II transcriptional activator (CIITA) sind die Hauptregulatoren der Transkription der Haupthistokompatibilitätskomplexe (MHC) Klasse I respektive Klasse II. Beide Proteine translozieren in den Zellkern, wo sie ihre regulatorischen Effekte entfalten. Sowohl NLRC5 als auch CIITA binden nicht direkt an die DNA, sondern interagieren hierfür mit einem gemeinsamen Multiproteinkomplex, dem MHC Enhanceosom. Des Weiteren rekrutieren sie Proteine die als transkriptionelle Regulatoren wirken. Obwohl die Komponenten des Enhanceosoms, soweit aktuell bekannt, identisch sind, sind NLRC5 und CIITA spezifisch für ihre Zielgene. In dieser Arbeit verwendeten wir verschiedene Methoden zur Identifikation neuer Interaktionspartner von NLRC5, um die zu Grunde liegenden Mechanismen der Spezifität zu verstehen. Da in vorhergehenden Arbeiten gezeigt werden konnte, dass die N-terminale Domäne (DD) von NLRC5 hierfür wichtig ist, haben wir verschiedene Methoden zur Identifikation potenzieller Interaktoren dieser Domäne angewendet. Zum einen wurde dafür ein *proximity ligation assay* adaptiert, in dem, mittels Fusion der NLRC5 N-terminalen Domäne an die modifizierte Biotinligase von *Aquifex aeolicus* (BioID2), Proteine in räumlicher Nähe des Fusionsproteins mit Biotin markiert werden. Streptavidin-Biotin Präzipitation und anschließende LC-MS/MS Analyse identifizierte neue Interaktoren von NLRC5 mit Funktionen in der transkriptionellen Regulation. Dieser Ansatz wurde durch einen Hefe Zwei-Hybrid Screen mit der N-terminalen Domäne von NLRC5 als bait gegen eine cDNA Bibliothek aus humanen CD4⁺ und CD8⁺ T Zellen komplementiert. Hierbei wurden das paired amphipathic helix Protein Sin3A (Sin3A), sowie der negative elongation factor B (NELFB) als Interaktoren der N-terminalen Domäne von NLRC5 identifiziert. Die Untersuchung der Rolle der beiden Proteine in der Induktion von MHC Klasse I zeigte eine inhibitorische Funktion beider Proteine. Da jedoch ebenfalls eine Repression der CIITA-vermittelten MHC Klasse II Transkription beobachtet wurde, sind diese beiden Proteine wohl nicht in der Vermittlung der Spezifität von NLRC5 für MHC Klasse I involviert.

Der Import von NLRC5 in den Zellkern ist essenziell für die Initiation der MHC Klasse I Transkription. Eine erzwungene nukleäre Lokalisation von NLRC5 reduziert jedoch die transaktivierende Aktivität.

Zusammenfassung

Ko-Immunopräzipitation cytosolisch und nukleär lokalisierter NLRC5-Konstrukte identifizierte Kandidaten, die in der post-translationalen Kontrolle der NLRC5 Aktivität involviert sein könnten.

Des Weiteren wurde erfolgreich ein Protokoll zur rekombinanten Expression und Aufreinigung der N-terminalen Domäne von NLRC5 etabliert, um Untersuchung der Proteinstruktur dieser Domäne zu erlauben.

Der zweite Teil dieser Arbeit befasste sich mit NLRP11, welches zu Beginn der Arbeit noch nicht funktionell beschrieben war. Im Laufe der Arbeit wurde NLRP11 dann als negativer Regulator der Typ I Interferonantwort, sowie anderer pro-inflammatorischer Immunantworten beschrieben. Typ I Interferone sind zentrale Zytokine in der antiviralen Immunreaktion und induzieren eine Vielzahl interferon-induzierter Gene. Die effektive Regulation der inflammatorischen Zytokin- und Interferonproduktion des angeborenen Immunsystems ist essenziell, um Pathogenen unter Kontrolle zu halten, sowie zur Vermeidung von Immunopathologien die durch eine überschießende Immunreaktion hervorgerufen werden können. In dieser Arbeit haben wir Zelllinien mit stabiler, induzierbarer Expression von NLRP11-eGFP als neues Tool zur Untersuchung der Funktion von NLRP11 generiert. Um unser Verständnis der zu Grunde liegenden regulatorischen Mechanismen zu vertiefen, wurden mittels dieser Zellen durch Ko-Immunopräzipitation und LC-MS/MS nach neuen Interaktionspartnern von NLRP11 gesucht. Hierbei wurde die ATP-abhängige RNA-Helikase DDX3X als neuer Interaktionspartner von NLRP11 identifiziert. DDX3X ist als positiver Regulator der Typ I Interferonantwort und des NLRP3 Inflammasoms bekannt. Wir zeigen hier, dass NLRP11 die IKK ϵ -vermittelte Phosphorylierung von DDX3X verhinderte, was zur Verminderung der Typ I Interferonantwort nach viraler Infektion führte. Dieser Effekt war von der Leucin-rich repeat (LRR) Domäne von NLRP11 abhängig, die wir als Interaktionsdomäne für DDX3X identifizieren konnten. Zusätzlich zeigen wir, dass NLRP11 die NLRP3-vermittelte Caspase-1 Aktivierung in Abhängigkeit der LRR Domäne inhibierte. Dies geschah in Abhängigkeit von DDX3X, was vermuten lässt, dass NLRP11 DDX3X sequestriert und damit verhindert, dass DDX3X die NLRP3-vermittelte Inflammasomaktivierung verstärkt. Unsere Daten zeigen, dass DDX3X ein zentraler Faktor für die negative Regulation der Typ I Interferonantwort, sowie des NLRP3 Inflammasoms durch NLRP11 ist. Dies vertieft unser Wissen über die zugrunde liegenden Mechanismen der regulatorischen Funktion von NLRP11 in der angeborenen Immunantwort und weist darauf hin, dass sowohl NLRP11 als auch DDX3X vielversprechende Kandidaten für Eingriffe in das angeborene Immunsystem darstellen.

1 Introduction

1.1 Recognition of pathogen associated molecular patterns is a prerequisite for innate immune responses

The mammalian immune system has co-evolved with a plethora of different microbial challenges, to prevent infections. To keep pathogens in check, a quick but broad innate immune response is mounted, which subsequently enables an adaptive immune response, tailored specifically towards the detected challenge. The prerequisite for the induction of any immune response is the recognition of pathogens. In case of the adaptive immune response, peptide antigens are recognized by highly specific antigen receptors which arise from extensive somatic gene-rearrangement (Roth 2014), but require long time to form. The more rapid, innate immune response is initiated directly after recognition of highly conserved pathogen associated molecular patterns (PAMPs) via germline-encoded pattern recognition receptors (PRRs). Those structures include components of microbial cell walls like peptidoglycan (PGN) (Girardin *et al.* 2003, Girardin *et al.* 2003) or lipopolysaccharides (LPS) (Poltorak *et al.* 1998), highly conserved proteins such as flagellin (Miao *et al.* 2007), or microbial nucleic acids (Gürtler and Bowie 2013). This concept was initially proposed by Charles Janeway in 1989, introducing the idea that immune responses are induced by a molecular trigger. At the same time, this broke with the concept, that self/nonself discrimination relied solely on clonally selected receptors of the adaptive immune system, such as T cell and B cell receptors (Janeway 1989).

PRRs have since been understood as a diverse group of proteins, which can be broadly divided by their subcellular localization. Membrane-bound Toll-like receptors (TLR), C-type lectins and scavenger receptors monitor the extracellular space, and in case of TLRs also endosomes and lysosomes, for the presence of PAMPs (Canton *et al.* 2013, Kawasaki and Kawai 2014, Dambuza and Brown 2015). NOD-like receptors (NLRs), RIG-I like receptors (RLRs) and cyclic GMP-AMP synthase (cGAS) detect PAMPs present in the cytosol (**Figure 1**).

The activation of all classes of PRRs results in the regulation of a well-defined set of inflammatory signaling pathways which culminate in either transcriptional regulation, or post-translational activation of pro-inflammatory cytokines and other pro-inflammatory genes (**Figure 1**).

Introduction

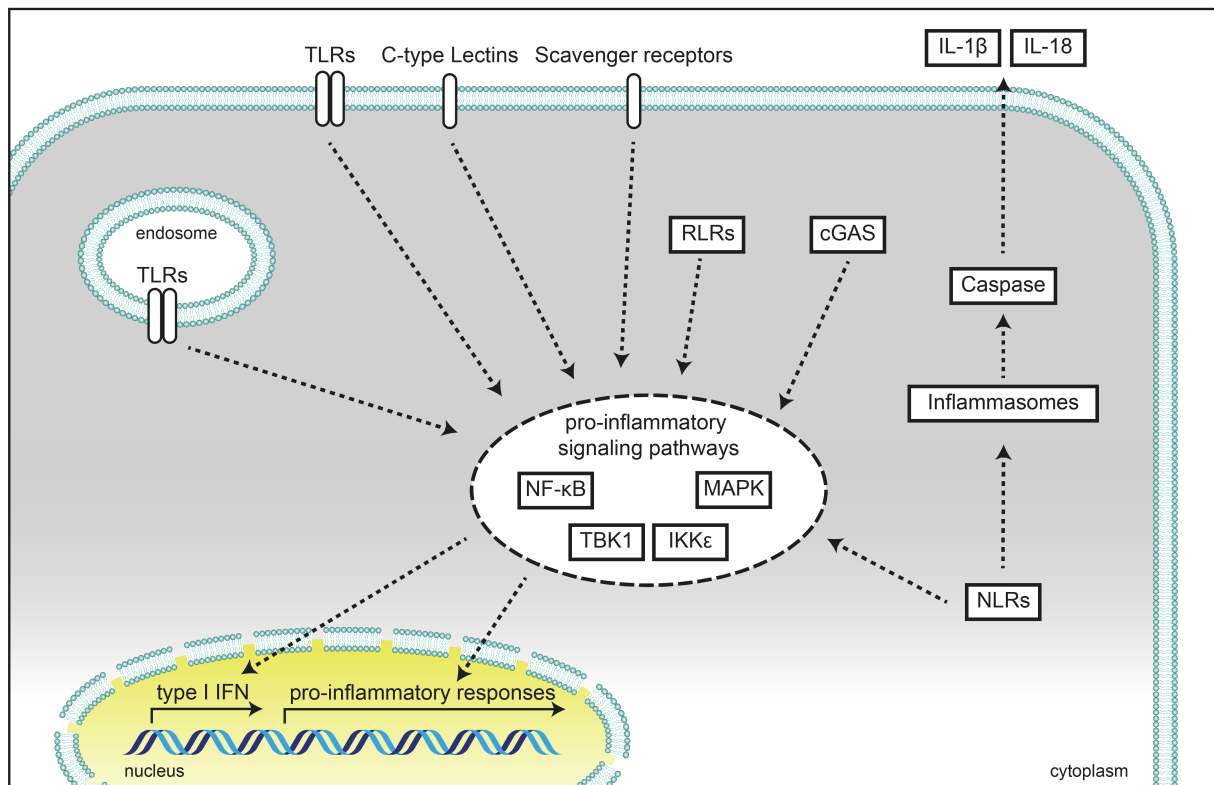


Figure 1: **Schematic representation of the localization of different pattern recognition receptors and the signaling pathways they regulate.** Membrane bound receptors, such as Toll-like receptors (TLRs), C-type lectins and scavenger receptors monitor the extracellular and endosomal space for the presence of conserved microbial structures. NOD-like receptors (NLRs), RIG-I-like receptors (RLRs) and cyclic GMP AMP synthase (cGAS) recognize pathogen associated molecular patterns in the cytoplasm. Activation of PRRs results in the regulation of a defined set of pro-inflammatory signaling pathways and subsequent transcriptional and post-translational regulation of pro-inflammatory responses. IFN: interferon; NF-κB: nuclear factor 'kappa-light-chain-enhancer' of activated B cells; MAPK: mitogen-activated protein kinase; TBK1: TANK-binding kinase 1; IKKε: Inhibitor of nuclear factor kappa B kinase subunit epsilon; IL: interleukin.

1.2 NOD-like receptors

NLRs are a class of cytosolic PRRs, which, in humans, consists of 22 proteins (Liwinski *et al.* 2020). They are characterized as a protein family by a common tripartite structure, consisting of a variable number of C-terminal leucine-rich repeats (LRRs), a central nucleotide binding and oligomerization (NACHT) domain and a variable N-terminal effector domain. Based on the type of effector domain, NLRs are subcategorized into four groups. Of those, the pyrin domain (PYD) containing NLRP subfamily is the largest with 14 proteins (NLRP1-14), followed by caspase activation and recruitment domain (CARD) containing NLRCs with five group members (NOD1, NOD2, NLRC3-5). There further are the baculovirus inhibitor of apoptosis (BIR) domain containing NLRB, and CARD transcription and activation domain (CARD-AD) containing NLRA subclasses with one member each (Ting and Davis 2005). NLRX1 contains an N-terminal mitochondrial localization sequence (MLS) and shares no homology to the N-terminal domains of the other NLR family members (Moore *et al.* 2008). It has been proposed, that the LRRs serve as a recognition domain for their respective activation signal, resulting in conformational changes and oligomerization via the NACHT domain. This in turn allows recruitment

Introduction

of adaptor proteins, which initiate NLR specific signaling cascades (Motta *et al.* 2015). This is best described for the founding member of the NLR family, the nucleotide-binding and oligomerization domain containing protein 1 (NOD1) (Inohara *et al.* 2000, Girardin *et al.* 2001, Girardin *et al.* 2005), as well as for its closest relative NOD2 (Ogura *et al.* 2001, Tanabe *et al.* 2004), which are activated by different forms of bacterial PGN (Chamaillard *et al.* 2003, Girardin *et al.* 2003, Girardin *et al.* 2003, Inohara *et al.* 2003). However, as the activating stimuli of many NLRs and the mechanisms of recognition are still unknown, it remains to be determined, whether this serves as a general model.

Upon activation, several NLR proteins of the PYD-family form high molecular weight multiprotein complexes, so-called inflammasomes. Inflammasomes act as activation platforms for caspase-1 and induce the processing and release of interleukin (IL)-1 β and IL-18, and the activation of gasdermin D (GSDMD), which is needed for IL-1 β release from the cells and can result in a specific form of cell death, termed pyroptosis. NLRP1, NLRP3 and the CARD-domain containing NLRC4 are the best characterized inflammasome-forming NLRs to date. Inflammasome formation has also been proposed for NLRP6, NLRP7, NLRP12 and NLRC5 (Grenier *et al.* 2002, Wang *et al.* 2002, Davis *et al.* 2011, Khare *et al.* 2012).

NLRP3 oligomerization after activation is in dependence of the ATPase function of the NACHT domain (Duncan *et al.* 2007). This multimerization enables recruitment of the adaptor apoptosis-associated speck-like protein containing a CARD (ASC). ASC consists of a PYD, and a CARD domain joined by a linker sequence. Heterodimeric PYD-PYD interactions of ASC and NLRP3 result in the formation of ASC filaments which then form one single ASC-speck in the cell (Lu *et al.* 2014). The exposure of the CARD domains of the oligomerized ASC leads to recruitment of caspase-1 by CARD-CARD interactions and results in caspase-1 self-cleavage by induced proximity. The active caspase-1 subsequently cleaves the immature pro-IL-1 β and pro-IL-18 to give rise to biologically active cytokines (Kronheim *et al.* 1992, Thornberry *et al.* 1992, Akita *et al.* 1997). Caspase-1 was hence initially named interleukin-1 beta converting enzyme (ICE) (Howard *et al.* 1991). Activation of the NLRP3 inflammasome requires two independent signals. A priming signal, which can be one of various PAMPs, induces transcriptional upregulation of inflammasome components (Bauernfeind *et al.* 2009), and a secondary step activates NLRP3. A broad range of different activating stimuli have been described to trigger the NLRP3 inflammasome. These different secondary signals have in common that they induce cellular stress. But how exactly the cellular stress is sensed by NLRP3, and which role alterations of the local environment play still needs to be elucidated (Swanson *et al.* 2019). Mounting evidence suggests, that the activation of inflammasomes is controlled by post-translational modifications (PTM) of the inflammasome complex (Yang *et al.* 2017). Besides PTM of NLRP3, ASC, or caspase-1 (Liang *et al.* 2021), modification of accessory proteins is also involved in NLRP3 inflammasome regulation. For example phosphorylation of NIMA-related kinase 7 (NEK7), an essential component of

Introduction

NLRP3 inflammasome formation (He *et al.* 2016, Schmid-Burgk *et al.* 2016, Shi *et al.* 2016), by polo-like kinase 4 (PLK4) results in the inhibition of NLRP3 inflammasome activation (Yang *et al.* 2020). This inhibitory effect of PLK4 is itself also regulated by deubiquitylation of PLK4 (Yang *et al.* 2020).

Besides recruitment of the adaptor protein ASC, inflammasome formation by direct interaction of the NLR with caspase-1 has also been described. Several CARD-containing proteins, such as CARD8 (Razmara *et al.* 2002), or NLRC4 (Zhang *et al.* 2015), have been shown to directly interact with the CARD-domain of pro-caspase-1, albeit the physiological relevance of these findings is not clear.

Understanding the regulation of the NLRP3 inflammasomes is critical to target NLRP3-driven immunopathologies such as arteriosclerosis (Düwell *et al.* 2010), gout (Martinon *et al.* 2006) and Alzheimer's disease (Halle *et al.* 2008). Blocking IL-1 signal (Dinarello *et al.* 2012), as well as targeting NLRP3 directly (Swanson *et al.* 2019) by biologicals and small compounds, respectively, are strategies for future therapeutic intervention for those diseases.

1.2.1 NOD-like receptors as master regulators of antigen presentation

However, not all NLRs act as PRRs. Some were shown to exhibit functions aside from pathogen recognition (Kufer and Sansonetti 2011, Kienes *et al.* 2021). For the major histocompatibility complex (MHC) class II transcriptional activator (CIITA) no PAMP activation has been described. Instead, it was shown by complementation cloning, that CIITA can rescue MHC class II expression in RJ2.2.5 cells, a cell line representing bare lymphocyte syndrome (BLS) (Steimle *et al.* 1993). The lack of MHC class II on lymphocytes in BLS is not caused by genetic defects in the MHC class II genes, but rather in one of the genes encoding the regulatory factor X (RFX) protein family, RFXANK, RFX5, RFXAP, or in CIITA. This manifests in reoccurring infections, as patients cannot mount humoral immune responses (Reith and Mach 2001).

The severity of the clinical manifestations caused by a lack of MHC class II, underscores the central role of presentation of peptide antigens in defense against pathogens and the initiation of an adaptive immune response. Exogenous proteins are taken up by antigen presenting cells (APCs) and processed by proteolysis in the endo-lysosome. MHC class II molecules, consisting of an α -chain and a β -chain subunit, are assembled in the endoplasmic reticulum (ER). They are stabilized by the presence of an invariant chain and are transported to late endosomal compartments, which fuse with the peptide containing endosomes. Human leukocyte antigen DM (HLA-DM), an accessory protein for the loading of MHC class II, facilitates the binding of the peptide antigens onto the MHC class II antigen-binding groove. Loaded MHC class II molecules are then presented on the cell surface where they can be recognized by CD4⁺ T cells (Cresswell 1994).

Introduction

Adaptive immune responses to intracellular pathogens, such as viruses and invasive bacteria, are initiated by antigen presentation on MHC class I. Proteasomal degradation of intracellular proteins by the so-called immunoproteasome, generates peptides, which are suitable to bind to the peptide-binding groove of MHC class I. The generated peptides are transported into the ER by the transporter associated with antigen processing (TAP). There, they are loaded onto MHC class I molecules, comprised of a heavy chain (HLA-A, HLA-B, or HLA-C in humans) and the β_2 microglobulin. The peptides are loaded onto MHC class I molecules by the peptide loading complex, consisting of TAP, tapasin, ERp57, calreticulin and the MHC class I, before the MHC-peptide complex is transported to the cell surface, where it can be recognized by CD8⁺ T cells (Leone *et al.* 2013). This results in direct killing of the infected cell, the release of several cytokines and chemokines and the recruitment of inflammatory cells (Harty *et al.* 2000). Antigen presentation by MHC class I molecules is also important to prevent natural killer (NK) cell-mediated lysis, which occurs when no MHC class I is present on the cell surface (Thielens *et al.* 2012).

During viral infection, as well as in tumor development, inhibition of antigen presentation by MHC class I is a common immune evasion strategy, nicely illustrating the importance of MHC class I for efficient defense against viruses and tumors (Maeurer *et al.* 1996, Alcami and Koszinowski 2000).

1.2.2 CIITA - the master regulator of major histocompatibility complex class II expression

Due to the importance of antigen presentation in the adaptive immune response, a tight regulation of the involved processes has evolved. The genes for the MHC class II proteins are clustered on the short arm of chromosome 6 in the class II region of the MHC locus. MHC class II transcription is controlled by a group of regulatory elements, termed S, X and Y boxes. CIITA itself does not have intrinsic DNA-binding capacities and thus, those elements are bound by other regulatory proteins. As previously described, mutations of the RFX-protein family members RFX5, RFX-ANK and RFX-AP are causal for BLS. These RFX proteins assemble into a trimeric RFX complex, which can bind to the X1 region of the MHC class II promoter (Steimle *et al.* 1995, Durand *et al.* 1997, Masternak *et al.* 1998, Nagarajan *et al.* 1999). Further, the X2 binding protein (X2BP), consisting of both cAMP response element binding protein (CREB) and activating transcription factor (ATF), is associated with the X2 region (Moreno *et al.* 1995, Gobin *et al.* 2001). Nuclear factor Y (NF-Y) binds the Y box (Louis-Plence *et al.* 1997, Jabrane-Ferrat *et al.* 2002). These transcription factors form a multiprotein complex, termed MHC enhanceosome, which serves as a basis for the recruitment of CIITA (**Figure 2**). This in turn enables recruitment of histone-modifying proteins, the transcription complex, and elongation factors by CIITA (Reith *et al.* 2005, Wright and Ting 2006).

MHC class II expression is restricted to APCs, such as dendritic cells (DCs), macrophages and B cells, and to epithelial cells of the thymus (Benoist and Mathis 1990, Boss 1997). While expression of the

Introduction

RFX-, X2BP- and NF-Y-complexes are ubiquitous, CIITA expression is limited to aforementioned cells and thus functions as a licensing factor for MHC class II transcription (Boss 1997). Interferon (IFN) γ strongly induces MHC class II transcription by the induction of CIITA expression (Steimle *et al.* 1994).

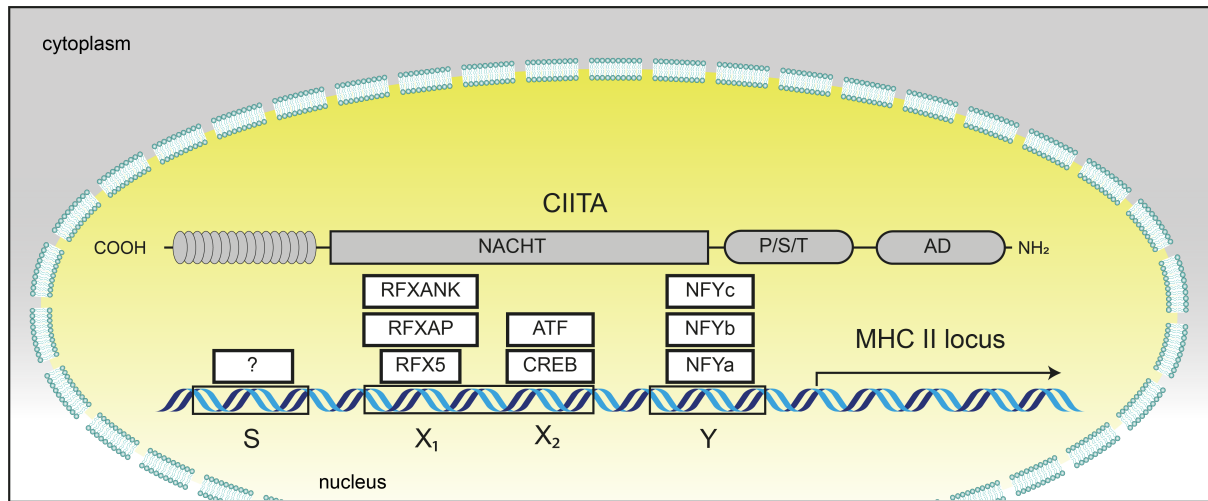


Figure 2: **Schematic representation of the MHC class II promoter region and the MHC enhanceosome.** The MHC class II transactivator (CIITA) is recruited to the promoter region of the MHC class II locus by interaction with the MHC enhanceosome. This multiprotein complex consists of the three regulatory factor X (RFX) proteins RFX5, RFXAP and RFXANK, which bind the X1 box of the promoter, the cAMP response element binding protein (CREB) and activating transcription factor (ATF) which bind the X2 region, as well as of the trimeric nuclear factor Y (NFY) complex, which binds the Y box. The CIITA-MHC complex serves as the basis for the recruitment of histone-modifying enzymes and transcription factors, to enable transcription of MHC class II genes. NACHT: Nucleotide binding and oligomerization domain; P/S/T: proline/serin/threonine rich region; AD: transcriptional activation domain.

CIITA shares the NLR-typical C-terminal LRRs and central NACHT domain. The N-terminal domain, however, consists of a transcriptional activation domain (AD) and a proline/serin/threonine rich region (P/S/T) (Chin *et al.* 1997) (**Figure 2**). To bind the enhanceosome, CIITA needs to be able to translocate into the nucleus. Intact GTP-binding function of the NACHT domain is needed for this (Harton *et al.* 1999). Furthermore, several residues within the LRRs were identified to be essential for nuclear translocation (Camacho-Carvajal *et al.* 2004). Additionally, a truncated version of CIITA, lacking the N-terminal AD and P/S/T domains (CIITA-L335), is not able to translocate into the nucleus and, when forced there by a nuclear localization sequence, is a dominant negative inhibitor of MHC class II transcription (Bontron *et al.* 1997).

1.3 The role of NLRC5 in major histocompatibility complex class I expression

S, X and Y boxes are also present within the MHC class I locus, upstream of the genes, encoding for MHC class I and β_2 microglobulin (Gobin *et al.* 1997, Martin *et al.* 1997, Gobin *et al.* 2001), and initial *in vitro* data implied a role of CIITA in the regulation of MHC class I (Martin *et al.* 1997, Gobin *et al.* 2001). This, however, was not reflected in mouse models (Itoh-Lindstrom *et al.* 1999). The NLR protein NLRC5 was only later identified as the transcriptional regulator of MHC class I (Steimle *et al.* 1993, Meissner *et al.* 2010, Neerinx *et al.* 2010). *In vitro* experiments revealed that the RFX complex is also essential for the interaction of NLRC5 with the MHC class I promoter region

Introduction

(Meissner *et al.* 2012), and that the region is occupied by the other regulatory factors of the MHC enhanceosome as well (van den Elsen 2011). *In vivo* experiments in knockout mouse models showed that NLRC5 and CIITA are non-redundant and specific for their respective set of genes (Ludigs *et al.* 2015). Analysis of the promoter consensus sequences bound by NLRC5 and CIITA, respectively, showed a general similarity. However certain residues within the X box and several in the S box differ strongly between regions transactivated by NLRC5 and CIITA (Ludigs *et al.* 2015). Exchange of the S boxes between the consensus promoter for NLRC5 and CIITA results in abolished transcription by NLRC5, when the MHC class II S box is used together with MHC class I X and Y box motifs. The MHC class I S box is further sufficient for transcription from the MHC class II promoter by NLRC5 (Ludigs *et al.* 2015). The SXY motif has recently been reported to be present upstream of genes of the butyrophilin (BTN) protein family, which are also regulated by NLRC5. It was shown that destruction of the S box *in vitro* severely impacted transcriptional activation by NLRC5, while CIITA-mediated transcription remained unaltered. This underlines the importance of the S box for the specificity of transcriptional activation by NLRC5 (Dang *et al.* 2021). However, it is still unclear how the specificity of NLRC5 for the MHC class I promoter region is conferred. Our recent work suggests that the N-terminal DD of NLRC5 is a determinant of this. We showed that the DD of NLRC5 has low transcriptional activity and generation of chimeric constructs, in which the N-terminal domain of CIITA was exchanged with the NLRC5 DD, results in a protein that activated both MHC class I and class II genes (Neerincx *et al.* 2014), indicating that the N-terminal domain of NLRC5 determines the specificity for MHC class I transcription. To understand the specificity of transcriptional regulation of NLRC5 it is thus critical to identify the mechanisms, by which the DD activates transcription, as it seems likely, that this, and the proteins binding to the S box of the respective MHC promoter region are the determining factors.

NLRC5 is a CARD-containing member of the NLR family. Although its N-terminal domain shows homology to CARD, it was found by nuclear magnetic resonance (NMR) analysis and computational modeling to differ in several structural features (Mótyán *et al.* 2013, Gutte *et al.* 2014). NLRC5 further stands out from the other NLRs as it contains 27 LRR and thus by far more than any other human NLR. This is also reflected in its size of 1,866 amino acids and a calculated molecular weight of approximately 205 kDa. It is highly expressed in the spleen and lymph nodes both in humans and mice, as well as in barrier tissues, such as the lung and the gastrointestinal tract, which are gateways for several pathogens (Benko *et al.* 2010, Cui *et al.* 2010, Kuenzel *et al.* 2010, Neerincx *et al.* 2010, Davis *et al.* 2011, Staehli *et al.* 2012). Characterization of the expression within the different cell populations of the immune system showed highest expression in both CD4⁺ and CD8⁺ T cells, as well as in B cells (Neerincx *et al.* 2010, Davis *et al.* 2011). Like CIITA, IFN- γ -induced signaling also results in increased expression of NLRC5 (Benko *et al.* 2010, Kuenzel *et al.* 2010, Lech *et al.* 2010, Neerincx *et al.* 2010), further enhancing MHC class I expression and antigen presentation.

Introduction

Import of NLRC5 into the nucleus is controlled by a bipartite nuclear localization sequence between the DD and the NACHT domain (Meissner *et al.* 2010, Meissner *et al.* 2012) and by the ATPase function within the NLRC5 NACHT domain, which was shown for the ATPase deficient K234A mutation in the Walker A motif of this domain (Neerinx *et al.* 2012). After transient presence in the nucleus, NLRC5 is exported via exportin 1 (CRM1), as was shown through nuclear accumulation after CRM1 inhibition by leptomycin B (Benko *et al.* 2010, Meissner *et al.* 2012, Neerinx *et al.* 2012). The LRRs of NLRC5 appear to be critical for nuclear export, as NLRC5 isoform 3, which lacks the LRRs, predominantly localizes in the nucleus. However, MHC induction capabilities of the predominantly nuclear isoform 3, that lacks the LRRs, as well as of NLRC5, forced to the nucleus by fusion of two NLS, are strongly reduced (Neerinx *et al.* 2012). This indicates an important role of the LRRs, as well as the presence of a cytosolic „licensing mechanism“, which enhances NLRC5’s transactivation capacity (Neerinx *et al.* 2012).

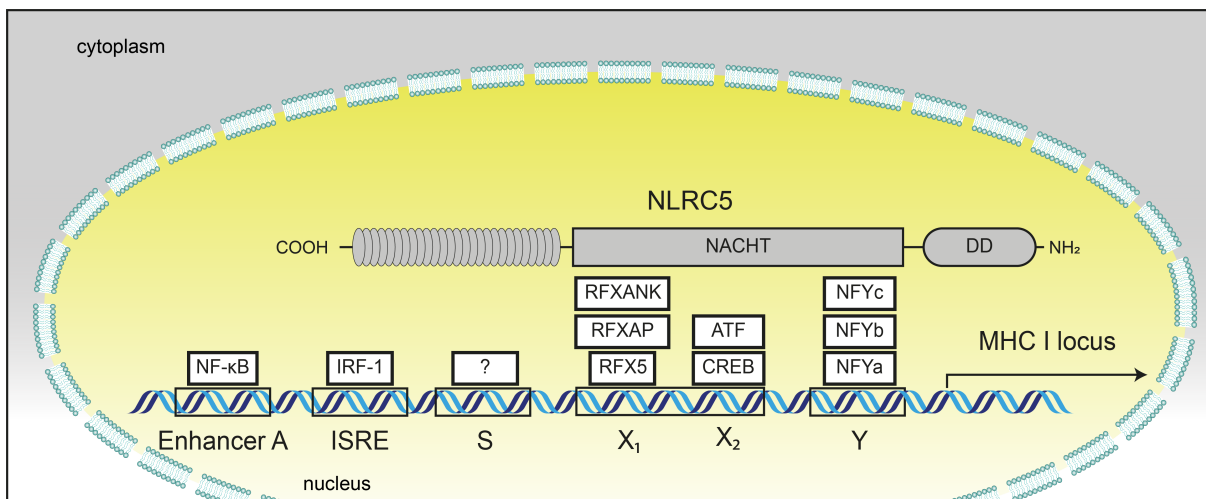


Figure 3: **Schematic representation of the MHC class I promoter region and the MHC enhanceosome.** NLRC5 is recruited to the promoter region of the MHC class I locus by interaction with the MHC enhanceosome. As for the MHC class II locus, this multiprotein complex consists of the three regulatory factor X (RFX) proteins RFX5, RFXAP and RFXANK, which bind the X1 box of the promoter, the cAMP response element binding protein (CREB) and activating transcription factor (ATF) which bind the X2 region, as well as of the trimeric nuclear factor Y (NFY) complex, which binds the Y box. The NLRC5-MHC enhanceosome complex serves as the basis for the recruitment of histone-modifying enzymes and transcription factors, to enable transcription of MHC class II genes. Additional binding factors for the S box remain to be identified. NACHT: Nucleotide binding and oligomerization domain; DD: Death domain-like fold; NF-κB: Nuclear factor 'kappa-light-chain-enhancer' of activated B cells; IRF-1: interferon regulatory factor 1.

MHC class I expression is detectable on almost all nucleated cells (van den Elsen *et al.* 2004), in contrast to MHC class II. This is due to several differences between the MHC I promoter region from the corresponding region of MHC class II. In addition to the SXY boxes, an IFN-sensitive response element (ISRE) is present upstream of the MHC class I locus, through which IFN-γ-dependent transcription of MHC class I molecules can be induced (Gobin *et al.* 1999). In addition to this site, which can bind interferon regulatory factor 1 (IRF1) (Gobin *et al.* 1999), an enhancer A region is present, to which nuclear factor 'kappa-light-chain-enhancer' of activated B cells (NF-κB) can bind (Gobin *et al.* 1998) (**Figure 3**). Nevertheless, NLRC5 is still critical for the induction of MHC class I through

Introduction

enhanceosome-dependent mechanisms. Deletion of *Nlrc5* (*Nlrc5*^{-/-}) in mice results in significantly reduced expression of MHC class I proteins as well as reduced expression of β_2 microglobulin, transporter associated with antigen processing 1 (TAP1) and large multifunctional protease 2 (LMP2) (Meissner *et al.* 2010, Biswas *et al.* 2012, Robbins *et al.* 2012, Staehli *et al.* 2012, Tong *et al.* 2012, Yao *et al.* 2012). However, in bone marrow derived macrophages and dendritic cells from *Nlrc5* deficient animals, only minor changes in MHC class I expression were observed (Biswas *et al.* 2012, Staehli *et al.* 2012) and only reduced numbers of CD8⁺ T cells are observed in *Nlrc5* knockout animals (Staehli *et al.* 2012), suggesting that NLRC5 only partly contributes to MHC class I expression in antigen presenting cells and positive selection of thymocytes.

As alluded to above, reduced MHC class I expression is an immune evasion strategy often observed in cells infected with viruses and in tumors. Malignant cells can be recognized by CD8⁺ T cells through cancer specific antigens presented on MHC class I (Chen and Mellman 2013, Motz and Coukos 2013). Yoshihama *et al.* showed that in 16 different cancers, NLRC5 expression is correlated with MHC class I expression, and that reduction of MHC surface expression by genetic alterations most often targeted NLRC5 (Yoshihama *et al.* 2016). Reconstitution of NLRC5 expression in B16-F10 melanoma cells rescued their ability to activate cognate CD8⁺ T cells. This resulted in attenuated tumor growth and reduced number of tumor foci after intravenous injection into C57BL/6 mice (Rodriguez *et al.* 2016). Reconstitution of defective MHC class I expression through NLRC5 thus is a highly interesting strategy to combat immune evasion of cancers. Additionally, transcriptional upregulation of NLRC5 by radiotherapy was shown to be important for CD8⁺ T cell-mediated killing (Zebertavage *et al.* 2020). Contrary to that, increased NLRC5 expression was observed in gastric (Li *et al.* 2018) and brain (Yoshihama *et al.* 2016) cancer, where it was also linked to poor prognosis. This makes NLRC5 an interesting candidate for therapeutical approaches and research to elucidate the underlying mechanisms of utmost importance.

In addition to its function in transcriptional regulation of MHC class I, NLRC5 has been described as a modulator of innate immune responses. While in vitro assays for both positive (Kuenzel *et al.* 2010, Neerinx *et al.* 2010, Ranjan *et al.* 2015) and negative (Cui *et al.* 2010) regulation of type I IFNs have been published, *Nlrc5*^{-/-} mice in which exon 4 was targeted, do not respond differently to poly(I:C) stimulation (Kumar *et al.* 2011). However, *Nlrc5*^{-/-} mice in which NLRC5 was knocked-out by targeting exon 8, presented with higher IFN- β levels and increased IRF3 phosphorylation after VSV challenge (Tong *et al.* 2012). While the role of NLRC5 as an enhancer of MHC class I transcription is well established and was confirmed by several independent findings, more work is needed to clarify its role in innate immunity and elimination of tumors.

1.3.1 Histone deacetylases – Sin3A

As elaborated above, changes in gene transcription can have major consequences on the cellular state. Dysregulated expression of proteins has the potential to transform cells and can give rise to tumors (Di Gennaro *et al.* 2004). Regulation of protein expression has hence evolved into a highly complex network of positive and negative acting transcription factors, a complex transcriptional and translational machinery, post-translational control of protein expression, and a plethora of factors which regulate the functions of the above.

DNA in cells is structurally organized as chromatin, by tight packaging of DNA around a complex of eight histone proteins. At least eight different covalent modifications of histones are known, which include small molecular modifications, such as phosphorylation, methylation, or acetylation but also modification with the small proteins ubiquitin, or the small ubiquitin related modifier (SUMO). Each of these modifications has implications on the regulation of transcription (reviewed in (Kouzarides 2007)). Specialized enzymes are required for each of these modifications, of which most are specific for particular sites within the histones. As transcriptional regulation is a highly dynamic process, which needs to be attenuated at an appropriate time, several more enzymes exist to reverse these modifications (reviewed in (Kouzarides 2007)). Chromatin modification can on the one hand alter the structure of the chromatin, and on the other hand result in the recruitment of specific proteins. Histone modifications help to organize the chromatin into transcriptionally accessible euchromatin and inaccessible heterochromatin.

Acetylation of histones by histone acetylases is associated with activation of transcription (Barnes *et al.* 2019), with replication (Bar-Ziv *et al.* 2016), and with DNA repair (Hunt *et al.* 2013). Reversion of histone acetylation by histone deacetylases (HDACs) is hence associated with the repression of transcription. However, as with many biological functions, the consequences of histone acetylation and deacetylation depend on the environmental context and the requirement for HDACs in transcriptional activation has been shown in several reports (Bernstein *et al.* 2000, Kim *et al.* 2013, Greer *et al.* 2015).

The HDAC1 complex assembles along the Sin3A protein as a molecular scaffold (Kadamb *et al.* 2013). Sin3A interacts with eight core proteins of the HDAC complex and it can recruit several proteins and transcription factors which add enzymatic function to the complex, and can help to direct it to the targeted regulatory DNA elements (Silverstein and Ekwall 2005). Interactions between Sin3A and the recruited proteins are mediated by six conserved motifs in Sin3A, which are four paired amphipathic helices, a histone deacetylase interaction domain, and the highly conserved region (Bansal *et al.* 2016). The Sin3A protein and the HDAC complex are highly conserved in eukaryotes from yeast to mammals (Silverstein and Ekwall 2005, Bansal *et al.* 2016).

Introduction

Sin3A is involved in the regulation of diverse cellular functions such as the cell cycle, energy metabolism and stem cell differentiation but also in embryonic development (Kadamb *et al.* 2013). And, as for the entire HDAC complex, it has been described as both a positive and negative regulator of transcription (Silverstein and Ekwall 2005). While transcriptional repression is achieved through deacetylation, the mechanisms of transcriptional activation by Sin3A are not well defined yet (Baymaz *et al.* 2015), but appear to be dependent on the cellular environment and further interactors (Lin *et al.* 2005, Baltus *et al.* 2009).

Histone acetylation and deacetylation play an important role in CIITA-mediated transcriptional regulation of MHC class II. It was shown that inhibition of histone deacetylases increases the expression of MHC class II genes (Magner *et al.* 2000), and the presence of CIITA at the MHC class II promoter correlates with acetylation of histones H3 and H4 (Beresford and Boss 2001). Moreover, the HDAC1-Sin3A complex is involved in the termination of MHC class II transcription (Zika *et al.* 2003).

1.3.2 The negative elongation factor complex

Within euchromatin, further regulatory mechanisms fine tune the transcription of protein coding genes. Stimulus-dependent binding of transcription factors to promoter elements, and the recruitment of the ribonucleic acid (RNA) polymerase II complex (Pol II) induces transcription of proteins. The transcription machinery of Pol II is further controlled by a broad range of regulatory factors (Roeder 2019), including Pol II elongation factors. These proteins interact with the Pol II complex at early stages of transcription and can either promote, or inhibit the transcription process (Schier and Taatjes 2020).

The tetrameric negative elongation factor complex (NELF), consisting of NELFA, NELFB, NELFC/D and NELFE, binds the Pol II complex at the promoter and within 25 – 50 nucleotides downstream of the transcription start site (Nechaev *et al.* 2010, Li *et al.* 2013). This association between the NELF complex with Pol II, together with the DRB sensitivity inducing factor (DSIF) complex (Wada *et al.* 1998), causes a halt to the transcription process, which is termed promoter proximal pausing (Yamaguchi *et al.* 1999). Phosphorylation of the inhibitory factors by the positive transcription elongation factor b (p-TEFb), consisting of cyclin-dependent kinase 9 and cyclin T, releases the NELF complex from Pol II, allowing transcription (Core and Adelman 2019). The mechanism behind promoter proximal pausing involves competition of the NELF complex with the Pol II complex component transcription elongation factor SII (TFIIS), which inhibits rescue from Pol II arrest and backtracking, which describes a proofreading mechanism during which the 3' end of the RNA is detached from the active site and RNA Pol II moves backwards on the DNA template (Palangat *et al.* 2005, Lisica *et al.* 2016).

Promoter proximal pausing is a common mechanism in gene transcription and its duration and intensity are regulated by the p-TEFb activity. Local p-TEFb activity seems to be modified by either gene specific

Introduction

recruitment of p-TEFb through other proteins (Lis *et al.* 2000, Peterlin and Price 2006, Zhou and Yik 2006), or by the disruption of p-TEFb sequestration in a large ribonucleoprotein complex, where p-TEFb is kept in an inactive state (Peterlin and Price 2006). Interestingly, the NELF complex does not appear to be required for the initiation of promoter proximal pausing, but rather to determine its duration (Cheng and Price 2007, Henriques *et al.* 2013, Vos *et al.* 2018). Besides controlling the overall transcription levels of a gene, pausing Pol II is thought to be a mechanism which enables rapid activation of the transcriptional response upon the appropriate stimulus, as the steps leading to recruitment of Pol II to the transcribed gene have already taken place (Gariglio *et al.* 1981, Wu *et al.* 2003, Core and Adelman 2019).

As NELFB and NELFC/D were proposed to form the structural scaffold of the complex it is difficult to decipher the functional role of single components of the NELF complex. They each recruit one of the other NELF subunits, NELFE and NELFA, respectively, into the complex (Narita *et al.* 2003, Vos *et al.* 2016). NELF subunit expression levels were also shown to correlate with each other, making experiments based on overexpression and knockdown difficult to interpret (Sun *et al.* 2008). Nevertheless, several approaches to elucidate the functions of NELFB were tried. NELFB was initially identified as cofactor of breast cancer susceptibility gene (COBRA1) (Ye *et al.* 2001), and is associated with the regulation of several breast cancer related genes in both estrogen-dependent and -independent fashion (Aiyar *et al.* 2007). Expression levels inversely correlate with disease progression, with less NELFB protein levels in patients with distant metastasis and local recurrence (Sun *et al.* 2008). Enhanced expression of NELFB was found in a majority of primary upper gastrointestinal adenocarcinomas (McChesney *et al.* 2006). Besides regulating estrogen-dependent transcription, NELFB was also found to bind to androgen receptor and repress androgen receptor-dependent transcription (Sun *et al.* 2007). Roles of NELFB in regulation of proliferation, apoptosis and oncogenesis might be explained by its interaction with activator protein 1 (AP-1) (Zhong *et al.* 2004).

Deeper understanding of the mechanisms leading to the transcription of MHCs is necessary to find the differences between MHC class I and II, and to unravel how specificity is conferred by either NLRC5 or CIITA. Identification of recruited histone modifying enzymes or other transcriptional regulators might serve as an important tool on our path to understand the precise mechanisms through which MHC expression is regulated.

1.4 NOD-like receptors as inhibitors of type I interferon responses

Type I IFNs play a critical role in antiviral defense, but also in the protection against other pathogens. IFNs were initially discovered by Alick Isaacs and Jean Lindemann in 1957 in supernatants of chorioallantoic membranes, exposed to heat inactivated influenza virus, as a soluble factor that could interfere with viral infection in cells (Isaacs and Lindenmann 1957). They both act in an autocrine and paracrine manner by binding to the heterodimeric IFN- α/β receptor (IFNAR) (Uzé *et al.* 1990, Novick *et al.* 1994, Domanski *et al.* 1995). The IFNAR is present on most cell types, and signals through activation of the janus kinase (JAK) - signal transducer and activator of transcription (STAT) signaling cascade, culminating in the transcription of a plethora of antiviral response genes, regulated by interferon stimulated response elements (ISRE) (Rawlings *et al.* 2004) (**Figure 4**). This multitude of interferon stimulated genes (ISG) is the main driving force behind the antiviral effect of IFNs. Paracrine signaling primes bystander cells towards a state of defense or tolerance for upcoming viral infection (Stetson and Medzhitov 2006).

Insufficient innate immune responses generally lead to higher pathogen burden upon infection. Mice deficient in either of the type I IFN receptor subunits, or their downstream signaling molecule STAT1, are thus highly susceptible to several viral infections (Muller *et al.* 1994, Koerner *et al.* 2007, Shepardson *et al.* 2018). On the other hand, inability to keep the innate immune response in reign can be equally detrimental for the host (Rodero and Crow 2016, Crayne *et al.* 2019). Also, loss of balance between type I IFN and pro-inflammatory responses can lead to severe pathology (Chi *et al.* 2006, Rotger *et al.* 2011, Channappanavar *et al.* 2019, Acharya *et al.* 2020, Jamilloux *et al.* 2020). As mentioned above, NLRC5 is controversially discussed as an inhibitor of innate immune responses. NLRC5, however, is not the only NLR for which such a PRR-independent role is discussed. It has become apparent, that several NLRs do not initiate an innate immune response, but rather function as inhibitors (Kienes *et al.* 2021).

Besides the induction of antiviral response genes, binding of type I IFNs to their receptor also induces other pro-inflammatory pathways, such as mitogen-activated protein kinase (MAPK), mammalian target of rapamycin (mTOR) and NF- κ B pathway, resulting in growth inhibition, chromatin remodeling and the induction of pro-inflammatory cytokines (Uddin *et al.* 1997, Caraglia *et al.* 1999, Lin *et al.* 2000) (**Figure 4**). Furthermore, type I IFNs drive the formation of the adaptive immune response by controlling cell expansion, differentiation, and by shaping the cytokine and chemokine response of lymphoid cells (McNab *et al.* 2015).

Introduction

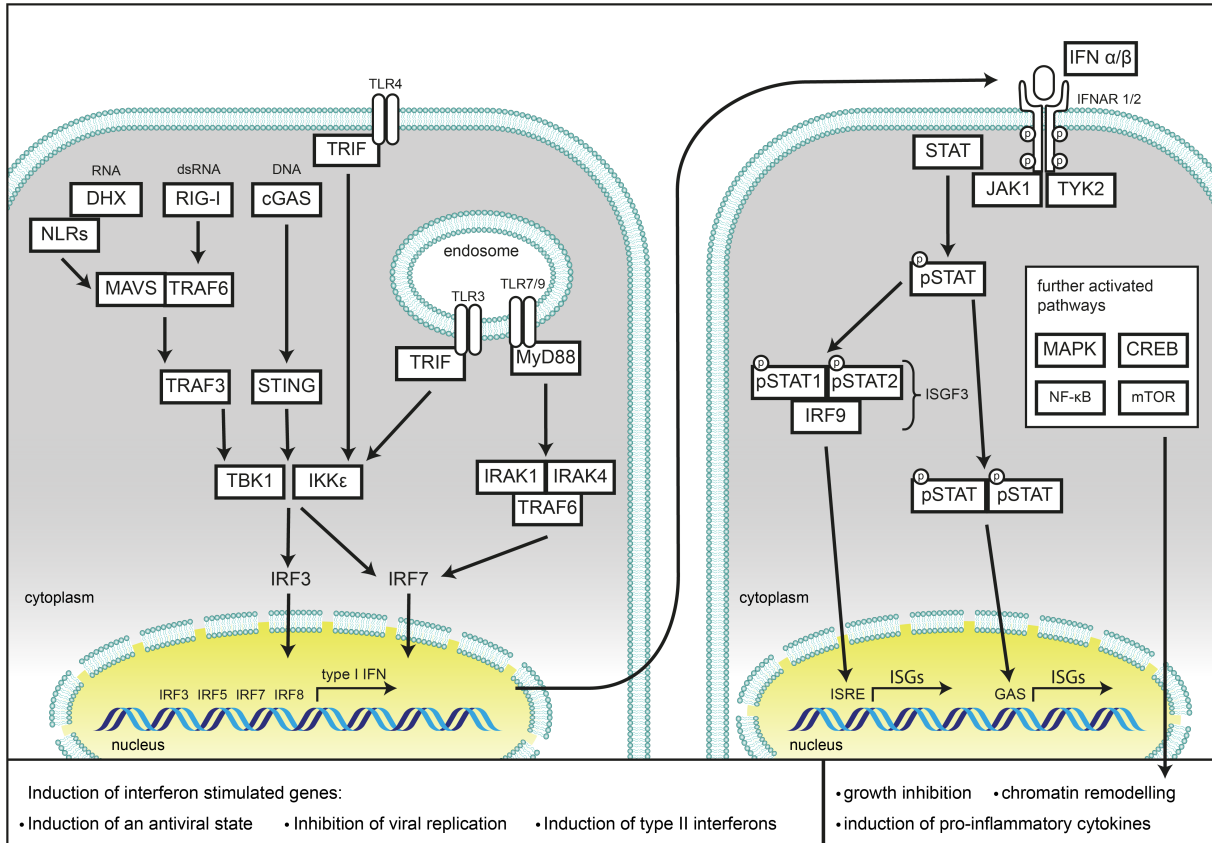


Figure 4: Schematic representation of type I interferon induction (left) and type I interferon induced signaling (right). Several pattern recognition receptors can induce the expression and secretion of type I interferons (IFN) upon recognition of their respective ligands. Recognition of pathogen associated molecular patterns initiates a signaling cascade, culminating in the activation and nuclear translocation of interferon regulatory factors (IRF) which can induce transcription of type I IFNs. Secreted type I IFNs then can be bound in an autocrine or paracrine manner by the type I IFN receptor (IFNAR) which induces a signaling cascade, resulting in the transcription of interferon stimulated genes (ISGs), and the activation of several other pro-inflammatory pathways. TLR: Toll-like receptor; TRIF: TIR-domain-containing adapter-inducing interferon- β ; cGAS: Cyclic GMP-AMP synthase; RIG-I: Retinoic acid-inducible gene I; DHX: DEXD-box helicases; NLR: NOD-like receptor; MAVS: Mitochondrial antiviral-signaling protein; TRAF: TNF receptor associated factor; STING: Stimulator of interferon genes; TBK1: TANK-binding kinase 1; IKK ϵ : Inhibitor of nuclear factor kappa B kinase subunit epsilon; MyD88: Myeloid differentiation primary response 88; IRAK: Interleukin 1 receptor associated kinase; STAT: Signal transducer and activator of transcription; JAK: Janus kinase; TYK2: Tyrosine kinase 2; p: phosphorylation; MAPK: Mitogen-activated protein kinase; CREB: CAMP responsive element binding protein; NF- κ B: Nuclear factor 'kappa-light-chain-enhancer' of activated B cells; mTOR: Mechanistic target of rapamycin kinase.

Type I IFNs are induced predominantly upon intercellular sensing of nucleic acids which can occur by TLRs, RLRs, cGAS, as well as by some NLRs. The main class of PRRs responsible for the detection of viral RNAs, are the RLRs. This protein family contains the retinoic acid-inducible gene I protein (RIG-I), melanoma differentiation-associated proteins 5 (MDA5), and laboratory of genetics and physiology 2 (LGP2). RIG-I senses the 5' di- and tri-phosphates of short, blunt end double stranded RNAs (dsRNA) (Rehwinkel and Gack 2020). RNA-binding is mediated by a DEXD/H box domain with ATPase function. The C-terminus of RIG-I contains an inhibitory domain, which keeps the protein in an inactive state until conformational changes are conferred by RNA binding (Cui *et al.* 2008). Upon activation, the two N-terminal CARD-domains homotetramerize (Kowalinski *et al.* 2011) and bind the CARD domain of the mitochondrial antiviral signaling protein (MAVS) (Hou *et al.* 2011). MAVS in turn recruits several adaptor proteins, which enable the activation of TANK-binding kinase 1 (TBK1)

Introduction

and inhibitor of nuclear factor kappa B kinase subunit epsilon (IKK ϵ). TBK1 and IKK ϵ phosphorylate the transcription factors IRF3 and IRF7, which results in their homodimerization and translocation into the nucleus, where they initiate the transcription of type I IFNs (Au *et al.* 1995, Au *et al.* 1998, Juang *et al.* 1998, Lin *et al.* 1998) (**Figure 4**).

1.4.1 Functions of NLRP11

Several NLRs have been described as negative regulators of the type I IFN response (Kienes *et al.* 2021). Of those, NLRC3 and NLRX1 are the best characterized ones. NLRX1 localizes to the mitochondria (Moore *et al.* 2008, Tattoli *et al.* 2008, Arnoult *et al.* 2009), where it disrupts the interaction of MAVS and RIG-I (Moore *et al.* 2008, Allen *et al.* 2011), and impairs induction of an antiviral response (Ma *et al.* 2017, Qin *et al.* 2017). NLRC3 inhibits the response towards cytosolic DNA and herpes simplex virus 1 (HSV1) by inhibition of the interaction between the stimulator of interferon genes (STING) and TBK1 (Zhang *et al.* 2014). In 2012, NLRP4 was shown to inhibit the type I IFN responses by initiating TBK1 degradation through the E3 ubiquitin ligase deltex-4 (DTX4) (Cui *et al.* 2012). The *NLRP4* gene lies on chromosome 19q13.42 in a cluster, together with the genes of three other NLRs, *NLRP11*, *NLRP8* and *NLRP13*, where it is organized in a bidirectional manner with *NLRP11* (**Figure 5**). Bidirectionally arranged genes are abundant within the human genome. These genes are often regulated by a common promoter and are thus co-expressed (Trinklein *et al.* 2004). Such a correlation of expression was also found for NLRP11 and NLRP4 by the analysis of gene chip expression sets (Ellwanger *et al.* 2018). Within cells of the immunological niche, different expression patterns have been reported for NLRP11. Ellwanger *et al.* showed highest expression in resting and activated B cells, while expression in monocytes was only weak. In contrast, Wu *et al.* reported only minimal expression in B cells, but high expression in monocytes (Wu *et al.* 2017, Ellwanger *et al.* 2018). Induction of NLRP11 by poly(I:C) and Pam3CSK4, but not by LPS in human myeloid THP-1 cells was observed by our group (Ellwanger *et al.* 2018), while Wu *et al.* reported strong induction in THP-1 cells by both LPS and Pam3CSK4 (Wu *et al.* 2017). However, both groups demonstrated induction of NLRP11 by LPS in peripheral blood mononuclear cells (PBMCs) at 16 h post stimulation (Wu *et al.* 2017, Ellwanger *et al.* 2018).

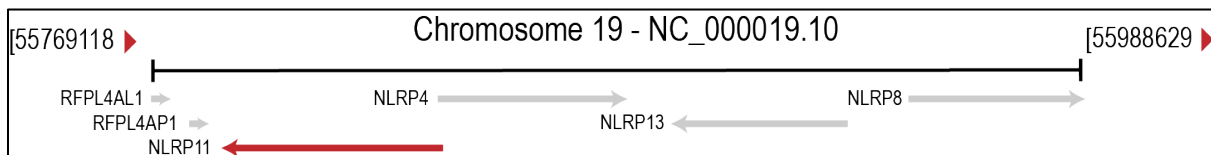


Figure 5: **Genomic organization of the *NLRP11* containing locus.** NLRP11 is encoded in a genomic region, together with the genes for *NLRP4*, *NLRP13* and *NLRP8*. It is organized in a bidirectional manner with *NLRP4*, indicating possible co-expression and functions in similar cellular context.

Introduction

Besides the expression in immune cells, NLRP11 is highly expressed in testicular and ovarian tissues, as well as in the liver (Tian *et al.* 2009, Wu *et al.* 2017, Ellwanger *et al.* 2018). In humans and other primates, NLRP11 mRNA transcription in oocytes was reported to decrease during maturation (McDaniel and Wu 2009).

NLRP11 encodes a 1,033 amino acid polypeptide of an approximate molecular weight of 118 kDa. It shows the typical tripartite structure of NLRs, consisting of an N-terminal PYD domain, a central NACHT domain, and six C-terminal LRRs. In line with its bidirectional organization and co-expression with NLRP4, it was suspected to exert similar functions as NLRP4. NLRP11 was reported to negatively regulate TLR-induced NF- κ B responses (Wu *et al.* 2017). Wu *et al.* showed that overexpression of NLRP11 in THP-1 cells resulted in reduced phosphorylation of IKK β , I κ B α , and several MAPK kinases upon stimulation with several TLR ligands, but not with TNF or poly(I:C), resulting in reduced cytokine secretion. They found NLRP11 to specifically interact with TRAF6 and to induce its degradation by recruiting the E3 ubiquitin ligase RING finger protein 19A (RFG19A) by K48-linked ubiquitylation (Wu *et al.* 2017).

Besides its inhibitory role in TLR-induced NF- κ B responses, NLRP11 was also implicated as an inhibitor of the antiviral type I IFN response (Qin *et al.* 2017, Ellwanger *et al.* 2018). It was shown to inhibit type I IFN production and ISG transcription in response to poly(I:C), poly(dA:dT), as well as to Sendai virus (SeV) challenge in overexpression experiments (Qin *et al.* 2017, Ellwanger *et al.* 2018). Reduction of NLRP11 expression, induced either by siRNA (Ellwanger *et al.* 2018), or by CRISPR-knockout (Qin *et al.* 2017), resulted in increased type I IFN response upon SeV challenge. While Wu *et al.* reported no inhibitory effect of NLRP11 on the TBK1-induced IFN β response (Wu *et al.* 2017), our group showed that overexpression of NLRP11 resulted in dose-dependent inhibition of type-I IFN responses induced by either TRAF2, TRAF6, or TBK1 (Ellwanger *et al.* 2018). This inhibitory function was also exerted by overexpression of the LRRs of NLRP11 and, in line with that, was independent of the functionality of the Walker A ATPase motif within the NACHT domain of NLRP11 (Ellwanger *et al.* 2018).

While the role of NLRP11 as a negative regulator of the type I IFN response emerges, it still remains unclear at which level NLRP11 inhibits this pathway, or if this interference might occur at multiple steps.

1.4.2 DDX3X

Besides the modulation of type I IFN responses, several NLRs can directly induce type I IFNs in response to cytoplasmic nucleic acids (Sabbah *et al.* 2009, Lupfer *et al.* 2013, Wang *et al.* 2015, Vegna *et al.* 2016, Zhu *et al.* 2017, Bauernfried *et al.* 2021). Interestingly, two of these were shown to rely on DExD-box helicases for sensing of viral RNA and activation. In case of murine *Nlrp9b*, *Dhx9*

Introduction

serves as a sensor for dsRNA, which in turn induces the formation of the Nlrp9b inflammasome (Zhu *et al.* 2017). Similarly, Dhx15 is a cytosolic sensor for viral RNA which enables interaction between Nlrp6 and Mavs to induce type I and type III IFNs (Wang *et al.* 2015).

DDX3X is another DExD-box helicase with a central role in type I IFN induction. It consists of 662 amino acids, organized in an N-terminal region, which mediates TBK1- and IKK ϵ -dependent induction of IFN β (Schröder *et al.* 2008), and a central ATPase and helicase domain. DDX3X is expressed in many tissues (Kim *et al.* 2001), and shuttles between the cytoplasm and the nucleus in a CRM1-dependent manner (Owsianka and Patel 1999, Yedavalli *et al.* 2004, Schröder *et al.* 2008), but also via the nuclear RNA export factor 1 (NXF1)-dependent mRNA export pathway (Lai *et al.* 2008). A first description of the function of DDX3X was provided by Owsianka and Patel, who showed that the DDX3X C-terminus interacts with Hepatitis C virus core protein in distinct spots in the perinuclear region (Owsianka and Patel 1999).

The role of DDX3X in type I IFN induction was discovered back to back as a enhancer of TBK1 activation (Soulat *et al.* 2008), and as a target of Vaccinia virus protein K7, which inhibits type I IFN induction (Schröder *et al.* 2008). Both groups showed that overexpression of DDX3X results in enhancement of TBK1- and IKK ϵ -induced *ifnb* promoter activation and that knockdown of the protein inhibited the activation of IRF3 and subsequent IFN β transcription. It was reported early on that activation of DDX3X by TBK1 results in its phosphorylation which coincides with phosphorylation of IRF3 (Soulat *et al.* 2008). The binding of DDX3X to IKK ϵ enables the autophosphorylation of IKK ϵ at Serine172 (S172), and subsequent phosphorylation of DDX3X at S102 (Gu *et al.* 2013). This phosphorylation of DDX3X facilitates recruitment of the transcription factor IRF3 to the signaling complex and thus its phosphorylation by IKK ϵ (Gu *et al.* 2013). DDX3X enhances the induction of type I IFNs at various steps in the pathway. It was shown to directly interact with MAVS (Oshiumi *et al.* 2009), IKK ϵ (Schröder *et al.* 2008), TBK1 (Soulat *et al.* 2008), TRAF3 (Gu *et al.* 2017), and IRF3 (Gu *et al.* 2013). Besides regulation of the type I IFN response, DDX3X is also involved as an enhancer of the NF- κ B pathway (Wang *et al.* 2017). Recently, a new role of DDX3X within innate immunity was reported. It was shown that the availability of DDX3X serves as a live or die checkpoint for the activation of the NLRP3 inflammasome and subsequent pyroptosis (Samir *et al.* 2019). The authors showed that DDX3X is a critical part in the formation of the NLRP3 inflammasome, and that sequestration into stress granules prevents the formation of NLRP3 inflammasomes (Samir *et al.* 2019).

Although DDX3X plays important roles in antiviral responses, dependence on DDX3X has been reported for efficient replication and virion production of 18 different viruses, making it an interesting target for broad antiviral intervention (Winnard *et al.* 2021). Targeting the RNA binding site of DDX3X, as well as the ATP binding site by small molecular inhibitors, has shown promising effect in the inhibition of several viruses (Brai *et al.* 2016, Brai *et al.* 2019, Brai *et al.* 2019, Brai *et al.* 2020,

Introduction

Brai *et al.* 2020, Yang *et al.* 2020). However, DExD box helicases are proteins which regulate a wide range of functions in cellular RNA metabolism, such as processing, export, transcription, translation, and degradation (de la Cruz *et al.* 1999). Thus, the plethora of pathways and cellular mechanisms in which DDX3X is involved also means that alterations of DDX3X levels and functionality will have consequences that are highly dependent on the cellular environment. For example, in oncogenesis, DDX3X can either act as a tumor suppressor, or as an oncogene, depending on its expression levels, the presence of mutations which influence only selective DDX3X functions, and on the tumor type (Riva and Maga 2019). Similarly, depending on modulations by the infecting virus, the stage of infection, and by the cellular background, DDX3X can either be beneficial for viral replication, or for antiviral immunity (Riva and Maga 2019). Understanding of the environmental contexts determining the benefits of DDX3X for either antiviral response, or viral replication, will help to specifically target DDX3X therapeutically without disturbing the important functions of DDX3X in cell cycle progression and mRNA processing.

1.5 Aim of the study

Tight regulation of innate immune responses is of utmost importance to ensure the balance between defense against pathogens on the one side, and tissue damage caused by the immune response on the other side. This is true for both innate immune responses, but also for antigen presentation and subsequent adaptive immune responses.

In this thesis the function of two NLR proteins were further characterized: NLRC5 and NLRP11.

For NLRC5 its role in MHC class I regulation is well establish, however the nature of the specificity of NLRC5 for MHC class I gene regulation over MHC class II genes still is not well understood, besides the fact that the NLRC5 N-terminal domain and the S box of the promoter are determining factors. As many viral infections and cell transformations achieve immune evasion through reduction of MHC class I surface expression, understanding the mechanisms behind the regulation of MHC class I could help to facilitate treatment of several viral diseases and tumors. In the first part of this thesis, I thus set out to identify the NLRC5 interactome in specific cellular compartments and, by this, identify and characterize factors which could play a critical role in conferring selective transcription of MHC class I. Furthermore, I aimed to gain novel insights into the structure of the NLRC5 DD. For this I optimized the recombinant expression of the NLRC5 DD and established a purification strategy for subsequent crystallization studies.

NLRP11 was only recently experimentally characterized during the conduction of this thesis and shown to affect type I interferon pathways in a still not well understood manner. Failure to properly dampen the antiviral IFN response at the appropriate moment results in increased disease burden either by host or viral factors (Rodero and Crow 2016, Davidson *et al.* 2018, Crayne *et al.* 2019). It is thus important

Introduction

to understand how negative regulators of the innate immune response keep the immune system in check. In the second part of the thesis, I thus set out to elucidate how NLRP11 exerts its inhibitory functions in the type I IFN response and characterize the underlying mechanisms behind inhibition of the type I IFN response. This was approached by identification of NLRP11 interactors and characterization of the effects of the interplay between NLRP11 and those novel interaction partners in the inhibition of innate immune responses.

2 Material and Methods

2.1 Materials

2.1.1 Cell lines and bacteria

All mammalian cell lines were maintained at 37°C and 5% CO₂ in a humid atmosphere in medium containing 50 U/ml penicillin and 50 µg/ml streptomycin (Gibco) (Pen/Strep), if not stated otherwise. Cell lines were routinely monitored for mycoplasma contamination by PCR.

Bacteria were grown at 37°C in Lysogeny Broth (LB) (Carl Roth), if not specified otherwise.

HEK293T

Human embryonic kidney 293T cells (HEK293T, ATCC, CRL-3216) were cultured in DMEM (ThermoFisher), supplemented with 10% heat inactivated FBS (Merck; PAN Biotech).

HEK Blue

HEK Blue IFN- α/β (hkb-ifnab, InvivoGen) cells were maintained in DMEM, supplemented with 10% two-times heat inactivated FBS, 30 µg/ml blasticidin (InvivoGen) and 100 µg/ml zeocin (InvivoGen). Genes encoding for IRF9 and STAT2 are stably integrated into these reporter cells to complete the type I IFN signaling pathway. They further express secreted embryonic alkaline phosphatase (SEAP) under the control of the type I IFN-inducible ISG54 promoter, which can be used to indirectly measure the levels of type I IFNs in cell supernatants.

HEK293 FlpIn T-REx

Maternal HEK293 FlpIn T-REx cells (ThermoFisher, R78007) were cultured in DMEM, supplemented with 10% heat inactivated FBS, 10 µg/ml blasticidin and 100 µg/ml zeocin. Upon insertion of the gene of interest by Flp recombinase, they were maintained under selective pressure with 100 µg/ml hygromycin B (InvivoGen) and 10 µg/ml blasticidin. Expression of the gene of interest is controlled by Tet-repressor (T-REx) and can be induced by 1 µg/ml doxycycline (Dox) (Sigma-Aldrich).

HEK293 FlpIn NLRP11-eGFP were generated in this study. HEK293 FlpIn eGFP-NLRC5, eGFP-NLRC5 isoform 3, eGFP-NLRC5 2xNLS, eGFP-NLRC5 NLS I and eGFP were previously generated by Patrick Suren.

HeLa

HeLa cells (ATCC, CCL-2) were maintained in DMEM, supplemented with 10% heat inactivated FBS.

HeLa FlpIn T-REx

Maternal HeLa FlpIn T-REx cells were kindly provided by the Hentze Lab (EMBL Heidelberg). They were cultured in DMEM, supplemented with 10% heat inactivated FBS, 10 µg/ml blasticidin and 100 µg/ml zeocin. Upon insertion of the gene of interest by Flp recombinase, they were maintained under selective pressure with 600 µg/ml hygromycin B and 10 µg/ml blasticidin. Expression of the gene of

Material and Methods

interest is controlled by Tet-repressor and can be induced by 1 µg/ml doxycycline. HeLa FlpIn eGFP cells were previously generated in our lab (Ellwanger *et al.* 2019). HeLa NLRP11-eGFP, eGFP-NLRC5, eGFP-NLRC5 isoform 3, eGFP-NLRC5 2xNLS and eGFP-NLRC5 NLS I were generated in this study.

K562 FlpIn

Maternal K562 FlpIn cells were a kind gift from the Superti-Furga lab. Cells were maintained in suspension in RPMI 1640 (ThermoFisher) containing 10% heat inactivated FBS, 2 mM L-Glutamin (Gibco), 30 µg/ml blasticidin, and 100 µg/ml zeocin. Upon insertion of the gene of interest, they were maintained in medium containing 200 µg/ml hygromycin B and 30 µg/ml blasticidin. K562 BioID2-HA and K562 DD-BioID2-HA cells were generated in this study.

THP-1

Human monocytic leukemia cell line THP-1 (ATCC TIB-202) cells were cultured in suspension in RPMI 1640, supplemented with 10% heat inactivated FBS and 2 mM L-Glutamin. Differentiation into adherent macrophage like cells was performed by treatment with 100 nM phorbol 12-myristate 13-acetate (PMA) (InvivoGen) for 16 h.

THP-1 shRNA

THP-1 cells with a doxycycline-inducible shRNA targeting DDX3X and respective controls are described in (Fullam *et al.* 2018). Cells were grown in suspension in RPMI 1640 supplemented with 10% FBS, 2 µg/ml puromycin (InvivoGen). Knockdown of DDX3X was induced by 1 µg/ml doxycycline for 48 h.

***Escherichia coli* DH5α**

The nonpathogenic laboratory strain *E. coli* DH5α [F⁻ Φ80*lacZ*ΔM15 Δ(*lacZYA-argF*)U169 *deoR recA1 endA1 bsdR17* (r_k⁺, m_k⁺) *phoA supE44 thi-1 gyrA96 relA1 λ*⁻], derived from apathogenic *E. coli* K12 were used for plasmid amplification. According to the resistance conferred by the transformed plasmid, bacteria were cultured with either 100 µg/ml ampicillin (Carl Roth), or 50 µg/ml kanamycin (Carl Roth).

***Escherichia coli* Rosetta**

The nonpathogenic *E. coli* Rosetta strain (Novagen) [B F⁻ *ompT gal dcm hsdS_B(r_B⁻m_B⁻) λ(*DE3 [*lacI lacUV5-T7p07 ind1 sam7 nin5*)] [*malB*⁺]_{K-12}(λ^S) pLysSRARE[*T7p20 ileX argU thrU tyrU glyT thrT argW metT leuW proL ori_{p15A}*](Cm^R)], derived from *E. coli* BL21, is complemented with tRNAs for codons, rarely used in *E. coli* and hence used for expression of eukaryotic genes, containing codons not common in *E. coli*. As a selection antibiotic 34 µg/ml chloramphenicol (Carl Roth) was used.

***Escherichia coli* BL21 (DE3)**

E. coli BL21 (DE3) [B F⁻ *ompT gal dcm lon hsdS_B(r_B⁻m_B⁻)* λ(DE3 [*lacI lacUV5-T7p07 ind1 sam7 nin5*]) [*malB*⁺]_{K-12}(λ^S)], derived from *E. coli* B834 were used for expression of recombinant proteins. This strain of *E. coli* carries the λ3 DE3 prophage which enables expression of the T7 RNA polymerase under control of a lacUV5 promoter, facilitating induction of T7 RNA polymerase expression by Isopropyl-β-D-thiogalactopyranosid (IPTG). The strain was used for recombinant protein expression.

***Escherichia coli* BL21 (DE3) pLysS**

Derived from *E. coli* BL21 (DE3), the BL21 (DE3) pLysS *E. coli* strain [B F⁻ *ompT gal dcm lon hsdS_B(r_B⁻m_B⁻)* λ(DE3 [*lacI lacUV5-T7p07 ind1 sam7 nin5*]) [*malB*⁺]_{K-12}(λ^S) pLysS[*T7p20 ori_{p15A}*](Cm^R)] contains a plasmid encoding the T7 phage lysozyme, which reduces the leaky expression of genes controlled by a T7 promoter, while not affecting IPTG induced expression. This is beneficial when recombinant proteins are expressed, which, even at low concentrations, result in reduced fitness of transformed bacteria. 34 µg/ml chloramphenicol was used as a selection antibiotic.

***Escherichia coli* Tuner**

The *E. coli* tuner strain [F⁻ *ompT hsdS_B (r_B⁻ m_B⁻) gal dcm lacY1*(DE3)] is derived from *E. coli* BL21 and contains a lac permease (lacY) mutation, which allows uniform entry of IPTG into all cells of the population, allowing for homogenous expression levels, which are concentration-dependent.

***Escherichia coli* C41 (DE3)**

Derived from *E. coli* BL21 (DE3) this strain [F⁻ *ompT hsdS_B (r_B⁻ m_B⁻) gal dcm* (DE3)] contains at least one uncharacterized mutation that prevents cell death upon overexpression of many toxic proteins.

***Escherichia coli* C43 (DE3)**

E. coli C43 (DE3) [F⁻ *ompT hsdS_B (r_B⁻ m_B⁻) gal dcm* (DE3)] were derived from *E. coli* C41 (DE3) by selection for resistance against a different toxic protein than the one used to select *E. coli* C41 (DE3). It can be used to express a broader range of toxic proteins than *E. coli* C41 (DE3).

E. coli strains BL21 (DE3), BL21 (DE3) pLysS, Tuner, C41 (DE3) and C43 (DE3) were kindly provided by Julia Fritz-Steuber (University of Hohenheim).

2.1.2 Chemicals and reagents

Table 1: Chemicals and reagents used in this study.

Chemicals and Reagents	Supplier
Acetic acid	Carl Roth
Ammoniumperoxidesulfate (APS)	Carl Roth
Adenoside-triphosphate	Carl Roth
β -mercaptoethanol	Carl Roth
β -Glycerophosphate	Fluka
Biotin	Sigma-Aldrich
Bromphenol Blue	Carl Roth
CaCl ₂	Carl Roth
Deoxycholic acid	Carl Roth
D-luciferin	Sigma-Aldrich
Dimethyl sulfoxide (DMSO)	Carl Roth
dNTPs	Genaxxon
Ethylenediaminetetraacetic acid (EDTA)	Carl Roth
Ethylene glycol-bis(β -aminoethyl ether)-N,N,N',N'-tetraacetic acid (EGTA)	Carl Roth
Glycerol	Carl Roth
Glycin	Carl Roth
HCl	Carl Roth
HEPES	Gibco
KCl	Carl Roth
Luminol	Sigma-Aldrich
Methanol	Carl Roth
MgCl ₂	Genaxxon
MgSO ₄	Carl Roth
Milk powder	Carl Roth
MnCl ₂	Carl Roth
NaF	Sigma-Aldrich
Na ₂ HPO ₄	Carl Roth
NaH ₂ PO ₄	Carl Roth
NaCl	Carl Roth
NaOH	Carl Roth
NP-40	Sigma-Aldrich
Ortho-Nitrophenyl- β -galactoside (ONPG)	Carl Roth
Paraformaldehyde	Carl Roth
p-Coumaric acid	Sigma-Aldrich
Phorbol 12-myristate 13-acetate (PMA)	InvivoGen
PIPES	Carl Roth
PonceauS	Carl Roth
ROTIPHORESE®NF-Acrylamid/Bis-Lösung 30 (29:1)	Carl Roth
Sodium dodecyl sulfate	Carl Roth
Sodium orthovanadate	Sigma-Aldrich
Succhrose	Carl Roth
Tetramethylethylenediamine (TEMED)	Carl Roth
tris(hydroxymethyl)aminomethane (Tris)	Carl Roth
Polyethylene glycol p-(1,1,3,3-tetramethylbutyl)-phenyl ether (Triton-X100)	Carl Roth
Polyoxyethylene (20) sorbitan monolaurate (Tween-20)	Carl Roth

Material and Methods

Trypsin	Biochrome
Urea	Carl Roth

2.1.3 Kits

Table 2: Kits used in this study.

Kit	Manufacturer
NucleoSpin	Macherey Nagel
DuoSet ELISAs (IL-1 β , IFN β , IL-8)	R&D Systems
cDNA Synthese Kit	BioRAD
RNeasy Mini Kit	Quiagen
SYBR-Green Reaction Mix	BioRAD

2.1.4 Plasmids

Table 3: Plasmids used for overexpression in mammalian cells (expression plasmids), recombinant expression in bacteria (recombinant expression) and reporter gene plasmids used in this study.

Plasmid	Insert	Tag	Backbone	Reference/obtained from
Expression plasmids				
AIM2	AIM2	eGFP	pEFBOS	(Bartok <i>et al.</i> 2013)
ASC-HA	ASC	HA	pCI	(Hornung <i>et al.</i> 2009)
β -galactosidase	β -galactosidase	none	pcDNA3.1	(Kufer <i>et al.</i> 2006)
Caspase-1	Caspase-1	none	pCI	(Bartok <i>et al.</i> 2013)
COBRA1-Flag	NELFB	FLAG	pcDNA3	Kind gift of Patrick Mehlen
DD-BioID2-HA	BioID2 C-terminal of NLRC5 DD; aa 1 – 139	HA	MCS-BioID2-HA	This work
eGFP-DDX3X	DDX3X	eGFP	pEGFP	This work
eGFP-NLRC5	NLRC5; aa 1 – 1866	eGFP	pcDNA5 FRT/TO	Patrick Suren
eGFP-NLRC5 2xNLS	NLRC5; aa 1 – 1866 fused with 2x SV40 NLS	eGFP	pcDNA5 FRT/TO	Patrick Suren
eGFP-NLRC5 isoform 3	NLRC5 isoform 3; aa 1 - 720	eGFP	pcDNA5 FRT/TO	Patrick Suren
eGFP-NLRC5 NLS I	NLRC5; aa 1 – 1866 mutations: RRK132/133/134 A	eGFP	pcDNA5 FRT/TO	Patrick Suren
eGFP-NLRP11	NLRP11	eGFP	pcDNA3.1	This work
FLAG-IKK ϵ	IKK ϵ	FLAG	pcDNA3.1	Kindly provided by E. F. Meurs
FLAG-TBK1	TBK1	FLAG	pcDNA3	Kindly provided by Kate Fitzgerald
HA-p62	p62	HA	pcDNA4/TO	(Fan <i>et al.</i> 2010)
Isoform3-BioID2-HA	BioID2 C-terminal of NLRC5 isoform 3; aa 1 – 720	HA	MCS-BioID2-HA	This work
LRR-BioID2-HA	BioID2 C-terminal of NLRC5 LRR; aa 550 – 1866	HA	MCS-BioID2-HA	This work

Material and Methods

MCS-BioID2-HA	BioID2	HA	pcDNA3.1	(Kim <i>et al.</i> 2016)
Myc-DDX3X	DDX3X	myc	pCMV-Myc	(Schröder <i>et al.</i> 2008)
Myc-DDX3X 4A	DDX3X; mutations: S71/82/83/102A	myc	pCMV-Myc	(Gu <i>et al.</i> 2013)
Myc-DDX3X S102A	DDX3X; mutations: S102A	myc	pCMV-Myc	(Gu <i>et al.</i> 2013)
Myc-BioID2-DD	BioID2 N-terminal of NLRC5 DD; aa 1 – 139	myc	Myc-BioID2-MCS	This work
myc-BioID2-isoform3	BioID2 N-terminal of NLRC5 isoform 3; aa 1 -720	myc	Myc-BioID2-MCS	This work
Myc-BioID2-MCS	BioID2	myc	pcDNA3.1	(Kim <i>et al.</i> 2016)
Myc-NLRC5	NLRC5; aa 1 – 1866	myc	pcDNA3.1-3xmyc-B	(Neerinx <i>et al.</i> 2012)
Myc-NLRC5 DD	NLRC5; aa 1 – 133	myc	pcDNA3.1-3xmyc-B	(Neerinx <i>et al.</i> 2012)
Myc-NLRC5 ΔDD	NLRC5; aa 134 – 1866	myc	pcDNA3.1-3xmyc-B	(Neerinx <i>et al.</i> 2012)
Myc-NLRC5 isoform 3	NLRC5 isoform 3; aa 1 - 720	myc	pcDNA3.1-3xmyc-B	(Neerinx <i>et al.</i> 2012)
Myc-NLRP3	NLRP3	myc	pcDNA3.1-3xmyc-B	Roland Wagner
Myc-NLRP11	NLRP11; aa 1 – 1033	myc	pcDNA3.1-3xmyc-B	(Ellwanger <i>et al.</i> 2018)
Myc-NLRP11 ΔPYD	NLRP11; aa 125 – 1033	myc	pcDNA3.1-3xmyc-B	(Ellwanger <i>et al.</i> 2018)
Myc-NLRP11 LRR	NLRP11 aa 518 - 1033	myc	pcDNA3.1-3xmyc-B	(Ellwanger <i>et al.</i> 2018)
Myc-NLRP11 NACHT	NLRP11 aa 125 – 523	myc	pcDNA3.1-3xmyc-B	(Ellwanger <i>et al.</i> 2018)
Myc-NLRP11 PYD	NLRP11; aa 1 – 128	myc	pcDNA3.1-3xmyc-B	(Ellwanger <i>et al.</i> 2018)
MyD88	MyD88; aa 13 – 296	none	pEX145	Kindly provided by Alex Weber
NLRP11	NLRP11	none	pcDNA3.1	(Ellwanger <i>et al.</i> 2018)
NLRP11-eGFP	NLRP11 aa 1 – 1033	eGFP	pcDNA5 FRT/TO	This work
pcDNA3.1	none	none	pcDNA3.1	Invitrogen
pcDNA5 FRT/TO	none	none	pcDNA5 FRT/TO	ThermoFisher
pcDNA5 FRT/TO DD-BioID2-HA	BioID2 C-terminal of NLRC5 DD; aa 1 – 139	HA	pcDNA5 FRT/TO	This work
pcDNA5 FRT/TO MCS-BioID2-HA	BioID2	HA	pcDNA5 FRT/TO	This work
pcDNA5 FRT/TO NLRP11-eGFP	NLRP11	eGFP	pcDNA5 FRT/TO	This work
pCMV Tag2B FLAG-Sin3A	Sin3A	FLAG	pCMV Tag2B	This work
pOG44	Flp recombinase	none	pOG44	ThermoFisher

Material and Methods

Recombinant expression				
Codon optimized NLRC5	Human NLRC5 codon optimized for expression in <i>E. coli</i>	none	pBSK	Epoch life science
pLicE codon opt. NLRC5	Codon optimized NLRC5; aa 1 – 1866	6xHis-TrxA	pLicE	This work
pLicE codon opt. NLRC5 DD	Codon optimized NLRC5; aa 1 – 139	6xHis-TrxA	pLicE	This work
pLicE codon opt. NLRC5 isoform 3	Codon optimized NLRC5; aa 1 – 720	6xHis-TrxA	pLicE	This work
pLicE codon opt. NLRC5 LRR	Codon optimized NLRC5; aa 588 – 1866	6xHis-TrxA	pLicE	This work
Reporter plasmids				
H2K	Luciferase under the control of the murine H2-K promoter	none	pGL3 min	(Ludigs <i>et al.</i> 2015)
H2E	Luciferase under the control of the murine H2-E promoter	none	pGL3 min	(Ludigs <i>et al.</i> 2015)
HLA B250	Luciferase under the control of the HLA B250 promoter	none	pGL3	(Gobin <i>et al.</i> 1997)
HLA DRA	Luciferase under the control of the HLA DRA promoter	none	pGL3	(Gobin <i>et al.</i> 1997)
IFN β -luciferase	125 bp fragment of the promoter of IFN β with two ISRE sites, one NF- κ B site and an Jun/IRF2 site	none	/	Kindly provided by AG Bowie
MHC Hybrid 1	Luciferase under the control of the murine H2-E S box and the H2-K X and Y boxes.	none	pGL3 min	(Ludigs <i>et al.</i> 2015)
MHC Hybrid 2	Luciferase under the control of the murine H2-E X box and the H2-K S and Y boxes.	none	pGL3 min	(Ludigs <i>et al.</i> 2015)
MHC Hybrid 3	Luciferase under the control of the murine H2-E Y box and the H2-K S and X boxes.	none	pGL3 min	(Ludigs <i>et al.</i> 2015)
MHC Hybrid 4	Luciferase under the control of the murine H2-K S box and the H2-E X and Y boxes.	none	pGL3 min	(Ludigs <i>et al.</i> 2015)
MHC Hybrid 5	Luciferase under the control of the murine H2-K X box and the H2-E S and Y boxes.	none	pGL3 min	(Ludigs <i>et al.</i> 2015)
MHC Hybrid 6	Luciferase under the control of the murine H2-K Y box and the H2-E S and X boxes.	none	pGL3 min	(Ludigs <i>et al.</i> 2015)

Material and Methods

NF- κ B	3x immunoglobulin κ chain enhancer κ B site upstream of the conalbumin promoter followed by the luciferase gene	none	p(Ig κ)3-conaluc	(Muñoz <i>et al.</i> 1994)
pGL3 min	none	none	pGL3 min	(Ludigs <i>et al.</i> 2015)
pIG-Luc	Fusion protein of pro-IL-1 β and luciferase of <i>Gaussia princeps</i>	none	pEFBOS	(Bartok <i>et al.</i> 2013)

2.1.5 Oligonucleotides

All oligonucleotides for this study were obtained from Eurofins Genomics.

Table 4: **Oligonucleotides used for Endpoint PCR, Cloning and Sequencing in this study.** Overhang regions of primers used for cloning are depicted in lower case letters, binding regions in uppercase letters.

Primer	Application	Primer #	Sequence
Endpoint PCR			
DDDX3X fwd	Endpoint PCR to detect expression of human DDX3X	935	TGC TGG CCT AGA CCT GAA CT
DDDX3X rev		936	TTG ATC CAC TTC CAC GAT CA
GAPDH fwd	Endpoint PCR to detect expression of human GAPDH	1	GGT ATC GTG GAA GGA CTC ATG AC
GAPDH rev		2	ATG CCA GTG AGC TTC CCG TTC AG
NLRP11 fwd	Endpoint PCR to detect expression of human NLRP11	779	GTT CAC CTC ACT GCT CAC GA
NLRP11 rev		780	CGC TTC AGG ACA GTA CAC GT
Cloning			
eGFP fwd KpnI	PCR of eGFP for generation of NLRP11-eGFP and NLRP11-eGFP	810	gcg cgg tac cAT GGT GAG CAA GGG CGA GG
eGFP rev BamhI		811	gcg cgg atc cCT TGT ACA GCT CGT CCA TGC
PYD-NLRP11 fwd	PCR of NLRP11 for generation of NLRP11-eGFP	686	gcg cgg tac cTA TGG CAG AAT CGG ATT CTA CTG ACT T
NLRP11-rev + AgeI		809	atg cac cgg tGG AAG GGG TTG CCT AGA TGC TGT A
GFP-DDX3 fwd	Cloning eGFP-DDX3X	970	gca taa gct tcG AGT CAT GTG GCA GTG GAA AAT G
GFP-DDX3 rev		971	cgT aga att cTC AGT TAC CCC ACC AGT CAA C
DDX3-GFP fwd	Cloning of DDX3X-eGFP	972	cgT aga att cTC AGT TAC CCC ACC AGT CAA C
DDX3-GFP rev		973	gca tcc cgg gAT GAG TCA TGT GGC AGT GGA AA
hSin3A_fw	Cloning of FLAG-Sin3A	729	gcg cgt cga cAA GCG GCG TTT GGA TGA CC
hSin3A_rev		728	gcg cct cga gTT AAG GGG CTT TGA ATA CTG TG
myc-BioID2-DD fw	Cloning of NLRC5 DD into myc-BioID2 vector (Addgene #74223)	711	gcg cct cga ggg agg cgg agg cag tAT GGA CCC CGT TGG CCT C
myc-BioID2-DD rv		712	gcg cga tat ctc aCT GCT TCT TGC ACT GCT TCC

Material and Methods

DD-BioID2-HA fw	Cloning of NLRC5 DD into BioID2-HA	717	gcg cgc tag cAT GGA CCC CGT TGG CCT C
DD-BioID2-HA rv	vector (Addgene #74224)	718	gcg cac egg tGC TGC TTC TTG CAC TGC TTC C
myc-BioID2-iso 3 fw	Cloning of NLRC5 isoform 3 into myc-BioID2 vector	715	gcg cct cga ggg agg egg agg cag tAT GGA CCC CGT TGG CCTC
myc-BioID2-iso 3 rv	(Addgene #74223)	716	gcg cga tat ctc ACC CCA GCA TCT GCA GC
iso 3-BioID2-HA fw	Cloning of NLRC5 isoform 3 into BioID2-HA vector	721	gcg cgc tag cAT GGA CCC CGT TGG CCT C
iso 3-BioID2-HA rv	(Addgene #74224)	722	gcg cac egg tcT CCT GCT AAC CCC AGC ATC T
LRR-BioID2-HA fw	Cloning of NLRC5 LRR into BioID2-HA vector	719	gcg cgc tag cAT GAC CAA AAG CTA GAC TGG GCC T
LRR-BioID2-HA rv	(Addgene #74224)	720	gcg cac egg tcA GTA CCC CAA GGG GCC TG
fwd DD-BioID2-HA	Cloning of DD-BioID2-HA from pcDNA3.1 into pcDNA5 FRT/TO	736	Gca tcc egg ggc cac cAT GGA CCC CGT TGG CCT C
rev DD-BioID2-HA		737	atg cct cga GCT ATG CGT AAT CCG GTA CAT C
fwd BioID2-HA empty	Cloning of BioID2-HA from pcDNA3.1 into pcDNA5	738	gca tcc egg ggc cac cat gTT CAA GAA CCT GAT CTG GCT G
rev BioID2-HA empty	FRT/TO	737	atg cct cga gCT ATG CGT AAT CCG GTA CAT C

Sequencing

BGH Reverse	Plasmid Sequencing;	---	TAGAAGGCACAGTCGAAG
CMV-F	GATC standard	---	CGCAAATGGGCGGTAGGCGTG
T7	primer	---	TAATACGACTCACTATAGGG
NLRP11_Seq1	Sequencing	670	CCTCATCTCTCAAGGCC
NLRP11_Seq2	NLRP11;	671	CTTATTTGGCATGTGGGTC
Seq NLRC5(E.Coli)_1	Sequencing codon optimized NLRC5	939	ACGTCTGCTGACCAAAGACC
Seq NLRC5(E.Coli)_2		940	GACGTTAAGGTTGAGGATGG
Seq NLRC5(E.Coli)_3		941	GAATACGTTAACCACCTTCTTCTCC
Seq NLRC5(E.Coli)_4		942	TGGTGCTAAACAGGCTGCTGTG
Seq NLRC5(E.Coli)_5		943	ACTGGTCCGAAAGTAGTAGAAC
Seq NLRC5(E.Coli)_6		944	AGGAGTCCGATGGTCAGCGTAAAG
Seq NLRC5(E.Coli)_7		945	TGGTACGCTGTTTCTCTACTCTGC
Seq NLRC5(E.Coli)_8		946	GCTGGACCTGTCTCATAACTC
Seq NLRC5(E.Coli)_9		947	TTTCGTCTGACCTCCTCCTG
Seq NLRC5(E.Coli)_10		948	TGAATCCCTGGTTCTGTGCC
Seq_NLRC5_1	Sequencing human NLRC5	97	GGCAGCCCCACGCCTTC
Seq_NLRC5_2		98	CAATGGGACCCTCCTGCCTG
Seq_NLRC5_3		99	CACAGGCCCTGGGCACCAG
Seq_NLRC5_4		100	CTGGATTTTGATGGCTGTCCCCTG
Seq_NLRC5_5		101	GTGACGGCCAGAGGAAAGGG
Seq_NLRC5_6		102	GAAGCTGCCACCTCGGTCAC
Seq_NLRC5_7		103	GCTGCAGCTGAGCCAGACGG
Seq_NLRC5_8		104	CTCCGGCCAGAGCACGTGTC
Seq_NLRC5_9		105	CTGAAGACATTTTCGGCTGACCTCCAG
Seq_NLRC5_10		106	GATGCTTGGCTGCAATGCCCTG

Material and Methods

 Table 5: **Oligonucleotides used for Gibson assembly.** Overhang regions of primers used for cloning are depicted in lower case letters, binding regions in uppercase letters. Bdg: binding. Tm: melting temperature.

Primer name	Length		T _m		Sequence
	total	bdg.	total	bdg.	
DD fwd Ligation Site 1 (Pair 1)	40	19	68	58	aac ctg tac ttc caa tcc aat GAC CCA GTA GGT CTG CAA C
DD rev Ligation Site 2 (Pair 2)	43	23	66	58	cgt tat cca ctt cca att taT TGT TTC TTA CAC TGC TTG CGA C
Backbone DD rev Ligation Site 1 (Pair 1)	40	22	68	57	gca gac cta ctg ggt cat tgg ATT GGA AGT ACA GGT TCT C
Backbone DD fwd Ligation Site 2 (Pair 2)	42	23	67	60	gca gtg taa gaa aca ata aAT TGG AAG TGG ATA ACG GAT CCG
LRR fwd Ligation Site 1 (Pair 3)	40	19	69	60	aac ctg tac ttc caa tcc aat GGT GCT AAA CAG GCT GCT G
LRR rev Ligation Site 2 (Pair 4)	40	19	69	59	gat ccg tta tcc act tcc aat TTA AGT ACC CCA CGG TGC C
Backbone LRR rev Ligation Site 1 (Pair 3)	40	24	67	57	cag cct gtt tag cac cAT TGG ATT GGA AGT ACA GGT TCT C
Backbone LRR fwd Ligation Site 2 (Pair 4)	40	23	68	59	cac cgt ggg gta ctt aaA TTG GAA GTG GAT AAC GGA TCC G
iso 3 fwd Ligation Site 1 (Pair 5)	40	19	68	58	aac ctg tac ttc caa tcc aat GAC CCA GTA GGT CTG CAA C
iso 3 rev Ligation Site 2 (Pair 6)	40	17	69	56	cgg atc cgt tat cca ctt cca att taA CCC AGC ATC TGC AGA C
Backbone iso 3 rev Ligation Site 1 (Pair 5)	40	24	68	57	gca gac cta ctg ggt cat tgg ATT GGA AGT ACA GGT TCT C
Backbone iso 3 fwd Ligation Site 2 (Pair 6)	40	23	69	60	gtc tgc aga tgc tgg gtt aaA TTG GAA GTG GAT AAC GGA TCC G
hNLRC5 fwd in FastBAC Ligation Site 1 (Pair 7)	40	19	74	64	gat gac gat gac aaa gga tcc GAC CCC GTT GGC CTC CAG C
hNLRC5 rev in FastBAC Ligation Site 2 (Pair 8)	35	21	75	63	ccg cgc gct tgc gac cgT CAA GTA CCC CAA GGG GCC TG
hNLRC5 in FastBAC Backbone rev Ligation Site 1 (Pair 7)	39	26	74	63	agg cca acg ggg tcG GAT CCT TTG TCA TCG TCA TCG CTG C
hNLRC5 in FastBAC Backbone fwd Ligation Site 2 (Pair 8)	33	16	75	64	ggc ccc ttg ggg tac ttg aCG GTC CGA AGC GCG CG

2.1.6 siRNAs

Table 6: Small interfering RNAs (siRNAs) used for the knockdown of protein expression in mammalian cells.

siRNA	Target	Sequence	Manufacturer
Allstar Negative	Non-targeting	proprietary	Qiagen
siNELFB_5	NELFB	CGT GGT GAT GTG CGT CAT GAA	Qiagen
siNELFB_6	NELFB	CTG GGA CAT GAT CGA CAG CCA	Qiagen
siNELFB_7	NELFB	AAG GTA CAA GAA GCT GGA AGA	Qiagen
siNELFB_8	NELFB	CCG GAC CTT GCC CAC CAT CCA	Qiagen
siNLRP11_6	NLRP11	CACGACCTTGACGCTGTCGAA	Qiagen
siSin3A_5	Sin3A	GAG CGT GTA AGC AAG CGT CTA	Qiagen
siSin3A_6	Sin3A	ATC CGG GTT CTG GAA GCA ATA	Qiagen

2.1.7 Antibodies

Primary antibodies

Table 7: Primary antibodies used in this study. WB: Western Blot; IF: Indirect immunofluorescence staining.

Name	Target	Species	Use	Manufacturer/Reference
C4; sc-47778	Actin	Mouse, monoclonal	WB	Santa Cruz Biotechnology
4642	AIF	Rabbit, polyclonal	IF	Cell Signaling Technologies
A300-474A	DDX3X	Rabbit, polyclonal	WB, IF	Bethyl Laboratories
M2; F1804	FLAG	Mouse, monoclonal	WB	Sigma-Aldrich
11814460001	GFP	Mouse, monoclonal	WB	Roche
Y-11; sc-805	HA	Rabbit, polyclonal	WB, IF	Santa Cruz Biotechnology
/	HLA B/C	Mouse monoclonal	WB	Kind gift of Victor Steimle
9E10; M4439	myc	Mouse	WB, IF	Sigma-Aldrich
3H8	NLRC5	Rat	WB	(Neerincx <i>et al.</i> 2010)
D6O1M; #29047	pIRF3 (Ser396)	Rabbit, monoclonal	WB	Cell Signaling Technologies
K-20, sc-994	Sin3A	Rabbit, polyclonal	WB	Santa Cruz Biotechnology

Secondary Antibodies

Table 8: Secondary antibodies used in this study.

Antibody	Manufacturer
Immunoblot	
Goat anti mouse HRP	Jackson ImmunoResearch
Goat anti rabbit HRP	Jackson ImmunoResearch
Goat anti rat HRP	Jackson ImmunoResearch
Immunofluorescence	
Goat anti mouse Alexa Fluor 405	Molecular Probes
Goat anti rabbit Alexa Fluor 488	Molecular Probes
Goat anti rabbit Alexa Fluor 488	Molecular Probes

2.1.8 Instruments

Table 9: Instruments used in this study.

Name	Manufacturer
DMi8	Leica
Orca Flash	Hamamatsu
Eclipse Ts 100	Nikon
Enspire Multimode Plate Reader	Perkin Elmer
Power Pac HC	BioRAD
Fusion FX	Vilber
T100 Thermal Cycler	BioRAD
Cfx Connect Real-Time PCR Detection System	BioRAD
Hera Cell 150i CO ₂ Incubator	ThermoFisher
Inolab pH 7110	WTW
Mini Protean Tetra System	BioRAD
Nanophotometer p360	Implen
Trans-Blot Turbo Transfer System	BioRAD

2.1.9 Software

Table 10: Software used for data analysis in this study.

Name	Version	Company
Adobe Illustrator	2020	Adobe
Cfx Manager	3.1	BioRAD
Las X	3.7.4	Leica
Graphpad Prism	7.05	GraphPad Software, Inc
Microsoft Office	365	Microsoft
Interactivevenn.net	May 2021	(Heberle <i>et al.</i> 2015)
Snapgene	4.2	GSL Biotech
Cytoscape	3.8.2	(Shannon <i>et al.</i> 2003)
Cytoscape String App	1.6.0	(Doncheva <i>et al.</i> 2019)

2.2 Methods

2.2.1 Cell biological methods

Reporter gene assays

HEK293T cells were seeded at a density of 30,000 cells per well of a 96 well plate and transiently transfected, using X-tremeGENE 9 transfection reagent (Roche), with a total of 51 ng of DNA. 8.6 ng β -galactosidase plasmid, 13 ng of the respective reporter plasmid, and the indicated amounts of plasmids (Table 3) were added up with pcDNA3.1 empty vector to constant DNA levels. Cells were lysed 24 h post transfection in 100 μ l lysis buffer (25 mM Tris pH 8.0, 8 mM MgCl₂, 1% Triton X-100, 15% glycerol) for 30 min at room temperature (RT). 50 μ l of the lysates were transferred into a non-transparent 96 well plate and luciferase activity was measured, in a multiplate reader (Enspire, PerkinElmer LifeSciences), as relative light units (RLU) 2 sec post automatic dispersion of 100 μ l substrate solution (1,3 μ M ATP, 770 ng/ml D-luciferin in lysis buffer) per well. 100 μ l of 1 mg/ml o-Nitrophenyl- β -D-galactopyranoside (ONPG) (in 60 mM Na₂HPO₄, 40 mM NaH₂PO₄, 10 mM KCl, 1 mM MgSO₄, pH 7.0) were added to the remaining 50 μ l cell lysate and incubated at 37°C until yellow color had developed. Absorption was measured at 405 nm against 620 nm reference wavelength as β -galactosidase activity. RLU was normalized (nRLU) to β -galactosidase activity. All assays were performed in technical triplicates.

Caspase activation reporter gene assays

For iGLuc caspase-1 reporter assays, HEK293T cells were seeded in a 96 well plate at a density of 35,000 cells per well and transiently transfected, using Xtreme Gene 9 transfection reagent, with 8.6 ng β -galactosidase plasmid, 42 ng of the iGLuc reporter plasmid (Bartok *et al.* 2013), and expression plasmids of NLRP3, NLRP11, ASC, caspase-1, DDX3X, DDX3X S102A, or DDX3X 4A (Table 3) as indicated. 20 h after transfection, cells were stimulated with 15 μ M nigericin (InvivoGen) for 3 h. Cells were then lysed in 100 μ l passive lysis buffer (Promega) per well. 50 μ l of the cell lysate were transferred into a non-transparent 96 well plate. Luciferase activity was measured after addition of 100 μ l of 3.33 μ M Coelenterazine (Carl Roth) (in ddH₂O) per well. 100 μ l of 1 mg/ml ONPG (in 60 mM Na₂HPO₄, 40 mM NaH₂PO₄, 10 mM KCl and 1 mM MgSO₄) were added to the remaining 50 μ l lysate, incubated at 37°C until yellow color had developed. Absorption was measured at 405 nm (620 nm reference) as β -galactosidase activity. Luciferase activity was normalized to β -galactosidase activity. All assays were performed in technical triplicates.

Transient DNA transfection

Transient transfection of plasmid DNA (Table 3) in adherent cells was performed using Lipofectamin 2000 (ThermoFisher). Adherent cells were seeded in DMEM containing FBS and Pen/Strep at 50 – 70 % cell density at least 4 h prior to transfection. Plasmid dilutions were prepared in an appropriate volume of OptiMEM (ThermoFisher) and the transfection reagent was added in a ratio

Material and Methods

of 1:2.5 ($\mu\text{g DNA}:\mu\text{l transfection reagent}$). The transfection mixtures were then incubated for 20 min at RT for the formation of transfection complexes. Right before transfection of the cells, the medium was replaced with fresh DMEM containing FBS and Pen/Strep.

Stimulation and infection of cells

For viral infection, cells were incubated with 160 hemagglutination units (HAU) of Sendai virus (SeV) (Cantell Strain in allantoic fluid, Charles River).

For the activation of the NLRP3 inflammasome in THP-1 cells, 100,000 cells were seeded in wells of 24 well plates and differentiated with 100 nM PMA for 16 h. Medium was changed, and cells were treated according to experimental setup. Cells were then stimulated with 100 ng/ml LPS (InvivoGen) for 4 h, followed by stimulation with 10 μM nigericin for 2 h.

For activation of NF- κB -signaling by TNF α , HEK293T cells were seeded and transfected according to the corresponding experimental procedure and stimulated with 10 ng/ml TNF α (InvivoGen) overnight.

For the inhibition of protein neo-synthesis, cells were seeded and treated according to the experimental procedure. Cells were then treated with 30 $\mu\text{g/ml}$ cycloheximide for up to 6 h.

siRNA transfection

THP-1 and THP-1shDDX3X cells were differentiated with 100 nM PMA for 16 h. Medium was changed, and cells rested for 24 h prior to siRNA-mediated knockdown with 100 nM siRNA (Table 6), transfected using HiPerFect transfection reagent (Qiagen) according to (Neerinx *et al.* 2010). AllStars negative control siRNA and siNLRP11_6 (Qiagen) (Ellwanger *et al.* 2018) were used. Knockdown of NLRP11 was performed for 72 h. For double knockdown of NLRP11 and DDX3X, 24 h after transfection of the siRNA, THP-1 shDDX3X cells were induced with 1 $\mu\text{g/ml}$ doxycycline for 48 h.

Knockdown efficiency of NLRP11 was monitored with endpoint PCR as described in (Ellwanger *et al.* 2018). Knockdown of DDX3X was monitored by end-point PCR.

For knockdown in HEK293T and HeLa cells, cells were seeded in serum free media according to experimental procedure, and directly transfected with 20 nM siRNA (Table 6), using HiPerFect transfection reagent. Cells were incubated for 6 h with the siRNA mixture, before one volume of complete media was added. The medium was replaced the next day and cells were incubated for 48 h before experiments were conducted.

HEK-IFN- α/β reporter assay (QuantiBlue)

Detection of type I interferons was performed using HEK Blue IFN- α/β cells (InvivoGen). HEK Blue IFN- α/β cells were seeded at a density of 50,000 cells in 96 well plates, stimulated for 20 h with the supernatant of SeV infected cells and SEAP activity in the supernatant of HEK Blue IFN- α/β cells was measured by QuantiBlue solution (InvivoGen) according to the manufacturer's protocol.

Generation of stable FlpIn cell lines

Stable, inducible cell lines expressing NLRP11-eGFP in HEK293 Flp-In T-REx (Invitrogen/ThermoFisher) and HeLa FlpIn T-REx (kindly provided by the Hentze Lab, EMBL Heidelberg) background and eGFP-NLRC5, eGFP-NLRC5 isoform 3, eGFP-NLRC5 2xNLS and eGFP NLS I in HeLa FlpIn T-REx cells, were generated by co-transfection of pOG44 and the corresponding pcDNA5/FRT/TO-gene of interest plasmid (Table 3) at 9:1 ratio using Lipofectamin 2000. Successful insertion at the Flp recombinase site was selected by incubation with 10 µg/ml blasticidin and either 100 µg/ml (HEK293) or 600 µg/ml (HeLa) hygromycin B and single clones were isolated. Expression was induced by 1 µg/ml doxycycline for at least 16 h prior to all experiments. All cell culture media were supplemented with Pen/Strep.

K562 FlpIn BioID2-HA and DD-BioID2-HA cells were transfected analogous and transferred to semi-solid, methylcellulose-based ClonaCell™-TCS medium (StemCell Technologies) 3 days post transfection, to ensure survival of monoclonal populations. Selection was carried out with 10 µg/ml blasticidin and 200 µg/ml hygromycin B.

Transformation of chemically competent bacteria

For amplification of mammalian expression plasmids (Table 3) 0.5 – 10 µl low concentration plasmid solution and 25 or 50 µl chemically competent *E. coli* DH5α were mixed gently and incubated on ice for 30 min. Heat shock was performed at 42°C for 30 sec and bacteria were placed on ice immediately afterwards for 5 minutes. 1 ml LB medium without antibiotics was added to the bacteria and they were incubated at 37°C for 1 h under constant shaking at 180 rounds per minute (rpm), before an appropriate volume was plated on LB-agar, containing the appropriate selection-antibiotic and grown overnight.

Transformation of electrocompetent bacteria

For bacterial expression of recombinant proteins, electrocompetent bacteria were thawed on ice, transferred into an electroporation cuvette (Biozym) and mixed with 1 µl containing 100 ng plasmid DNA (Table 3). Cells were pulsed for 1 second (sec) in an AMAXA BIOSYSTEMS Nucleofactor I (program bacteria 3). 1 ml of prewarmed, antibiotic-free LB medium was added, cells were transferred into a fresh, sterile 1.5 ml reaction tube and incubated at 37°C for 1 h under constant shaking. An appropriate volume of cell suspension was then plated onto LB-agar plates, containing the appropriate selection-antibiotics, and grown overnight.

Recombinant expression of NLRC5 constructs in *E. coli*

Transformed bacteria were grown overnight, diluted to an OD₆₀₀ of 0.3 and induced for 22 h with 0.5 M IPTG (Gerbu Biotechnik). After determination of the OD, equal numbers of cells were spun down, and either lysed with FastBreak Cell Lysis Reagent (Promega) in fresh LB, cleared of debris by centrifugation and denatured with Laemmli sodium dodecyl sulfate (SDS) buffer (7 ml Tris pH 6.8,

containing 0.4% SDS, 3 ml glycerol, 1 g SDS, bromphenole blue, 60 mM β -mercaptoethanol), or lysed directly in Laemmli buffer.

Large scale expression and purification of recombinant NLRC5 DD in *E. coli*

A total of 400 ml overnight cultures of *E. coli* BL21 (DE3) transformed with pLicE NLRC5 DD were grown at 37°C in LB medium containing 100 μ g/ml ampicillin (LB-Amp) and were then completely used to inoculate 2 L of LB Amp. These cultures were grown at 20°C for 2 h before induction of protein expression with 0.5 M IPTG. After growth overnight, bacterial cells were spun down (8,000 x g, 15 min, 4°C) and pellets were resuspended in lysis buffer (25 mM HEPES pH 8.0, 500 mM NaCl) and processed 2 times at 30 kPsi and 40 kPsi, respectively, in a French press. Lysates were cleared by centrifugation (30,000 x g, 15 min 4°C) and subsequently loaded at 4 ml/min onto a HisTrap HP 5 ml column (GE Healthcare), equilibrated according to manufacturer's instructions. Elution was performed by FPLC with a gradient of elution buffer (25 mM HEPES pH 8.0, 150 mM NaCl, 500 mM Imidazole), and fractions as well as the flow through were collected. After SDS-PAGE and Coomassie staining, protein-containing fractions were pooled, and protein concentration was determined by measurement of A_{280} . 1 mg TEV protease was added to the protein solution which was then dialyzed against dialysis buffer (25 mM HEPES pH 8.0, 150 mM NaCl) overnight in SnakeSkin™ Dialysis Tubing, 3.5K MWCO, 35 mm (ThermoFisher). Subsequently the solution was cleared from any precipitate by centrifugation (30,000 x g, 15 min 4°C) and loaded onto a HiTRAP 5 ml FF column (GE Healthcare), prepared according to manufacturer's instructions. Flowthrough and fractions were collected and subjected to SDS-PAGE on a 12% polyacrylamide gel. DD containing fractions were pooled and dialyzed for 3 h at 4°C against 2 L of Ion exchange buffer A (25 mM HEPES pH 8.0). The salt free samples were concentrated by repeated centrifugation (4,000 x g, 10 min,) in an Amicon Ultracentrifuge filter with a pore size of 3.5 kDa (Merck Millipore), until the sample was reduced to a volume of 4 ml. Subsequently the sample was loaded onto a MonoQ 5/50 GL column (Sigma-Aldrich) and run with a gradient from 0 – 100% Ion exchange buffer B (25 mM HEPES pH 8.0, 1 M NaCl). Fractions of 1 ml, or 0.5 ml were collected. And analyzed by SDS-PAGE. DD containing fractions were combined and protein concentration was determined by measuring A_{280} . All buffers were filtered (0.22 μ m) and degassed prior to use.

2.2.2 Molecular methods

Polymerase chain reaction

Cloning

For the generation of expression plasmids, the desired inserts were amplified, either from sequenced plasmids (Table 3), or from genomic DNA, by polymerase chain reaction (PCR) according to the following setup (Table 11). Oligonucleotides (Table 4) were designed with an overhang, containing the desired restriction site for restriction enzyme digest and a four-nucleotide overhang. Additionally, when

Material and Methods

necessary, start- (ATG) or stop-codons (TAA, TAG, or TGA) were inserted in frame with the desired insert. Further, a Kozak consensus sequence (ACCATGG) was inserted between the restriction site and the start-codon of the gene of interest. PCR products were cleaned up using the NucleoSpin Gel and PCR Clean-up, Mini kit (Macherey-Nagel), according to manufacturer's instructions.

For Gibson assembly, oligonucleotides (Table 5) were designed and tested *in silico* using the SnapGene Software. DNA was amplified by PCR according to following setup (Table 11). Amplification products were run on a 0.5% agarose gel and cut out bands were purified using the NucleoSpin Gel and PCR Clean-up, Mini kit, according to manufacturer's instructions.

DNA concentration and purity in eluates was determined by nanodrop photometry.

Table 11: **Amplification of DNA for cloning**; Composition of PCR reaction and PCR protocol.

Reagent	Volume	Temperature	Time	Cycles
Template DNA (10 ng/ml)	1 μ l	98°C	2 min	1x
2x Phusion Mastermix (NEB)	15 μ l	98°C	10 sec	
fwd primer	0.6 μ l	57 - 63°C	20 sec	8x
rev primer	0.6 μ l	72°C	30 sec per kbp	
H ₂ O	12.8 μ l	98°C	10 sec	
		72°C	30 sec per kbp	15x
		72°C	10 min	1x

Endpoint PCR

Confirmation of siRNA- or shRNA-mediated knockdowns was performed by endpoint reverse transcription PCR using following protocol (Table 12). The PCR products were analyzed on a 1 – 2% agarose gel.

Table 12: **Endpoint RT PCR composition of PCR reaction and amplification protocol.**

Reagent	Volume	Temperature	Time	Cycles
cDNA	50-200 ng	98°C	2 min	1x
Go-Taq Puffer (5x)	5 μ l	98°C	10 sec	20-40 x
MgCl ₂ (25 Mm)	4 μ l	57 - 63°C	20 sec	depending of target gene
dNTPs (10 Mm)	2 μ l	72°C	20 sec	
fwd primer	0.6 μ l	72°C	5 min	1x
rev primer	0.6 μ l			
H ₂ O	Ad 25 μ l			

Sanger sequencing

Insert sequence of newly acquired, or generated plasmids was verified by Sanger sequencing. Sequencing was performed by GATC, respectively Eurofins Genomics.

cDNA synthesis

cDNA synthesis was performed with the iScript cDNA synthesis Kit (BioRad) according to the manufacturer's instructions. A total of 200 – 1000 ng of RNA was transcribed per reaction.

Restriction digestion of plasmid DNA

Restriction enzyme digest was performed with the selected restriction enzyme and its recommended buffer (ThermoFisher) according to the manufacturer's instructions. Double digests were performed, whenever possible, according to the Thermo Fisher DoubleDigest Calculator (<https://www.thermofisher.com/de/de/home/brands/thermo-scientific/molecular-biology/thermo-scientific-restriction-modifying-enzymes/restriction-enzymes-thermo-scientific/double-digest-calculator-thermo-scientific.html>).

Ligation of DNA fragments

Digested DNA fragments were ligated using 1 µl T4 DNA ligase (ThermoFisher), 2 µl T4 Ligation buffer (10x; ThermoFisher), vector and insert in a molar ratio of 1:5 to 1:9 in a total volume of 20 µl. The reactions were either incubated at 37°C for 20 min, or at RT for 1 h.

Ligation of DNA fragments by Gibson assembly was performed at a molar ratio of 1:2 (vector:insert) using the Gibson Assembly® Master Mix (New England Biolabs; E2611) according to manufacturer's instructions.

Isolation of plasmid DNA from bacteria

Plasmid DNA from transformed *E. coli* DH5α was isolated, using either NucleoBond Xtra Midi kit for transfection-grade plasmid DNA, or the NucleoSpin Plasmid, Mini kit for plasmid DNA (Macherey-Nagel) according to manufacturer's instructions.

Generation of chemically competent bacteria

Bacteria were grown at 37°C in 5 ml LB medium for at least 6 – 10 h. 1 ml of the bacterial culture was used to inoculate 250 ml fresh LB medium and grown at 20°C overnight until an OD₆₀₀ between 0.33 and 0.36 was reached. When the desired OD₆₀₀ was reached, the culture was chilled in an ice-bath for 10 min before cells were pelleted by centrifugation at 4°C. Bacterial pellets were washed once in a total volume of 200 ml sterile filtered, ice cold Transformation buffer (15 mM CaCl₂, 250 mM KCl, 10 mM PIPES, 55 mM MnCl₂, pH 6.4), pelleted again and then resuspended in a total volume of 20 ml ice-cold transformation buffer with 1.5 ml DMSO. 500 µl Aliquots were frozen in liquid nitrogen and stored at - 80°C until use.

Generation of electrocompetent bacteria

Bacteria were grown overnight in LB medium at 30°C before a 200 ml LB culture was inoculated at an OD₆₀₀ of 0.2. Cells were grown to an OD₆₀₀ of 0.6 and pelleted by centrifugation at 4°C. Pellets were resuspended twice in a total of 200 ml ice cold, sterile 10% glycerol by vortexing and spun down again.

After the second washing step, cells were resuspended in 1 ml of sterile, ice cold 10% glycerol, divided into 40 μ l aliquots and frozen in liquid nitrogen. Electrocompetent cells were stored until use at - 80°C.

RNA Isolation from mammalian cells

Isolation of mammalian RNA was performed with the RNeasy Plus Mini Kit (Quiagen) according to manufacturer's instruction. RNA concentration and purity were assessed by measurement of absorbance at 260 and 280 nm using a nanodrop photometer.

Agarose gel electrophoresis

To separate DNA fragments, agarose NEEO (CarlRoth) was dissolved in Tris-Acetic acid-EDTA (TAE) buffer (40 mM Tris, 20 mM acetic acid, 1 mM EDTA) at a concentration of 0.5 – 2 g/100 ml. DNA solution was mixed with DNA Gel Loading Dye (ThermoFisher) and GelRed (Carl Roth) and loaded onto the agarose gel. Separation was performed at a constant voltage of 90 V. DNA was visualized with UV light in the Vilber Fusion FX gel documentation system. Gene Ruler 100 bp, or GeneRuler 1 kb DNA ladder (ThermoFisher) were used as standards.

2.2.3 Biochemical methods

Indirect immunofluorescence microscopy (IF)

HEK293T cells were seeded at 100,000 cells per well on poly-L-lysine (Sigma-Aldrich) pretreated glass-coverslips and treated according to the experimental procedure. HeLa FlpIn cells were seeded into 24 well plates at a density of 75,000 cells per well on glass coverslips, HEK293 FlpIn cells at 100,000 cells per well on poly-L-lysine pretreated glass-coverslips and expression of eGFP or eGFP-NLRP11 was induced by 1 μ g/ml doxycycline. After overnight expression, cells were either infected with SeV for different durations, or directly fixed with 4% paraformaldehyde (PFA) in phosphate-buffered saline (PBS), permeabilized with 0.5% Triton X-100 and blocked with 5% FBS in PBS. Cells were then incubated with primary (**Table 7**) and secondary antibody (**Table 8**) sequentially. DNA was stained with Hoechst 33258 (Sigma-Aldrich). Slides were mounted in Mowiol 4-88 (Carl Roth). Images were captured with a Leica DMI8 microscope using a HCX PL FL L 40X/0.60 or a HC PL APO 63X/1.40-0.60 OIL objective and processed using the Leica LasX software and ImageJ. For 3D deconvolution, Z-stacks of 4.05 μ m depth were captured, with individual planes every 0.2 μ m. Blind 3D-deconvolution was performed using the Leica LasX software, performing 10 iterations at a refractive index of 1.52. For quantitative analysis, sample pictures were blinded and counted by eye.

SDS-PAGE and immunoblot

For immunoblot, proteins were separated by sodium dodecyl sulfate polyacrylamide gel electrophoresis (SDS-PAGE). For this, cells were harvested in Laemmli loading buffer containing β -mercaptoethanol and boiled for 5 min at 95°C. Samples were loaded onto 7.5%, 10% or 12% Tris-buffered SDS-Polyacrylamide gels and were run in running buffer (25 mM Tris, 192 mM glycine, 3.467 mM SDS in

Material and Methods

H₂O) between 80 and 180 V until the dye completely passed through the gel. For immunoblot, proteins were transferred from the gel to a nitrocellulose membrane (0.2 µm pore size) (Sigma-Aldrich) by semi-dry blot in transfer buffer (25 mM Tris, 192 mM glycine 20% methanol) using the Trans-Blot Turbo Transfer System (BioRad). Efficient and uniform transfer was confirmed by PonceauS staining (0.2% PonceauS, 3% Acetic acid in ddH₂O). Membranes were then washed in PBS-T (137 mM NaCl, 2.7 mM KCl, 8.1 mM Na₂HPO₄, 1.47 mM KH₂PO₄, 0.05% Tween-20), and blocked in Roche blocking solution (Roche) (0.5% in PBS) for 60 min. The membrane was incubated with primary antibody (**Table 7**) at 4°C overnight, washed thrice for 5 min each, and incubated with secondary antibody (**Table 8**) for 1 h at room temperature (RT). The membrane was washed again three times for 5 min each and chemiluminescence was detected after incubation with either ECL solution (Solution A: 0.25 mg/ml Luminol in 0.1 M Tris pH 8.8; Solution B: 1.1 mg/ml para-hydroxy coumaric acid in DMSO; mixed 9:1), or SuperSignal™ West Femto Maximum Sensitivity Substrate (ThermoFisher) according to manufacturer's instructions.

Separation gel: 2.1 ml H₂O, 1.65 ml 30% Acrylamide, 1.25 ml 1.5 M Tris pH 8.8 containing 0.4% SDS, 30 µl 10% APS, 6.5 µl TEMED.

The recipe is for a 10% SDS-polyacrylamide gel. For higher, or lower concentrations, the volume of 30% Acrylamide solution and H₂O have to be adjusted accordingly.

Stacking gel: 1.5 ml H₂O, 350 µl 30% Acrylamide, 650 µl 0.5 M Tris pH6.8 containing 0.4% SDS, 12.5 µl 10% APS, 10 µl TEMED.

Coomassie staining

For in-gel staining of proteins, SDS-PAGE gels were incubated in Coomassie staining solution (50% methanol, 10% Acetic acid, in H₂O) until uniform blue staining of the gel was achieved. Gels were destained in destaining buffer (5% methanol, 7.5% acetic acid, in H₂O) until the protein bands were clearly distinguishable from the clear background.

Immunoprecipitation

Co-Immunoprecipitation (co-IP) of NLRP11-eGFP, from HEK293T and HeLa FlpIn eGFP and NLRP11-eGFP cell lines, or of eGFP-DDX3X from HEK293T cells, transiently transfected with Lipofectamine 2000 (ThermoFisher) was performed with GFP-Trap Agarose resin (Chromotek). Cells were lysed in Triton buffer (50 mM Tris/HCl pH 7.4, 150 mM NaCl, 1% Triton-X100, 1% Na-Deoxycholate, 100 nM β-glycerophosphate, 100 nM sodium orthovanadate, 1 mM NaF and cOmplete Mini Protease inhibitor Cocktail (Roche)), or, if subcellular fractionation was performed, as described in (**Subcellular fractionation**). Lysates were cleared by centrifugation (15 min, 4°C, 21,000 x g) before the supernatants were loaded onto the matrix. Precipitation was performed at 4°C for 3 h, before the

Material and Methods

matrix was washed with washing buffer (50 mM Tris/HCl pH 7.4, 150 mM NaCl, 1% Na-Deoxycholate).

Precipitation of biotinylated proteins was performed with Dynabeads™ M-280 Streptavidin (Invitrogen). When no subcellular fractionation was performed, BioID2 expressing cells were incubated with 25 μ M biotin for 16 h, harvested and washed in PBS and lysed in Triton lysis buffer (50 mM Tris, 500 mM NaCl, 0.2% SDS, 2% Triton X-100 pH 7.4, 100 nM β -glycerophosphate, 100 nM sodium orthovanadate, 1 mM NaF and cOmplete Mini Protease inhibitor Cocktail (Roche)) on ice. Lysates were diluted with one volume of 50 mM Tris pH 7.4 and cleared by centrifugation. Beads were washed in lysis buffer. When immunoprecipitation was preceded by subcellular fractionation of K562 cells, the lysis protocol was performed as described in (**Subcellular fractionation**). An appropriate volume of washed beads was added to the cleared lysates and precipitation was performed for 3 h at 4°C. The beads were washed twice in 2% SDS, followed by washing steps in wash buffer (50 mM HEPES, 500 mM NaCl, 1 mM EDTA, 1% Triton X-100, 0.1% Deoxycholic acid pH 7.5). Two further washing steps were performed in NP-40 wash buffer (10 mM Tris, 250 mM NaCl, 1 mM EDTA, 0.5% NP-40, 0.5% Deoxycholic acid) (adapted from (Roux *et al.* 2013)). For mass spectrometry analysis, beads were then washed twice in PBS, before being taken up in 6 M urea in 10 mM Tris pH 7.4.

Co-IP of FLAG-tagged Sin3A and NELFB were performed with anti-FLAG M2 affinity gel (Sigma-Aldrich) HEK293T cells were seeded according to the experimental procedure and co-transfected with either FLAG-Sin3A, or FLAG-NELFB and either myc-NLRC5, myc-NLRC5 isoform 3, myc-NLRC5 Δ DD, or myc-NLRC5 DD only with Lipofectamin 2000. Cells were lysed in NP-40 lysis buffer (10 mM HEPES, 50 mM NaCl, 0.1 mM EDTA, 0.1 mM EGTA, 0.1% NP 40 100 nM β -glycerophosphate, 100 nM sodium orthovanadate, 1 mM NaF and cOmplete Mini Protease inhibitor Cocktail) and incubated with the agarose matrix for 3 h. The beads were then washed three times with lysis buffer, before proteins were eluted by boiling in SDS-Laemmli buffer at 95°C for 5 min.

Subcellular fractionation

For the separation of the nuclear and cytosolic fractions of K562 cells, the cells were seeded and treated according to the experimental procedure and 6×10^7 cells were harvested in 3 ml cold harvest buffer (10 mM HEPES, 10 mM KCl, 0.5 M succhrose, 0.1 mM EDTA, 0.5% Triton-X100, 100 nM β -glycerophosphate, 100 nM sodium orthovanadate, 1 mM NaF and cOmplete Mini Protease inhibitor Cocktail) and incubated for 5 min on ice. Nuclei were pelleted by centrifugation (500 x g, 10 min, 4°C) and the supernatant was transferred into fresh, precooled 1.5 ml reaction tubes and cleared by centrifugation. The nuclei were washed once in cold wash buffer (10 mM HEPES, 10 mM KCl, 0.1 mM EDTA, 0.1 mM EGTA) and pelleted by centrifugation (500 x g, 10 min, 4°C). Nuclei were lysed in 1.4 ml nuclear lysis buffer (10 mM HEPES, 50 mM NaCl, 0.1 mM EDTA, 0.1 mM EGTA, 0.1% NP-40). DNA was digested using RQ1 RNase free DNase (Promega). Samples were cleared by

Material and Methods

centrifugation and supernatants were transferred into fresh, precooled 2 ml reaction tubes. If samples were not used right away, they were frozen in liquid nitrogen and stored at -80°C .

For GFP co-IP after subcellular fractionation, HEK293 FlpIn cells were seeded and induced according to protocol, harvested in PBS and lysed in 1 ml lysis buffer (10 mM HEPES, 10 mM KCl, 0.1 mM EGTA, 0.6% NP-40 100 nM β -glycerophosphate, 100 nM sodium orthovanadate, 1 mM NaF and cOmplete Mini Protease inhibitor Cocktail) on ice for 30 min. Nuclei were pelleted by centrifugation ($500 \times g$, 15 min, 4°C) and cytosolic fractions were transferred into fresh, precooled 2 ml reaction tubes and add one volume of Tris-NaCl buffer (50 mM Tris pH 7.5, 390 mM NaCl). Nuclei were resuspended in 500 μl nuclear buffer (20 mM HEPES pH 7.5, 400 mM NaCl, 1 mM EGTA, 100 nM β -glycerophosphate, 100 nM sodium orthovanadate, 1 mM NaF and cOmplete Mini Protease inhibitor Cocktail) and incubated on ice for 10 min. Nuclear lysates were cleared by centrifugation. Supernatants were transferred into fresh, pre-cooled 1.5 ml reaction tubes and diluted with one volume of NP-40 buffer (50 mM Tris pH 7.5, 0.6% NP-40). Samples were either used directly for GFP co-IP, or frozen in liquid nitrogen and stored at -80°C .

Measurement of cytokines

IL-1 β and IFN β release was measured in cell supernatants by ELISA (DY201, DY814, R&D Systems) according to the manufacturer's instructions. A bioassay for type I interferons was performed using HEK Blue IFN- α/β cells (InvivoGen) as described in (**HEK-IFN- α/β reporter assay (QuantiBlue)**).

NanoLC-MS/MS analysis

Proteins were digested on beads using trypsin (Roche, Germany) in 6 M urea, 50 mM Tris-HCl pH 8.5. Cysteines were reduced using 1,4-dithiothreitol (DTT) and then alkylated by chloroacetamide. Samples were then diluted to a final concentration of 2 M urea. 750 ng trypsin were added, and samples were digested overnight at 25°C . The digests were stopped by adding trifluoroacetic acid (TFA). Next, peptide mixtures were concentrated and desalted on C18 stage tips and dried under vacuum. Samples were dissolved in 0.1 % TFA and were subjected to nanoLC-MS/MS analysis on an EASY-nLC 1000 system (ThermoFisher) coupled to a Q-Exactive Plus mass spectrometer (ThermoFisher) using an EASY-Spray nanoelectrospray ion source (ThermoFisher). The system was controlled by Xcalibur 3.0.63 software. Tryptic peptides were directly injected to a 25 cm x 75 μm EASY-Spray analytical column (2 μm , 100 \AA , PepMap C18) operated at 35°C . Peptides were separated at a flow rate of 250 nL/min using a 120 min gradient with the following profile: 3 – 10% solvent B in 50 min, 10 – 22% solvent B in 40 min, 22 – 45% solvent B in 30 min, 45 – 90% solvent B in 10 min, 15 min isocratic at 90% solvent B, followed by 90 – 3% solvent B in 10 min and re-equilibration at 3% solvent B for 15 min (solvent A: 0.5% acetic acid; solvent B: acetonitrile/H₂O (80/20, v/v), 0.5% acetic acid).

MS spectra ($m/z = 300 - 1600$) were detected at a resolution of 70,000 ($m/z = 200$) using a maximum injection time (MIT) of 100 ms and an automatic gain control (AGC) value of 1×10^6 . MS/MS spectra

Material and Methods

were generated for the 10 most abundant peptide precursors using high energy collision dissociation (HCD) fragmentation at a resolution of 17,500, normalized collision energy of 27 and an intensity threshold of 1.3×10^5 . Only ions with charge states from +2 – +5 were selected for fragmentation using an isolation width of 1.6 Da. For each MS/MS scan, the AGC was set at 5×10^5 and the MIT was 100 ms. Mascot 2.6 (Matrix Science, UK) was used as search engine for protein identification. Spectra were searched against the human UniProt database (UniProt Consortium 2018). Scaffold 4.8.6. (Proteome Software, USA) was used to evaluate peptide identifications. These were accepted with a peptide probability greater than 80% as specified by the Peptide Prophet algorithm (Keller *et al.* 2002). Proteins had to be identified by at least one unique peptide and a protein probability of at least 99% to be accepted. NanoLC-MS/MS analysis was performed by the Core facility Hohenheim.

2.2.4 Bioinformatic methods

Generation of interaction networks

Proteins lists, identified in LC-MS/MS analysis after co-immunoprecipitation were curated manually to contain only proteins of which either no peptides were identified in the appropriate control, or, if peptides were identified under control conditions, of which at least twice the number of peptides were identified in the bait condition. For eGFP co-IP Experiments data sets of two independent experiments were compared and proteins were considered specific, if they met the criteria above in both experiments. Those proteins were termed high confidence interactors. To compare interactors of different experimental conditions, for example different bait constructs, the lists of interactors were analyzed with the open-source software Cytoscape (Shannon *et al.* 2003). To generate interaction networks of the interactors of one specific experimental condition, the protein identifiers of the interactors from this setting were analyzed with the stringApp plugin in Cytoscape using a 0.4 confidence (score) cutoff and 0 maximum additional interactors. Venn diagrams were generated via the InteractiVenn service (Heberle *et al.* 2015).

2.2.5 Yeast two-hybrid screening

ULTimate yeast two-hybrid (Y2H) screening was performed by Hybrigenics. The N-terminal domain of human NLRC5 (amino acids 1 – 139) were cloned into pB66 and pB35 vectors to encode for GAL4-NLRC5 DD fusion proteins, which encompass the DNA binding domain of the Regulatory protein Gal4 of *Saccharomyces cerevisiae*. Screening was performed with both constitutive pB66 and inducible pB35 vectors against a human thymocyte cDNA prey library of both CD4⁺ and CD8⁺ T cells. Results were scored by global predicted biological score (PBS[®]) ranking.

3 Results

3.1 NLRC5

The role of the MHC enhanceosome in MHC class II transcription has been discovered some time ago (Masternak *et al.* 2000) and its involvement in NLRC5-dependent MHC transcription is also well established (Meissner *et al.* 2012, Neerinx *et al.* 2012). Nevertheless, it is still unclear, how the high specificity of NLRC5 for MHC class I promoters is conferred. We therefore set out to identify novel interaction partners of NLRC5 through which selective MHC class I transcription is conferred.

3.1.1 Identification of NLRC5 interaction partners by co-immunoprecipitation following fractionation

To better understand the function of NLRC5 and potential licensing mechanisms in the cytoplasm, we wanted to identify novel interaction partners which are specific for either cytoplasmic or nuclear localized NLRC5. To this end, we performed immunoprecipitations (IPs) of eGFP-NLRC5 (NLRC5 FL), or the predominantly nuclear eGFP-NLRC5 isoform 3 and a version of NLRC5, tagged with the strong nuclear localization sequence (NLS) of Simian virus 40 (eGFP-NLRC5 2xNLS) from stably expressing HEK293 FlpIn cells (Neerinx *et al.* 2012). Co-precipitated proteins were analyzed by LC-MS/MS analysis.

We were able to identify several proteins that specifically bound to one of the constructs in two independent experiments (**S. Table I**, **S. Table II**, **S. Table III**), termed high confidence candidates below. Several proteins thereby were identified with more than one NLRC5-bait construct (**Figure 6A**, **S. Table IV**, **S. Table V**, **S. Table VI**, **S. Table VII**). Most of the high confidence candidates were either chaperones (BAG family of proteins, heat shock proteins (HSPs), DNAJ family of proteins), parts of the proteasomal degradation machinery (proteasomal subunits), ribosomal proteins (RPS29), or involved in vesicular trafficking (RAB5C, AP3M1). However, several proteins with known functions in epigenetic regulation by acetylation (TRRAP) or methylation (DPX30) were identified as interactors of NLRC5 FL, and NLRC5 isoform 3, or the 2xNLS construct of NLRC5, respectively (**Figure 6A**).

In co-IPs of HEK293 FlpIn eGFP-NLRC5 2xNLS and eGFP-NLRC5 NLS I, performed after separation of the cytosolic and the nuclear fractions, several proteins were identified as specific interactors of either NLRC5 NLS I, or NLRC5 2xNLS (**Figure 6B**, **S. Table VIII**, **S. Table IX**). Although differently localizing NLRC5 constructs were used, and nuclear and cytosolic fractions were separated, some proteins were identified as high confidence interactors of NLRC5 in both conditions (**Figure 6B**). Not much overlap was obtained between the co-IPs performed in whole cell lysates (**Figure 6A**) or in the subcellular fractions (**Figure 6B**), and it consisted mainly of chaperones (**Figure 6C**).

Results

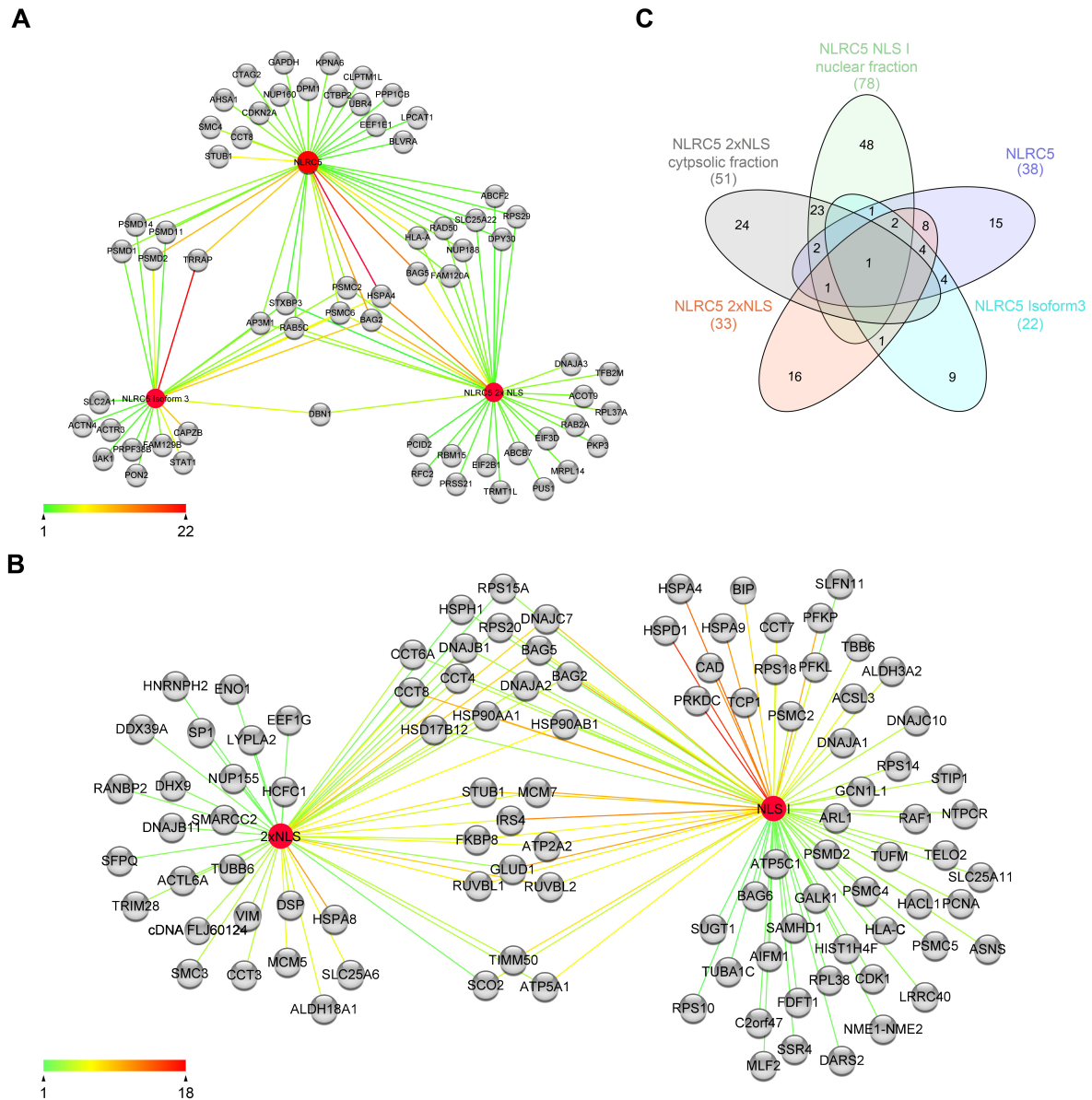


Figure 6: **Identification of novel interaction partners of NLRC5 by co-immunoprecipitation.** (A,B) Network of proteins identified as specific interactors of (A) HEK293 eGFP-NLRC5, eGFP-NLRC5 2xNLS and HEK293 eGFP-NLRC5 isoform 3, or (B) HEK293 eGFP-NLRC5 2xNLS and HEK293 eGFP-NLRC5 NLS I in comparison to HEK293 eGFP. Co-IPs from (A) whole cell lysates, or (B) subcellular fractionations, from stably overexpressing cells, induced overnight with 1 μ g/ml doxycycline, were analyzed by LC-MS/MS. Proteins, of which at least 2 peptides were identified in the eGFP-NLRC5 samples, while none were identified in the eGFP control sample, or proteins of which at least twice the number of peptides were identified in the sample, compared to the control were considered, if they were present in at least two independent experiments. The identified proteins were plotted around their respective bait, using Cytoscape, to identify proteins specific for each NLRC5 construct. (A,B) The number of peptides identified in each experiment is indicated by the color of the edge between the protein and the bait, as indicated by the scale bar. (B) Analysis of experiments, which were performed by Felix Hezel. (C) Venn-Diagram of proteins identified as specific hits in at least two independent experiments of (A) and (B).

To gain a better overview of the identified NLRC5 interactome, chaperones, proteasomal subunits, and ribosomal subunits were subtracted from the candidate lists and an interaction network of the remaining proteins was generated. For many of the putative interactors identified from whole cell lysates, no interactions amongst each other are known (Figure 7). Full-length eGFP-NLRC5 interacted with two proteins of the nuclear pore complex (NUP160, NUP188) and importin subunit alpha 7 (KPNA6), as

Results

expected for the nuclear translocation of NLRC5. Furthermore, a cluster of proteins, which are known to be associated with transcriptional regulation or replication (TRRAP, RAD50, SMC4, DPY30, PP1CB, GAPDH, CTBP2, CDKN2A), was identified here, potentially representing interesting candidates for further analysis (**Figure 7A**). Interactors of the predominantly nuclear eGFP-NLRC5 isoform 3 were mainly involved in actin organization (ACTN4, ACTR3, DBN1, CAPZB) and protein transport (RAB5C). Interestingly, this construct specifically interacted with JAK1 and STAT1, two proteins involved in signaling downstream of the type I IFN receptor, potentially implicating this isoform in the regulation of type I IFN signaling (**Figure 7B**).

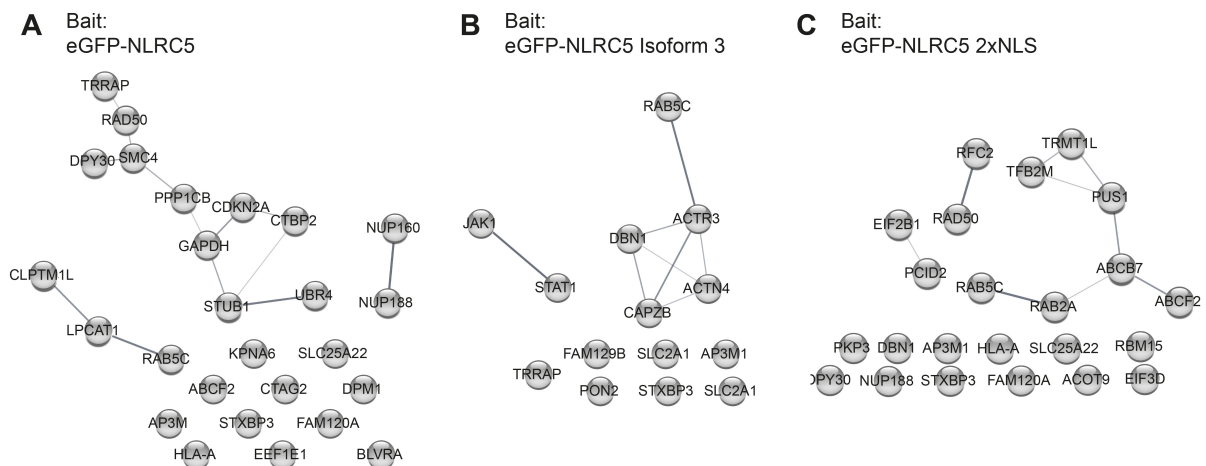


Figure 7: Interaction networks of proteins identified as specific interactors of differently localizing NLRC5 constructs. (A-C) Proteins identified in co-IPs of (A) NLRC5, (B) NLRC5 isoform 3, or (C) NLRC5 2xNLS, were manually curated to remove all proteasomal subunits, ribosomal subunits and chaperones. Curated lists were then analyzed for known and predicted protein-protein interactions of the putative interactors by STRINGApp in Cytoscape. Width of edges represents the confidence score of the interactions.

The interactors of eGFP-NLRC5 2xNLS are organized in an interaction network of proteins involved in RNA metabolism (TRMT1L, TFB2M, PUS1), efflux pumps (ABCB7, ABCF2), and protein transport (RAB2A, RAB5C). Further, two interesting groups of proteins, involved in DNA replication (RFC2, RAD50) and translation (EIF2B1), or mRNA export (PCID2), were identified (**Figure 7C**).

Of the proteins identified as specific interactors of cytosolic eGFP-NLRC5 NLS I, in which the amino-terminal NLS in NLRC5 is mutated, or nuclear eGFP-NLRC5 2xNLS none were previously described to interact with NLRC5 (**Figure 8A, B**). Interestingly, several proteins with known function in transcriptional activation (RUVBL1, RUVBL2, HCF2, ACTL6A, SMARCC2) were identified in the nuclear fraction. Further, proteins involved in DNA replication (SMC3, MCM2, MCM7) were identified here (**Figure 8A**). Although only the cytosolic fraction was used for GFP-IPs of eGFP-NLRC5 NLS I, one large cluster of proteins, associated with DNA repair and replication (MCM7, PCNA, RUVBL1, RUVBL2, TELO; PRKDC, CDK1) was identified. The second large cluster contained proteins associated with intracellular membranes (TIMM50, ATP5A1, ATP5C1, ATP2A2, TUFM, SSR4).

Results

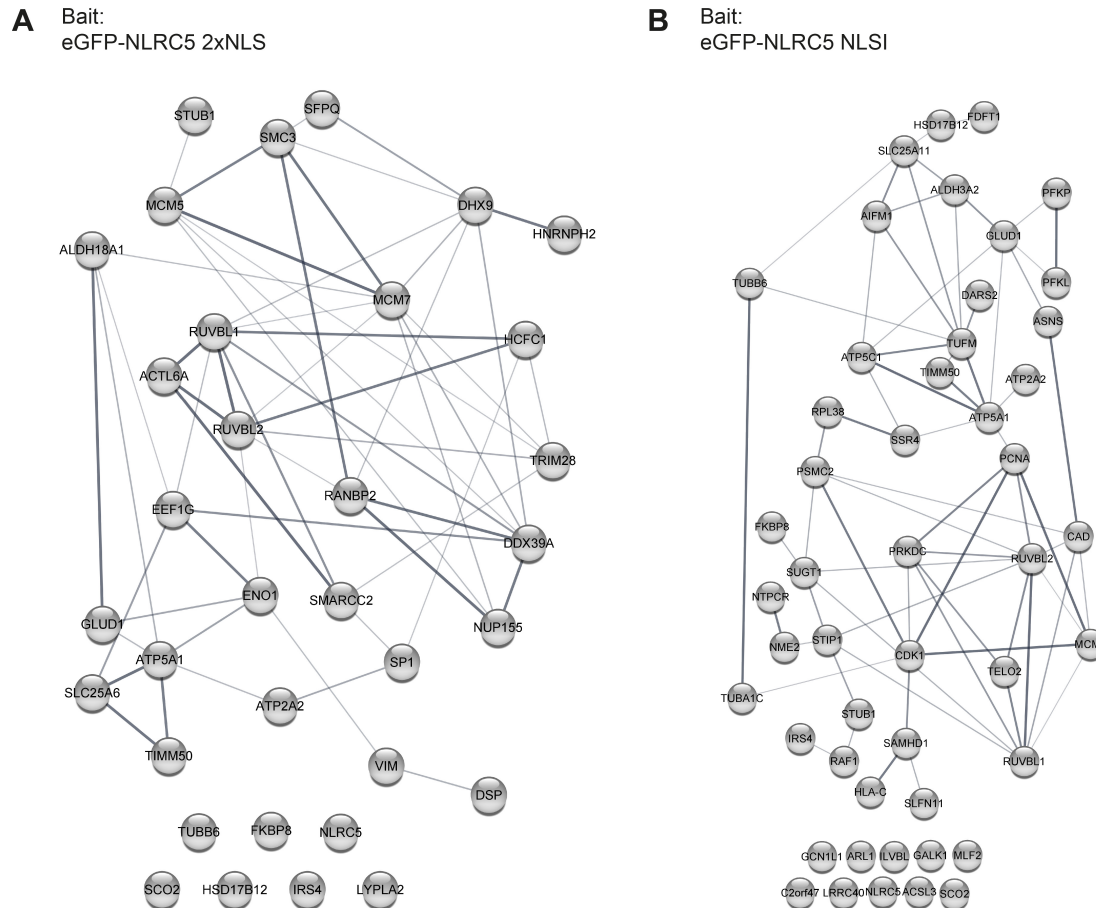


Figure 8: **Interaction network of proteins identified as specific interactors of NLRC5 in different subcellular compartments.** (A,B) Proteins identified in (A) the nuclear, or (B) the cytosolic compartment in co-IPs from (A) NLRC5 2xNLS or (B) NLRC5 NLS I were manually curated to remove all proteasomal subunits, ribosomal subunits and chaperones. Curated lists were then analyzed for known and predicted protein-protein interactions of the putative interactors by STRINGapp in Cytoscape. Width of edges represents the confidence score of the interactions.

In conclusion, several interesting candidates with known functions in transcriptional regulation were identified in this approach. Of note, with transformation/transcription domain-associated protein (TRRAP) (**Figure 7A, B**), RuvB-like1 (RUVBL1) and RUVBL2 (**Figure 8A, B**), several proteins of the NuA4 histone acetylase complex (Doyon and Côté 2004) co-precipitated with different NLRC5 bait constructs. This makes the NuA4 complex an interesting candidate for a potential role in NLRC5-mediated regulatory mechanisms. However, as none of the proteins previously described to interact with NLRC5 were identified here, the results have to be interpreted cautiously. Moreover, we did not normalize to eventual changes in protein abundance induced by the expression of the respective construct thus some hits might be the results of increase in protein expression over the control.

3.1.2 Establishment of a proximity biotin ligation system (BioID2) for identification of further NLRC5 interaction partners

As co-IPs depend on long lasting high affinity binding and thus have the limitation that they are not well suited to identify transient interactions, we established a proximity ligation system to bypass this

Results

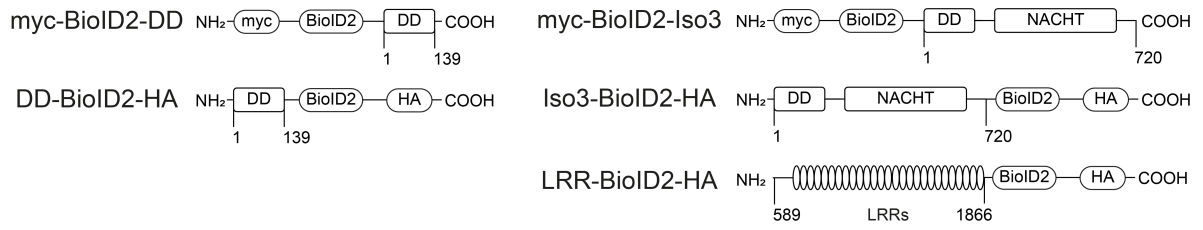
constraint. This system employs the biotin ligase function of a mutated version of the bifunctional ligase/repressor (BirA) from *Aquifex aeolicus* (Kim *et al.* 2016) to label proteins in close proximity of the protein of interest. Biotinylation is a rarely occurring PTM in mammalian cells (Chapman-Smith and Cronan 1999), and hence well suitable as a tagging system. Subsequently biotin-labelled proteins can be precipitated by biotin-streptavidin interaction and identified via mass spectrometry. R40G mutation of the biotin ligase, results in premature release of biotinoyl-5'AMP from the catalytic site, which can react with the nucleophilic ϵ -amino group of near-by lysin, resulting in promiscuous biotinylation of proteins in direct vicinity (Choi-Rhee *et al.* 2004, Cronan 2005, Roux *et al.* 2012, Kim *et al.* 2016). This property of the mutated biotin ligase, hence forward termed BioID2, can be harnessed by generating fusion proteins consisting of the BioID2 and a protein of interest to tag proteins in close proximity of the desired bait (Roux *et al.* 2012, Kim *et al.* 2016).

BioID2 constructs of the NLRC5 DD and NLRC5 isoform 3 were generated by molecular cloning with the BioID2 at the C-terminus (BioID2-HA), or at the N-terminus (myc-BioID2). Further, a NLRC5 LRR-BioID2-HA construct was generated (**Figure 9A**). Their expression was verified in transiently transfected HEK293T cells. Except for LRR-BioID2-HA, all constructs expressed well and at comparable levels (**Figure 9B**). Neerinx *et al.* established that the N-terminal DD-like fold of NLRC5 is the domain responsible for the MHC class I specificity of NLRC5 (Neerinx *et al.* 2014), suggesting that regulatory proteins bind to the DD. We thus performed precipitation of biotinylated proteins from either HEK293T cells, transiently transfected with DD-BioID2-HA (**Figure 9C DD-BioID2 HEK293T**), or myc-BioID2-DD (**Figure 9C BioID2-DD**). This identified several proteins, which were biotinylated specifically by BioID2 constructs of the DD, compared to cells transfected with the BioID2 as control (**S. Table XI, S. Table XII**). However, the overlap of identified proteins between the two experiments was only small (**Figure 9C, right side**).

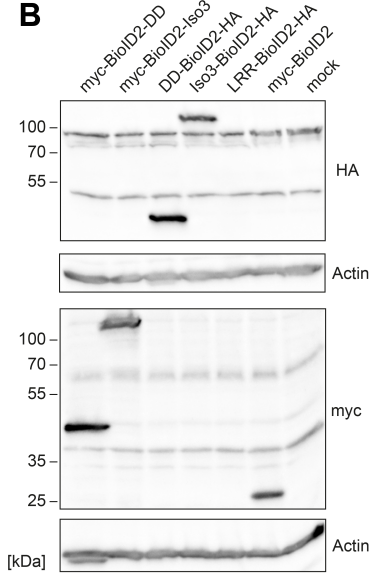
Transient expression in HEK293T cells results in unphysiologically high protein load, likely yielding high levels of unspecifically biotinylated background. We thus generated cell lines, stably expressing DD-BioID2-HA, or the BioID2-HA control in myeloid K562 cells. We regarded this cell line as more representative for the transcriptional regulation of MHC class I than epithelial HEK293T cells, as NLRC5 is endogenously expressed in myeloid cells (Neerinx *et al.* 2010). Expression of the BioID2 construct and biotinylation of cellular proteins was confirmed by immunoblot (**Figure 9D**). Precipitation of biotinylated proteins from the nuclear fractions of those cells revealed several specific hits in two independent experiments (**Figure 9C, S. Table XIII, S. Table XIV**). However, in total only 10 proteins were identified in two independent experiments (**Figure 9C**). As the aim was to identify NLRC5 specific interactors, involved in transcriptional regulation, two proteins associated with the cytoskeleton (DSTN, LASP1) were excluded.

Results

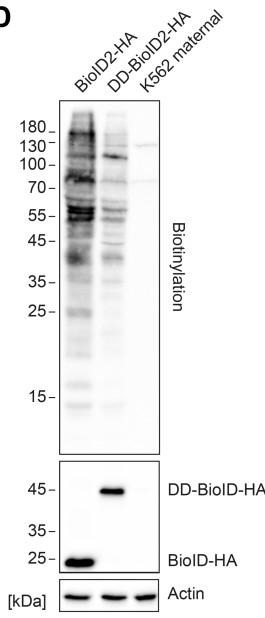
A



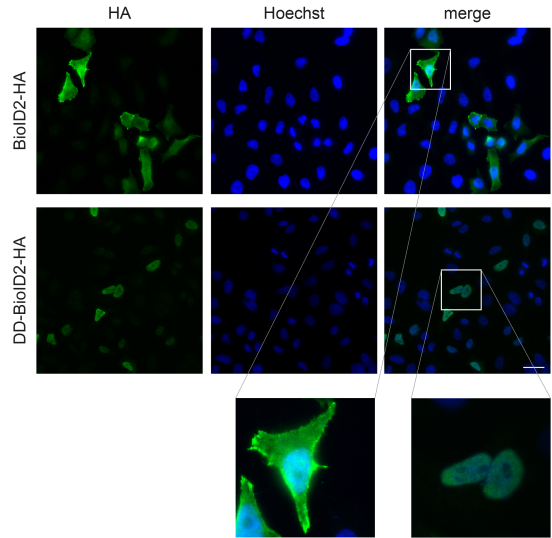
B



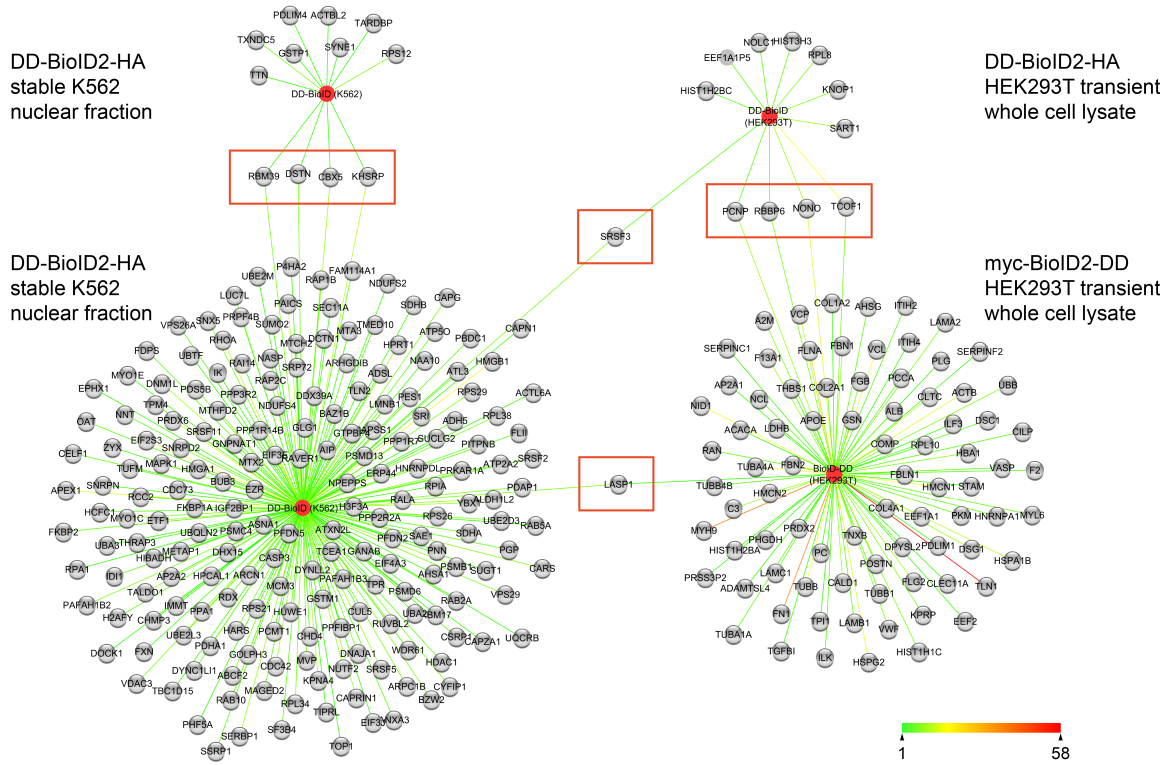
D



E



C



Results

Figure 9: Identification of novel NLRC5 interactors by BioID2. (A) Schematic representation of generated BioID2 constructs for the NLRC5 N-terminal DD-like fold (DD), NLRC5 isoform 3 and NLRC5 leucine-rich repeats (LRRs). The numbers indicate the corresponding amino acid positions in full-length NLRC5. (B) Immunoblot analysis of HEK293T cells, transiently transfected with the indicated plasmids. Membranes were probed against HA- and myc-tags, as well as for actin as loading control. (C) Proteins identified as specifically biotinylated by DD-BioID2-HA by mass spectrometry after Streptavidin-biotin precipitation, in four independent experiments. Proteins, of which at least 2 peptides were identified in the DD-BioID2-HA sample, while none were identified in the BioID2 control sample, or proteins of which at least twice the number of peptides were identified in the sample, as in the control were considered. The identified proteins of each experiment were plotted around their bait using Cytoscape. Proteins identified in more than one experiment are marked by a red rectangle. The number of peptides identified in each experiment is indicated by the color of the edge between the protein and the bait, as indicated by the scale bar. Precipitations were performed in either whole cell lysates of HEK293T cells, transiently transfected with DD-BioID2-HA, or myc-BioID2-DD, or in the nuclear fraction of K562 cells, stably expressing DD-BioID2-HA, as indicated. (D) Immunoblot of stably expressing K562 BioID2-HA, DD-BioID2-HA cells, or maternal K562 FlpIn cells as control. Membranes were probed with Streptavidin-HRP, and antibodies against the HA-tag, or actin as a control. (E) Indirect immunofluorescence micrographs of HEK293T cells, transiently transfected with BioID2-HA or DD-BioID2-HA. Staining for the HA-tag (green) and Hoechst (blue) are depicted. Scale bar = 25 μ m.

Identified nuclear proteins with known DNA binding capacities were chromobox 5 (CBX5), also known as heterochromatin protein 1 homologue alpha (HP1 α), which is associated with transcriptional silencing (Cheutin *et al.* 2003), and non-POU domain-containing octamer-binding protein (NONO), which is a known transcriptional activator (Sewer *et al.* 2002). Three RNA associated factors, RNA binding protein 39 (RBM39), serine/arginine-rich splicing factor 3 (SRSF3) and far upstream element-binding protein 2 (KHSRP), were also identified (Min *et al.* 1997, Dowhan *et al.* 2005, Xiao *et al.* 2016). Furthermore, treacle protein (TCOF1), a regulator of the RNA Polymerase I (Hayano *et al.* 2003), and the E3 ubiquitin-protein ligase RB binding protein 6 (RBBP6), which is involved in replication (Miotto *et al.* 2014), were found in more than one experiment. When we verified the nuclear localization of DD-BioID2-HA by indirect immunofluorescence microscopy in transiently transfected HEK293T cells (**Figure 9E**), we observed that the BioID2-HA control was predominantly localized in the cytoplasm (**Figure 9E**). Thus, interaction of the identified proteins with NLRC5 DD needs to be carefully evaluated, as the cytosolic BioID2-HA might result in overestimation of nuclear interactors. Efforts to target BioID2-HA to the nucleus by tagging it with the SV40 NLS did not succeed (data not shown).

Although the BioID2 approach was more promising than the identification of interactors by co-IP, the identification of putative interaction partners of the N-terminal domain by biotin labelling varied strongly between N- and C-terminally tagged constructs, between transient expression in HEK293T and stable expression in K562, as well as between independent experiments within the stable K562 cells. Combined with the high background, we therefore decided to perform a complimentary approach to circumvent these problems. To this end, we applied a yeast two-hybrid (Y2H) screen using the DD domain of NLRC5 as bait.

3.1.3 Sin3A interacts with NLRC5 at the Death Domain and inhibits major histocompatibility complex transcription

Besides identification of novel NLRC5 interactors by co-IP and proximal ligation assays, we also approached this by a Y2H screen. Here, the N-terminal DD of NLRC5 (amino acids 1 – 139) was used

Results

as a bait against a human thymocyte cDNA prey library prepared from both CD4⁺ and CD8⁺ T cells. 128 clones were sequenced and results ranked according to the predicted biological score which takes into account known false positives from other screens (Rain *et al.* 2001). Notably, the screen identified several importin subunit alpha proteins as interaction partners, providing confidence in the approach (**S. Table XV**). Amongst the very high and high confidence candidates, two proteins with known functions in transcriptional regulation, Sin3A and NELFB, caught our interest (**S. Table XV**). We considered these as the most promising hits from all screening approaches and further characterized their interaction with NLRC5.

The sequencing results of the prey showed that NLRC5 interacted with the HDAC interaction site of Sin3A (schematic representation in **Figure 10A**). In co-IP experiments, from transiently expressed proteins in HEK293T cells, we could confirm that FLAG-Sin3A interacted with NLRC5, NLRC5 isoform 3, lacking the LRRs, and the DD of NLRC5 alone, while a truncation mutant of NLRC5 lacking the DD (Δ DD) did not co-precipitate with FLAG-Sin3A (**Figure 10B**), showing that the DD was both sufficient and necessary for interaction.

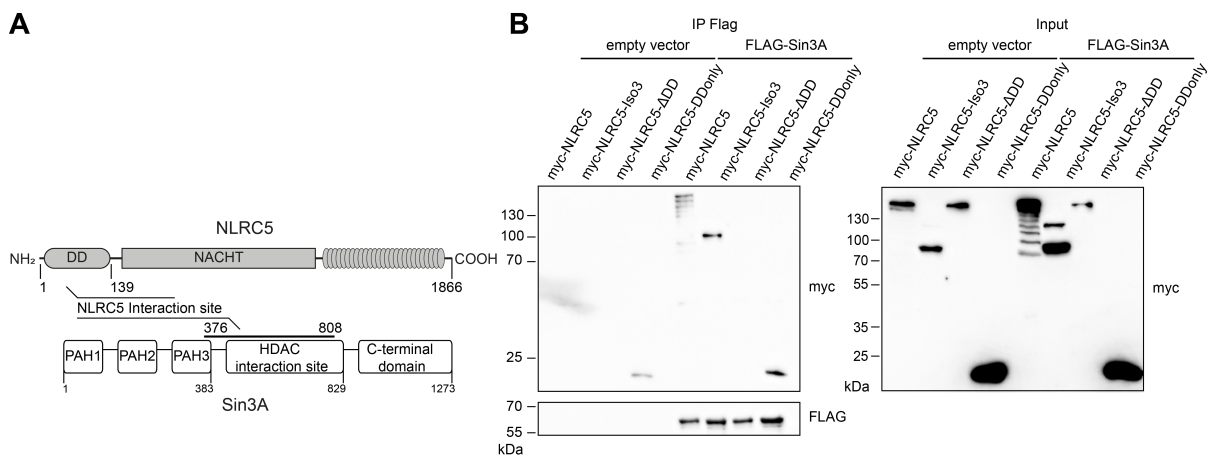


Figure 10: **Sin3A interacts with the N-terminal DD of NLRC5.** (A) Schematic representation of the NLRC5 DD-Sin3A interaction site, as revealed by Y2H screening. (B) Immunoblot of FLAG-immunoprecipitation of FLAG-Sin3A, co-expressed with the indicated myc-NLRC5 truncation constructs in HEK293T cells. Membranes of inputs were probed with an antibody against the myc-tag. Membranes of IPs were probed with antibodies against myc- and FLAG-tags. Experiments performed by Felix Hezel. Blots are representative of two independent experiments. PAH: paired amphipathic helix.

To characterize the function of this interaction in NLRC5-mediated MHC gene regulation, we performed reporter gene assays with MHC class I (HLA-B250) and II (HLA-DRA) promoter regions. Here we observed a dose-dependent reduction of NLRC5-induced MHC class I transcription (**Figure 11A**). Induction of the HLA-DRA reporter construct by CIITA overexpression was also reduced by titration of Sin3A (**Figure 11A**), as previously shown (Zika *et al.* 2003). We next used hybrid reporter gene constructs, in which the S, X or Y boxes of the MHC class I and class II promoter were interchanged (schematically depicted in **Figure 11C**) (Ludigs *et al.* 2015). As previously described, NLRC5 induced transcription from hybrids 2 and 4, which contain the MHC class I S box and either the

Results

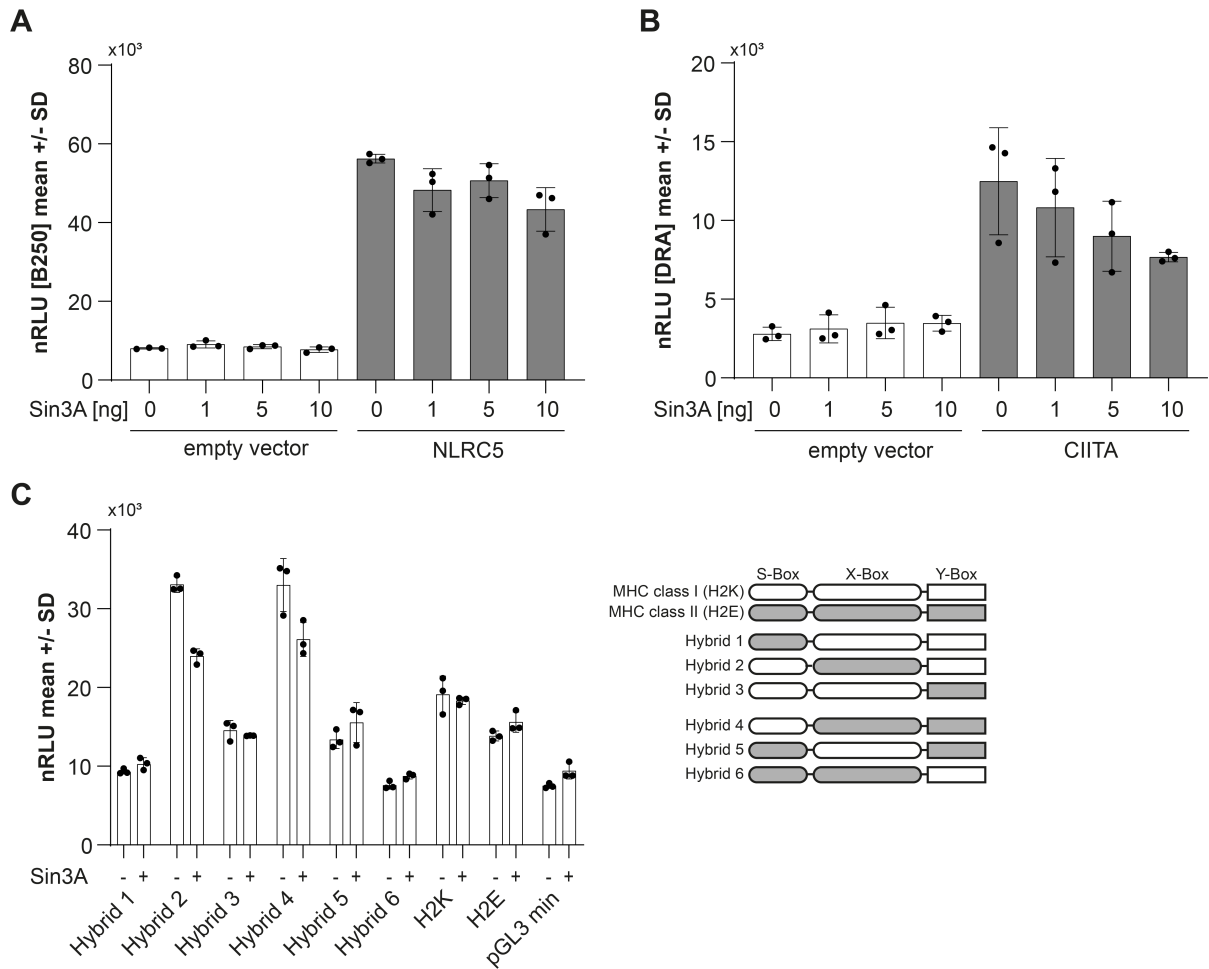


Figure 11: **Sin3A does not alter NLRC5-induced MHC class I transcription.** (A-C) Reporter gene assays for (A) HLA-B250, (B) HLA-DRA, or (C) hybrid reporter regions. Sin3A was overexpressed at the indicated amounts, together with the indicated reporter gene constructs. Transcriptional activation was induced by the overexpression of either (A,C) NLRC5, or (B) CIITA. Luciferase activity was normalized against β -galactosidase activity (nRLU). Representative results of at least two independent experiments performed in technical triplicates by Felix Hezel. (C) Schematic representation of the hybrid promoter regions.

MHC class II X box and the MHC class I Y box (hybrid 2), or both MHC class II X box and Y box (**Figure 11C**) (Ludigs *et al.* 2015). Sin3A inhibited NLRC5-induced expression of both constructs (**Figure 11C**). However, no effect was seen for the MHC class I and II wild-type promoters (H2K and H2E).

We then knocked down Sin3A in HEK293 FlpIn eGFP and eGFP-NLRC5 cells by two siRNA duplexes. We observed no differences in protein levels of MHC class I with either siRNA, although both siRNAs strongly reduced Sin3A protein levels compared to control siRNA treated cells (**Figure 12**).

Results

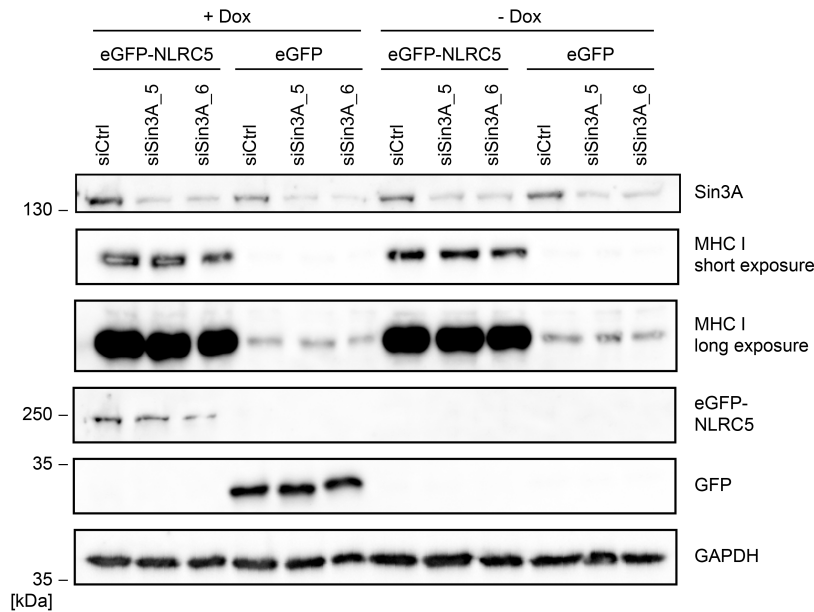


Figure 12: **Knockdown of Sin3A does not alter MHC class I expression levels.** Immunoblots from HeLa eGFP-NLRC5 cells. Cells were treated with the 20 nM of indicated siRNAs for 72 h before NLRC5 expression was induced with 1 μ g/ml doxycycline (+Dox). Membranes were probed for Sin3A, HLA B/C, eGFP, and GAPDH as loading control.

In conclusion, we could confirm the interaction of NLRC5 with Sin3A, which was identified in our Y2H screen, by co-IP and immunoblot. However, the effect of Sin3A overexpression on MHC class I induction by NLRC5 was only marginal and siRNA-mediated reduction of Sin3A did not result in a robust change in NLRC5-induced MHC class I expression. Furthermore, Sin3A overexpression also reduced CIITA-induced transcription from the MHC class II promoter, suggesting that the effect was not specific for MHC class I induction by NLRC5.

3.1.4 NELFB interacts with NLRC5 via its Death Domain and inhibits major histocompatibility complex transcription

Besides Sin3A, NELFB, a central component of the negative elongation factor complex, was identified as a high confidence interactor of the NLRC5 DD in our Y2H screen (**Figure 13A**). In line with the Y2H data, co-IP of overexpressed FLAG-NELFB in HEK293T cells confirmed the interaction with the NLRC5 DD (**Figure 13B**). Further, NLRC5 FL and NLRC5 isoform 3 coprecipitated with NELFB, while NLRC5- Δ DD did not bind to NELFB, indicating that the NLRC5 DD is critical for the interaction, as expected from the screen.

Results

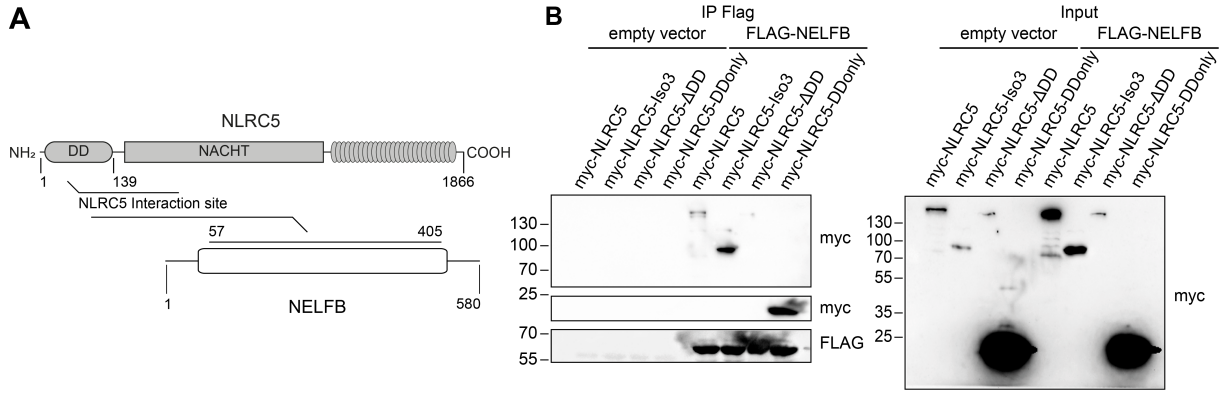


Figure 13: **NELFB interacts with the N-terminal DD of NLRC5.** (A) Schematic representation of the NLRC5 DD-NELFB interaction site, as revealed by Y2H screening. (B) Immunoblot of FLAG-immunoprecipitation of FLAG-NELFB, co-expressed with the indicated myc-NLRC5 truncation constructs in HEK293T cells. Membranes of inputs were probed with an antibody against the myc-tag, Membranes of IPs were probed with antibodies against myc- and FLAG-tags. Experiments performed by Felix Hezel. Blots are representative of two independent experiments.

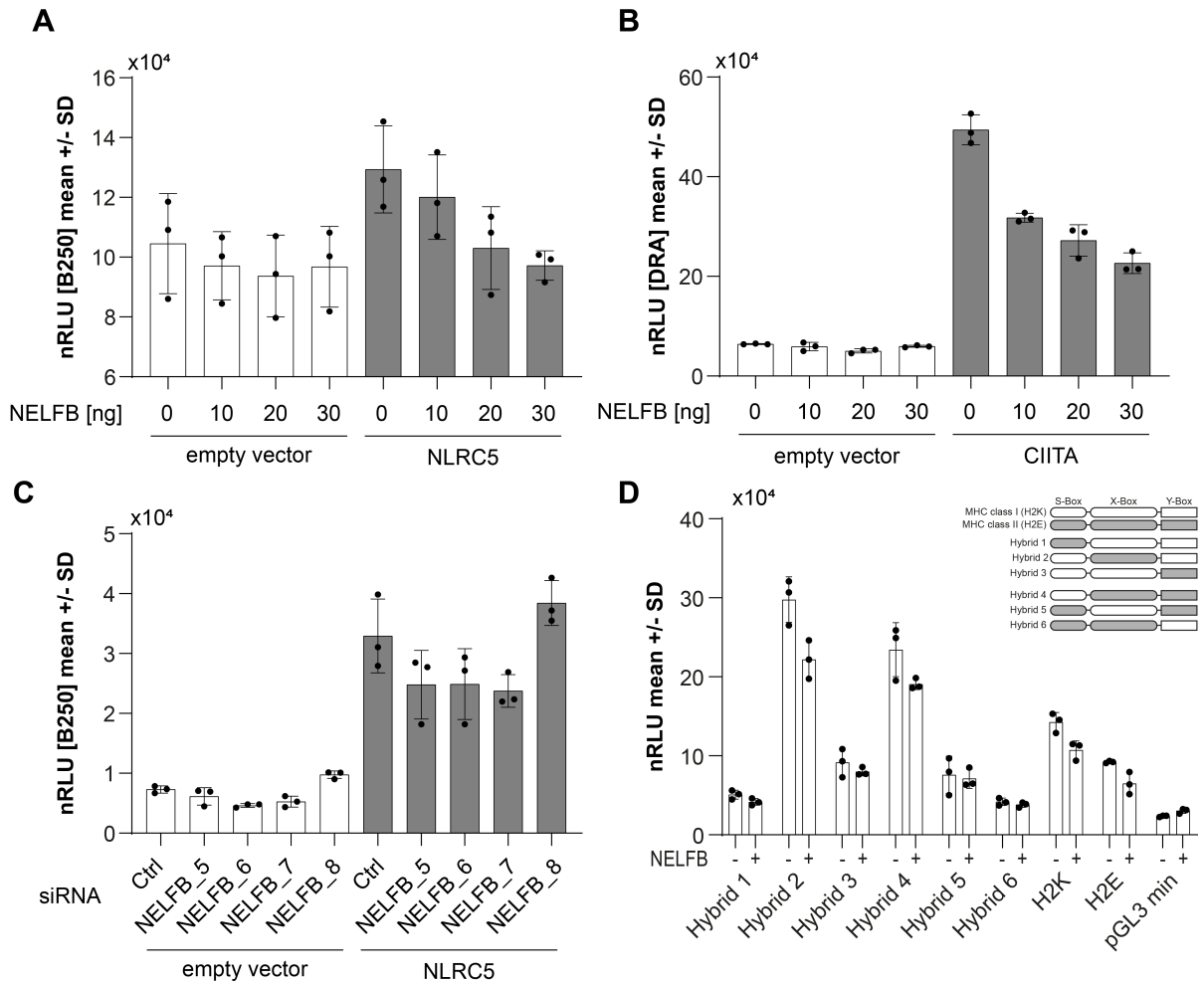


Figure 14: **NELFB inhibits both NLRC5-induced MHC class I and CIITA-induced MHC class II transcription.** (A-D) Reporter gene assays for (A,C) HLA-B250, (B) HLA-DRA, or (D) hybrid reporter regions. NELFB was overexpressed at the indicated amounts, together with the indicated reporter gene constructs. Transcriptional activation was induced by the overexpression of either (A,C,D) NLRC5, or (B) CIITA. Luciferase activity was normalized against β -galactosidase activity (nRLU). Representative results of at least two independent experiments performed in technical triplicates by Felix Hezel.

Results

When we overexpressed NELFB we observed dose-dependent reduction of NLRC5-mediated transcriptional activation of the HLA-B promotor (**Figure 14A**). However, as for Sin3A, this was also observed for CIITA-induced transcriptional activation of the MHC class II DRA reporter construct (**Figure 14B**). Knockdown of NELFB did not result in significant alterations of MHC class I transcription in HEK293T cell-based reporter gene assays (**Figure 14C**). This might indicate that the effect observed during NELFB overexpression might rather be due to a more general transcriptional repression by promoter proximal pausing, instead of specific repression of MHC transcription, although no clear trend is observable in baseline transcription from the promoter region. Overexpression of NELFB in the context of MHC hybrid reporter showed reduction of both wild-type reporter constructs. Further, similar to Sin3A, transcription from both hybrid 2 and hybrid 4 promoter constructs (**Figure 14D**), which are activated by NLRC5 and contain the MHC class I S box (**Figure 11C**), was inhibited by NELFB overexpression.

In conclusion, we could confirm interaction of NELFB with the NLRC5 DD, however, as for Sin3A, transcriptional repression by NELFB, seemed not to be specific for NLRC5.

To provide further evidence whether the inhibitory effect of NELFB and Sin3A in MHC reporter gene assays was specific, or rather due to their general inhibitory functions, we evaluated the effect of Sin3A and NELFB overexpression on transcriptional regulation of innate immune signaling pathways. Overexpression of NELFB inhibited myeloid differentiation primary response 88 (MyD88) induced transcription of an NF- κ B reporter gene construct in a dose-dependent manner. Overexpression of NLRC5 did not alter the negative effect of NELFB overexpression (**Figure 15A**). Interestingly, inhibition of NF- κ B activation by NELFB appeared to be specific for MyD88 induction and not due to general transcriptional of the reporter plasmid, as TNF α -induced NF- κ B activation remained unaltered (**Figure 15B**). Sin3A on the other hand did not influence the MyD88-induced NF- κ B response, neither in presence nor absence of NLRC5 (**Figure 15C**).

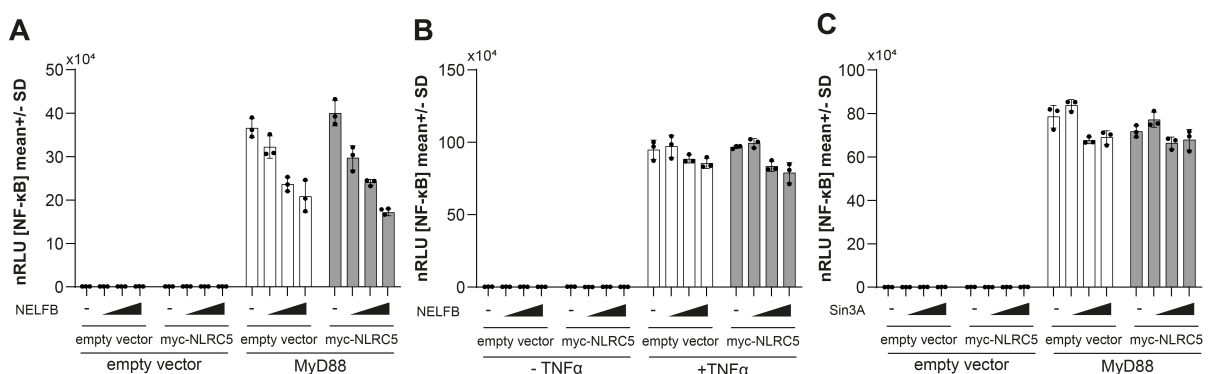


Figure 15: **NELFB and Sin3A do not synergize with NLRC5 in the regulation of NF- κ B responses.** (A-C) Reporter gene assays for NF- κ B. (A,B) NELFB, or (C) Sin3A were expressed at increasing amounts together with NLRC5. Activation of the NF- κ B response was either achieved by overexpression of MyD88, or stimulation with 10 ng/ml TNF. Luciferase activity was normalized against β -galactosidase activity (nRLU). Representative results of two independent experiments, conducted in triplicates.

Results

In conclusion, NELFB appears to possess an inhibitory role in MyD88-induced NF- κ B response independent of NLRC5, hinting towards a more general means of inhibition.

Overall, I employed several approaches to identify novel interaction partners of NLRC5 which might play a role in conferring specificity for MHC class I transcription, as well as interaction partners, specific for the subcellular compartments, in which NLRC5 is present. We further analyzed the role of two NLRC5 interaction partners, Sin3A and NELFB, with known roles in transcriptional regulation, in NLRC5-mediated MHC class I regulation, and the regulation of innate immune responses. Here we observed, that both Sin3A and NELFB were negative regulatory factors of MHC induction by both NLRC5, as well as CIITA, and that NELFB negatively influenced innate immune responses, regardless of NLRC5.

3.1.5 Structural analysis of NLRC5

Recombinant expression of NLRC5 in bacteria

Besides by identification of novel interaction partners, protein functions can be unraveled by solving the protein structure and identifying structurally related proteins and domains. Recombinant expression of human proteins in bacteria is a helpful tool for the production and purification of large amounts of proteins, which are needed for structural analysis. To optimize recombinant expression in *E. coli*, we generated a codon optimized version of NLRC5 and subcloned expression constructs of codon optimized NLRC5, the NLRC5 DD, the LRRs and isoform 3 (schematic representation **Figure 16**).

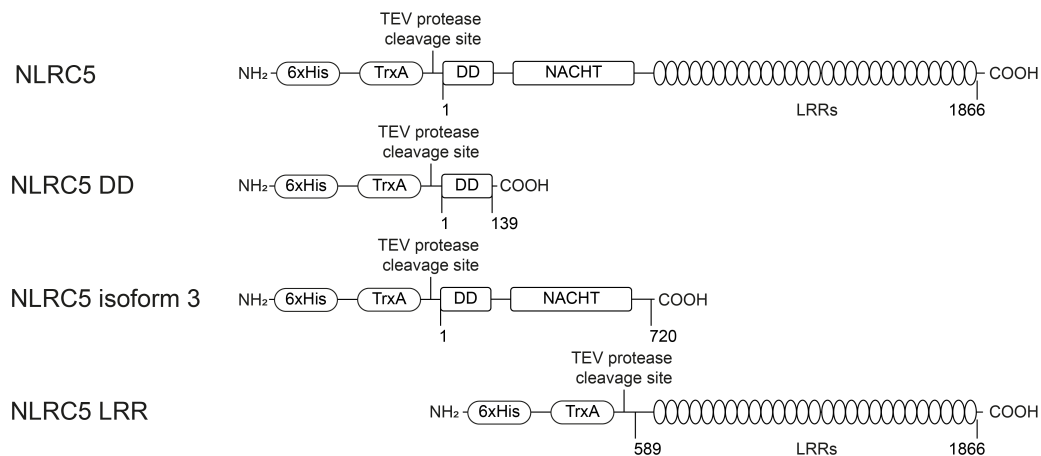


Figure 16: Schematic representation of constructs for recombinant expression. NLRC5, codon optimized for expression in *E. coli*, was used to generate expression constructs, encompassing either full-length NLRC5, the NLRC5 death domain like fold (NLRC5 DD), NLRC5 isoform 3 (NLRC5 isoform 3), or the NLRC5 leucine-rich repeats (NLRC5 LRR). The constructs were generated as fusion proteins with bacterial thioredoxin A (TrxA) for stabilization of bacterial expression and a 6x histidine-tag (6xHis) for purification. The linker region between the tag and the NLRC5 domain construct encompassed a restriction site (ENLYFQS) for tobacco etch virus protease (TEV) to remove the tag after purification. Numbers indicate the first and last amino acid of the construct in the original NLRC5 protein. NACHT: Nucleotide binding and oligomerization domain.

For enhanced expression and purification, the genes of interest were cloned, in frame, at the C-terminus of the *E. coli* protein thioredoxin 1 (TrxA), with an N-terminal 6xHis tag. TrxA serves as an expression

Results

scaffold, which has been shown to increase the solubility and biological activity of several recombinantly expressed proteins (LaVallie *et al.* 1993). The linker region contained a tobacco etch virus (TEV) protease recognition and cleavage site, which can be used to cleave the protein of interest from the N-terminal tag (**Figure 16**).

To obtain optimal conditions, expression was tested in *E. coli* strains BL21 (DE3), BL21 (DE3) tuner, BL21 (DE3) pLysS, C41 (DE3), and C43 (DE3) and at 20°C and 30°C. Full-length NLRC5 could not be visualized as a distinct protein band by colloidal Coomassie staining in any of the tested conditions (**Figure 17A**). When lysates were subjected to immunoblot analysis, protein bands at the expected size of NLRC5 were observed in BL21 (DE3) and, to lower extent, in BL21 (DE3) pLysS (**Figure 17B**). Here expression at 20°C yielded higher protein levels than at 30°C (**Figure 17B**, WCL, upper and lower panel). However, the protein was not soluble under any of the tested conditions (**Figure 17B**, soluble fraction).

Similarly, the NLRC5 LRRs were not observed in Coomassie staining of whole cell lysates in any of the tested conditions (**Figure 18A**), but proteins could be readily detected in immunoblots of whole cell lysates of BL21 (DE3) and BL21 (DE3) pLysS (**Figure 18B**, WCL upper and lower panel). Like NLRC5 FL, the LRRs were only present in the whole cell lysates but were not soluble (**Figure 18 B** soluble fraction).

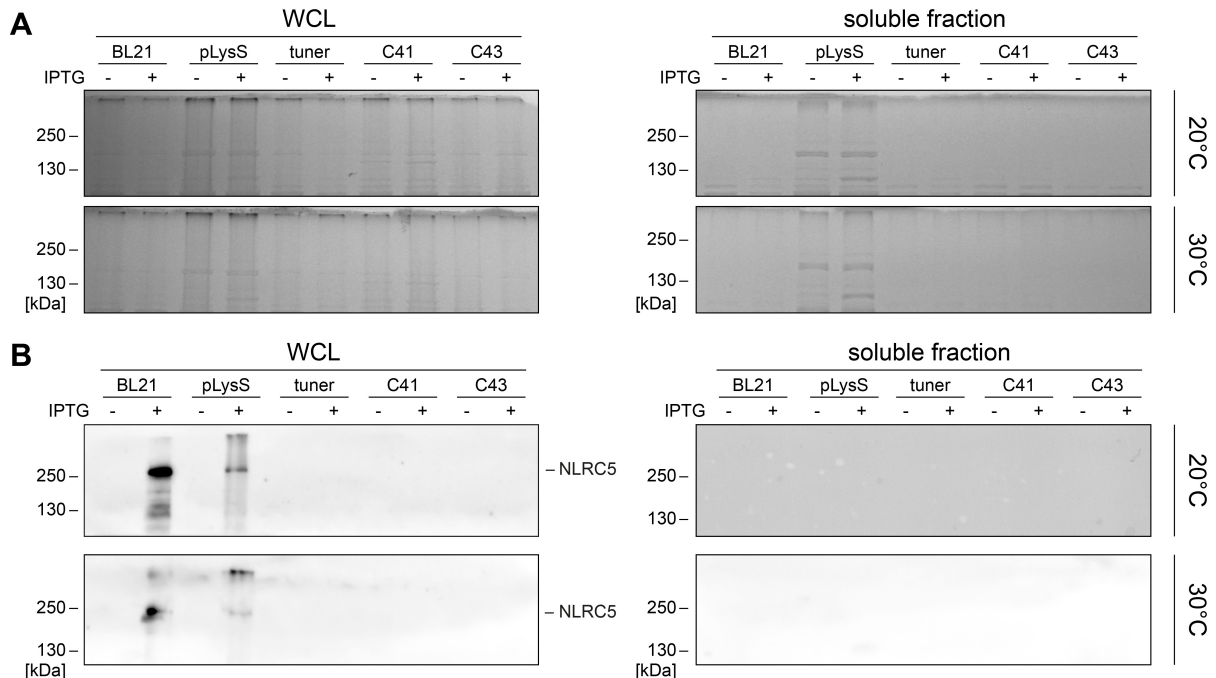


Figure 17: *E. coli* BL21 and pLysS express recombinant but insoluble NLRC5 FL. (A,B) Transformed bacteria were grown at 37°C for 5 h, diluted to an OD₆₀₀ of 0.3 and incubated at either 20°C or 30°C. Of each bacterial strain, one culture was left untreated, and one was induced with 0.5 mM IPTG and incubated for 22 h. An equal number of bacteria were either lysed directly in Laemmli buffer (WCL) or lysed in fresh LB medium with FastBreak lysis buffer and cleared by centrifugation (soluble fraction). (A) Coomassie staining of *E. coli* WCL or soluble fractions (B) Immunoblot of *E. coli* WCL or soluble fractions. NLRC5 was detected with 3H8 antibody.

Results

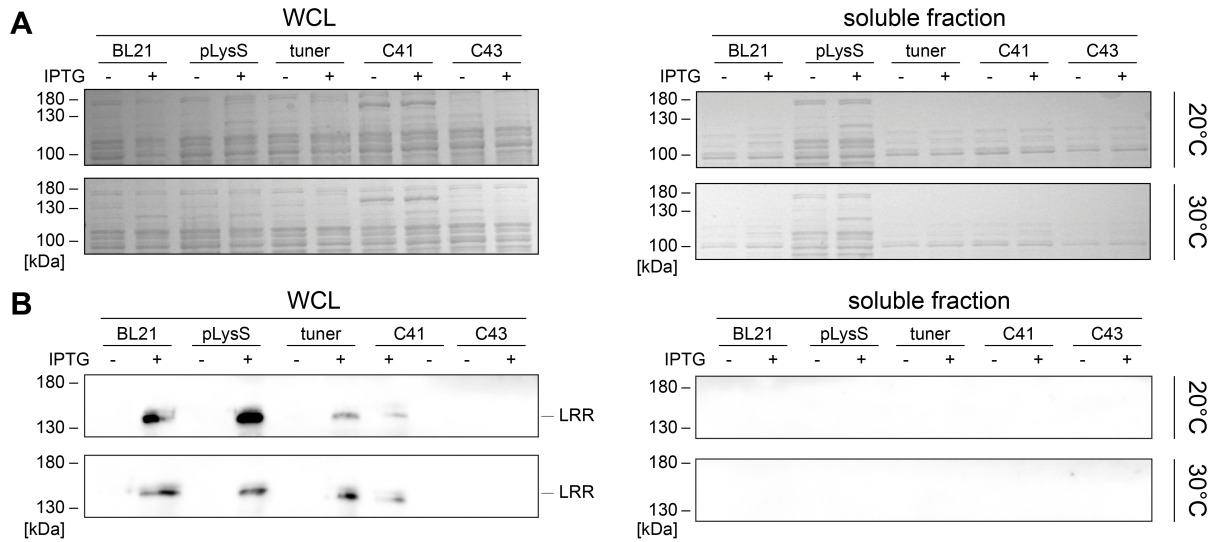


Figure 18: *E. coli* BL21, pLysS, tuner and C41 express recombinant, but insoluble NLRC5 LRR. (A,B) Transformed bacteria were grown at 37°C for 5 h, diluted to an OD600 of 0.3 and incubated at either 20°C or 30°C. Of each bacterial strain, one culture was left untreated, and one was induced with 0.5 mM IPTG and incubated for 22 h. An equal number of bacteria were either lysed directly in Laemmli buffer (WCL) or lysed in fresh LB medium with FastBreak lysis buffer and cleared by centrifugation (soluble fraction). (A) Coomassie staining of *E. coli* WCL or soluble fractions. (B) Immunoblot of *E. coli* WCL or soluble fractions. NLRC5 LRRs were detected with 3H8 antibody.

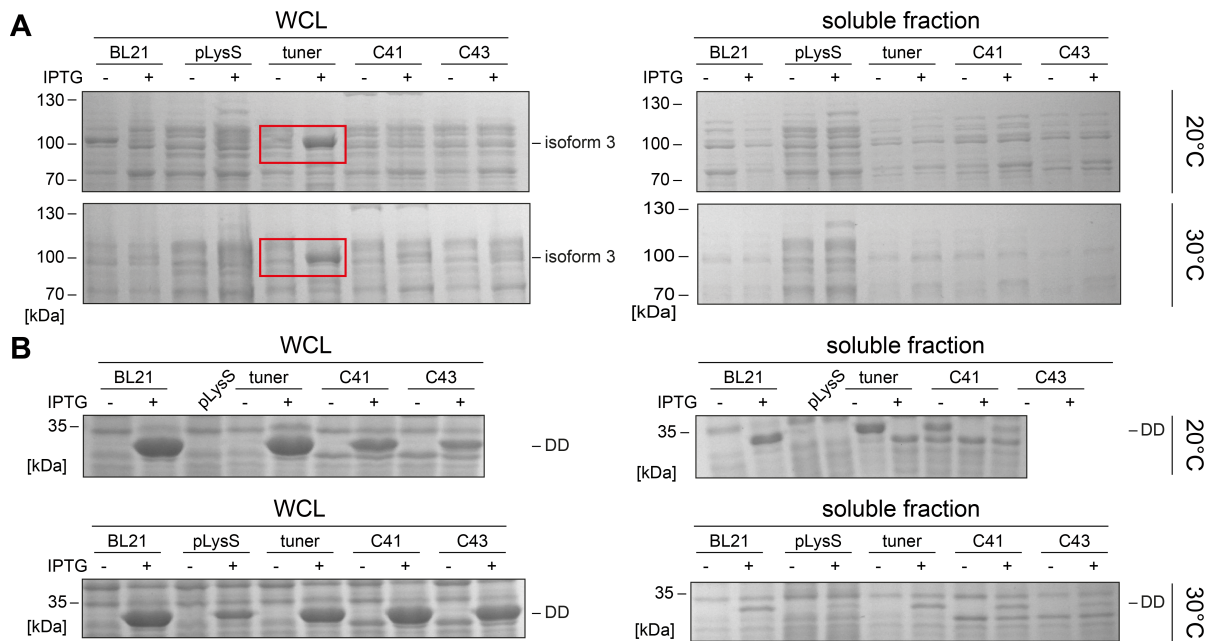


Figure 19: NLRC5 isoform 3 and the NLRC5 death domain like fold are well expressed in *E. coli*. (A,B) Transformed bacteria were grown at 37°C for 5 h, diluted to an OD600 of 0.3 and incubated at either 20°C or 30°C. Of each bacterial strain, one culture was left untreated, and one was induced with 0.5 mM IPTG and incubated for 22 h. An equal number of bacteria were either lysed directly in Laemmli buffer (WCL) or lysed in fresh LB medium with FastBreak lysis buffer and cleared by centrifugation (soluble fraction). Coomassie staining of *E. coli* whole cell lysate (WCL) and soluble fraction of bacteria transformed with (A) NLRC5 isoform 3 and (B) the NLRC5 death domain like fold (DD). Expressed isoform 3 in BL21 (DE3) tuner is highlighted with a red box.

In contrast to recombinantly expressed NLRC5 FL and LRR, the isoform 3 of NLRC5 was detectable by Coomassie staining of protein lysates from transformed BL21 (DE3) tuner, both at 20°C and 30°C, at comparable levels (Figure 19A, WCL), however not in the corresponding soluble fractions

Results

(**Figure 19A**, soluble fraction). NLRC5 DD was abundantly expressed in WCL of all tested strains, with exception of the pLysS strain, in which the protein band was much less prominent, at 30°C (**Figure 19B**, WCL). In contrast to the other recombinantly expressed constructs, the DD was also found in the soluble fractions of the BL21 (DE3), tuner and C41 strains (**Figure 19B**, soluble fraction). It showed higher solubility when expressed at 20°C, compared to 30°C (**Figure 19B**, soluble fraction).

In conclusion, we were able to express all generated constructs of NLRC5 in at least one distinct expression condition. However, except for the NLRC5 DD, all proteins were not soluble and thus require additional refolding steps after purification. Furthermore, expressed NLRC5 FL and the LRRs were only detectable in immunoblot, indicating only low protein yield.

Large scale expression and purification of NLRC5 DD

To obtain a sufficient amount of NLRC5 DD protein for subsequent crystallization trials and structure determination, a large-scale expression and purification protocol was established. This was performed in collaboration with Dr. Begoña Heras at LaTrobe University in Melbourne. Cell lysates of 2 L IPTG-induced *E. coli* BL21 (DE3) bacterial cultures were subjected to immobilized metal affinity chromatography (IMAC) on a HisTrap column to retain the 6x His-tagged TrxA-DD fusion protein. Following fast protein liquid chromatography (FPLC) the fusion-protein containing fractions 4 to 7 (**Figure 20A**) were pooled and a total protein amount of 84 mg was determined by measurement of A_{280} . After tobacco etch virus protease cleavage overnight the protein solution was again loaded onto a HisTrap column, to retain the 6xHis-TrxA-tag. However, analysis of the flowthrough and the collected fractions revealed, that both TrxA, as well as the NLRC5 DD, were retained by the nickel column and, eluted together in fractions 2 and 3 (**Figure 20B**). The protein containing fractions were pooled and dialyzed against a salt free HEPES buffer, concentrated and subjected to MonoQ anion exchange chromatography (**Figure 20D**). Elution of NLRC5 DD started as early as in fraction 5, however, the bulk of the protein was present in fractions later than 22. The band at the size of TrxA was present from fraction 22 onward (**Figure 20D**). Thus, fractions 7 to 21 were pooled, and protein concentration was determined by measurement of A_{280} , revealing a total amount of 720 ng of protein. A next step of size exclusion chromatography to try to separate the NLRC5 DD from larger, contaminating proteins, could unfortunately not be performed, due to the developments of the SARS-CoV2 pandemic in the spring of 2020, which forced us to end the stay at LaTrobe University ahead of schedule. The collaboration will be continued to further the approaches for the purification and crystallization of the NLRC5 DD.

In conclusion, we laid the foundation for structural analysis of NLRC5 DD by generating expression constructs for recombinant expression in bacteria and we established a suitable purification protocol.

Results

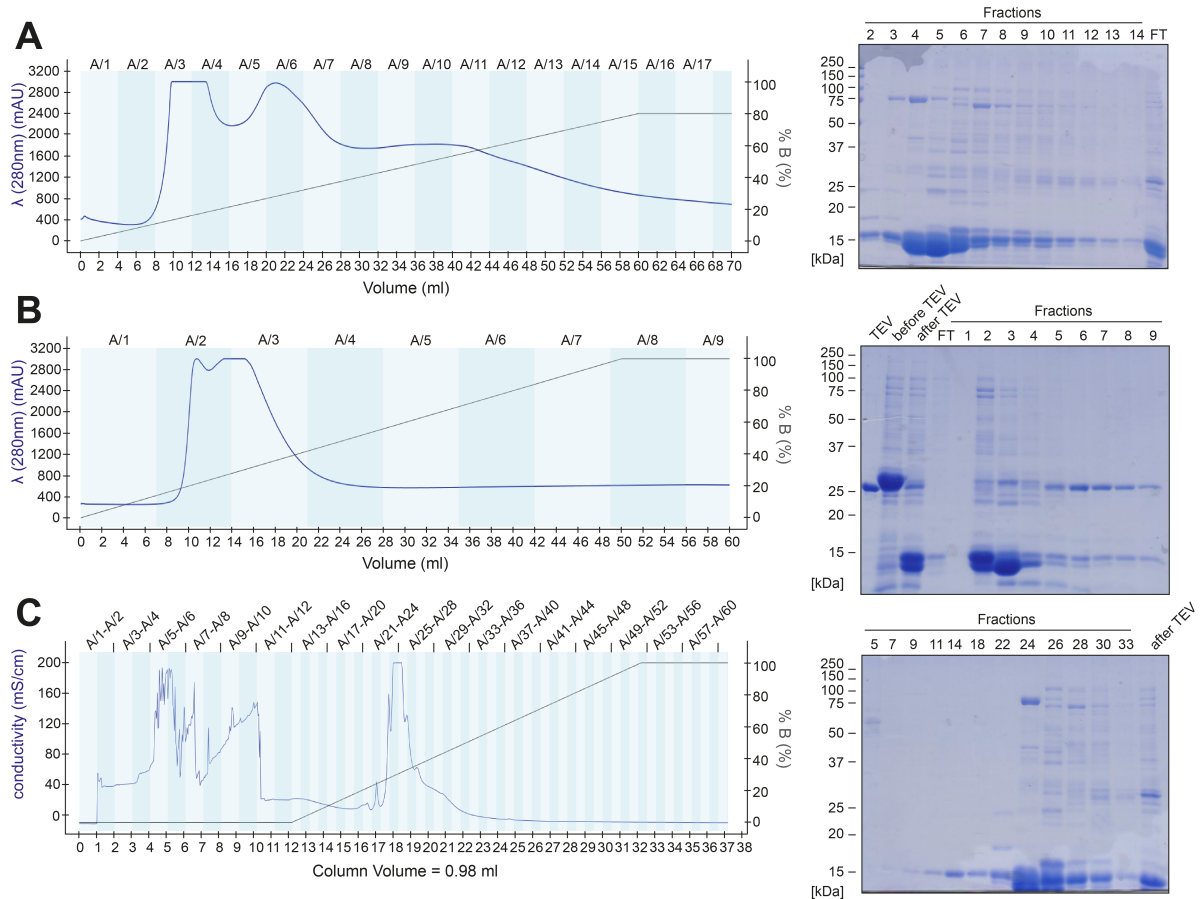


Figure 20: Recombinant expression and purification of NLRC5 DD. (A) Lysates of *E. coli* BL21 (DE3) expressing 6xHis-TrxA-DD fusion proteins were subjected to HisTrap immobilized metal affinity purification with an elution buffer gradient up to 80%. Fractions were collected, subjected to SDS-PAGE and visualized by Coomassie staining. (B) Pooled protein containing fractions were subjected to HisTrap FPLC after TEV cleavage and dialysis overnight. Elution of bound proteins was performed with a gradient of elution buffer up to 100%. Eluted fractions were subjected to SDS-PAGE and visualized by Coomassie staining. (C) MonoQ Anion exchange chromatography of NLRC5 DD-containing fractions. After flow through of 12 column volumes of buffer A, bound proteins were eluted with a gradient of elution buffer. Fractions were collected, subjected to SDS-PAGE and visualized by Coomassie staining. (A,B) Protein concentrations in milli arbitrary units (mAU), as determined by λ_{280} measurement, or (C) conductivity in mS/cm are plotted as a blue line against the volume, passed through the column. The percentage of elution buffer (%B) is indicated as grey lines. Elution was performed with elution buffer, containing (A,B) 25 mM HEPES pH 8.0, 150 mM NaCl, 500 mM Imidazole, or (C) 25 mM HEPES pH 8.0, 1 M NaCl. FT: Flow-through; TEV: Tobacco etch virus protease.

3.2 DDX3X links NLRP11 to the regulation of type I interferon responses and NLRP3 inflammasome activation

The second part of the thesis focused on the mechanisms behind the regulatory effect of NLRP11 in type I IFN responses (Qin *et al.* 2017, Ellwanger *et al.* 2018). As it was reported that NLRP11 inhibits type I interferon by the initiation of TRAF6 degradation (Qin *et al.* 2017), but also downstream of TBK1 overexpression (Ellwanger *et al.* 2018), we wanted to understand the underlying mechanisms behind the inhibition of TBK1-induced type I interferon response.

3.2.1 Identification of novel NLRP11 interaction partners

Cloning of NLRP11-eGFP

In a first step to gain deeper insight into the function of NLRP11 and to create new tools to monitor the spatiotemporal distribution of NLRP11 in living cells, we generated NLRP11-eGFP and eGFP-NLRP11 expression constructs. Expression of the NLRP11 constructs was verified by transient transfection in HEK293T cells and subsequent immunoblotting. Here the construct for N-terminal fusion of eGFP (eGFP-NLRP11) did not express (**Figure 21A**), thus further experiments were conducted with the C-terminally tagged NLRP11-eGFP. As also previously observed for myc-NLRP11 (data not shown), NLRP11-eGFP formed an SDS-stable, high molecular weight complex (**Figure 21A**). Additionally, two protein products at approximately 28 and 20 kDa were observed, when the membranes were probed with an antibody directed against GFP, likely representing eGFP transcribed from internal start-codons or degradation products (**Figure 21A**).

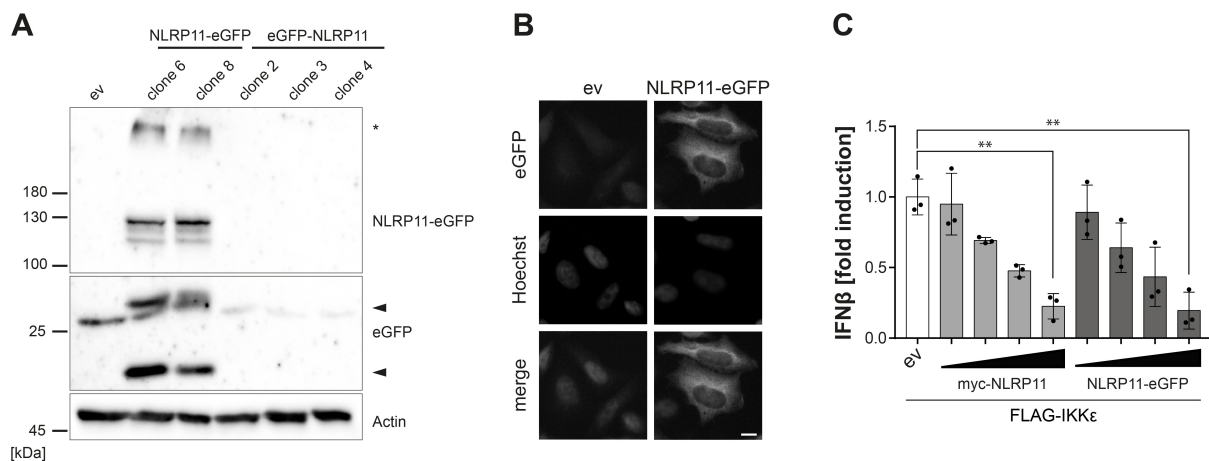


Figure 21: **Functional validation of NLRP11-eGFP and eGFP-NLRP11 plasmids.** (A) Immunoblot of NLRP11-eGFP and eGFP-NLRP11 transiently overexpressed in HEK293T cells. Membranes were probed with antibodies against eGFP and actin as a loading control. ►: eGFP likely expressed from internal START-codons. (B) Immunofluorescence micrographs of HeLa cells transiently transfected with either NLRP11-eGFP, or empty vector (ev). eGFP signal (green) and Hoechst-stained DNA (blue) are shown. Scale bar = 10 μ m. (C) *ifnb* luciferase assay in HEK293T cells transfected with IKK ϵ and either empty vector (ev), myc-NLRP11, or NLRP11-eGFP. Mean of three independent experiments conducted in triplicates \pm SEM relative to ev is shown. **, $p < 0.01$. Welch's two-sided t-test.

Results

Localization and functionality of the constructs were verified by transient expression in HEK293T cells and subsequent indirect immunofluorescence, and *ifn β* luciferase reporter gene assay. We observed a cytosolic distribution (**Figure 21B**), as well as a negative effect on IKK ϵ -induced *ifn β* induction comparable to myc-NLRP11 (**Figure 21C**).

Generation and characterization of stable, NLRP11-eGFP expressing cell lines

Next, the above characterized NLRP11-eGFP construct was used to generate stable, doxycycline (Dox)-inducible cell lines using the HEK293 FlpIn and HeLa FlpIn lines. Based on expression levels and tightness of expression, one clone for each HEK293 and HeLa FlpIn NLRP11-eGFP lines was selected and the following experiments were performed using HEK293 FlpIn NLRP11-eGFP clone 34 and HeLa FlpIn NLRP11-eGFP clone 15 (**Figure 22A**).

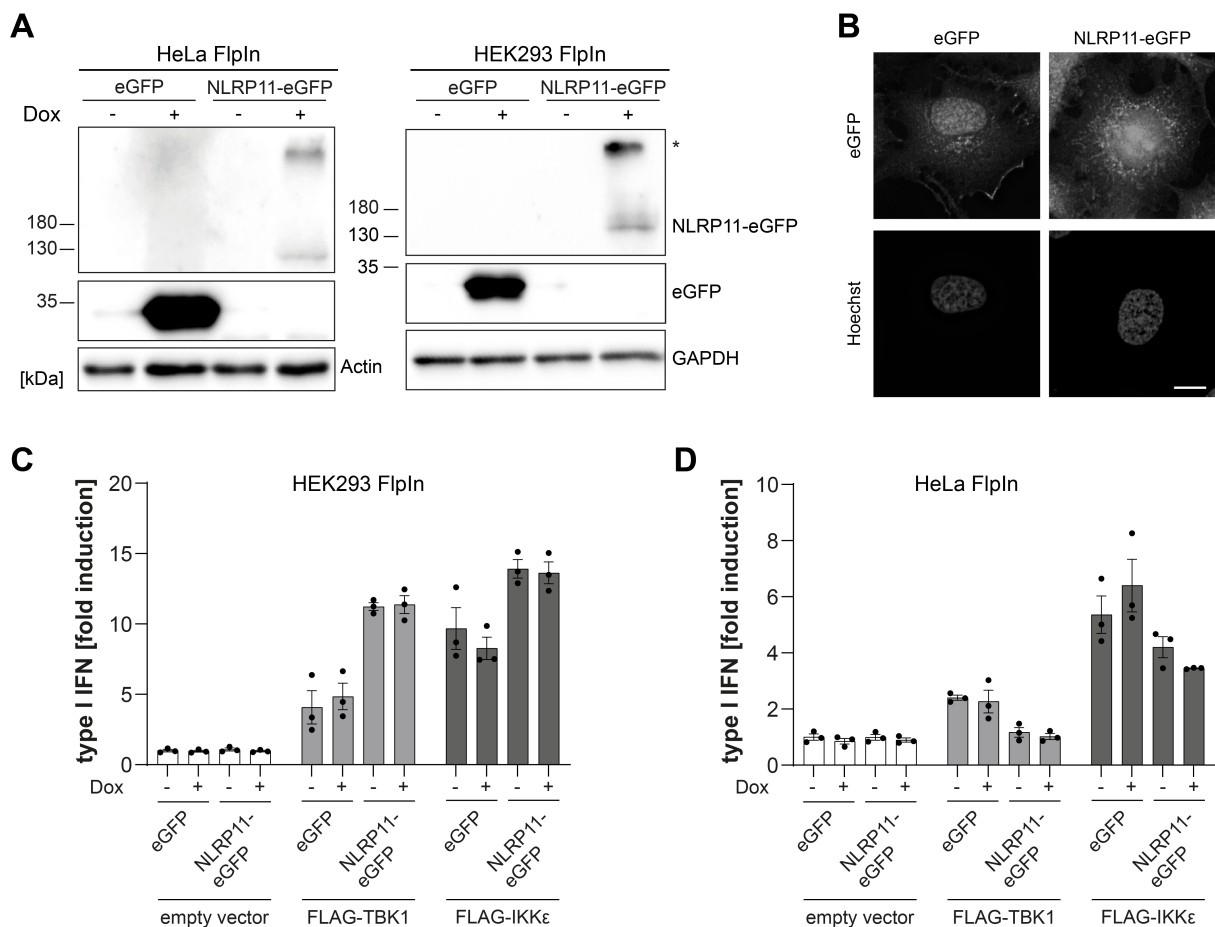


Figure 22: Characterization of HEK293 and HeLa NLRP11-eGFP FlpIn cells. (A) Immunoblot of HeLa and HEK293 FlpIn eGFP and NLRP11-eGFP mono-clonal populations. Membranes were probed for eGFP and either actin or GAPDH as loading control. (B) Immunofluorescence micrographs of HeLa FlpIn NLRP11-eGFP cells. Cells were induced with 1 μ g/ml doxycycline overnight, fixed and nuclei were stained with Hoechst. 3D-deconvolution of z-stacks of the signal of Hoechst-stained DNA (blue) and eGFP (green) are shown. Stack size = 0.2 μ m. Scale bar = 10 μ m. (C,D) Type I IFN response of (C) HEK293 and (D) HeLa FlpIn eGFP and NLRP11-eGFP cells in response to overexpression of TBK1, or IKK ϵ . Cells were induced with 1 μ g/ml doxycycline overnight and transfected with equal amounts of either empty vector, FLAG-TBK1, or FLAG-IKK ϵ . Supernatants were collected 20 h after transfection and used to stimulate HEK blue IFN α/β cells. Means \pm SEM of three independent experiments, of which SEAP assays were performed in technical duplicates are shown.

Results

All tested clones showed the previously observed high molecular weight signal, when NLRP11-eGFP was expressed (**Figure 22A**). The localization of induced NLRP11-eGFP was confirmed to be cytosolic. However, closer inspection showed that NLRP11 tended to form perinuclear clusters (**Figure 22B**).

As NLRP11 is an inhibitor of the type I IFN response downstream of TBK1 (Ellwanger *et al.* 2018), we analyzed the type I IFN response of the selected clones after overexpression of either FLAG-TBK1, or FLAG-IKK ϵ . HEK293 FlpIn NLRP11 cells responded with higher type I IFN secretion to either overexpression of TBK1 or IKK ϵ , compared to HEK293 eGFP cells, as visualized in HEK blue IFN α/β reporter cell lines (**Figure 22C**). Induction of NLRP11 by doxycycline did not result in a further change of the response (**Figure 22C**). HeLa NLRP11-eGFP cells showed less induction of type I IFN after overexpression of TBK1 or IKK ϵ , in comparison to unstimulated cells, than the HeLa eGFP controls (**Figure 22D**). Additionally, induction of NLRP11 by treatment with doxycycline resulted in a trend towards a lower type I IFN response upon IKK ϵ overexpression (**Figure 22D**).

Identification of novel NLRP11 interactors by co-immunoprecipitation and mass spectrometry

HeLa NLRP11-eGFP and HeLa eGFP cells were used to identify novel interaction partners of NLRP11 by GFP-IP and LC-MS/MS. A list of candidate proteins was identified which were found in both experiments but were not present in any precipitates from HeLa eGFP cells (**Table 13**).

From this list of candidate interaction partners, sequestosome 1, also known as p62, was selected due to its known functions in autophagy (Johansen and Lamark 2011), and DDX3X due to its well described functions in antiviral innate immune signaling (Schröder *et al.* 2008, Soulat *et al.* 2008, Szappanos *et al.* 2018). Both proteins were promising candidates as targets of NLRP11 in negative regulation of the type I IFN response.

Results

Table 13: **List of proteins that co-precipitated with NLRP11-eGFP.** Proteins identified by nano LC-ESI-MS/MS in two independent co-immunoprecipitation experiments (#1, #2). Number of identified unique peptides are shown of proteins of which no peptides were identified in the control immunoprecipitation (eGFP). Proteins selected for further evaluation are displayed in bold letters.

Gene symbol	Protein name	Unique peptides	
		#1	#2
NLRP11	NACHT, LRR and PYD domains-containing protein 11	38	50
ABCD3	ATP-binding cassette subfamily D member 3	1	1
ACTN1	Alpha-actinin 1	2	1
ALDH3A2	Fatty aldehyde dehydrogenase	2	2
ANP32A	Acidic leucine-rich nuclear phosphoprotein 32 family member A	1	2
BAG6	Large proline-rich protein BAG 6	1	8
BASP1	Brain acid soluble protein 1	5	2
DDX3X	ATP-dependent RNA helicase DDX3X	1	2
DNAJB1	DnaJ homolog subfamily B member 1	1	7
GNAS	Guanine nucleotide-binding protein G(s) subunit alpha isoforms XLas	10	4
GNB2	Guanine nucleotide-binding protein G(I)/G(S)/G(T) subunit beta-2	11	3
GNG12	Guanine nucleotide-binding protein G(I)/G(S)/G(O) subunit gamma-12	4	1
HAX-1	HCLS1-associated protein X-1	2	3
HSPH1	Heat shock protein 105 kDa	1	8
PSMC5	26S proteasome regulatory subunit 8	1	4
PSMD1	26S proteasome non-ATPase regulatory subunit 1	3	5
PSMD2	26S proteasome non-ATPase regulatory subunit 2	1	6
PSMD3	26S proteasome non-ATPase regulatory subunit 3	1	3
PSMD6	26S proteasome non-ATPase regulatory subunit 6	1	1
PSMD11	26S proteasome non-ATPase regulatory subunit 11	2	5
PSMD13	26S proteasome non-ATPase regulatory subunit 13	2	2
PSMD14	26S proteasome non-ATPase regulatory subunit 14	1	6
RPN2	Dolichyl-diphosphooligosaccharide-protein-glycosyltransferase subunit 2	1	4
RPS24	40S ribosomal protein S24	2	2
RTN4	Reticulon-4	1	1
SQSTM1	Sequestosome 1	3	5
STIP1	Stress-induced-phosphoprotein 1	14	27
STUB1	E3 ubiquitin protein ligase CHIP	8	10
TKT	Transketolase	1	1
TUBB2A	Tubulin beta-2A chain	1	1
UBL4A	Ubiquitin-like protein 4A	2	7

NLRP11 interacts with DDX3X and p62

For the validation of the identified interactions, GFP-IPs were performed after transient overexpression of HA-p62 in HEK293 eGFP, or NLRP11-eGFP cells. HA-p62 co-precipitated well with NLRP11-eGFP, however a slight band was also visible in the eGFP control (**Figure 23A**). Endogenous DDX3X was also shown to interact specifically with stably expressing NLRP11-eGFP in HEK293 NLRP11-eGFP cells (**Figure 23A**). Lack of an antibody recognizing NLRP11 prevented us from verifying the interaction between endogenous NLRP11 and endogenous DDX3X. Both a commercially available antibody against NLRP11 (Novus, NBP 1-92189), and an in house generated antibody against

Results

an NLRP11 peptide (Eurogentech), were not able to specifically detect endogenous NLRP11 (data not shown).

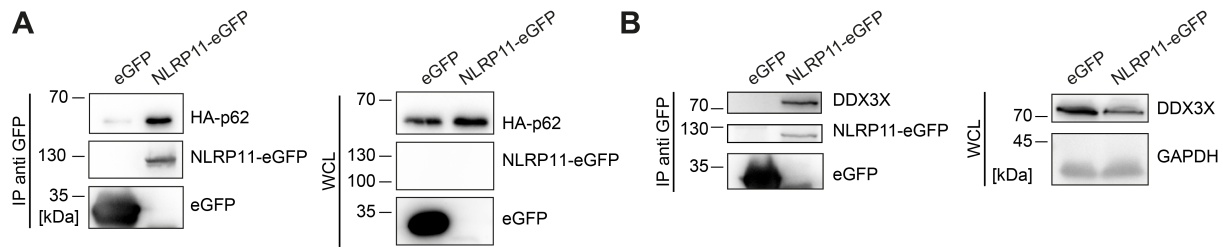


Figure 23: **Validation of the interaction of NLRP11 with DDX3X and p62.** (A) Immunoblots from anti-GFP-immunoprecipitations (IP) from HEK293 eGFP and NLRP11-eGFP cells induced overnight with 1 μ g/ml doxycycline and transiently transfected with HA-p62. Membranes of IPs and whole cell lysates (WCL) were probed for the HA-tag and eGFP. Representative blots of two independent experiments are shown. (B) Immunoblots from anti-GFP IPs from HEK293 NLRP11-eGFP cell induced overnight with doxycycline. Membranes of IPs were probed for DDX3X and GFP, membranes of WCL for DDX3X, and GAPDH as loading control. Blots are representative of at least two independent experiments. Experiments were performed by Clarissa Gottschild.

In conclusion, we identified novel interaction partners for NLRP11 by co-IP and LC-MS/MS analysis from HeLa NLRP11-eGFP cells, of which we could validate DDX3X and p62 as specific interactors for NLRP11-eGFP in HEK293 NLRP11 cells. In the subsequent studies we focused on DDX3X due to its well-known role in interferon responses (Schröder *et al.* 2008, Soulat *et al.* 2008, Oshiumi *et al.* 2010)

3.2.2 Functional characterization of the interplay between NLRP11 and DDX3X

NLRP11 interacts with DDX3X via its leucine-rich repeats

To map the DDX3X interaction domain within NLRP11 we first generated an eGFP-tagged version of DDX3X by molecular cloning. eGFP-DDX3X strongly bound NLRP11 and the NLRP11 Δ PYD (Figure 24A, B). Robust co-precipitation was also observed with the LRR domain of NLRP11 (Figure 24B). As the NACHT domain of NLRP11 by itself did not specifically interact with eGFP-DDX3X (Figure 24B), this indicates that the LRRs are the domain through which NLRP11 binds to DDX3X.

We next set out to analyze the functional relevance of the DDX3X-NLRP11 interaction. First, we tested whether the NLRP11-DDX3X complex changed during SeV infection. Starting at 4 h post infection, we observed increased expression levels and co-IP of endogenous DDX3X with NLRP11-eGFP in HEK293 FlpIn cells. This was strongest at 6 h and 16 h post infection (Figure 25A). We next analyzed the subcellular localization dynamics of NLRP11 and DDX3X during SeV infection by indirect immunofluorescence microscopy. We confirmed co-localization of NLRP11 and DDX3X in the cytosol of HEK293 NLRP11-eGFP cells. This co-localization persisted and appeared even slightly enhanced during SeV infection with more pronounced co-localization at 16 h post infection, compared to steady-state levels (Figure 25 B). Co-localization of DDX3X and NLRP11-eGFP was also observed in HeLa NLRP11-eGFP cells, where NLRP11-eGFP continued to co-localize with DDX3X over the course of infection in the majority of cells up to 16 h post infection (Figure 25C). However, NLRP11 was not

Results

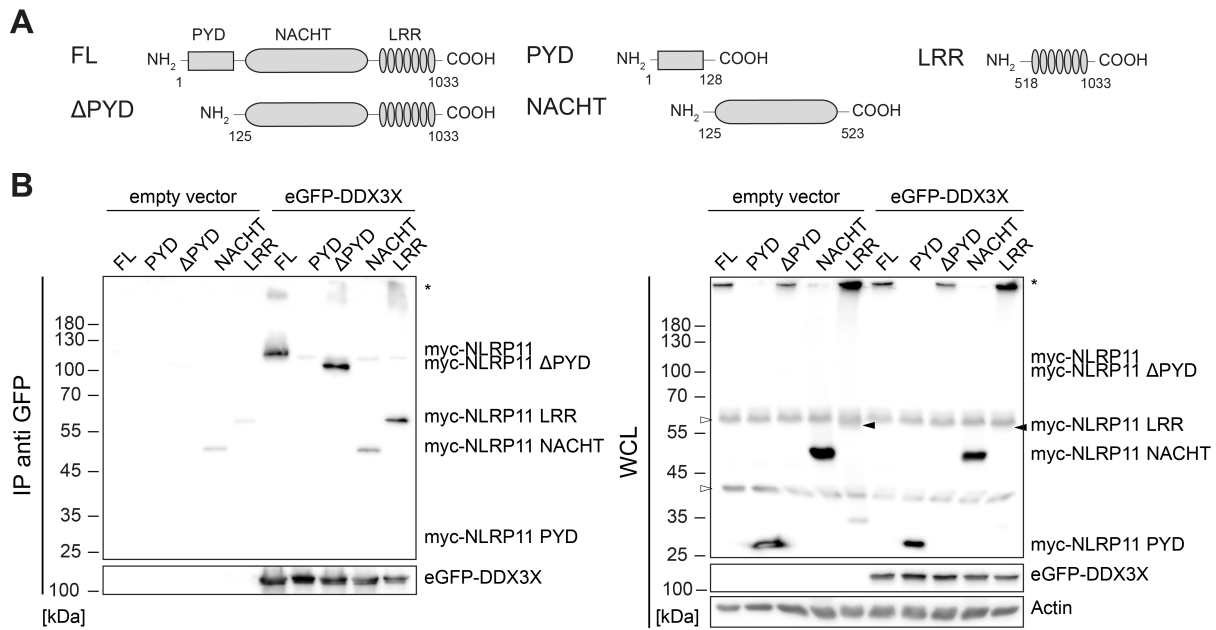


Figure 24: **DDX3X interacts with the LRRs of NLRP11.** (A) Schematic representation of myc-NLRP11 truncation mutants. Corresponding protein domains are indicated above, amino acid positions within full-length NLRP11 are indicated below. (B) Immunoblots of anti-eGFP-immunoprecipitations (IP) from HEK293T cells transfected with either an empty vector, or eGFP-DDX3X and the indicated myc-NLRP11 truncation mutants. Membranes of IPs and whole cell lysate (WCL) were probed against the myc-tag and eGFP. Membranes of WCL were additionally probed for actin as a loading control. * high-molecular weight NLRP11 aggregate; ► myc-NLRP11-LRR; ▷ unspecific bands.

recruited to distinct DDX3X clusters that appeared 16 h post infection in a minority of cells (**Figure 25D**). These structures likely represent stress granules, to which DDX3X is known to be recruited (Shih *et al.* 2012, Pene *et al.* 2015, Samir *et al.* 2019). The formation of those structures was not influenced by the presence, or absence of NLRP11 (**Figure 25D**).

Qin *et al.* reported that NLRP11 exerts its inhibitory function in type I IFN induction by being recruited to the MAVS signaling complex, where it induces the degradation of TRAF6 (Qin *et al.* 2017). As recruitment of DDX3X to MAVS has also been reported, we wanted to investigate, whether the interaction between NLRP11 and DDX3X might take place at the mitochondria. In line with the data published by Qin *et al.* (Qin *et al.* 2017), NLRP11 did not show co-localization with the mitochondrial marker apoptosis-inducing factor (AIF) in HEK293 cells at steady-state conditions, but we observed recruitment of NLRP11 to mitochondria at 16 h post infection (**Figure 26A**). In HeLa NLRP11-eGFP cells, NLRP11 was localized in proximity to mitochondria in untreated cells and this localization pattern persisted during 16 h of SeV infection with partial co-localization observed at 16 h post infection (**Figure 26B**).

Taken together, we demonstrated that NLRP11 localized in proximity to mitochondria and that the interaction between NLRP11 and DDX3X occurred in the cytosol.

Results

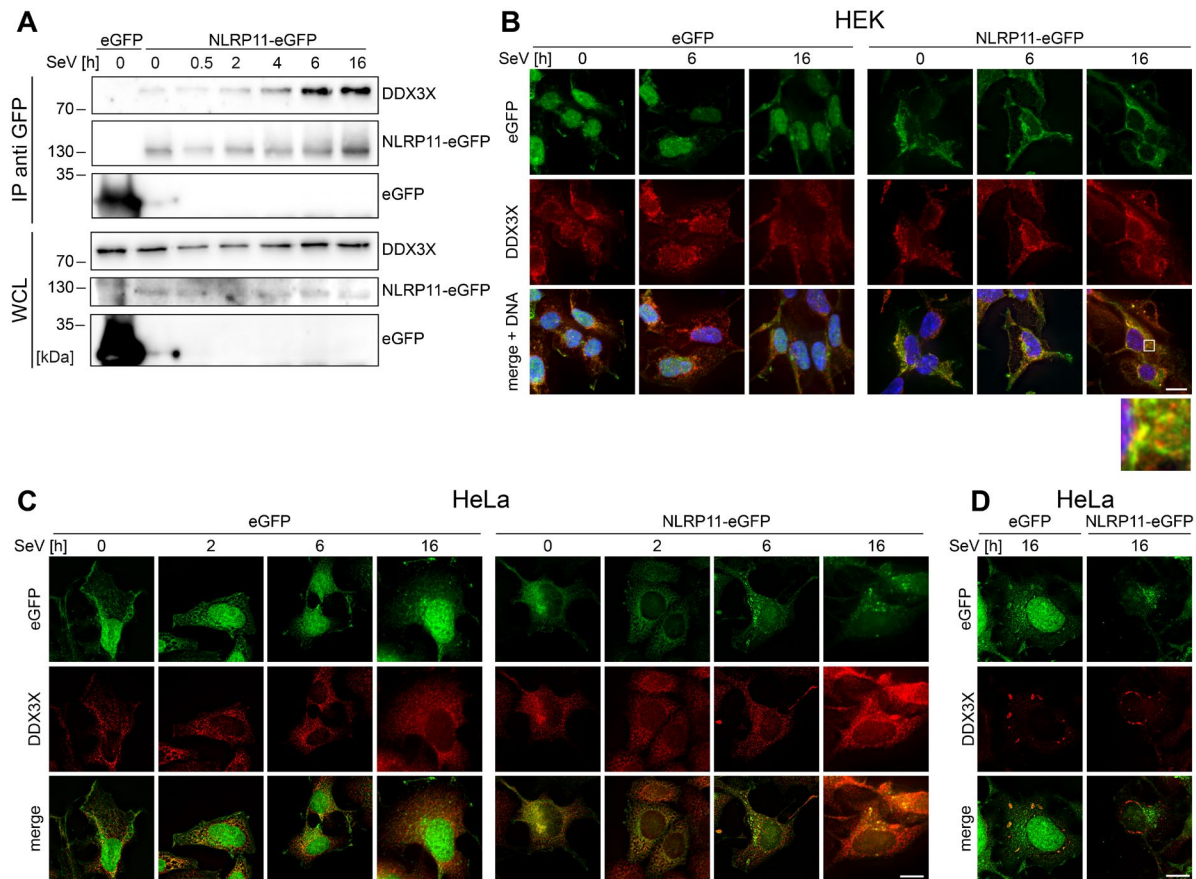


Figure 25: **Sub-cellular localization of NLRP11 and DDX3X upon infection.** (A) Immunoblot of anti-GFP-immunoprecipitation (IP) from HEK293 eGFP and NLRP11-eGFP cells after induction with 1µg/ml doxycycline overnight and subsequent infection with SeV for the indicated time. Membranes of IPs and whole cell lysates (WCL) were probed for DDX3X and GFP. (B-D) Indirect immunofluorescence micrographs of (B) HEK293, or (C,D) HeLa-eGFP, or NLRP11-eGFP cells induced with 1µg/ml doxycycline overnight and subsequently infected with Sendai virus (SeV) for the indicated time. 3D deconvolution of staining of DDX3X (red) together with the eGFP signal (green) are shown. Nuclei are stained with Hoechst (blue). Scale bar = 10 µm.

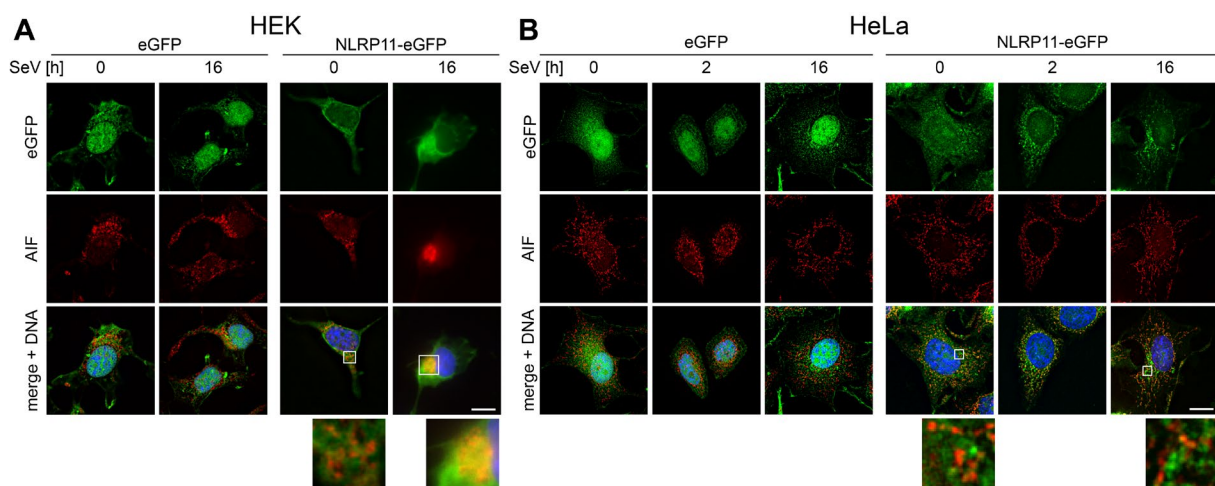


Figure 26: **Investigation of NLRP11-recruitment to mitochondria during SeV infection.** (A,B) Indirect immunofluorescence micrographs of (A) HEK293 or (B) HeLa-eGFP, or NLRP11-eGFP cells induced with 1µg/ml doxycycline overnight and subsequently infected with SeV for the indicated time. 3D deconvolution of AIF-staining (red) together with the eGFP signal (green) are shown. Nuclei are stained with Hoechst (blue). Scale bar = 10 µm.

Results

NLRP11 prevents IKK ϵ induced phosphorylation of DDX3X

Alteration of the status of PTMs is a common mechanism by which inhibitory effects are conferred. Gu *et al.* reported that phosphorylation of DDX3X by IKK ϵ is a prerequisite for the activation of IRF3 and subsequent transcription from the *Ifnb* promoter (Gu *et al.* 2013). We therefore investigated whether NLRP11 inhibits this phosphorylation of DDX3X by IKK ϵ . As previously shown, co-expression of IKK ϵ and DDX3X in HEK293T cells resulted in a shift of the electrophoretic mobility of DDX3X, which is indicative of phosphorylation at its N-terminus (Gu *et al.* 2013). Co-expression of NLRP11 clearly suppressed this up-shift (**Figure 27A**).

Our previous data indicates that the ability of NLRP11 to inhibit TBK1-induced transcription from the *Ifnb* promoter is dependent on its LRRs (Ellwanger *et al.* 2018). Given that the LRR region also interacted with DDX3X (**Figure 24B**), we investigated, whether this domain was also required for the inhibition of DDX3X phosphorylation and subsequent activation of IRF3. Expression of full-length NLRP11, NLRP11 Δ PYD and NLRP11 LRR reduced the IKK ϵ -induced upshift of DDX3X, while this was not observed for the PYD or NACHT domains of NLRP11 (**Figure 27B**). NLRP11, as well as NLRP11 Δ PYD and the NLRP11 LRRs, inhibited IKK ϵ -mediated phosphorylation of DDX3X, while no changes were apparent in presence of the PYD, or the NACHT domain (**Figure 27B**). Accordingly, serine 396 phosphorylation of IRF3, indicative of activation and a prerequisite for the induction of type I IFNs, was strongly reduced when NLRP11, NLRP11 Δ PYD or the NLRP11 LRRs were overexpressed (**Figure 27B**).

To investigate the consequences of the NLRP11-DDX3X interaction on IFN β induction, we performed siRNA-mediated knockdown of NLRP11 in macrophage-like differentiated THP-1 cells, in which DDX3X expression was suppressed by Tet-inducible expression of a DDX3X-specific short hairpin RNA (shRNA) (THP-1 shDDX3X) (Fullam *et al.* 2018). We employed THP-1 cells as a model, as they show higher expression levels of endogenous NLRP11 than HEK293T or HeLa cells (Ellwanger *et al.* 2018). In accordance with recent data (Qin *et al.* 2017, Ellwanger *et al.* 2018), knockdown of NLRP11 resulted in significantly increased IFN β production in response to SeV infection (**Figure 27C**). Knockdown of DDX3X resulted, as reported previously (Schröder *et al.* 2008), in reduced IFN β secretion (**Figure 27C**). However, DDX3X depletion (+Dox) led to a similar ration of IFN β reduction compared to control (-Dox) in both siCtrl and siNLRP11 treated cells (**Figure 27C**). Measurement of the type I IFN response by a bioassay showed a qualitatively similar result (**Figure 27C**).

Results

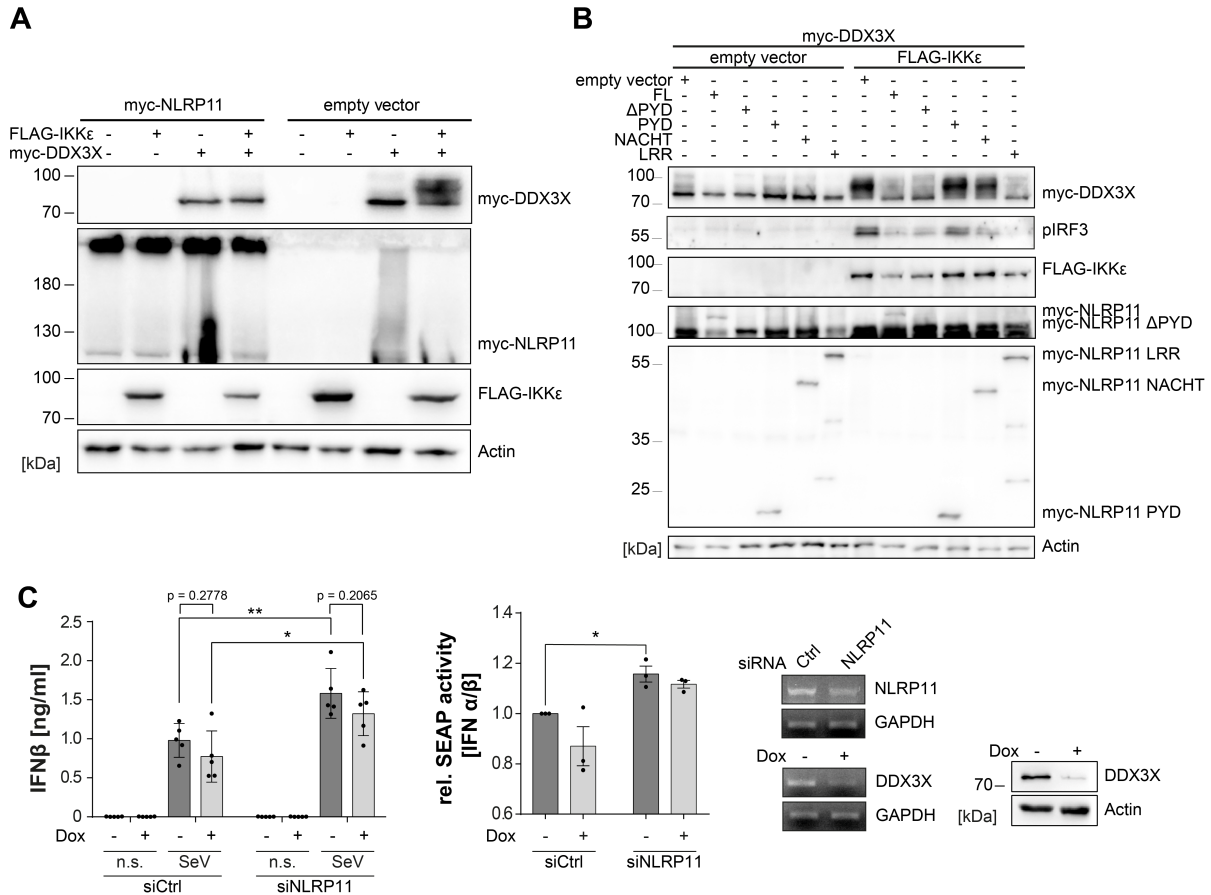


Figure 27: NLRP11 inhibits the phosphorylation of DDX3X by IKKε. (A,B) Immunoblot of whole cell lysates from HEK293T cells expressing FLAG-IKKε, myc-DDX3X and either (A) myc-NLRP11, or (B) myc-NLRP11 deletion constructs as indicated. Membranes were probed for the myc- and FLAG-tags, pIRF3, and actin as loading control. Representative blots of at least two independent experiments are shown. (C) IFN release from macrophage-like differentiated shDDX3 THP-1 cells. DDX3X targeting shRNA was expressed by induction with 1μg/ml doxycycline (Dox) for 48 h and NLRP11 was targeted by siRNA transfection for 72 h, as indicated. Cells were infected with SeV for 16 h. IFNβ levels, determined by ELISA, and relative type I IFN levels, determined by HEK IFNα/β blue assay ± SEM are depicted (IFNβ n = 5; type I IFN n = 3). * p < 0.05; ** p < 0.01 Welch's two-sided t-test. Knockdown efficiency of NLRP11 and DDX3X was validated by endpoint PCR and protein levels of DDX3X by immunoblot. Membranes were probed for DDX3X and actin as a loading control (right panels). n.s.: not stimulated.

In conclusion, we were able to show that NLRP11 inhibits the hyperphosphorylation of DDX3X by IKKε, and subsequent activation of IRF3 via the LRR domain. The interaction of DDX3X and NLRP11 took place in the cytoplasm, and we could corroborate the recruitment of NLRP11 to the mitochondria in HEK293 NLRP11-eGFP cells. However, in HeLa NLRP11-eGFP cells, no co-localization between NLRP11 and the mitochondrial marker AIF was observed during the course of infection.

NLRP11 affects the NLRP3 inflammasome

Since NLRP11 belongs to the class of PYD containing NLR proteins, and it was further identified in a shRNA screen as a candidate contributing to *Mycobacterium tuberculosis*-induced IL-1β secretion (Mishra *et al.* 2010), we asked whether NLRP11 is an inflammasome forming NLR protein. Indirect immunofluorescence of overexpressed myc-NLRP11 together with HA-ASC revealed that, contrary to myc-NLRP3, myc-NLRP11 was not recruited to ASC-specks (**Figure 28A**).

Results

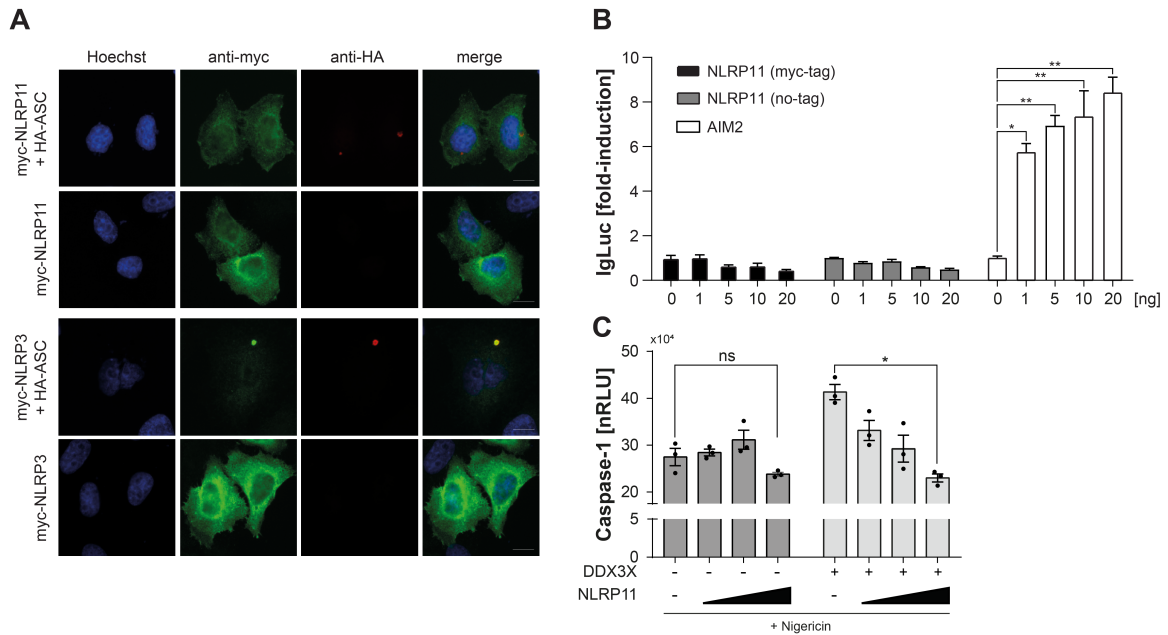


Figure 28: NLRP11 inhibits NLRP3 inflammasome via DDX3X. (A) Indirect immunofluorescence micrographs of HeLa cells, transiently transfected HA-ASC, myc-NLRP3 and myc-NLRP11 as indicated. Staining for the myc- (red) and HA-tags (green) is shown. Scale bar = 10 μ m. (B) iGLuc caspase-1 activation assay in HEK293T cells transiently transfected with caspase-1 (10 ng), HA-ASC (10 ng), together with the indicated amount of either myc-NLRP11, NLRP11, or HA-ASC. Mean \pm SD of three independent experiments is depicted. *, $p < 0.05$; **, $p < 0.005$. (C) iGLuc caspase-1 activation assay in HEK293T cells transiently transfected with caspase 1 (10 ng), HA-ASC (10 ng), myc-NLRP3 (15 ng) together with the indicated proteins. After expression for 20 h, cells were treated with 15 μ M nigericin for 3 h. Mean of three independent experiments conducted in triplicates \pm SEM are depicted. * $p < 0.05$; Welch's two-sided t-test.

Further evaluation of the effect of overexpressed myc-NLRP11 on caspase-1 activity, using caspase-1 luciferase reporter assay (Bartok *et al.* 2013), revealed no activation of overexpressed caspase-1 by NLRP11, but rather a dose-dependent inhibitory effect (**Figure 28B**). As DDX3X was recently identified as a positive regulator of NLRP3-inflammasome formation (Samir *et al.* 2019), we next investigated whether NLRP11 affects the function of DDX3X in this context. In line with the report from the Kanneganti lab (Samir *et al.* 2019), DDX3X enhanced nigericin-induced pro-caspase-1 cleavage in the luciferase reporter system. Overexpression of NLRP11 dose-dependently counteracted this effect of exogenous DDX3X (**Figure 28C**). To determine, whether the LRRs of NLRP11 were involved in the negative regulation of the NLRP3 inflammasome, we performed caspase-1 activation assays with our different NLRP11 truncation mutants. Expression of full-length NLRP11, or the LRRs, led to a significant reduction of nigericin-induced caspase-1 activation, while the PYD and the NACHT domain both showed no effect when the system was activated by nigericin (**Figure 29A**). The same trend was also observed in cells expressing only endogenous DDX3X (**Figure 29A**).

Results

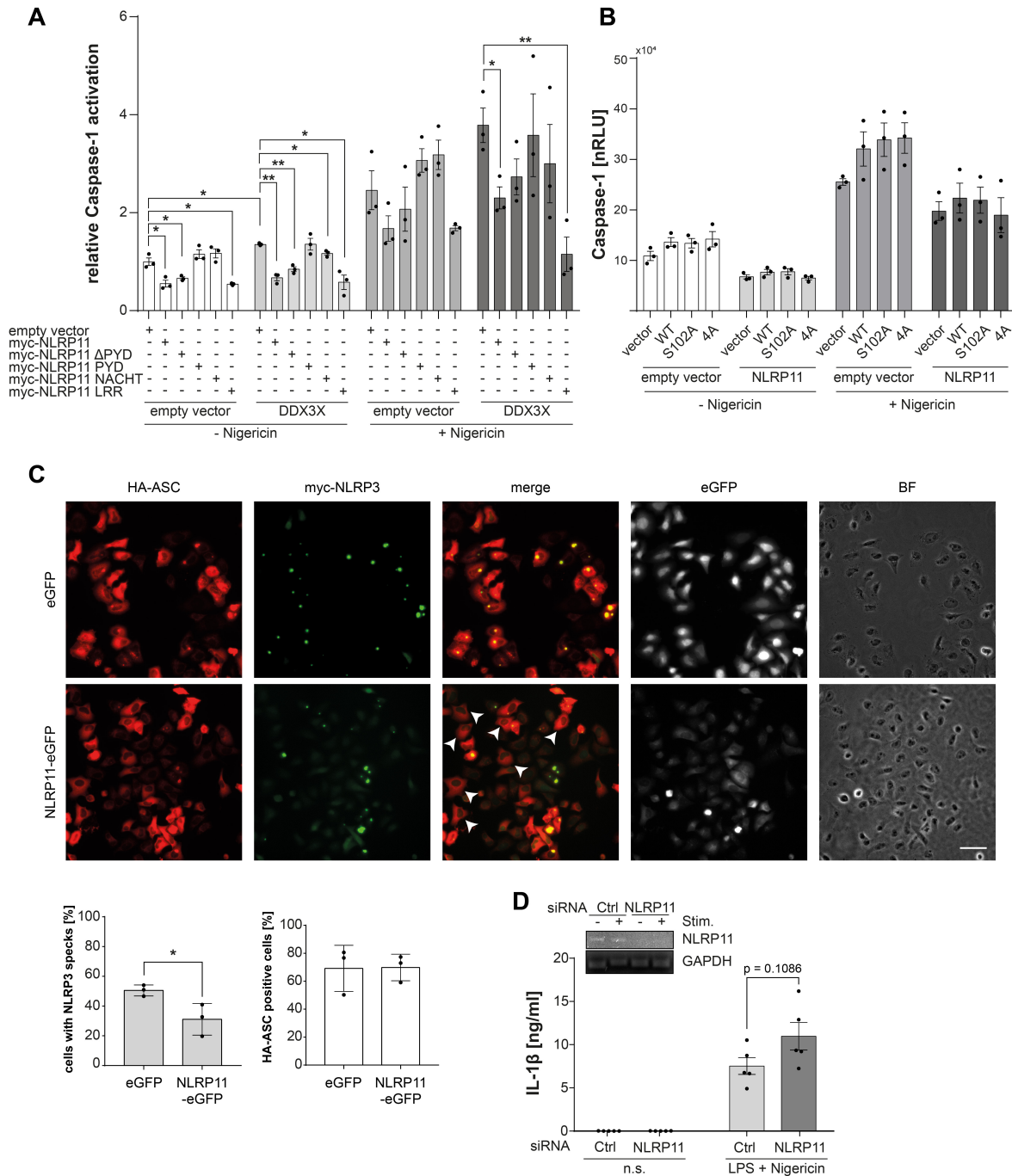


Figure 29: NLRP11 counteracts DDX3X during NLRP3 inflammasome activation. (A,B) iGLuc caspase-1 activation assay in HEK293T cells transiently transfected with caspase 1 (10 ng), HA-ASC (10 ng), myc-NLRP3 (15 ng) together with the indicated NLRP11 domain constructs and DDX3X, or the indicated DDX3X mutant. After expression for 20 h, cells were treated with 15 μM nigericin for 3 h. Mean from three independent experiments conducted in triplicates ± SEM. (A) Values are depicted relative to the mean of cells transfected with the reporter plasmid, myc-NLRP3, HA-ASC and caspase-1, not treated with nigericin. *, p < 0.05; **, p < 0.01. Welch's two-sided t-test. (C) Indirect fluorescence micrographs of HeLa eGFP or HeLa NLRP11-eGFP cells, induced with 1 μg/ml doxycycline overnight and transfected with HA-ASC and myc-NLRP3. Staining for the myc- (green) and HA-tags (red), as well as eGFP signal (white) and bright field images are shown. Images are representative of three independent experiments. Scale bar = 50 μm. HA-ASC expressing cells without speck-formation are indicated with white arrow heads. Right panels: Quantification of cells with myc-NLRP3 specks and quantification of cells with HA-ASC staining (blinded counting of 150 cells per condition from n = 3). (D) IL-1β release from macrophage-like differentiated THP-1 cells after 72 h of siRNA-mediated knockdown. Cells were primed for 4 h with 100 ng/ml LPS followed by stimulation with 10 μM nigericin for 2 h. Means of two independent experiments ± SEM are shown. Inlay: endpoint PCR for NLRP11 and GAPDH of a representative experiment for validation of knockdown efficiency. n.s.: not stimulated, n.d.: not detectable.

Results

As the data showed inhibition of caspase-1 activation in dependence of the LRRs, which were required for the inhibition of IKK ϵ -mediated phosphorylation (**Figure 27B**), we investigated whether DDX3X hyperphosphorylation at the N-terminus was relevant for both the positive effect of DDX3X on the NLRP3-inflammasome, as well as for the inhibition by NLRP11. For this, we overexpressed DDX3X mutants S102A and DDX3X 4A, in which either serine 102 (S102A), or 4 different potential IKK ϵ -dependent phosphorylation sites (S71A, S82A, S83A, S102A) (4A) in the N-terminus of DDX3X were replaced by alanine (Gu *et al.* 2013). Here we did not observe any differences between the WT and both mutants regarding caspase-1 activation and inhibition by NLRP11 (**Figure 29B**). To provide further evidence for the inhibition of NLRP3 inflammasome formation by NLRP11, we performed ASC-speck formation assays. When we overexpressed HA-ASC and myc-NLRP3 in HeLa NLRP11-eGFP cells, we observed fewer ASC-specks in NLRP11-eGFP expressing cells, compared to eGFP-expressing cells. Blinded quantification of both specks, as well as HA-ASC positive cells, showed a reduction from about 51% speck containing cells in HeLa eGFP to about 31% in HeLa NLRP11-eGFP (**Figure 29C**). Equal transfection rates were confirmed by blinded counting of HA-ASC positive cells (**Figure 29C**). To corroborate the negative regulatory role of NLRP11 in NLRP3-induced caspase-1 activation, we knocked down endogenous NLRP11 expression in macrophage-like differentiated THP-1 cells by specific siRNA, followed by activation of the NLRP3 inflammasome by priming with LPS and activation with nigericin. Knockdown of NLRP11 resulted in increased secretion of IL-1 β , although the increase did not reach significance ($p = 0.1086$) (**Figure 29D**).

Taken together, this data shows that the LRRs of NLRP11 are both necessary and sufficient to dampen NLRP3 inflammasome activation, which might be a result of DDX3X recruitment and possibly sequestration via the LRR domain of NLRP11. This effect is independent of DDX3X phosphorylation events, which are necessary for IFN β activation. Reduced numbers of ASC-speck formation in presence of NLRP11 strongly suggests that NLRP11 can inhibit the assembly of NLRP3 inflammasomes.

4 Discussion

It was previously shown that NLRC5 2xNLS, which is targeted to the nucleus, was much less efficient in inducing MHC class I transcription, than wild-type NLRC5, which shuttles between the cytoplasm and the nucleus (Neerincx *et al.* 2012). This indicates that temporary cytoplasmic localization might go hand in hand with protein-protein interactions of NLRC5 which are necessary for its activation. Such a mechanism would resemble, for example, a broad range of transcription factors, which need to be phosphorylated by different kinases for nuclear translocation and subsequent activation of transcription (Filtz *et al.* 2014). To date, however, no such mechanism is known for NLRC5. Here, we approached the identification of factors potentially relevant for this, by IP of either wild-type NLRC5, or predominantly nuclear localized NLRC5 2xNLS, and NLRC5 isoform 3. We further wanted to characterize the specific cytoplasmic and nuclear interactome of NLRC5 by analyzing the interactions of a nuclear (NLRC5 2xNLS) and cytoplasmic targeted (NLRC5 NLS I) form of NLRC5, in the corresponding subcellular fractions.

The identification of proteins from the nuclear pore complex in samples of NLRC5, and NLRC5 2xNLS, which both transition between the cytoplasm and the nucleus, indicates correct localization and translocation of the analyzed constructs, and validates the experimental procedure. However, the identification of exclusively nuclear localized proteins, such as Histone H4 and MCM7 in the cytosolic fraction, indicates that the fractionation protocol in the applied form was not optimal.

Several proteins with known DNA binding activity were identified specifically for full-length NLRC5. However, none of those factors are known transcriptional activators. Most of them are involved in DNA repair (RAD50 (Carney *et al.* 1998)), chromatin condensation (SMC4 (Kimura *et al.* 2001)), or cell cycle regulation (CDKN2A (Okamoto *et al.* 1994)), and we did not regard them as likely candidates for regulators of MHC class I transcription. Several components of the NuA4 histone acetyltransferase complex were identified in co-IPs with different NLRC5 bait constructs. Interaction of NLRC5 with RUVBL1 and RUVBL2 was found in both cytoplasmic and nuclear fractions, which however is not counterintuitive, as the proteins are also localized in both cellular fractions (Izumi *et al.* 2010, Taniuchi *et al.* 2014). Acetylation of CIITA by the histone acetyltransferase PCAF has been proposed to be required for nuclear translocation (Spilianakis *et al.* 2000), and a role of the highly conserved NuA4 (Doyon and Côté 2004) in nuclear translocation has recently been shown in yeast for several proteins (Walden *et al.* 2020). It thus appears plausible that acetylation of NLRC5 by the NuA4 complex might be involved in NLRC5 translocation into the nucleus and that the NuA4 complex might be an important regulatory mechanism in NLRC5-regulated MHC class I transcription.

Independent validation of co-IP data is needed to identify possible false positive results. For example, DBN1 and DPY30, two proteins identified as specific hits were flagged, when we compared our data

with the CRAPome (Mellacheruvu *et al.* 2013), a database dedicated to finding false positive proteins identified by different co-IP MS/MS approaches. As the database only contains a small number for eGFP-IPs with camelid antibodies, careful evaluation of the co-IP results is needed. Comparison with co-IPs of other NLR proteins, performed in our group, also revealed STUB1 as a consistently co-purifying protein of several human NLRs, indicating unspecific binding. Additionally, although co-IP and LC-MS/MS analysis identified several proteins as potential interactors of NLRC5, none of the proteins of the MHC enhanceosome were identified, although being ubiquitously expressed (Boss 1997). However, a similar observation, regarding the identification of RFX or NF-Y proteins in co-IP, has been made for CIITA (Masternak *et al.* 2000). This made it difficult to assess whether the identified interactors might be involved in transcriptional regulation of MHC class I. Thus, identification of NLRC5 interactors was additionally approached by other means.

4.1.1 Proximity ligation – a promising approach for the identification of novel interaction partners

Since the discovery, that NLRC5 engages the same MHC enhanceosome as CIITA (Meissner *et al.* 2012, Neerinx *et al.* 2012), it remains enigmatic, through which mechanisms both proteins confer their specificity. As it was shown that replacement of the N-terminal domain of CIITA with the NLRC5 DD was sufficient to induce transcription from the MHC class I promoter (Neerinx *et al.* 2014), we aimed to identify proteins specifically binding to the N-terminal DD of NLRC5. For this, we applied the BioID2 ligand system (Kim *et al.* 2016) and conducted a Y2H screen using the NLRC5 DD as bait.

Classical co-IP strategies are limited by the need of a highly stable protein-protein interaction and both transient and low affinity interactions, that are physiologically highly important can be missed (Perkins *et al.* 2010). To circumvent this problem, we employed the BioID2 system to gain deeper insights into the interactome of the NLRC5 DD. This proximity ligation approach is well suited to identify transient interactions and has also been widely applied for the identification of interaction networks of transcription factors (Kim *et al.* 2017, Trinkle-Mulcahy 2019, Carnesecchi *et al.* 2020, Ummethum and Hamperl 2020, Göös *et al.* 2021).

As NLRC5 is a very large protein with a complex tertiary structure (Mótyán *et al.* 2013), we expected that fusion of the BioID2 to the full-length protein would disturb folding and expression or result in impaired functionality. Indeed, lack of protein expression was observed for the LRR-BioID2 fusion protein. We thus only applied BioID2 to analyze the interactome of the well-expressed N-terminal DD, the domain likely responsible for MHC class I specificity (Neerinx *et al.* 2014). The use of the NLRC5-DD however raises the problem, that interactions, which might be dependent on prior complex formation by full-length NLRC5, might be missed, as the DD by itself is not sufficient to induce MHC class I transcription, although it translocates into the nucleus and has low intrinsic transcriptional activity (Neerinx *et al.* 2012). However, the identification of several histone proteins in three of the four

Discussion

conducted experiments indicated, that the NLRC5 DD itself is likely recruited to the chromatin. This was further substantiated by the identification of several proteins known to be involved in chromatin organization and translational regulation in some of the experiments. However, only three of them could be confirmed in independent replicates. With the BioID2 approach, we faced the problem that reproducibility between independent experiments was low. This is a major challenge for the identification of specific interactors, especially when no direct interaction between the two proteins is necessary. This was further complicated by the observation that the BioID2 control did not show the same subcellular localization as our bait. In further research, several strategies might be approached to overcome the challenges we faced. Although our approaches to target the BioID2 control into the nucleus were not successful (data not shown), nuclear localization was observed in the DD-BioID2 fusion protein. Thus, to generate a proper control, fusion proteins of BioID2 with a different nuclear localizing protein need to be used. The CIITA N-terminal domain, which also contains transcriptional activity (Raval *et al.* 2001), localizes to the nucleus due to a bipartite NLS between amino acids 141 to 159 (Spilianakis *et al.* 2000). It could thus serve as a viable candidate here, as this could already give an indication whether transcription factors are specific for either NLRC5 or CIITA and thus for MHC class I and class II, respectively.

Additionally, approaches to adapt proximal ligation could benefit from recent developments in the field. BioID2 is limited to non-dynamic processes, as 16 h of biotinylation are required to generate sufficient amounts of biotinylated proteins for efficient precipitation and identification (Kim *et al.* 2016, Sears *et al.* 2019). This has been overcome by the development of two new biotin ligases, termed TurboID and miniTurboID, which exhibit similar levels of biotinylation within 10 min, as BioID2 exhibits after 18 h (Branon *et al.* 2018). This system might be able to broaden the range of questions which can be addressed, for example to elucidate the differences in the NLRC5 interactome after stimulation with IFN γ . This would resemble the situation of MHC class I induction more closely than simple NLRC5 overexpression.

Due to the limited reproducibility between the independent replicates in stable K562 cells, and the discrepancies in subcellular localization between DD-BioID2 and the BioID2 control, the proteins identified here can only serve as an initial impression of possible nuclear interactors of the NLRC5 DD. We therefore shifted our focus from the identification of novel interaction partners by BioID2 towards the well-established Y2H system.

4.1.2 Sin3A and NELFB do not determine MHC class I specificity of NLRC5

Y2H screening has the benefit of screening large cDNA libraries for interactors with the desired bait. Besides high throughput, this means, that also interactions of proteins with low expression in the cellular models used for co-IP can be identified. Further, transient, and low-affinity interactions can be identified here, in contrast to co-IPs. Additionally, the hits are scored based on the results within the screen, but

Discussion

also based on bioinformatic data, facilitating a more robust interpretation of the results and reliable identification of artifacts (Rain *et al.* 2001). The screen was carried out against a human thymocyte library, containing cDNA from both CD4⁺ and CD8⁺ T cells, in which high expression of NLRC5 was reported (Neerinx *et al.* 2010). Physiological expression of NLRC5 and MHC I molecules in these cells makes it highly likely that factors, which are important for MHC class I transcription are represented in the library. As the NLRC5 DD translocates into the nucleus (Neerinx *et al.* 2012), the identification of interactions with several karyopherin α proteins, which mediate nuclear import (Oka and Yoneda 2018), supports the validity of the screen. The NLRC5 DD was described as the domain which confers transcriptional regulation (Neerinx *et al.* 2014). It is thus thought to recruit the Pol II complex and transcription factors to the MHC class I locus. However, Y2H screening only identified few proteins with known functions in transcriptional regulation, of which only NELFB and Sin3A reached high confidence scores. Sin3A is an essential scaffold for the histone deacetylase complex and controls transcriptional regulation (Silverstein and Ekwall 2005). Histone acetylation has been shown to be an important regulatory mechanism for CIITA-induced MHC class II transcription (Magner *et al.* 2000, Beresford and Boss 2001, Osborne *et al.* 2001). Although we confirmed the interaction between the NLRC5-DD and full-length NLRC5 with Sin3A in co-IPs, the effect of Sin3A overexpression in NLRC5-induced MHC class I transcription was only limited, and Sin3A did also inhibit CIITA-induced MHC class II transcription as previously described (Zika *et al.* 2003). It is thus likely, that regulation of histone acetylation by NLRC5 is a mechanism which might be involved in the regulation of MHC class I transcription, however, Sin3A is likely not a key determining factor for MHC class I specificity of NLRC5. Interestingly, C-terminal binding protein 2 (CtBP2), which we identified as an interactor in co-IPs, has been reported to interact with endogenous Sin3A and HDAC2 (Koipally and Georgopoulos 2000), supporting the notion that histone deacetylation by Sin3A and HDACs are involved in transcriptional regulation by NLRC5.

NELFB a subunit of the negative elongation factor complex was previously found to associate with a majority of expressed genes, including several MHC class I and MHC class II genes in mice (Sun *et al.* 2011). However, only a fraction of those genes, including H2-DMA and H2-M2, was differentially regulated, when *Nelfb* was knocked out (Sun *et al.* 2011). In line with that, and like Sin3A, the interaction with NELFB was not specific for NLRC5-induced MHC class I transcription, but also inhibited CIITA-induced MHC class II transcription. The observed inhibition is likely due to general promoter proximal pausing induced by NELFB overexpression. This is also in line with our observation, that NELFB overexpression, inhibits the MyD88-induced NF- κ B response. However, in macrophages, promoter proximal pausing has been described as a mechanism for the rapid initiation of pro-inflammatory response genes upon LPS-stimulation (Adelman *et al.* 2009). Accumulation of paused Pol II transcription complexes downstream of the promoter can lead to rapidly initiated transcription of target genes upon an appropriate stimulus, as the transcription machinery is already assembled and only

needs to be released (Gariglio *et al.* 1981, Wu *et al.* 2003, Adelman *et al.* 2009, Core and Adelman 2019). It thus remains to be answered whether promoter proximal pausing, initiated by the NELF complex is indeed solely inhibitory in the context of MHC transcription. Thus, the possibility remains, that NLRC5 recruits NELFB to the assembled Pol II complex in steady state conditions to initiate an immediate transcriptional response upon IFN γ stimulation. However, as for Sin3A, our data indicates, that this would not be a mechanism which determines the specificity of NLRC5 for MHC class I transcription.

4.1.3 Recombinant expression of NLRC5

Unraveling the structure of proteins can serve as a potent way to understand their functions by structural comparison to similarly structured proteins and domains with known functions, or by identifying important residues and secondary structures which form regions likely involved in protein-protein interactions. Hitherto no crystal structure of NLRC5 or its domains has been reported. Here, we set out to establish a protocol for recombinant expression and purification of NLRC5, the LRRs, isoform 3, and the DD. For several NLR proteins, such as NOD1, NLRP1, or NLRC4, structural analysis of recombinantly expressed proteins has successfully been performed (Askari *et al.* 2012, Hu *et al.* 2013, Reubold *et al.* 2014, Bentham *et al.* 2017). However, due to the large size of NLRC5 and the complex, predicted structure of its LRRs (Mótyán *et al.* 2013), recombinant expression proved difficult as only low yields could be obtained. This complicates crystallization approaches, during which several different conditions need to be tested to generate high quality protein crystals (McPherson and Gavira 2014). Additionally, as was also observed for isoform 3 and the LRRs, recombinantly expressed proteins were not present as soluble proteins, although TrxA fusion was used to enhance protein solubility (LaVallie *et al.* 1993). For those constructs additional refolding approaches need to be evaluated (Yamaguchi and Miyazaki 2014). Alternatively, baculoviral expression in insect cells has been applied for the expression and crystalization of several other NLRs (Hu *et al.* 2013, Sharif *et al.* 2019). This system provides the benefit of post-translational modifications which resemble the mammalian environment more closely than bacteria. This can positively influence solubility and expression levels of the recombinant proteins (Christian and Andreas 2013) and should thus be evaluated for the expression of NLRC5 and the LRRs. Only the TrxA-DD fusion protein was both expressed at sufficiently high levels for purification and crystallization and was present as soluble protein. Although the NMR structure of the N-terminal domain of murine NLRC5 has previously been solved (Gutte *et al.* 2014), structural analysis by NMR and crystallography are complementary methods. While NMR excels at solving flexible structures within proteins, X-ray crystallography typically provides higher resolution (Krishnan and Rupp 2012). Purification of recombinantly expressed 6xHis-TrxA-NLRC5 DD yielded large quantities of proteins. However, due to difficulties of separating the NLRC5 DD from 6xHis-TrxA due to unexpected binding of NLRC5-DD to the nickel IMAC column, most of the protein was lost. The small size difference between the NLRC5 DD (17 kDa) and TrxA (11kDa) is not sufficient to efficiently

Discussion

separate these proteins by size exclusion chromatography, and anion exchange chromatography also resulted in insufficient separation of these two proteins. Separation of NLRC5 DD and 6xHis-TrxA needs to be further optimized to yield larger quantities of purified NLRC5 DD in subsequent work. Alternatively, recombinant expression of the NLRC5 DD without TrxA needs to be evaluated, as has been successfully performed for several other NLR effector domains, such as the pyrin domains of NLRP4 and NLRP9, or the CARD domain of NLRC4 (Eibl *et al.* 2012, Matyszewski *et al.* 2018, Ha and Park 2020).

The generation of plasmids for recombinant expression of the NLRC5 DD, as well as for other domains of NLRC5, lays the foundation for further optimization of the recombinant expression and purification of NLRC5 and its domains for the solution of their crystal structures.

4.1.4 The role of NLRP11 as a negative regulator of innate immune responses

The second part of this work focused on the characterization of the function of human NLRP11. Our group and others have previously shown, that NLRP11 is a negative regulator of innate immune responses, in particular the type I IFN response (Qin *et al.* 2017, Ellwanger *et al.* 2018), and the NF- κ B response (Wu *et al.* 2017). In this work, we were able to substantiate our knowledge about the underlying mechanisms of type I IFN regulation by NLRP11. We show, that NLRP11 is also a negative regulator of the NLRP3 inflammasome and that both inhibitory functions of NLRP11 are mediated, at least partially, through the interaction with and inhibition of DDX3X.

Besides the interaction with DDX3X, we also identified the autophagy related protein p62 as a specific interaction partner of NLRP11. p62 is an autophagy adaptor protein, which binds to ubiquitylated proteins and targets them to autophagosomes, where they are degraded (Pankiv *et al.* 2007). Autophagic clearance after poly-ubiquitylation is one of the pathways through which misfolded proteins, are cleared from cells (Ding and Yin 2008) and in several diseases conferred by protein aggregates such as Parkinson's disease and Alzheimer's disease, p62 is present in inclusion bodies of the aggregated proteins (Zatloukal *et al.* 2002). As p62 was also identified in co-IP of eGFP-NLRP8, this might indicate a role of p62 in the degradation of misfolded NLRPs, rather than a functional role in NLRP11-regulated signaling. This is further supported by the observed low expression levels and the high-molecular weight SDS-stable complexes of exogenous NLRP11.

4.1.5 The interaction between NLRs and DExD-box helicases is an emerging synergistical pattern

Several interactions between NLRs and members of DExD-box helicase families have recently been reported with functions in the induction of innate immune responses. Often, DExD-box proteins act as sensors for microbial nucleotides which in turn activate the interacting NLR. This has been reported for murine Dhx9, which senses dsRNA and activates Nlrp9b (Zhu *et al.* 2017), as well as for murine Dhx15,

Discussion

which mediates the interaction between Nlrp6 and Mavs upon recognition of viral RNA (Wang *et al.* 2015). Furthermore, the NLRP3 inflammasome was previously reported to be activated by DHX33 upon recognition of viral and bacterial RNA, resulting in inflammasome formation and the activation of caspase-1 (Mitoma *et al.* 2013). For both interactions of Nlrp6 and Dhx15, as well as for NLRP3 and DHX33, dependency on the NLR NACHT domain has been reported. The interaction between NLRP3 and DDX3X, recently shown as a prerequisite for activation of the NLRP3 inflammasome, is also dependent on the NACHT domain of NLRP3 (Samir *et al.* 2019). In contrast to this, we observed the interaction between NLRP11 and DDX3X in dependence of the NLRP11 LRRs. The difference in the interacting domains on the NLR might give an indication to why previously described interactions between NLRs and DExD-box proteins enhance the innate response, while we described an inhibitory role of the NLRP11-DDX3X interaction. In this context, it would be interesting to elucidate, which NLR domain is responsible for the interactions between Nlrp9b and Dhx9. Oshiumi *et al.* proposed, that DDX3X is directly involved in the recognition of viral RNA upon which it activates MAVS signaling (Oshiumi *et al.* 2010). Considering the emerging reports of DExD box helicases, which serve as sensors for NLR activation, it is interesting to speculate, whether recognition of viral RNA by DDX3X might also be an activating factor for NLRP11, especially as there is still no knowledge about a direct PAMP ligand of NLRP11.

4.1.6 Role of the NLRP11-DDX3X complex in antiviral type I interferon response

We identified DDX3X as the central protein, through which NLRP11 exerts its inhibitory function in the type I IFN response downstream of RIG-I. This signaling occurs through MAVS, and it has been previously proposed, that in SeV infected HEK293T cells, NLRP11 is recruited to the mitochondria, where it inhibits RIG-I induced signaling through degradation of TRAF6 (Qin *et al.* 2017). We also observed co-localization of NLRP11-eGFP with the mitochondrial marker AIF in SeV infected HEK293 NLRP11-eGFP cells. However, when we infected HeLa NLRP11-eGFP cells with SeV, no direct co-localization of NLRP11-eGFP with AIF was observed during the course of infection. The NLRP11-eGFP signal was only observed in the periphery of the mitochondria. Oshiumi *et al.* showed, that upon recognition of viral RNA, ectopically expressed DDX3X directly interacts with overexpressed MAVS at the mitochondria in HeLa cells (Oshiumi *et al.* 2010). Albeit we did not find co-localization of NLRP11 with AIF at the mitochondria in those cells, it would be interesting to see, whether the recruitment of NLRP11 to the mitochondria in HEK293 NLRP11-eGFP cells might be dependent on DDX3X and whether this is abrogated by the presence of NLRP11-eGFP in HeLa NLRP11-eGFP cells. This would add a further point at which the interaction of NLRP11 with DDX3X might target the RLR-induced type I IFN response (**Figure 30**).

We further observed differences between HEK293 and HeLa NLRP11-eGFP cells in the response mediated by TBK1 and IKK ϵ overexpression. While, compared to eGFP control cells, HeLa

Discussion

NLRP11-eGFP cells showed reduced type I IFN secretion upon overexpression of TBK1 or IKK ϵ , HEK293 NLRP11-eGFP cells reacted with higher levels of type I IFN secretion. It needs to be determined which differences in these two cell lines account for this. However, when antiviral responses are investigated in HEK293 cells, it needs to be kept in mind, that they do not recapitulate endogenous IFN responses upon dsRNA challenge well, as these cells express the adenoviral E1A protein (Graham *et al.* 1977), which interferes with the antiviral response and the induction of ISGs (Anderson and Fennie 1987, Lau *et al.* 2015, Bachmann *et al.* 2016).

As we found NLRP11 to inhibit DDX3X phosphorylation by IKK ϵ and subsequent IRF3 phosphorylation, and we previously reported that NLRP11 inhibits the induction of transcription from the *Irf3* promoter upon TBK1 overexpression, it is interesting to speculate, whether NLRP11 also inhibits phosphorylation of DDX3X by TBK1 (Soulat *et al.* 2008). Although different serine residues within DDX3X are phosphorylated by the two kinases (Soulat *et al.* 2008, Gu *et al.* 2013), the inhibitory role of NLRP11 is mediated by the LRRs in both cases, arguing for a similar mechanism by which the activation of IRF3 is prevented. The inhibition of TBK1-induced IFN β response in HeLa NLRP11-eGFP cells, which was even more pronounced than the inhibition of IKK ϵ -induced IFN β , also hints towards a role of NLRP11 as a negative inhibitor of DDX3X activation by both TBK1 and IKK ϵ .

Furthermore, the activation of IRF3 by TBK1 or IKK ϵ is a central step during type I IFN responses downstream of several PRRs. Detection of PAMPs by cGAS, TLR3 and TLR4 all result in the activation of IRF3 by TBK1 (Zhang *et al.* 2019). DDX3X deficiency in bone-marrow derived macrophages results in reduced transcription of IFN β , when the cells are treated with either poly(I:C), poly(dA:dT), or LPS, indicating a role of DDX3X in TLR4 and cGAS induced type I IFN responses (Szappanos *et al.* 2018). Interestingly, Qin *et al.* reported an increase in ISRE and IFN β levels after stimulation of NLRP11 knockout cells with the cGAS ligand poly(dA:dT), similar to that of the RLR ligand poly(I:C) (Qin *et al.* 2017). However, they used HEK293T cells for their knockdown, which, in our hands, have barely detectable levels of NLRP11 mRNA expression (Ellwanger *et al.* 2018). It would thus be highly interesting to further elucidate, whether NLRP11 also plays a role in the regulation of RIG-I-independent induction of type I IFNs, or if its negative regulation is specific for the type I IFN response initiated by RIG-I.

When we knocked down NLRP11 in macrophage like differentiated THP-1 cells, with inducible DDX3X knockdown, we observed the expected increase in IFN β secretion after infection with SeV which we and others previously published (Qin *et al.* 2017, Ellwanger *et al.* 2018). As we proposed that NLRP11 exerts its inhibitory function in type I IFN response by blocking DDX3X phosphorylation and subsequent IRF3 phosphorylation, we were surprised to see an increase of the IFN β response when both NLRP11 and DDX3X were knocked down. However, as our knockdown was not complete residual DDX3X might be sufficient to mediate IFN induction. Incomplete knockdown of DDX3X in those

Discussion

experiments was also indicated by the marginal reduction of IFN β secretion when only DDX3X was knocked down. Another hypothesis, which might explain the discrepancy between the observed increase in IFN β secretion, compared to the control, after combined DDX3X and NLRP11 knockdown and the expected reduction of the IFN β response levels might stem from the different roles TBK1 and IKK ϵ play within the type I IFN response. Although both proteins ultimately phosphorylate the transcription factors IRF3 and IRF7, IKK ϵ is more involved in the induction of ISGs (Matsui *et al.* 2006, Tenoever *et al.* 2007) than in the induction of type I IFNs which are mainly governed by TBK1 (Hemmi *et al.* 2004, Perry *et al.* 2004). Elucidating the specific impact of NLRP11 on TBK1 and IKK ϵ -mediated responses, ideally in cells in which either one of the kinases is knocked out, will greatly benefit our understanding of the exact role of NLRP11 within RIG-I, and possibly cGAS-, TLR3- or TLR4-mediated type I IFN responses.

Besides activation of IRF3, IRF7 also is a critical transcription factor in the type I IFN response. However, the roles of IRF3 and IRF7 differ. While IRF3 is the initial transcription factor, responsible for type I IFN induction, it also induces transcription of IRF7, mediating a positive feedback loop for a second wave of type I IFN transcription (Honda *et al.* 2006). As NLRP11 is induced at later timepoints during SeV infection (Wu *et al.* 2017, Ellwanger *et al.* 2018), a possible role in inhibition of IRF7 activation seems likely. However, the enhancing function of DDX3X in IRF7 activation might be independent of IRF phosphorylation by TBK1 or IKK ϵ , as DDX3X enhances the IFN response by a constitutively active version of IRF7 in absence of TBK1 and IKK ϵ (Szappanos *et al.* 2018).

The initial finding that NLRP11 is a negative regulator of the type I IFN response, was based on luciferase reporter gene assays. Although those assays are a widely used and well accepted tool to assess the effect of proteins, or therapeutics in innate signaling pathways, one has to keep in mind that they are a highly artificial system. HEK293T cells are commonly used for reporter gene assays due to their great transfection and protein expression rates. Furthermore, those cells are great tools to analyze the functions of specific, transfected PRRs, as they themselves barely express any TLRs (Hornung *et al.* 2002). However, it is thus highly likely, that their proteome also does not correctly represent the regulatory mechanisms behind the corresponding signaling pathways. Furthermore, as previously mentioned, transformation of the cells with sheared fragments of the human adenovirus 5 genome results in the expression of adenoviral proteins (Graham *et al.* 1977), which can influence the antiviral response (Anderson and Fennie 1987, Lau *et al.* 2015, Bachmann *et al.* 2016). Besides the limitations of reporter gene assays based on their cellular environment, expression of some NLRs was shown to negatively regulate luciferases from *Photinus pyralis*, and *Renilla remiformis* by a post-translational mechanism (Ling *et al.* 2012). Although this has to be kept in mind when interpreting the inhibitory effects NLRP11 displays in reporter gene assays, the negative regulatory role of NLRP11 has been also corroborated by measurement of type I IFN by ELISA after NLRP11 knockdown (Ellwanger *et al.* 2018), or in CRISPR

Discussion

knockout cells (Qin *et al.* 2017). Overexpression of NLRP11 also showed a clear effect on IRF3 phosphorylation downstream of IKK ϵ overexpression in immunoblot. Our cumulative data thus makes it unlikely, that the inhibition, observed in reporter gene assays, is conferred by unspecific post-translational inhibition of the luciferase.

Although we provided a first functional analysis of the interaction between NLRP11 and DDX3X, the question about the physiological relevance of this interaction remains unanswered. We studied the interaction mainly in HEK and HeLa cells, which barely transcribe NLRP11 (Ellwanger *et al.* 2018), and evaluated our findings by siRNA-mediated knockdown of NLRP11 in THP-1 cells, in which we described detectable, but still low levels of NLRP11 transcription (Ellwanger *et al.* 2018). The observation of low NLRP11 levels in THP-1 cells are contrasted by the report from Wu *et al.*, in which even robust protein levels of NLRP11 were shown in THP-1 cells (Wu *et al.* 2017). However, they also show pronounced protein levels of NLRP11 in HEK293T cells, which, in our hands, barely express NLRP11 (Qin *et al.* 2017, Ellwanger *et al.* 2018). The nature of these discrepancies remains elusive.

4.1.7 Inhibition of the NLRP3 inflammasome by NLRP11

We showed here, that NLRP11 is a negative regulator of the NLRP3 inflammasome. NLRP11 inhibits NLRP3 induced caspase-1 activation through its interaction with DDX3X, which was recently shown to be a crucial factor during activation of the NLRP3 inflammasome (Samir *et al.* 2019).

As previously elaborated for the analysis of the function of NLRP11 in type I IFN response, we must keep in mind, that the activity of luciferase can be inhibited by some NLRs in a post-translational manner (Ling *et al.* 2012). Although only the luciferases from *Photinus pyralis*, and *Renilla remiformis* were analyzed, this might also be the case for the *Gaussia princeps* luciferase, used in caspase-1 reporter assays. Here however, we did not observe an inhibitory effect of NLRP11 unless we co-transfected DDX3X, indicating that the observed inhibitory effect was specific for the presence of DDX3X. In contrast to the role of NLRP11 in type I IFN response, increased IL-1 β levels after knockdown of NLRP11 in the context of NLRP3 inflammasome activation did not reach significance, leaving the question about the physiological role of NLRP11 in NLRP3 inflammasome activation in macrophage-like differentiated THP-1 cells unanswered. Furthermore, Mishra *et al.* identified NLRP11 as an enhancer of the IL-1 β response towards *Mycobacterium tuberculosis* in an siRNA screen in macrophage-like differentiated THP-1 cells (Mishra *et al.* 2010); the discrepancy to my data is unclear at present.

4.1.8 The physiological role of the NLRP11-DDX3X interaction

It remains elusive, in which cell types and under which conditions the interaction between NLRP11 and DDX3X could be of physiological relevance *in vivo* and what exactly the roles of this interaction are in the broad context of innate immune responses. Lack of mouse models, as NLRP11 is a primate specific NLR (Tian *et al.* 2009), additionally makes this question challenging to address.

One physiological context in which the interplay of NLRP11 and DDX3X might be of high relevance could be indicated by high expression levels of both NLRP11, as well as DDX3X in oocytes (Li *et al.* 2014, Wu *et al.* 2017, Ellwanger *et al.* 2018). As the fertilization process, as well as the embryonic development, are immuno-privileged events (Clark and Schust 2013), high expression levels of DDX3X, as they have been reported to be crucial for murine oocytes and during the initial stages of development (Li *et al.* 2014), potentially present the risk of unwanted innate immune responses. A role of NLRP11 during fertilization is also suggested by the reports of age-related decrease of NLRP11 expression levels in human, as well as in simian oocytes (McDaniel and Wu 2009, Zhang *et al.* 2014). Inhibition of type I IFN response during oocytes fertilization by inhibition of TBK1, has already been proposed for NLRP14 (Abe *et al.* 2017).

Another possible role of NLRP11 might be deduced from the ambivalent role of DDX3X during viral infections. Although DDX3X enhances the antiviral response via diverse mechanisms, several viruses have been reported to require DDX3X for efficient replication. HIV and HCV are both able to co-opt DDX3X and use it to benefit their own replication (Ariumi *et al.* 2007). We and others have previously shown that NLRP11 is well expressed in the liver (Wu *et al.* 2017, Ellwanger *et al.* 2018), the main site of HCV tropism, as well as in B cells, which are also discussed as a site of infection (Chen *et al.* 2017). One could speculate on a possible role for NLRP11 in the HCV replication cycle or the development of self-limiting versus chronic HCV infections. A possible role of NLRP11 in this might give a handle for site specific therapeutic interventions by targeted gene therapy instead of proposed systemic treatment with DDX3X inhibitors (Kwong *et al.* 2005, Schröder 2010, Brai *et al.* 2016). As DDX3X has a multifaced role in the cell and is also involved in cell cycle regulation and RNA metabolism, knowledge of the functional interplay between NLRP11 and DDX3X in the context of viral infection will broaden our understanding of the regulation of DDX3X in the specific context. Shedding light on the DDX3X domain responsible for binding to NLRP11 might facilitate the development of directed interventions, which are limited to only one specific function of DDX3X.

Furthermore, activation of the inflammasome is a major contributing factor in several liver pathologies, (Szabo and Csak 2012, Al Mamun *et al.* 2020). Since NLRP11 was shown to be robustly expressed in the liver (Wu *et al.* 2017, Ellwanger *et al.* 2018), a role of NLRP11 in inflammasome attenuation might be likely. Activation of the NLRP3 inflammasome has been shown in several non-immune cells in the liver (Csak *et al.* 2011), and hepatocytes (Gaul *et al.* 2021), as well as in liver-resident macrophages,

Discussion

termed Kupffer cells (Belkaya *et al.* 2019). Given that activation of the NLRP3 inflammasome plays a significant role in liver pathologies, both in infection, as well as in sterile inflammation (Tsutsui *et al.* 2015, Gaul *et al.* 2021), it would be important to understand hepatic NLRP11 expression regarding the expression in different cell populations, to further evaluate the function of NLRP11 in IL-1 β driven liver pathology.

Besides high expression levels in oocytes and liver, our group reported strong transcription of NLRP11 in B cells, and several B cell tumors (Ellwanger *et al.* 2018). However, this was in contrast to data from Wu *et al.*, who described low transcription of NLRP11 in B cells (Wu *et al.* 2017). Recently, a first report described the potential of B cells and B-lymphoma-cell lines to activate inflammasomes (Lim *et al.* 2020). They described that B cell activating factor (BAFF) can serve as both priming and activating factor of the NLRP3 inflammasome (Lim *et al.* 2020). Increased BAFF serum levels and B cell-derived IL-1 β was described in patients with essential thrombocythemia (Liu *et al.* 2014, Lim *et al.* 2017), giving rise to the possibility, that NLRP11 might be involved in the regulation of this yet barely characterized mechanism.

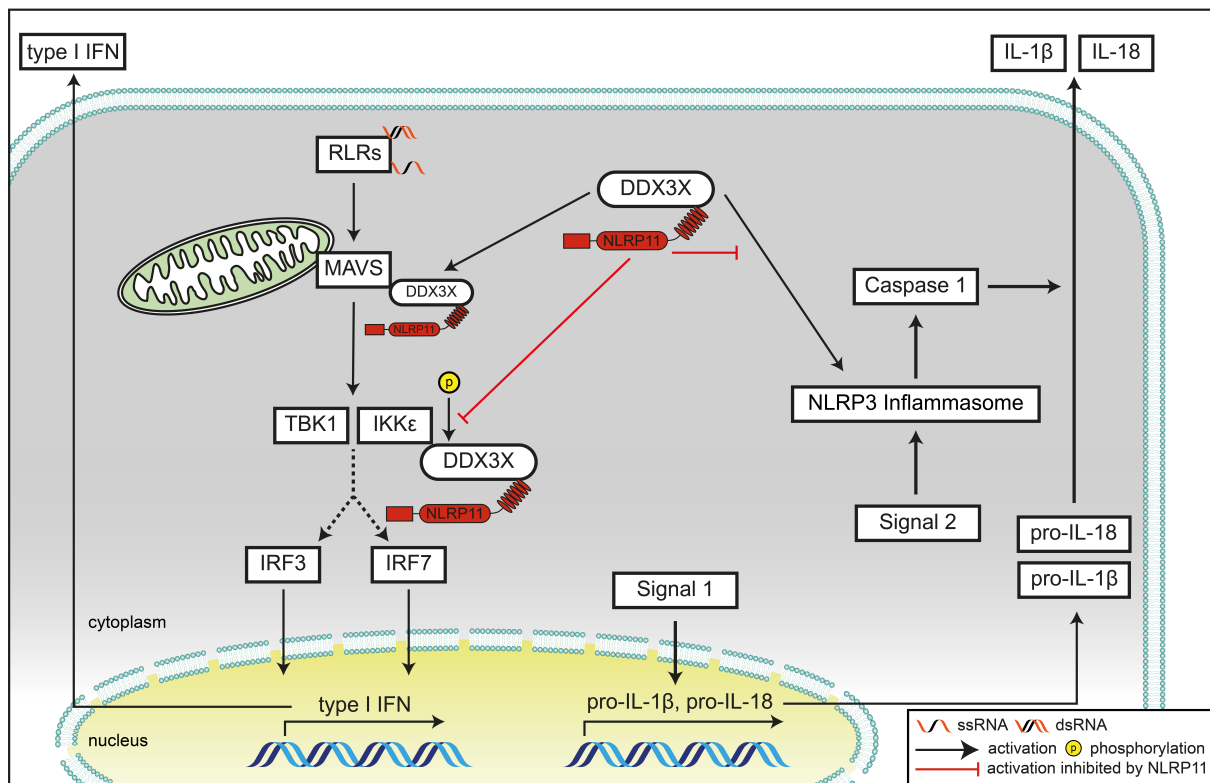


Figure 30: Schematic representation of the proposed functional interplay between NLRP11 and DDX3X. The role of NLRP11 in attenuation of RIG-I-induced type I IFN response (left side) and NLRP3 inflammasome activation (right side) are depicted. NLRP11 interacts with DDX3X via its LRRs and reduces type I IFN induction downstream of RIG-I by preventing IKK ϵ -mediated phosphorylation of DDX3X and thus subsequent activation of IRF3. Interaction with DDX3X also inhibits DDX3X-mediated activation of the NLRP3 inflammasome, resulting in reduced IL-1 β secretion.

Discussion

In summary, the second part of this thesis identified DDX3X as a novel interaction partner of NLRP11 through which NLRP11 exerts its inhibitory effect in RIG-I induced type I IFN response. This is conferred by inhibition of IKK ϵ -mediated DDX3X phosphorylation (**Figure 30**). We further identified a novel role for NLRP11 as an inhibitor of the NLRP3 inflammasome. This as well is mediated through inhibition of DDX3X in its role as an enhancer of NLRP3 inflammasome activation. Here however, the exact mechanism still remains to be elucidated (**Figure 30**).

In conclusion we identified potential interaction partners of NLRC5 by several different approaches. We found Sin3A and NELFB to be interactors of the NLRC5 DD by Y2H screening and verified their interaction by co-IP and immunoblot. However, we observed, that their transcriptional repression of this process was not limited to NLRC5, but also affected CIITA-driven MHC class II transcription and, in case of NELFB, also the MyD88-induced NF- κ B response. We found several other interesting candidate proteins whose interaction with NLRC5 need to be verified and whose role in NLRC5-mediated MHC class I transcription need to be elucidated. We further provided the basis for recombinant expression of NLRC5 and its domains for purification and structural analysis by crystallography. Our research further substantially broadened our understanding of the mechanisms behind NLRP11-mediated inhibition of the type I IFN response. Here we identified DDX3X as an essential interactor of NLRP11, through which IKK ϵ -induced phosphorylation of IRF3 was inhibited. We further identified a novel function of NLRP11 in the regulation of the NLRP3-inflammasome. Here, NLRP11 counteracted the positive role of DDX3X in NLRP3-inflammasome activation.

References

- Abe, T., A. Lee, R. Sitharam, J. Kesner, R. Rabadan and S. D. Shapira (2017). "Germ-Cell-Specific Inflammasome Component NLRP14 Negatively Regulates Cytosolic Nucleic Acid Sensing to Promote Fertilization." *Immunity* **46**(4): 621-634.
- Acharya, D., G. Liu and M. U. Gack (2020). "Dysregulation of type I interferon responses in COVID-19." *Nature Reviews Immunology* **20**(7): 397-398.
- Adelman, K., M. A. Kennedy, S. Nechaev, D. A. Gilchrist, G. W. Muse, Y. Chinenov and I. Rogatsky (2009). "Immediate mediators of the inflammatory response are poised for gene activation through RNA polymerase II stalling." *Proc Natl Acad Sci U S A* **106**(43): 18207-18212.
- Aiyar, S. E., A. L. Blair, D. A. Hopkinson, S. Bekiranov and R. Li (2007). "Regulation of clustered gene expression by cofactor of BRCA1 (COBRA1) in breast cancer cells." *Oncogene* **26**(18): 2543-2553.
- Akita, K., T. Ohtsuki, Y. Nukada, T. Tanimoto, M. Namba, T. Okura, R. Takakura-Yamamoto, K. Torigoe, Y. Gu, M. S. Su, M. Fujii, M. Satoh-Itoh, K. Yamamoto, K. Kohno, M. Ikeda and M. Kurimoto (1997). "Involvement of caspase-1 and caspase-3 in the production and processing of mature human interleukin 18 in monocytic THP.1 cells." *J Biol Chem* **272**(42): 26595-26603.
- Al Mamun, A., A. Akter, S. Hossain, T. Sarker, S. A. Safa, Q. G. Mustafa, S. A. Muhammad and F. Munir (2020). "Role of NLRP3 inflammasome in liver disease." *Journal of Digestive Diseases* **21**(8): 430-436.
- Alcami, A. and U. H. Koszinowski (2000). "Viral mechanisms of immune evasion." *Trends in Microbiology* **8**(9): 410-418.
- Allen, I. C., C. B. Moore, M. Schneider, Y. Lei, B. K. Davis, M. A. Scull, D. Gris, K. E. Roney, A. G. Zimmermann, J. B. Bowzard, P. Ranjan, K. M. Monroe, R. J. Pickles, S. Sambhara and J. P. Ting (2011). "NLRX1 protein attenuates inflammatory responses to infection by interfering with the RIG-I-MAVS and TRAF6-NF- κ B signaling pathways." *Immunity* **34**(6): 854-865.
- Anderson, K. P. and E. H. Fennie (1987). "Adenovirus early region 1A modulation of interferon antiviral activity." *J Virol* **61**(3): 787-795.
- Ariumi, Y., M. Kuroki, K.-i. Abe, H. Dansako, M. Ikeda, T. Wakita and N. Kato (2007). "DDX3 DEAD-Box RNA Helicase Is Required for Hepatitis C Virus RNA Replication." *Journal of Virology* **81**(24): 13922-13926.
- Arnoult, D., F. Soares, I. Tattoli, C. Castanier, D. J. Philpott and S. E. Girardin (2009). "An N-terminal addressing sequence targets NLRX1 to the mitochondrial matrix." *J Cell Sci* **122**(Pt 17): 3161-3168.
- Askari, N., R. G. Correa, D. Zhai and J. C. Reed (2012). "Expression, purification, and characterization of recombinant NOD1 (NLRC1): A NLR family member." *J Biotechnol* **157**(1): 75-81.
- Au, W. C., P. A. Moore, D. W. LaFleur, B. Tombal and P. M. Pitha (1998). "Characterization of the interferon regulatory factor-7 and its potential role in the transcription activation of interferon A genes." *J Biol Chem* **273**(44): 29210-29217.
- Au, W. C., P. A. Moore, W. Lowther, Y. T. Juang and P. M. Pitha (1995). "Identification of a member of the interferon regulatory factor family that binds to the interferon-stimulated response element and activates expression of interferon-induced genes." *Proc Natl Acad Sci U S A* **92**(25): 11657-11661.
- Bachmann, M., T. Breitwieser, C. Lipps, D. Wirth, I. Jordan, U. Reichl and T. Frensing (2016). "Impaired antiviral response of adenovirus-transformed cell lines supports virus replication." *J Gen Virol* **97**(2): 293-298.
- Baltus, G. A., M. P. Kowalski, A. V. Tutter and S. Kadam (2009). "A Positive Regulatory Role for the mSin3A-HDAC Complex in Pluripotency through Nanog and Sox2*." *Journal of Biological Chemistry* **284**(11): 6998-7006.
- Bansal, N., G. David, E. Farias and S. Waxman (2016). "Emerging Roles of Epigenetic Regulator Sin3 in Cancer." *Adv Cancer Res* **130**: 113-135.
- Bar-Ziv, R., Y. Voichek and N. Barkai (2016). "Chromatin dynamics during DNA replication." *Genome Res* **26**(9): 1245-1256.
- Barnes, C. E., D. M. English and S. M. Cowley (2019). "Acetylation & Co: an expanding repertoire of histone acylations regulates chromatin and transcription." *Essays Biochem* **63**(1): 97-107.

References

- Bartok, E., F. Bauernfeind, M. G. Khaminets, C. Jakobs, B. Monks, K. A. Fitzgerald, E. Latz and V. Hornung (2013). "iGLuc: a luciferase-based inflammasome and protease activity reporter." *Nat Methods* **10**(2): 147-154.
- Bauernfeind, F. G., G. Horvath, A. Stutz, E. S. Alnemri, K. MacDonald, D. Speert, T. Fernandes-Alnemri, J. Wu, B. G. Monks, K. A. Fitzgerald, V. Hornung and E. Latz (2009). "Cutting edge: NF-kappaB activating pattern recognition and cytokine receptors license NLRP3 inflammasome activation by regulating NLRP3 expression." *J Immunol* **183**(2): 787-791.
- Bauernfried, S., M. J. Scherr, A. Pichlmair, K. E. Duderstadt and V. Hornung (2021). "Human NLRP1 is a sensor for double-stranded RNA." *Science* **371**(6528).
- Baymaz, H. I., I. D. Karemaker and M. Vermeulen (2015). "Perspective on unraveling the versatility of 'co-repressor' complexes." *Biochimica et Biophysica Acta (BBA) - Gene Regulatory Mechanisms* **1849**(8): 1051-1056.
- Belkaya, S., E. Michailidis, C. B. Korol, M. Kabbani, A. Cobat, P. Bastard, Y. S. Lee, N. Hernandez, S. Drutman, Y. P. de Jong, E. Vivier, J. Bruneau, V. Béziat, B. Boisson, L. Lorenzo-Diaz, S. Boucherit, M. Sebah, E. Jacquemin, J. F. Emile, L. Abel, C. M. Rice, E. Jouanguy and J. L. Casanova (2019). "Inherited IL-18BP deficiency in human fulminant viral hepatitis." *J Exp Med* **216**(8): 1777-1790.
- Benko, S., J. G. Magalhaes, D. J. Philpott and S. E. Girardin (2010). "NLRC5 limits the activation of inflammatory pathways." *J Immunol* **185**(3): 1681-1691.
- Benoist, C. and D. Mathis (1990). "Regulation of major histocompatibility complex class-II genes: X, Y and other letters of the alphabet." *Annu Rev Immunol* **8**: 681-715.
- Bentham, A., H. Burdett, P. A. Anderson, S. J. Williams and B. Kobe (2017). "Animal NLRs provide structural insights into plant NLR function." *Ann Bot* **119**(5): 827-702.
- Beresford, G. W. and J. M. Boss (2001). "CIITA coordinates multiple histone acetylation modifications at the HLA-DRA promoter." *Nat Immunol* **2**(7): 652-657.
- Bernstein, B. E., J. K. Tong and S. L. Schreiber (2000). "Genomewide studies of histone deacetylase function in yeast." *Proc Natl Acad Sci U S A* **97**(25): 13708-13713.
- Biswas, A., T. B. Meissner, T. Kawai and K. S. Kobayashi (2012). "Cutting edge: impaired MHC class I expression in mice deficient for Nlrc5/class I transactivator." *J Immunol* **189**(2): 516-520.
- Bontron, S., V. Steimle, C. Ucla, M. M. Eibl and B. Mach (1997). "Two novel mutations in the MHC class II transactivator CIITA in a second patient from MHC class II deficiency complementation group A." *Hum Genet* **99**(4): 541-546.
- Boss, J. M. (1997). "Regulation of transcription of MHC class II genes." *Curr Opin Immunol* **9**(1): 107-113.
- Brai, A., A. Boccuto, M. Monti, S. Marchi, I. Vicenti, F. Saladini, C. I. Trivisani, A. Pollutri, C. M. Trombetta, E. Montomoli, V. Riva, A. Garbelli, E. M. Nola, M. Zazzi, G. Maga, E. Dreassi and M. Botta (2020). "Exploring the Implication of DDX3X in DENV Infection: Discovery of the First-in-Class DDX3X Fluorescent Inhibitor." *ACS Med Chem Lett* **11**(5): 956-962.
- Brai, A., R. Fazi, C. Tintori, C. Zamperini, F. Bugli, M. Sanguinetti, E. Stigliano, J. Esté, R. Badia, S. Franco, M. A. Martinez, J. P. Martinez, A. Meyerhans, F. Saladini, M. Zazzi, A. Garbelli, G. Maga and M. Botta (2016). "Human DDX3 protein is a valuable target to develop broad spectrum antiviral agents." *Proceedings of the National Academy of Sciences* **113**(19): 5388-5393.
- Brai, A., F. Martelli, V. Riva, A. Garbelli, R. Fazi, C. Zamperini, A. Pollutri, L. Falsitta, S. Ronzini, L. Maccari, G. Maga, S. Giannecchini and M. Botta (2019). "DDX3X Helicase Inhibitors as a New Strategy To Fight the West Nile Virus Infection." *J Med Chem* **62**(5): 2333-2347.
- Brai, A., V. Riva, F. Saladini, C. Zamperini, C. I. Trivisani, A. Garbelli, C. Pennisi, A. Giannini, A. Boccuto, F. Bugli, M. Martini, M. Sanguinetti, M. Zazzi, E. Dreassi, M. Botta and G. Maga (2020). "DDX3X inhibitors, an effective way to overcome HIV-1 resistance targeting host proteins." *Eur J Med Chem* **200**: 112319.
- Brai, A., S. Ronzini, V. Riva, L. Botta, C. Zamperini, M. Borgini, C. I. Trivisani, A. Garbelli, C. Pennisi, A. Boccuto, F. Saladini, M. Zazzi, G. Maga and M. Botta (2019). "Synthesis and Antiviral Activity of Novel 1,3,4-Thiadiazole Inhibitors of DDX3X." *Molecules* **24**(21).
- Branon, T. C., J. A. Bosch, A. D. Sanchez, N. D. Udeshi, T. Svinkina, S. A. Carr, J. L. Feldman, N. Perrimon and A. Y. Ting (2018). "Efficient proximity labeling in living cells and organisms with TurboID." *Nat Biotechnol* **36**(9): 880-887.

References

- Camacho-Carvajal, M. M., S. Klingler, F. Schnappauf, S. B. Hake and V. Steimle (2004). "Importance of class II transactivator leucine-rich repeats for dominant-negative function and nucleo-cytoplasmic transport." *Int Immunol* **16**(1): 65-75.
- Canton, J., D. Neculai and S. Grinstein (2013). "Scavenger receptors in homeostasis and immunity." *Nature Reviews Immunology* **13**(9): 621-634.
- Caraglia, M., A. Abbruzzese, A. Leardi, S. Pepe, A. Budillon, G. Baldassare, C. Selleri, S. De Lorenzo, A. Fabbrocini, G. Giuberti, G. Vitale, G. Lupoli, A. R. Bianco and P. Tagliaferri (1999). "Interferon- α induces apoptosis in human KB cells through a stress-dependent mitogen activated protein kinase pathway that is antagonized by epidermal growth factor." *Cell Death & Differentiation* **6**(8): 773-780.
- Carnesecchi, J., G. Sigismondo, K. Domsch, C. E. P. Baader, M.-R. Rafiee, J. Krijgsveld and I. Lohmann (2020). "Multi-level and lineage-specific interactomes of the Hox transcription factor Ubx contribute to its functional specificity." *Nature Communications* **11**(1): 1388.
- Carney, J. P., R. S. Maser, H. Olivares, E. M. Davis, M. Le Beau, J. R. Yates, 3rd, L. Hays, W. F. Morgan and J. H. Petrini (1998). "The hMre11/hRad50 protein complex and Nijmegen breakage syndrome: linkage of double-strand break repair to the cellular DNA damage response." *Cell* **93**(3): 477-486.
- Chamaillard, M., M. Hashimoto, Y. Horie, J. Masumoto, S. Qiu, L. Saab, Y. Ogura, A. Kawasaki, K. Fukase, S. Kusumoto, M. A. Valvano, S. J. Foster, T. W. Mak, G. Nuñez and N. Inohara (2003). "An essential role for NOD1 in host recognition of bacterial peptidoglycan containing diaminopimelic acid." *Nat Immunol* **4**(7): 702-707.
- Channappanavar, R., A. R. Fehr, J. Zheng, C. Wohlford-Lenane, J. E. Abrahante, M. Mack, R. Sompallae, P. B. McCray, Jr., D. K. Meyerholz and S. Perlman (2019). "IFN-I response timing relative to virus replication determines MERS coronavirus infection outcomes." *The Journal of Clinical Investigation* **129**(9): 3625-3639.
- Chapman-Smith, A. and J. E. Cronan, Jr. (1999). "Molecular biology of biotin attachment to proteins." *J Nutr* **129**(2S Suppl): 477s-484s.
- Chen, C. L., J. Y. Huang, C. H. Wang, S. M. Tahara, L. Zhou, Y. Kondo, J. Schechter, L. Su, M. M. Lai, T. Wakita, F. L. Cosset, J. U. Jung and K. Machida (2017). "Hepatitis C virus has a genetically determined lymphotropism through co-receptor B7.2." *Nat Commun* **8**: 13882.
- Chen, D. S. and I. Mellman (2013). "Oncology meets immunology: the cancer-immunity cycle." *Immunity* **39**(1): 1-10.
- Cheng, B. and D. H. Price (2007). "Properties of RNA polymerase II elongation complexes before and after the P-TEFb-mediated transition into productive elongation." *J Biol Chem* **282**(30): 21901-21912.
- Cheutin, T., A. J. McNairn, T. Jenuwein, D. M. Gilbert, P. B. Singh and T. Misteli (2003). "Maintenance of Stable Heterochromatin Domains by Dynamic HP1 Binding." *Science* **299**(5607): 721-725.
- Chi, B., H. L. Dickensheets, K. M. Spann, M. A. Alston, C. Luongo, L. Dumoutier, J. Huang, J.-C. Renauld, S. V. Kotenko, M. Roederer, J. A. Beeler, R. P. Donnelly, P. L. Collins and R. L. Rabin (2006). "Alpha and Lambda Interferon Together Mediate Suppression of CD4 T Cells Induced by Respiratory Syncytial Virus." *Journal of Virology* **80**(10): 5032-5040.
- Chin, K.-C., G. G.-X. Li and J. P.-Y. Ting (1997). "Importance of acidic, proline/serine/threonine-rich, and GTPbinding regions in the major histocompatibility complex class II transactivator: Generation of transdominant-negative mutants." *Proceedings of the National Academy of Sciences* **94**(6): 2501-2506.
- Chinnadurai, G. (2007). "Transcriptional regulation by C-terminal binding proteins." *Int J Biochem Cell Biol* **39**(9): 1593-1607.
- Choi-Rhee, E., H. Schulman and J. E. Cronan (2004). "Promiscuous protein biotinylation by Escherichia coli biotin protein ligase." *Protein Sci* **13**(11): 3043-3050.
- Christian, K. and V. Andreas (2013). "Production of Recombinant Proteins in Insect Cells." *American Journal of Biochemistry and Biotechnology* **9**(3).
- Clark, G. F. and D. J. Schust (2013). "Manifestations of immune tolerance in the human female reproductive tract." *Front Immunol* **4**: 26.
- Core, L. and K. Adelman (2019). "Promoter-proximal pausing of RNA polymerase II: a nexus of gene regulation." *Genes Dev* **33**(15-16): 960-982.

References

- Crayne, C. B., S. Albeituni, K. E. Nichols and R. Q. Cron (2019). "The Immunology of Macrophage Activation Syndrome." *Frontiers in Immunology* **10**(119).
- Cresswell, P. (1994). "Assembly, transport, and function of MHC class II molecules." *Annu Rev Immunol* **12**: 259-293.
- Cronan, J. E. (2005). "Targeted and proximity-dependent promiscuous protein biotinylation by a mutant *Escherichia coli* biotin protein ligase." *J Nutr Biochem* **16**(7): 416-418.
- Csak, T., M. Ganz, J. Pespisa, K. Kodys, A. Dolganiuc and G. Szabo (2011). "Fatty acid and endotoxin activate inflammasomes in mouse hepatocytes that release danger signals to stimulate immune cells." *Hepatology* **54**(1): 133-144.
- Cui, J., Y. Li, L. Zhu, D. Liu, Z. Songyang, H. Y. Wang and R. F. Wang (2012). "NLRP4 negatively regulates type I interferon signaling by targeting the kinase TBK1 for degradation via the ubiquitin ligase DTX4." *Nat Immunol* **13**(4): 387-395.
- Cui, J., L. Zhu, X. Xia, H. Y. Wang, X. Legras, J. Hong, J. Ji, P. Shen, S. Zheng, Z. J. Chen and R. F. Wang (2010). "NLRC5 negatively regulates the NF-kappaB and type I interferon signaling pathways." *Cell* **141**(3): 483-496.
- Cui, S., K. Eisenächer, A. Kirchhofer, K. Brzózka, A. Lammens, K. Lammens, T. Fujita, K. K. Conzelmann, A. Krug and K. P. Hopfner (2008). "The C-terminal regulatory domain is the RNA 5'-triphosphate sensor of RIG-I." *Mol Cell* **29**(2): 169-179.
- Dambuzá, I. M. and G. D. Brown (2015). "C-type lectins in immunity: recent developments." *Curr Opin Immunol* **32**: 21-27.
- Dang, A. T., J. Strietz, A. Zenobi, H. J. Khameneh, S. M. Brandl, L. Lozza, G. Conradt, S. H. E. Kaufmann, W. Reith, I. Kwee, S. Minguet, S. T. Chelbi and G. Guarda (2021). "NLRC5 promotes transcription of *BTN3A1-3* genes and $V\gamma 9V\delta 2$ T cell-mediated killing." *iScience* **24**(1): 101900.
- Davidson, S., A. Steiner, C. R. Harapas and S. L. Masters (2018). "An Update on Autoinflammatory Diseases: Interferonopathies." *Curr Rheumatol Rep* **20**(7): 38.
- Davis, B. K., R. A. Roberts, M. T. Huang, S. B. Willingham, B. J. Conti, W. J. Brickey, B. R. Barker, M. Kwan, D. J. Taxman, M. A. Accavitti-Loper, J. A. Duncan and J. P. Ting (2011). "Cutting edge: NLRC5-dependent activation of the inflammasome." *J Immunol* **186**(3): 1333-1337.
- de la Cruz, J., D. Kressler and P. Linder (1999). "Unwinding RNA in *Saccharomyces cerevisiae*: DEAD-box proteins and related families." *Trends Biochem Sci* **24**(5): 192-198.
- Di Gennaro, E., F. Bruzzese, M. Caraglia, A. Abruzzese and A. Budillon (2004). "Acetylation of proteins as novel target for antitumor therapy: review article." *Amino Acids* **26**(4): 435-441.
- Dinareello, C. A., A. Simon and J. W. van der Meer (2012). "Treating inflammation by blocking interleukin-1 in a broad spectrum of diseases." *Nat Rev Drug Discov* **11**(8): 633-652.
- Ding, W. X. and X. M. Yin (2008). "Sorting, recognition and activation of the misfolded protein degradation pathways through macroautophagy and the proteasome." *Autophagy* **4**(2): 141-150.
- Domanski, P., M. Witte, M. Kellum, M. Rubinstein, R. Hackett, P. Pitha and O. R. Colamonici (1995). "Cloning and expression of a long form of the beta subunit of the interferon alpha beta receptor that is required for signaling." *J Biol Chem* **270**(37): 21606-21611.
- Doncheva, N. T., J. H. Morris, J. Gorodkin and L. J. Jensen (2019). "Cytoscape StringApp: Network Analysis and Visualization of Proteomics Data." *J Proteome Res* **18**(2): 623-632.
- Dowhan, D. H., E. P. Hong, D. Auboeuf, A. P. Dennis, M. M. Wilson, S. M. Berget and B. W. O'Malley (2005). "Steroid hormone receptor coactivation and alternative RNA splicing by U2AF65-related proteins CAPERalpha and CAPERbeta." *Mol Cell* **17**(3): 429-439.
- Doyon, Y. and J. Côté (2004). "The highly conserved and multifunctional NuA4 HAT complex." *Current Opinion in Genetics & Development* **14**(2): 147-154.
- Duewell, P., H. Kono, K. J. Rayner, C. M. Sirois, G. Vladimer, F. G. Bauernfeind, G. S. Abela, L. Franchi, G. Nuñez, M. Schnurr, T. Espevik, E. Lien, K. A. Fitzgerald, K. L. Rock, K. J. Moore, S. D. Wright, V. Hornung and E. Latz (2010). "NLRP3 inflammasomes are required for atherogenesis and activated by cholesterol crystals." *Nature* **464**(7293): 1357-1361.
- Duncan, J. A., D. T. Bergstralh, Y. Wang, S. B. Willingham, Z. Ye, A. G. Zimmermann and J. P. Ting (2007). "Cryopyrin/NALP3 binds ATP/dATP, is an ATPase, and requires ATP binding to mediate inflammatory signaling." *Proc Natl Acad Sci U S A* **104**(19): 8041-8046.

References

- Durand, B., P. Sperisen, P. Emery, E. Barras, M. Zufferey, B. Mach and W. Reith (1997). "RFXAP, a novel subunit of the RFX DNA binding complex is mutated in MHC class II deficiency." *Embo j* **16**(5): 1045-1055.
- Eibl, C., S. Grigoriu, M. Hessenberger, J. Wenger, S. Puehringer, A. S. Pinheiro, R. N. Wagner, M. Proell, J. C. Reed, R. Page, K. Diederichs and W. Peti (2012). "Structural and functional analysis of the NLRP4 pyrin domain." *Biochemistry* **51**(37): 7330-7341.
- Ellwanger, K., E. Becker, I. Kienes, A. Sowa, Y. Postma, Y. Cardona Gloria, A. N. R. Weber and T. A. Kufer (2018). "The NLR family pyrin domain-containing 11 protein contributes to the regulation of inflammatory signaling." *J Biol Chem* **293**(8): 2701-2710.
- Ellwanger, K., S. Briese, C. Arnold, I. Kienes, V. Heim, U. Nachbur and T. A. Kufer (2019). "XIAP controls RIPK2 signaling by preventing its deposition in speck-like structures." *Life Sci Alliance* **2**(4).
- Fan, W., Z. Tang, D. Chen, D. Moughon, X. Ding, S. Chen, M. Zhu and Q. Zhong (2010). "Keap1 facilitates p62-mediated ubiquitin aggregate clearance via autophagy." *Autophagy* **6**(5): 614-621.
- Filtz, T. M., W. K. Vogel and M. Leid (2014). "Regulation of transcription factor activity by interconnected post-translational modifications." *Trends Pharmacol Sci* **35**(2): 76-85.
- Fullam, A., L. Gu, Y. Höhn and M. Schröder (2018). "DDX3 directly facilitates IKK α activation and regulates downstream signalling pathways." *Biochem J* **475**(22): 3595-3607.
- Gariglio, P., M. Bellard and P. Chambon (1981). "Clustering of RNA polymerase B molecules in the 5' moiety of the adult beta-globin gene of hen erythrocytes." *Nucleic Acids Res* **9**(11): 2589-2598.
- Gaul, S., A. Leszczynska, F. Alegre, B. Kaufmann, C. D. Johnson, L. A. Adams, A. Wree, G. Damm, D. Seehofer, C. J. Calvente, D. Povero, T. Kisseleva, A. Eguchi, M. D. McGeough, H. M. Hoffman, P. Pelegrin, U. Laufs and A. E. Feldstein (2021). "Hepatocyte pyroptosis and release of inflammasome particles induce stellate cell activation and liver fibrosis." *J Hepatol* **74**(1): 156-167.
- Girardin, S. E., I. G. Boneca, L. A. Carneiro, A. Antignac, M. Jehanno, J. Viala, K. Tedin, M. K. Taha, A. Labigne, U. Zahringer, A. J. Coyle, P. S. DiStefano, J. Bertin, P. J. Sansonetti and D. J. Philpott (2003). "Nod1 detects a unique muropeptide from gram-negative bacterial peptidoglycan." *Science* **300**(5625): 1584-1587.
- Girardin, S. E., I. G. Boneca, J. Viala, M. Chamaillard, A. Labigne, G. Thomas, D. J. Philpott and P. J. Sansonetti (2003). "Nod2 is a general sensor of peptidoglycan through muramyl dipeptide (MDP) detection." *J Biol Chem* **278**(11): 8869-8872.
- Girardin, S. E., M. Jehanno, D. Mengin-Lecreulx, P. J. Sansonetti, P. M. Alzari and D. J. Philpott (2005). "Identification of the critical residues involved in peptidoglycan detection by Nod1." *J Biol Chem* **280**(46): 38648-38656.
- Girardin, S. E., R. Tournebize, M. Mavris, A. L. Page, X. Li, G. R. Stark, J. Bertin, P. S. DiStefano, M. Yaniv, P. J. Sansonetti and D. J. Philpott (2001). "CARD4/Nod1 mediates NF-kappaB and JNK activation by invasive *Shigella flexneri*." *EMBO Rep* **2**(8): 736-742.
- Gobin, S. J., V. Keijsers, M. van Zutphen and P. J. van den Elsen (1998). "The role of enhancer A in the locus-specific transactivation of classical and nonclassical HLA class I genes by nuclear factor kappa B." *J Immunol* **161**(5): 2276-2283.
- Gobin, S. J., A. Peijnenburg, V. Keijsers and P. J. van den Elsen (1997). "Site alpha is crucial for two routes of IFN gamma-induced MHC class I transactivation: the ISRE-mediated route and a novel pathway involving CIITA." *Immunity* **6**(5): 601-611.
- Gobin, S. J., M. van Zutphen, S. D. Westerheide, J. M. Boss and P. J. van den Elsen (2001). "The MHC-specific enhanceosome and its role in MHC class I and beta(2)-microglobulin gene transactivation." *J Immunol* **167**(9): 5175-5184.
- Gobin, S. J., M. van Zutphen, A. M. Woltman and P. J. van den Elsen (1999). "Transactivation of classical and nonclassical HLA class I genes through the IFN-stimulated response element." *J Immunol* **163**(3): 1428-1434.
- Gobin, S. J. P., M. van Zutphen, S. D. Westerheide, J. M. Boss and P. J. van den Elsen (2001). "The MHC-Specific Enhanceosome and Its Role in MHC Class I and β -Microglobulin Gene Transactivation." *The Journal of Immunology* **167**(9): 5175-5184.
- Göös, H., M. Kinnunen, L. Yadav, Z. Tan, K. Salokas, Q. Zhang, G.-h. Wei and M. Varjosalo (2021). Human transcription factor protein interaction networks, Research Square.

References

- Graham, F. L., J. Smiley, W. C. Russell and R. Nairn (1977). "Characteristics of a Human Cell Line Transformed by DNA from Human Adenovirus Type 5." *Journal of General Virology* **36**(1): 59-72.
- Graham, F. L., J. Smiley, W. C. Russell and R. Nairn (1977). "Characteristics of a human cell line transformed by DNA from human adenovirus type 5." *J Gen Virol* **36**(1): 59-74.
- Greer, C. B., Y. Tanaka, Y. J. Kim, P. Xie, M. Q. Zhang, I. H. Park and T. H. Kim (2015). "Histone Deacetylases Positively Regulate Transcription through the Elongation Machinery." *Cell Rep* **13**(7): 1444-1455.
- Grenier, J. M., L. Wang, G. A. Manji, W. J. Huang, A. Al-Garawi, R. Kelly, A. Carlson, S. Merriam, J. M. Lora, M. Briskin, P. S. DiStefano and J. Bertin (2002). "Functional screening of five PYPAF family members identifies PYPAF5 as a novel regulator of NF-kappaB and caspase-1." *FEBS Lett* **530**(1-3): 73-78.
- Gu, L., A. Fullam, R. Brennan and M. Schröder (2013). "Human DEAD box helicase 3 couples IκB kinase ε to interferon regulatory factor 3 activation." *Mol Cell Biol* **33**(10): 2004-2015.
- Gürtler, C. and A. G. Bowie (2013). "Innate immune detection of microbial nucleic acids." *Trends Microbiol* **21**(8): 413-420.
- Gutte, P. G., S. Jurt, M. G. Grütter and O. Zerbe (2014). "Unusual structural features revealed by the solution NMR structure of the NLRC5 caspase recruitment domain." *Biochemistry* **53**(19): 3106-3117.
- Ha, H. J. and H. H. Park (2020). "Crystal structure of the human NLRP9 pyrin domain reveals a bent N-terminal loop that may regulate inflammasome assembly." *FEBS Letters* **594**(15): 2396-2405.
- Halle, A., V. Hornung, G. C. Petzold, C. R. Stewart, B. G. Monks, T. Reinheckel, K. A. Fitzgerald, E. Latz, K. J. Moore and D. T. Golenbock (2008). "The NALP3 inflammasome is involved in the innate immune response to amyloid-β." *Nature Immunology* **9**(8): 857-865.
- Harton, J. A., D. E. Cressman, K. C. Chin, C. J. Der and J. P. Ting (1999). "GTP binding by class II transactivator: role in nuclear import." *Science* **285**(5432): 1402-1405.
- Harty, J. T., A. R. Tvinnereim and D. W. White (2000). "CD8+ T cell effector mechanisms in resistance to infection." *Annu Rev Immunol* **18**: 275-308.
- Hayano, T., M. Yanagida, Y. Yamauchi, T. Shinkawa, T. Isobe and N. Takahashi (2003). "Proteomic analysis of human Nop56p-associated pre-ribosomal ribonucleoprotein complexes. Possible link between Nop56p and the nucleolar protein treacle responsible for Treacher Collins syndrome." *J Biol Chem* **278**(36): 34309-34319.
- He, Y., M. Y. Zeng, D. Yang, B. Motro and G. Núñez (2016). "NEK7 is an essential mediator of NLRP3 activation downstream of potassium efflux." *Nature* **530**(7590): 354-357.
- Heberle, H., G. V. Meirelles, F. R. da Silva, G. P. Telles and R. Minghim (2015). "InteractiVenn: a web-based tool for the analysis of sets through Venn diagrams." *BMC Bioinformatics* **16**(1): 169.
- Hemmi, H., O. Takeuchi, S. Sato, M. Yamamoto, T. Kaisho, H. Sanjo, T. Kawai, K. Hoshino, K. Takeda and S. Akira (2004). "The roles of two IκB kinase-related kinases in lipopolysaccharide and double stranded RNA signaling and viral infection." *J Exp Med* **199**(12): 1641-1650.
- Henriques, T., D. A. Gilchrist, S. Nechaev, M. Bern, G. W. Muse, A. Burkholder, D. C. Fargo and K. Adelman (2013). "Stable pausing by RNA polymerase II provides an opportunity to target and integrate regulatory signals." *Mol Cell* **52**(4): 517-528.
- Honda, K., A. Takaoka and T. Taniguchi (2006). "Type I interferon [corrected] gene induction by the interferon regulatory factor family of transcription factors." *Immunity* **25**(3): 349-360.
- Hornung, V., A. Ablasser, M. Charrel-Dennis, F. Bauernfeind, G. Horvath, D. R. Caffrey, E. Latz and K. A. Fitzgerald (2009). "AIM2 recognizes cytosolic dsDNA and forms a caspase-1-activating inflammasome with ASC." *Nature* **458**(7237): 514-518.
- Hornung, V., S. Rothenfusser, S. Britsch, A. Krug, B. Jahrsdörfer, T. Giese, S. Endres and G. Hartmann (2002). "Quantitative expression of toll-like receptor 1-10 mRNA in cellular subsets of human peripheral blood mononuclear cells and sensitivity to CpG oligodeoxynucleotides." *J Immunol* **168**(9): 4531-4537.
- Hou, F., L. Sun, H. Zheng, B. Skaug, Q. X. Jiang and Z. J. Chen (2011). "MAVS forms functional prion-like aggregates to activate and propagate antiviral innate immune response." *Cell* **146**(3): 448-461.
- Howard, A. D., M. J. Kostura, N. Thornberry, G. J. Ding, G. Limjuco, J. Weidner, J. P. Salley, K. A. Hogquist, D. D. Chaplin and R. A. Mumford (1991). "IL-1-converting enzyme requires aspartic acid

References

- residues for processing of the IL-1 beta precursor at two distinct sites and does not cleave 31-kDa IL-1 alpha." *The Journal of Immunology* **147**(9): 2964-2969.
- Hu, Z., C. Yan, P. Liu, Z. Huang, R. Ma, C. Zhang, R. Wang, Y. Zhang, F. Martinon, D. Miao, H. Deng, J. Wang, J. Chang and J. Chai (2013). "Crystal Structure of NLRC4 Reveals Its Autoinhibition Mechanism." *Science* **341**(6142): 172-175.
- Hunt, C. R., D. Ramnarain, N. Horikoshi, P. Iyengar, R. K. Pandita, J. W. Shay and T. K. Pandita (2013). "Histone modifications and DNA double-strand break repair after exposure to ionizing radiations." *Radiat Res* **179**(4): 383-392.
- Inohara, N., T. Koseki, J. Lin, L. del Peso, P. C. Lucas, F. F. Chen, Y. Ogura and G. Núñez (2000). "An induced proximity model for NF-kappa B activation in the Nod1/RICK and RIP signaling pathways." *J Biol Chem* **275**(36): 27823-27831.
- Inohara, N., Y. Ogura, A. Fontalba, O. Gutierrez, F. Pons, J. Crespo, K. Fukase, S. Inamura, S. Kusumoto, M. Hashimoto, S. J. Foster, A. P. Moran, J. L. Fernandez-Luna and G. Nuñez (2003). "Host recognition of bacterial muramyl dipeptide mediated through NOD2. Implications for Crohn's disease." *J Biol Chem* **278**(8): 5509-5512.
- Isaacs, A. and J. Lindenmann (1957). "Virus interference. I. The interferon." *Proc R Soc Lond B Biol Sci* **147**(927): 258-267.
- Itoh-Lindstrom, Y., J. F. Piskurich, N. J. Felix, Y. Wang, W. J. Brickey, J. L. Platt, B. H. Koller and J. P.-Y. Ting (1999). "Reduced IL-4-, Lipopolysaccharide-, and IFN- γ -Induced MHC Class II Expression in Mice Lacking Class II Transactivator Due to Targeted Deletion of the GTP-Binding Domain." *The Journal of Immunology* **163**(5): 2425-2431.
- Izumi, N., A. Yamashita, A. Iwamatsu, R. Kurata, H. Nakamura, B. Saari, H. Hirano, P. Anderson and S. Ohno (2010). "AAA+ Proteins RUVBL1 and RUVBL2 Coordinate PIKK Activity and Function in Nonsense-Mediated mRNA Decay." *Science Signaling* **3**(116): ra27-ra27.
- Jabrane-Ferrat, N., N. Nekrep, G. Tosi, L. J. Esserman and B. M. Peterlin (2002). "Major histocompatibility complex class II transcriptional platform: assembly of nuclear factor Y and regulatory factor X (RFX) on DNA requires RFX5 dimers." *Mol Cell Biol* **22**(15): 5616-5625.
- Jamilloux, Y., T. Henry, A. Belot, S. Viel, M. Fauter, T. El Jammal, T. Walzer, B. François and P. Sève (2020). "Should we stimulate or suppress immune responses in COVID-19? Cytokine and anti-cytokine interventions." *Autoimmunity Reviews* **19**(7): 102567.
- Janeway, C. A., Jr. (1989). "Approaching the asymptote? Evolution and revolution in immunology." *Cold Spring Harb Symp Quant Biol* **54 Pt 1**: 1-13.
- Johansen, T. and T. Lamark (2011). "Selective autophagy mediated by autophagic adapter proteins." *Autophagy* **7**(3): 279-296.
- Juang, Y. T., W. Lowther, M. Kellum, W. C. Au, R. Lin, J. Hiscott and P. M. Pitha (1998). "Primary activation of interferon A and interferon B gene transcription by interferon regulatory factor 3." *Proc Natl Acad Sci U S A* **95**(17): 9837-9842.
- Kadamb, R., S. Mittal, N. Bansal, H. Batra and D. Saluja (2013). "Sin3: Insight into its transcription regulatory functions." *European Journal of Cell Biology* **92**(8): 237-246.
- Kawasaki, T. and T. Kawai (2014). "Toll-like receptor signaling pathways." *Front Immunol* **5**: 461.
- Keller, A., A. I. Nesvizhskii, E. Kolker and R. Aebersold (2002). "Empirical statistical model to estimate the accuracy of peptide identifications made by MS/MS and database search." *Anal Chem* **74**(20): 5383-5392.
- Khare, S., A. Dorfleutner, N. B. Bryan, C. Yun, A. D. Radian, L. de Almeida, Y. Rojanasakul and C. Stehlik (2012). "An NLRP7-containing inflammasome mediates recognition of microbial lipopeptides in human macrophages." *Immunity* **36**(3): 464-476.
- Kienes, I., T. Weidl, N. Mirza, M. Chamaillard and T. A. Kufer (2021). "Role of NLRs in the Regulation of Type I Interferon Signaling, Host Defense and Tolerance to Inflammation." *Int J Mol Sci* **22**(3).
- Kim, B. R., E. Coyaud, E. M. N. Laurent, J. St-Germain, E. Van de Laar, M. S. Tsao, B. Raught and N. Moghal (2017). "Identification of the SOX2 Interactome by BioID Reveals EP300 as a Mediator of SOX2-dependent Squamous Differentiation and Lung Squamous Cell Carcinoma Growth." *Mol Cell Proteomics* **16**(10): 1864-1888.
- Kim, D. I., S. C. Jensen, K. A. Noble, B. Kc, K. H. Roux, K. Motamedchaboki and K. J. Roux (2016). "An improved smaller biotin ligase for BioID proximity labeling." *Mol Biol Cell* **27**(8): 1188-1196.

References

- Kim, Y. J., C. B. Greer, K. R. Cecchini, L. N. Harris, D. P. Tuck and T. H. Kim (2013). "HDAC inhibitors induce transcriptional repression of high copy number genes in breast cancer through elongation blockade." *Oncogene* **32**(23): 2828-2835.
- Kim, Y. S., S. G. Lee, S. H. Park and K. Song (2001). "Gene structure of the human DDX3 and chromosome mapping of its related sequences." *Mol Cells* **12**(2): 209-214.
- Kimura, K., O. Cuvier and T. Hirano (2001). "Chromosome condensation by a human condensin complex in *Xenopus* egg extracts." *J Biol Chem* **276**(8): 5417-5420.
- Koerner, I., G. Kochs, U. Kalinke, S. Weiss and P. Staeheli (2007). "Protective role of beta interferon in host defense against influenza A virus." *J Virol* **81**(4): 2025-2030.
- Koipally, J. and K. Georgopoulos (2000). "Ikaros interactions with CtBP reveal a repression mechanism that is independent of histone deacetylase activity." *J Biol Chem* **275**(26): 19594-19602.
- Kouzarides, T. (2007). "Chromatin modifications and their function." *Cell* **128**(4): 693-705.
- Kowalinski, E., T. Lunardi, A. A. McCarthy, J. Louber, J. Brunel, B. Grigorov, D. Gerlier and S. Cusack (2011). "Structural basis for the activation of innate immune pattern-recognition receptor RIG-I by viral RNA." *Cell* **147**(2): 423-435.
- Krishnan, V. and B. Rupp (2012). *Macromolecular Structure Determination: Comparison of X-ray Crystallography and NMR Spectroscopy*. eLS.
- Kronheim, S. R., A. Mumma, T. Greenstreet, P. J. Glackin, K. Van Ness, C. J. March and R. A. Black (1992). "Purification of interleukin-1 beta converting enzyme, the protease that cleaves the interleukin-1 beta precursor." *Arch Biochem Biophys* **296**(2): 698-703.
- Kuenzel, S., A. Till, M. Winkler, R. Hasler, S. Lipinski, S. Jung, J. Grotzinger, H. Fickenscher, S. Schreiber and P. Rosenstiel (2010). "The nucleotide-binding oligomerization domain-like receptor NLRC5 is involved in IFN-dependent antiviral immune responses." *J Immunol* **184**(4): 1990-2000.
- Kufer, T. A., E. Kremmer, D. J. Banks and D. J. Philpott (2006). "Role for erbin in bacterial activation of Nod2." *Infect Immun* **74**(6): 3115-3124.
- Kufer, T. A. and P. J. Sansonetti (2011). "NLR functions beyond pathogen recognition." *Nat Immunol* **12**(2): 121-128.
- Kumar, H., S. Pandey, J. Zou, Y. Kumagai, K. Takahashi, S. Akira and T. Kawai (2011). "NLRC5 deficiency does not influence cytokine induction by virus and bacteria infections." *J Immunol* **186**(2): 994-1000.
- Kwong, A. D., B. G. Rao and K. T. Jeang (2005). "Viral and cellular RNA helicases as antiviral targets." *Nat Rev Drug Discov* **4**(10): 845-853.
- Lai, M. C., Y. H. Lee and W. Y. Tarn (2008). "The DEAD-box RNA helicase DDX3 associates with export messenger ribonucleoproteins as well as tip-associated protein and participates in translational control." *Mol Biol Cell* **19**(9): 3847-3858.
- Lau, L., E. E. Gray, R. L. Brunette and D. B. Stetson (2015). "DNA tumor virus oncogenes antagonize the cGAS-STING DNA-sensing pathway." *Science* **350**(6260): 568-571.
- LaVallie, E. R., E. A. DiBlasio, S. Kovacic, K. L. Grant, P. F. Schendel and J. M. McCoy (1993). "A Thioredoxin Gene Fusion Expression System That Circumvents Inclusion Body Formation in the E. coli Cytoplasm." *Bio/Technology* **11**(2): 187-193.
- Lech, M., A. Avila-Ferruffino, V. Skuginna, H. E. Susanti and H. J. Anders (2010). "Quantitative expression of RIG-like helicase, NOD-like receptor and inflammasome-related mRNAs in humans and mice." *Int Immunol* **22**(9): 717-728.
- Leone, P., E.-C. Shin, F. Perosa, A. Vacca, F. Dammacco and V. Racanelli (2013). "MHC Class I Antigen Processing and Presenting Machinery: Organization, Function, and Defects in Tumor Cells." *JNCI: Journal of the National Cancer Institute* **105**(16): 1172-1187.
- Li, J., Y. Liu, H. S. Rhee, S. K. Ghosh, L. Bai, B. F. Pugh and D. S. Gilmour (2013). "Kinetic competition between elongation rate and binding of NELF controls promoter-proximal pausing." *Mol Cell* **50**(5): 711-722.
- Li, Q., P. Zhang, C. Zhang, Y. Wang, R. Wan, Y. Yang, X. Guo, R. Huo, M. Lin, Z. Zhou and J. Sha (2014). "DDX3X regulates cell survival and cell cycle during mouse early embryonic development." *J Biomed Res* **28**(4): 282-291.
- Li, Y., M. Zhang and X. Zheng (2018). "High Expression of NLRC5 is associated with prognosis of gastric cancer." *Open Medicine* **13**(1): 443-449.

References

- Liang, Z., A. Damianou, E. Di Daniel and B. M. Kessler (2021). "Inflammasome activation controlled by the interplay between post-translational modifications: emerging drug target opportunities." Cell Communication and Signaling **19**(1): 23.
- Lim, K. H., C. G. Chen, Y. C. Chang, Y. H. Chiang, C. W. Kao, W. T. Wang, C. Y. Chang, L. Huang, C. S. Lin, C. C. Cheng, H. I. Cheng, N. W. Su, J. Lin, Y. F. Chang, M. C. Chang, R. K. Hsieh, H. C. Lin and Y. Y. Kuo (2017). "Increased B cell activation is present in JAK2V617F-mutated, CALR-mutated and triple-negative essential thrombocythemia." Oncotarget **8**(20): 32476-32491.
- Lim, K. H., L. C. Chen, K. Hsu, C. C. Chang, C. Y. Chang, C. W. Kao, Y. F. Chang, M. C. Chang and C. G. Chen (2020). "BAFF-driven NLRP3 inflammasome activation in B cells." Cell Death Dis **11**(9): 820.
- Lin, R., P. Génin, Y. Mamane and J. Hiscott (2000). "Selective DNA Binding and Association with the CREB Binding Protein Coactivator Contribute to Differential Activation of Alpha/Beta Interferon Genes by Interferon Regulatory Factors 3 and 7." Molecular and Cellular Biology **20**(17): 6342-6353.
- Lin, R., C. Heylbroeck, P. M. Pitha and J. Hiscott (1998). "Virus-dependent phosphorylation of the IRF-3 transcription factor regulates nuclear translocation, transactivation potential, and proteasome-mediated degradation." Mol Cell Biol **18**(5): 2986-2996.
- Lin, T., C. Chao, S. i. Saito, S. J. Mazur, M. E. Murphy, E. Appella and Y. Xu (2005). "p53 induces differentiation of mouse embryonic stem cells by suppressing Nanog expression." Nature Cell Biology **7**(2): 165-171.
- Ling, A., F. Soares, D. O. Croitoru, I. Tattoli, L. A. Carneiro, M. Boniotto, S. Benko, D. J. Philpott and S. E. Girardin (2012). "Post-transcriptional inhibition of luciferase reporter assays by the Nod-like receptor proteins NLRX1 and NLRC3." J Biol Chem **287**(34): 28705-28716.
- Lis, J. T., P. Mason, J. Peng, D. H. Price and J. Werner (2000). "P-TEFb kinase recruitment and function at heat shock loci." Genes Dev **14**(7): 792-803.
- Lisica, A., C. Engel, M. Jahnel, É. Roldán, E. A. Galburt, P. Cramer and S. W. Grill (2016). "Mechanisms of backtrack recovery by RNA polymerases I and II." Proceedings of the National Academy of Sciences **113**(11): 2946-2951.
- Liu, C. C., S. C. Wang, C. W. Kao, R. K. Hsieh, M. C. Chang, Y. F. Chang, K. H. Lim and C. G. Chen (2014). "B cells facilitate platelet production mediated by cytokines in patients with essential thrombocythaemia." Thromb Haemost **112**(3): 537-550.
- Liwinski, T., D. Zheng and E. Elinav (2020). "The microbiome and cytosolic innate immune receptors." Immunol Rev **297**(1): 207-224.
- Louis-Pence, P., C. S. Moreno and J. M. Boss (1997). "Formation of a regulatory factor X/X2 box-binding protein/nuclear factor-Y multiprotein complex on the conserved regulatory regions of HLA class II genes." J Immunol **159**(8): 3899-3909.
- Lu, A., V. G. Magupalli, J. Ruan, Q. Yin, M. K. Atianand, M. R. Vos, G. F. Schröder, K. A. Fitzgerald, H. Wu and E. H. Egelman (2014). "Unified polymerization mechanism for the assembly of ASC-dependent inflammasomes." Cell **156**(6): 1193-1206.
- Ludigs, K., Q. Seguí-Estévez, S. Lemeille, I. Ferrero, G. Rota, S. Chelbi, C. Mattmann, H. R. MacDonald, W. Reith and G. Guarda (2015). "NLRC5 exclusively transactivates MHC class I and related genes through a distinctive SXY module." PLoS Genet **11**(3): e1005088.
- Lupfer, C., P. G. Thomas, P. K. Anand, P. Vogel, S. Milasta, J. Martinez, G. Huang, M. Green, M. Kundu, H. Chi, R. J. Xavier, D. R. Green, M. Lamkanfi, C. A. Dinarello, P. C. Doherty and T. D. Kanneganti (2013). "Receptor interacting protein kinase 2-mediated mitophagy regulates inflammasome activation during virus infection." Nat Immunol **14**(5): 480-488.
- Ma, Z., S. E. Hopcraft, F. Yang, A. Petrucelli, H. Guo, J. P. Ting, D. P. Dittmer and B. Damania (2017). "NLRX1 negatively modulates type I IFN to facilitate KSHV reactivation from latency." PLoS Pathog **13**(5): e1006350.
- Maeurer, M. J., S. M. Gollin, D. Martin, W. Swaney, J. Bryant, C. Castelli, P. Robbins, G. Parmiani, W. J. Storkus and M. T. Lotze (1996). "Tumor escape from immune recognition: lethal recurrent melanoma in a patient associated with downregulation of the peptide transporter protein TAP-1 and loss of expression of the immunodominant MART-1/Melan-A antigen." The Journal of Clinical Investigation **98**(7): 1633-1641.

References

- Magner, W. J., A. L. Kazim, C. Stewart, M. A. Romano, G. Catalano, C. Grande, N. Keiser, F. Santaniello and T. B. Tomasi (2000). "Activation of MHC class I, II, and CD40 gene expression by histone deacetylase inhibitors." *J Immunol* **165**(12): 7017-7024.
- Martin, B. K., K. C. Chin, J. C. Olsen, C. A. Skinner, A. Dey, K. Ozato and J. P. Ting (1997). "Induction of MHC class I expression by the MHC class II transactivator CIITA." *Immunity* **6**(5): 591-600.
- Martinon, F., V. Pétrilli, A. Mayor, A. Tardivel and J. Tschopp (2006). "Gout-associated uric acid crystals activate the NALP3 inflammasome." *Nature* **440**(7081): 237-241.
- Masternak, K., E. Barras, M. Zufferey, B. Conrad, G. Corthals, R. Aebersold, J. C. Sanchez, D. F. Hochstrasser, B. Mach and W. Reith (1998). "A gene encoding a novel RFX-associated transactivator is mutated in the majority of MHC class II deficiency patients." *Nat Genet* **20**(3): 273-277.
- Masternak, K., A. Muhlethaler-Mottet, J. Villard, M. Zufferey, V. Steimle and W. Reith (2000). "CIITA is a transcriptional coactivator that is recruited to MHC class II promoters by multiple synergistic interactions with an enhanceosome complex." *Genes Dev* **14**(9): 1156-1166.
- Matsui, K., Y. Kumagai, H. Kato, S. Sato, T. Kawagoe, S. Uematsu, O. Takeuchi and S. Akira (2006). "Cutting edge: Role of TANK-binding kinase 1 and inducible IkappaB kinase in IFN responses against viruses in innate immune cells." *J Immunol* **177**(9): 5785-5789.
- Matyszewski, M., W. Zheng, J. Lueck, B. Antiochos, E. H. Egelman and J. Sohn (2018). "Cryo-EM structure of the NLRC4CARD filament provides insights into how symmetric and asymmetric supramolecular structures drive inflammasome assembly." *Journal of Biological Chemistry* **293**(52): 20240-20248.
- McChesney, P. A., S. E. Aiyar, O. J. Lee, A. Zaika, C. Moskaluk, R. Li and W. El-Rifai (2006). "Cofactor of BRCA1: a novel transcription factor regulator in upper gastrointestinal adenocarcinomas." *Cancer Res* **66**(3): 1346-1353.
- McDaniel, P. and X. Wu (2009). "Identification of oocyte-selective NLRP genes in rhesus macaque monkeys (*Macaca mulatta*)." *Mol Reprod Dev* **76**(2): 151-159.
- McNab, F., K. Mayer-Barber, A. Sher, A. Wack and A. O'Garra (2015). "Type I interferons in infectious disease." *Nature Reviews Immunology* **15**(2): 87-103.
- McPherson, A. and J. A. Gavira (2014). "Introduction to protein crystallization." *Acta Crystallogr F Struct Biol Commun* **70**(Pt 1): 2-20.
- Meissner, T. B., A. Li, A. Biswas, K. H. Lee, Y. J. Liu, E. Bayir, D. Iliopoulos, P. J. van den Elsen and K. S. Kobayashi (2010). "NLR family member NLRC5 is a transcriptional regulator of MHC class I genes." *Proc Natl Acad Sci U S A* **107**(31): 13794-13799.
- Meissner, T. B., A. Li, Y. J. Liu, E. Gagnon and K. S. Kobayashi (2012). "The nucleotide-binding domain of NLRC5 is critical for nuclear import and transactivation activity." *Biochem Biophys Res Commun* **418**(4): 786-791.
- Meissner, T. B., Y. J. Liu, K. H. Lee, A. Li, A. Biswas, M. C. van Eggermond, P. J. van den Elsen and K. S. Kobayashi (2012). "NLRC5 cooperates with the RFX transcription factor complex to induce MHC class I gene expression." *J Immunol* **188**(10): 4951-4958.
- Mellacheruvu, D., Z. Wright, A. L. Couzens, J.-P. Lambert, N. A. St-Denis, T. Li, Y. V. Miteva, S. Hauri, M. E. Sardi, T. Y. Low, V. A. Halim, R. D. Bagshaw, N. C. Hubner, A. al-Hakim, A. Bouchard, D. Faubert, D. Fermin, W. H. Dunham, M. Goudreault, Z.-Y. Lin, B. G. Badillo, T. Pawson, D. Durocher, B. Coulombe, R. Aebersold, G. Superti-Furga, J. Colinge, A. J. R. Heck, H. Choi, M. Gstaiger, S. Mohammed, I. M. Cristea, K. L. Bennett, M. P. Washburn, B. Raught, R. M. Ewing, A.-C. Gingras and A. I. Nesvizhskii (2013). "The CRAPome: a contaminant repository for affinity purification-mass spectrometry data." *Nature Methods* **10**(8): 730-736.
- Miao, E. A., E. Andersen-Nissen, S. E. Warren and A. Aderem (2007). "TLR5 and Ipaf: dual sensors of bacterial flagellin in the innate immune system." *Seminars in Immunopathology* **29**(3): 275-288.
- Min, H., C. W. Turck, J. M. Nikolic and D. L. Black (1997). "A new regulatory protein, KSRP, mediates exon inclusion through an intronic splicing enhancer." *Genes Dev* **11**(8): 1023-1036.
- Miotto, B., M. Chibi, P. Xie, S. Koundrioukoff, H. Moolman-Smook, D. Pugh, M. Debatisse, F. He, L. Zhang and P. A. Defossez (2014). "The RBBP6/ZBTB38/MCM10 axis regulates DNA replication and common fragile site stability." *Cell Rep* **7**(2): 575-587.

References

- Mishra, B. B., P. Moura-Alves, A. Sonawane, N. Hacohen, G. Griffiths, L. F. Moita and E. Anes (2010). "Mycobacterium tuberculosis protein ESAT-6 is a potent activator of the NLRP3/ASC inflammasome." *Cell Microbiol* **12**(8): 1046-1063.
- Mitoma, H., S. Hanabuchi, T. Kim, M. Bao, Z. Zhang, N. Sugimoto and Y. J. Liu (2013). "The DHX33 RNA helicase senses cytosolic RNA and activates the NLRP3 inflammasome." *Immunity* **39**(1): 123-135.
- Moore, C. B., D. T. Bergstralh, J. A. Duncan, Y. Lei, T. E. Morrison, A. G. Zimmermann, M. A. Accavitti-Loper, V. J. Madden, L. Sun, Z. Ye, J. D. Lich, M. T. Heise, Z. Chen and J. P. Ting (2008). "NLRX1 is a regulator of mitochondrial antiviral immunity." *Nature* **451**(7178): 573-577.
- Moreno, C. S., P. Emery, J. E. West, B. Durand, W. Reith, B. Mach and J. M. Boss (1995). "Purified X2 binding protein (X2BP) cooperatively binds the class II MHC X box region in the presence of purified RFX, the X box factor deficient in the bare lymphocyte syndrome." *J Immunol* **155**(9): 4313-4321.
- Motta, V., F. Soares, T. Sun and D. J. Philpott (2015). "NOD-like receptors: versatile cytosolic sentinels." *Physiol Rev* **95**(1): 149-178.
- Mótyán, J. A., P. Bagossi, S. Benkó and J. Tózsér (2013). "A molecular model of the full-length human NOD-like receptor family CARD domain containing 5 (NLRC5) protein." *BMC Bioinformatics* **14**: 275.
- Motz, G. T. and G. Coukos (2013). "Deciphering and reversing tumor immune suppression." *Immunity* **39**(1): 61-73.
- Muller, U., U. Steinhoff, L. Reis, S. Hemmi, J. Pavlovic, R. Zinkernagel and M. Aguet (1994). "Functional role of type I and type II interferons in antiviral defense." *Science* **264**(5167): 1918-1921.
- Muñoz, E., G. Courtois, P. Veschambre, P. Jalinot and A. Israël (1994). "Tax induces nuclear translocation of NF-kappa B through dissociation of cytoplasmic complexes containing p105 or p100 but does not induce degradation of I kappa B alpha/MAD3." *J Virol* **68**(12): 8035-8044.
- Nagarajan, U. M., P. Louis-Pence, A. DeSandro, R. Nilsen, A. Bushey and J. M. Boss (1999). "RFX-B is the gene responsible for the most common cause of the bare lymphocyte syndrome, an MHC class II immunodeficiency." *Immunity* **10**(2): 153-162.
- Narita, T., Y. Yamaguchi, K. Yano, S. Sugimoto, S. Chanarat, T. Wada, D. K. Kim, J. Hasegawa, M. Omori, N. Inukai, M. Endoh, T. Yamada and H. Handa (2003). "Human transcription elongation factor NELF: identification of novel subunits and reconstitution of the functionally active complex." *Mol Cell Biol* **23**(6): 1863-1873.
- Nechaev, S., D. C. Fargo, G. dos Santos, L. Liu, Y. Gao and K. Adelman (2010). "Global analysis of short RNAs reveals widespread promoter-proximal stalling and arrest of Pol II in Drosophila." *Science* **327**(5963): 335-338.
- Neerincx, A., K. Jakobshagen, O. Utermöhlen, H. Büning, V. Steimle and T. A. Kufer (2014). "The N-terminal domain of NLRC5 confers transcriptional activity for MHC class I and II gene expression." *J Immunol* **193**(6): 3090-3100.
- Neerincx, A., K. Lautz, M. Menning, E. Kremmer, P. Zigrino, M. Hösel, H. Büning, R. Schwarzenbacher and T. A. Kufer (2010). "A role for the human nucleotide-binding domain, leucine-rich repeat-containing family member NLRC5 in antiviral responses." *J Biol Chem* **285**(34): 26223-26232.
- Neerincx, A., G. M. Rodriguez, V. Steimle and T. A. Kufer (2012). "NLRC5 controls basal MHC class I gene expression in an MHC enhanceosome-dependent manner." *J Immunol* **188**(10): 4940-4950.
- Novick, D., B. Cohen and M. Rubinstein (1994). "The human interferon alpha/beta receptor: characterization and molecular cloning." *Cell* **77**(3): 391-400.
- Ogura, Y., N. Inohara, A. Benito, F. F. Chen, S. Yamaoka and G. Nunez (2001). "Nod2, a Nod1/Apaf-1 family member that is restricted to monocytes and activates NF-kappaB." *J Biol Chem* **276**(7): 4812-4818.
- Oka, M. and Y. Yoneda (2018). "Importin α : functions as a nuclear transport factor and beyond." *Proc Jpn Acad Ser B Phys Biol Sci* **94**(7): 259-274.
- Okamoto, A., D. J. Demetrick, E. A. Spillare, K. Hagiwara, S. P. Hussain, W. P. Bennett, K. Forrester, B. Gerwin, M. Serrano, D. H. Beach and et al. (1994). "Mutations and altered expression of p16INK4 in human cancer." *Proc Natl Acad Sci U S A* **91**(23): 11045-11049.

References

- Osborne, A., H. Zhang, W. M. Yang, E. Seto and G. Blanck (2001). "Histone deacetylase activity represses gamma interferon-inducible HLA-DR gene expression following the establishment of a DNase I-hypersensitive chromatin conformation." *Mol Cell Biol* **21**(19): 6495-6506.
- Oshiumi, H., M. Matsumoto, S. Hatakeyama and T. Seya (2009). "Riplet/RNF135, a RING finger protein, ubiquitinates RIG-I to promote interferon-beta induction during the early phase of viral infection." *J Biol Chem* **284**(2): 807-817.
- Oshiumi, H., K. Sakai, M. Matsumoto and T. Seya (2010). "DEAD/H BOX 3 (DDX3) helicase binds the RIG-I adaptor IPS-1 to up-regulate IFN-beta-inducing potential." *Eur J Immunol* **40**(4): 940-948.
- Owsianka, A. M. and A. H. Patel (1999). "Hepatitis C Virus Core Protein Interacts with a Human DEAD Box Protein DDX3." *Virology* **257**(2): 330-340.
- Palangat, M., D. B. Renner, D. H. Price and R. Landick (2005). "A negative elongation factor for human RNA polymerase II inhibits the anti-arrest transcript-cleavage factor TFIIS." *Proc Natl Acad Sci U S A* **102**(42): 15036-15041.
- Pankiv, S., T. H. Clausen, T. Lamark, A. Brech, J. A. Bruun, H. Outzen, A. Øvervatn, G. Bjørkøy and T. Johansen (2007). "p62/SQSTM1 binds directly to Atg8/LC3 to facilitate degradation of ubiquitinated protein aggregates by autophagy." *J Biol Chem* **282**(33): 24131-24145.
- Pene, V., Q. Li, C. Sodroski, C. S. Hsu and T. J. Liang (2015). "Dynamic Interaction of Stress Granules, DDX3X, and IKK-alpha Mediates Multiple Functions in Hepatitis C Virus Infection." *J Virol* **89**(10): 5462-5477.
- Perkins, J. R., I. Diboun, B. H. Dessailly, J. G. Lees and C. Orengo (2010). "Transient Protein-Protein Interactions: Structural, Functional, and Network Properties." *Structure* **18**(10): 1233-1243.
- Perry, A. K., E. K. Chow, J. B. Goodnough, W. C. Yeh and G. Cheng (2004). "Differential requirement for TANK-binding kinase-1 in type I interferon responses to toll-like receptor activation and viral infection." *J Exp Med* **199**(12): 1651-1658.
- Peterlin, B. M. and D. H. Price (2006). "Controlling the Elongation Phase of Transcription with P-TEFb." *Molecular Cell* **23**(3): 297-305.
- Poltorak, A., X. He, I. Smirnova, M. Y. Liu, C. Van Huffel, X. Du, D. Birdwell, E. Alejos, M. Silva, C. Galanos, M. Freudenberg, P. Ricciardi-Castagnoli, B. Layton and B. Beutler (1998). "Defective LPS signaling in C3H/HeJ and C57BL/10ScCr mice: mutations in Tlr4 gene." *Science* **282**(5396): 2085-2088.
- Qin, Y., Z. Su, Y. Wu, C. Wu, S. Jin, W. Xie, W. Jiang, R. Zhou and J. Cui (2017). "NLRP11 disrupts MAVS signalosome to inhibit type I interferon signaling and virus-induced apoptosis." *EMBO Rep* **18**(12): 2160-2171.
- Qin, Y., B. Xue, C. Liu, X. Wang, R. Tian, Q. Xie, M. Guo, G. Li, D. Yang and H. Zhu (2017). "NLRX1 Mediates MAVS Degradation To Attenuate the Hepatitis C Virus-Induced Innate Immune Response through PCBP2." *J Virol* **91**(23).
- Rain, J. C., L. Selig, H. De Reuse, V. Battaglia, C. Reverdy, S. Simon, G. Lenzen, F. Petel, J. Wojcik, V. Schächter, Y. Chemama, A. Labigne and P. Legrain (2001). "The protein-protein interaction map of *Helicobacter pylori*." *Nature* **409**(6817): 211-215.
- Ranjan, P., N. Singh, A. Kumar, A. Neerincx, E. Kremmer, W. Cao, W. G. Davis, J. M. Katz, S. Gangappa, R. Lin, T. A. Kufer and S. Sambhara (2015). "NLRC5 interacts with RIG-I to induce a robust antiviral response against influenza virus infection." *Eur J Immunol* **45**(3): 758-772.
- Raval, A., T. K. Howcroft, J. D. Weissman, S. Kirshner, X.-S. Zhu, K. Yokoyama, J. Ting and D. S. Singer (2001). "Transcriptional Coactivator, CIITA, Is an Acetyltransferase that Bypasses a Promoter Requirement for TAFII250." *Molecular Cell* **7**(1): 105-115.
- Rawlings, J. S., K. M. Rosler and D. A. Harrison (2004). "The JAK/STAT signaling pathway." *J Cell Sci* **117**(Pt 8): 1281-1283.
- Razmara, M., S. M. Srinivasula, L. Wang, J. L. Poyet, B. J. Geddes, P. S. DiStefano, J. Bertin and E. S. Alnemri (2002). "CARD-8 protein, a new CARD family member that regulates caspase-1 activation and apoptosis." *J Biol Chem* **277**(16): 13952-13958.
- Rehwinkel, J. and M. U. Gack (2020). "RIG-I-like receptors: their regulation and roles in RNA sensing." *Nat Rev Immunol* **20**(9): 537-551.
- Reith, W., S. LeibundGut-Landmann and J. M. Waldburger (2005). "Regulation of MHC class II gene expression by the class II transactivator." *Nat Rev Immunol* **5**(10): 793-806.

References

- Reith, W. and B. Mach (2001). "The bare lymphocyte syndrome and the regulation of MHC expression." *Annu Rev Immunol* **19**: 331-373.
- Reubold, T. F., G. Hahne, S. Wohlgemuth and S. Eschenburg (2014). "Crystal structure of the leucine-rich repeat domain of the NOD-like receptor NLRP1: implications for binding of muramyl dipeptide." *FEBS Lett* **588**(18): 3327-3332.
- Riva, V. and G. Maga (2019). "From the magic bullet to the magic target: exploiting the diverse roles of DDX3X in viral infections and tumorigenesis." *Future Med Chem* **11**(11): 1357-1381.
- Robbins, G. R., A. D. Truax, B. K. Davis, L. Zhang, W. J. Brickey and J. P. Ting (2012). "Regulation of class I major histocompatibility complex (MHC) by nucleotide-binding domain, leucine-rich repeat-containing (NLR) proteins." *J Biol Chem* **287**(29): 24294-24303.
- Rodero, M. P. and Y. J. Crow (2016). "Type I interferon-mediated monogenic autoinflammation: The type I interferonopathies, a conceptual overview." *Journal of Experimental Medicine* **213**(12): 2527-2538.
- Rodriguez, G. M., D. Bobbala, D. Serrano, M. Mayhue, A. Champagne, C. Saucier, V. Steimle, T. A. Kufer, A. Menendez, S. Ramanathan and S. Ilangumaran (2016). "NLRC5 elicits antitumor immunity by enhancing processing and presentation of tumor antigens to CD8(+) T lymphocytes." *Oncoimmunology* **5**(6): e1151593.
- Roeder, R. G. (2019). "50+ years of eukaryotic transcription: an expanding universe of factors and mechanisms." *Nat Struct Mol Biol* **26**(9): 783-791.
- Rotger, M., J. Dalmau, A. Rauch, P. McLaren, S. E. Bosinger, R. Martinez, N. G. Sandler, A. Roque, J. Liebner, M. Battegay, E. Bernasconi, P. Descombes, I. Erkizia, J. Fellay, B. Hirschel, J. M. Miró, E. Palou, M. Hoffmann, M. Massanella, J. Blanco, M. Woods, H. F. Günthard, P. de Bakker, D. C. Douek, G. Silvestri, J. Martinez-Picado and A. Telenti (2011). "Comparative transcriptomics of extreme phenotypes of human HIV-1 infection and SIV infection in sooty mangabey and rhesus macaque." *The Journal of Clinical Investigation* **121**(6): 2391-2400.
- Roth, D. B. (2014). "V(D)J Recombination: Mechanism, Errors, and Fidelity." *Microbiol Spectr* **2**(6).
- Roux, K. J., D. I. Kim and B. Burke (2013). "BioID: a screen for protein-protein interactions." *Curr Protoc Protein Sci* **74**: 19.23.11-19.23.14.
- Roux, K. J., D. I. Kim, M. Raida and B. Burke (2012). "A promiscuous biotin ligase fusion protein identifies proximal and interacting proteins in mammalian cells." *J Cell Biol* **196**(6): 801-810.
- Sabbah, A., T. H. Chang, R. Harnack, V. Frohlich, K. Tominaga, P. H. Dube, Y. Xiang and S. Bose (2009). "Activation of innate immune antiviral responses by Nod2." *Nat Immunol* **10**(10): 1073-1080.
- Samir, P., S. Kesavardhana, D. M. Patmore, S. Gingras, R. K. S. Malireddi, R. Karki, C. S. Guy, B. Briard, D. E. Place, A. Bhattacharya, B. R. Sharma, A. Nourse, S. V. King, A. Pitre, A. R. Burton, S. Pelletier, R. J. Gilbertson and T. D. Kanneganti (2019). "DDX3X acts as a live-or-die checkpoint in stressed cells by regulating NLRP3 inflammasome." *Nature* **573**(7775): 590-594.
- Schier, A. C. and D. J. Taatjes (2020). "Structure and mechanism of the RNA polymerase II transcription machinery." *Genes Dev* **34**(7-8): 465-488.
- Schmid-Burgk, J. L., D. Chauhan, T. Schmidt, T. S. Ebert, J. Reinhardt, E. Endl and V. Hornung (2016). "A Genome-wide CRISPR (Clustered Regularly Interspaced Short Palindromic Repeats) Screen Identifies NEK7 as an Essential Component of NLRP3 Inflammasome Activation." *J Biol Chem* **291**(1): 103-109.
- Schröder, M. (2010). "Human DEAD-box protein 3 has multiple functions in gene regulation and cell cycle control and is a prime target for viral manipulation." *Biochem Pharmacol* **79**(3): 297-306.
- Schröder, M., M. Baran and A. G. Bowie (2008). "Viral targeting of DEAD box protein 3 reveals its role in TBK1/IKKepsilon-mediated IRF activation." *Embo j* **27**(15): 2147-2157.
- Sears, R. M., D. G. May and K. J. Roux (2019). "BioID as a Tool for Protein-Proximity Labeling in Living Cells." *Methods Mol Biol* **2012**: 299-313.
- Sewer, M. B., V. Q. Nguyen, C. J. Huang, P. W. Tucker, N. Kagawa and M. R. Waterman (2002). "Transcriptional activation of human CYP17 in H295R adrenocortical cells depends on complex formation among p54(nrb)/NonO, protein-associated splicing factor, and SF-1, a complex that also participates in repression of transcription." *Endocrinology* **143**(4): 1280-1290.

References

- Shannon, P., A. Markiel, O. Ozier, N. S. Baliga, J. T. Wang, D. Ramage, N. Amin, B. Schwikowski and T. Ideker (2003). "Cytoscape: a software environment for integrated models of biomolecular interaction networks." *Genome Res* **13**(11): 2498-2504.
- Sharif, H., L. Wang, W. L. Wang, V. G. Magupalli, L. Andreeva, Q. Qiao, A. V. Hauenstein, Z. Wu, G. Núñez, Y. Mao and H. Wu (2019). "Structural mechanism for NEK7-licensed activation of NLRP3 inflammasome." *Nature* **570**(7761): 338-343.
- Shepardson, K. M., K. Larson, L. L. Johns, K. Stanek, H. Cho, J. Wellham, H. Henderson and A. Rynda-Applé (2018). "IFNAR2 Is Required for Anti-influenza Immunity and Alters Susceptibility to Post-influenza Bacterial Superinfections." *Frontiers in Immunology* **9**(2589).
- Shi, H., Y. Wang, X. Li, X. Zhan, M. Tang, M. Fina, L. Su, D. Pratt, C. H. Bu, S. Hildebrand, S. Lyon, L. Scott, J. Quan, Q. Sun, J. Russell, S. Arnett, P. Jurek, D. Chen, V. V. Kravchenko, J. C. Mathison, E. M. Moresco, N. L. Monson, R. J. Ulevitch and B. Beutler (2016). "NLRP3 activation and mitosis are mutually exclusive events coordinated by NEK7, a new inflammasome component." *Nat Immunol* **17**(3): 250-258.
- Shih, J. W., W. T. Wang, T. Y. Tsai, C. Y. Kuo, H. K. Li and Y. H. Wu Lee (2012). "Critical roles of RNA helicase DDX3 and its interactions with eIF4E/PABP1 in stress granule assembly and stress response." *Biochem J* **441**(1): 119-129.
- Silverstein, R. A. and K. Ekwall (2005). "Sin3: a flexible regulator of global gene expression and genome stability." *Current Genetics* **47**(1): 1-17.
- Soulat, D., T. Bürckstümmer, S. Westermayer, A. Goncalves, A. Bauch, A. Stefanovic, O. Hantschel, K. L. Bennett, T. Decker and G. Superti-Furga (2008). "The DEAD-box helicase DDX3X is a critical component of the TANK-binding kinase 1-dependent innate immune response." *Embo j* **27**(15): 2135-2146.
- Spilianakis, C., J. Papamatheakis and A. Kretsovali (2000). "Acetylation by PCAF Enhances CIITA Nuclear Accumulation and Transactivation of Major Histocompatibility Complex Class II Genes." *Molecular and Cellular Biology* **20**(22): 8489-8498.
- Spilianakis, C., J. Papamatheakis and A. Kretsovali (2000). "Acetylation by PCAF enhances CIITA nuclear accumulation and transactivation of major histocompatibility complex class II genes." *Mol Cell Biol* **20**(22): 8489-8498.
- Staehli, F., K. Ludigs, L. X. Heinz, Q. Seguin-Estevez, I. Ferrero, M. Braun, K. Schroder, M. Rebsamen, A. Tardivel, C. Mattmann, H. R. MacDonald, P. Romero, W. Reith, G. Guarda and J. Tschoop (2012). "NLRC5 deficiency selectively impairs MHC class I- dependent lymphocyte killing by cytotoxic T cells." *J Immunol* **188**(8): 3820-3828.
- Steimle, V., B. Durand, E. Barras, M. Zufferey, M. R. Hadam, B. Mach and W. Reith (1995). "A novel DNA-binding regulatory factor is mutated in primary MHC class II deficiency (bare lymphocyte syndrome)." *Genes Dev* **9**(9): 1021-1032.
- Steimle, V., L. A. Otten, M. Zufferey and B. Mach (1993). "Complementation cloning of an MHC class II transactivator mutated in hereditary MHC class II deficiency (or bare lymphocyte syndrome)." *Cell* **75**(1): 135-146.
- Steimle, V., C. A. Siegrist, A. Mottet, B. Lisowska-Groszpiette and B. Mach (1994). "Regulation of MHC class II expression by interferon-gamma mediated by the transactivator gene CIITA." *Science* **265**(5168): 106-109.
- Stetson, D. B. and R. Medzhitov (2006). "Type I interferons in host defense." *Immunity* **25**(3): 373-381.
- Sun, J., A. L. Blair, S. E. Aiyar and R. Li (2007). "Cofactor of BRCA1 modulates androgen-dependent transcription and alternative splicing." *J Steroid Biochem Mol Biol* **107**(3-5): 131-139.
- Sun, J., H. Pan, C. Lei, B. Yuan, S. J. Nair, C. April, B. Parameswaran, B. Klotzle, J. B. Fan, J. Ruan and R. Li (2011). "Genetic and genomic analyses of RNA polymerase II-pausing factor in regulation of mammalian transcription and cell growth." *J Biol Chem* **286**(42): 36248-36257.
- Sun, J., G. Watkins, A. L. Blair, C. Moskaluk, S. Ghosh, W. G. Jiang and R. Li (2008). "Deregulation of cofactor of BRCA1 expression in breast cancer cells." *J Cell Biochem* **103**(6): 1798-1807.
- Swanson, K. V., M. Deng and J. P. Ting (2019). "The NLRP3 inflammasome: molecular activation and regulation to therapeutics." *Nat Rev Immunol* **19**(8): 477-489.
- Szabo, G. and T. Csak (2012). "Inflammasomes in liver diseases." *Journal of Hepatology* **57**(3): 642-654.

References

- Szappanos, D., R. Tschismarov, T. Perlot, S. Westermayer, K. Fischer, E. Platanitis, F. Kallinger, M. Novatchkova, C. Lassnig, M. Muller, V. Sexl, K. L. Bennett, M. Foong-Sobis, J. M. Penninger and T. Decker (2018). "The RNA helicase DDX3X is an essential mediator of innate antimicrobial immunity." *PLoS Pathog* **14**(11): e1007397.
- Tanabe, T., M. Chamaillard, Y. Ogura, L. Zhu, S. Qiu, J. Masumoto, P. Ghosh, A. Moran, M. M. Predergast, G. Tromp, C. J. Williams, N. Inohara and G. Núñez (2004). "Regulatory regions and critical residues of NOD2 involved in muramyl dipeptide recognition." *Embo j* **23**(7): 1587-1597.
- Taniuchi, K., M. Furihata, S. Iwasaki, K. Tanaka, T. Shimizu, M. Saito and T. Saibara (2014). "RUVBL1 directly binds actin filaments and induces formation of cell protrusions to promote pancreatic cancer cell invasion." *Int J Oncol* **44**(6): 1945-1954.
- Tattoli, I., L. A. Carneiro, M. Jehanno, J. G. Magalhaes, Y. Shu, D. J. Philpott, D. Arnoult and S. E. Girardin (2008). "NLRX1 is a mitochondrial NOD-like receptor that amplifies NF-kappaB and JNK pathways by inducing reactive oxygen species production." *EMBO Rep* **9**(3): 293-300.
- Tenoever, B. R., S. L. Ng, M. A. Chua, S. M. McWhirter, A. García-Sastre and T. Maniatis (2007). "Multiple functions of the IKK-related kinase IKKepsilon in interferon-mediated antiviral immunity." *Science* **315**(5816): 1274-1278.
- Thielens, A., E. Vivier and F. Romagné (2012). "NK cell MHC class I specific receptors (KIR): from biology to clinical intervention." *Curr Opin Immunol* **24**(2): 239-245.
- Thornberry, N. A., H. G. Bull, J. R. Calaycay, K. T. Chapman, A. D. Howard, M. J. Kostura, D. K. Miller, S. M. Molineaux, J. R. Weidner, J. Aunins and et al. (1992). "A novel heterodimeric cysteine protease is required for interleukin-1 beta processing in monocytes." *Nature* **356**(6372): 768-774.
- Tian, X., G. Pascal and P. Monget (2009). "Evolution and functional divergence of NLRP genes in mammalian reproductive systems." *BMC Evol Biol* **9**: 202.
- Ting, J. P. and B. K. Davis (2005). "CATERPILLER: a novel gene family important in immunity, cell death, and diseases." *Annu Rev Immunol* **23**: 387-414.
- Tong, Y., J. Cui, Q. Li, J. Zou, H. Y. Wang and R. F. Wang (2012). "Enhanced TLR-induced NF-κB signaling and type I interferon responses in NLRC5 deficient mice." *Cell Res* **22**(5): 822-835.
- Trinkle-Mulcahy, L. (2019). "Recent advances in proximity-based labeling methods for interactome mapping." *F1000Res* **8**.
- Trinklein, N. D., S. F. Aldred, S. J. Hartman, D. I. Schroeder, R. P. Otilar and R. M. Myers (2004). "An abundance of bidirectional promoters in the human genome." *Genome Res* **14**(1): 62-66.
- Tsutsui, H., X. Cai and S. Hayashi (2015). "Interleukin-1 Family Cytokines in Liver Diseases." *Mediators Inflamm* **2015**: 630265.
- Uddin, S., E. N. Fish, D. A. Sher, C. Gardziola, M. F. White and L. C. Platanius (1997). "Activation of the phosphatidylinositol 3-kinase serine kinase by IFN-alpha." *The Journal of Immunology* **158**(5): 2390-2397.
- Ummethum, H. and S. Hamperl (2020). "Proximity Labeling Techniques to Study Chromatin." *Frontiers in Genetics* **11**(450).
- UniProt Consortium, T. (2018). "UniProt: the universal protein knowledgebase." *Nucleic Acids Res* **46**(5): 2699.
- Uzé, G., G. Lutfalla and I. Gresser (1990). "Genetic transfer of a functional human interferon alpha receptor into mouse cells: cloning and expression of its cDNA." *Cell* **60**(2): 225-234.
- van den Elsen, P. J. (2011). "Expression regulation of major histocompatibility complex class I and class II encoding genes." *Front Immunol* **2**: 48.
- van den Elsen, P. J., T. M. Holling, H. F. Kuipers and N. van der Stoep (2004). "Transcriptional regulation of antigen presentation." *Curr Opin Immunol* **16**(1): 67-75.
- Vegna, S., D. Gregoire, M. Moreau, P. Lassus, D. Durantel, E. Assenat, U. Hibner and Y. Simonin (2016). "NOD1 Participates in the Innate Immune Response Triggered by Hepatitis C Virus Polymerase." *J Virol* **90**(13): 6022-6035.
- Vos, S. M., L. Farnung, H. Urlaub and P. Cramer (2018). "Structure of paused transcription complex Pol II-DSIF-NELF." *Nature* **560**(7720): 601-606.
- Vos, S. M., D. Pöllmann, L. Caizzi, K. B. Hofmann, P. Rombaut, T. Zimniak, F. Herzog and P. Cramer (2016). "Architecture and RNA binding of the human negative elongation factor." *Elife* **5**.

References

- Wada, T., T. Takagi, Y. Yamaguchi, A. Ferdous, T. Imai, S. Hirose, S. Sugimoto, K. Yano, G. A. Hartzog, F. Winston, S. Buratowski and H. Handa (1998). "DSIF, a novel transcription elongation factor that regulates RNA polymerase II processivity, is composed of human Spt4 and Spt5 homologs." *Genes Dev* **12**(3): 343-356.
- Walden, E. A., R. Y. Fong, T. T. Pham, H. Knill, S. J. Laframboise, S. Huard, M. E. Harper and K. Baetz (2020). "Phenomic screen identifies a role for the yeast lysine acetyltransferase NuA4 in the control of Bcy1 subcellular localization, glycogen biosynthesis, and mitochondrial morphology." *PLoS Genet* **16**(11): e1009220.
- Wang, L., G. A. Manji, J. M. Grenier, A. Al-Garawi, S. Merriam, J. M. Lora, B. J. Geddes, M. Briskin, P. S. DiStefano and J. Bertin (2002). "PYPAF7, a novel PYRIN-containing Apaf1-like protein that regulates activation of NF-kappa B and caspase-1-dependent cytokine processing." *J Biol Chem* **277**(33): 29874-29880.
- Wang, P., S. Zhu, L. Yang, S. Cui, W. Pan, R. Jackson, Y. Zheng, A. Rongvaux, Q. Sun, G. Yang, S. Gao, R. Lin, F. You, R. Flavell and E. Fikrig (2015). "Nlrp6 regulates intestinal antiviral innate immunity." *Science* **350**(6262): 826-830.
- Wang, X., R. Wang, M. Luo, C. Li, H. X. Wang, C. C. Huan, Y. R. Qu, Y. Liao and X. Mao (2017). "(DEAD)-box RNA helicase 3 modulates NF- κ B signal pathway by controlling the phosphorylation of PP2A-C subunit." *Oncotarget* **8**(20): 33197-33213.
- Winnard, P. T., Jr., F. Vesuna and V. Raman (2021). "Targeting host DEAD-box RNA helicase DDX3X for treating viral infections." *Antiviral Res* **185**: 104994.
- Wright, K. L. and J. P. Ting (2006). "Epigenetic regulation of MHC-II and CIITA genes." *Trends Immunol* **27**(9): 405-412.
- Wu, C., Z. Su, M. Lin, J. Ou, W. Zhao, J. Cui and R. F. Wang (2017). "NLRP11 attenuates Toll-like receptor signalling by targeting TRAF6 for degradation via the ubiquitin ligase RNF19A." *Nat Commun* **8**(1): 1977.
- Wu, C. H., Y. Yamaguchi, L. R. Benjamin, M. Horvat-Gordon, J. Washinsky, E. Enerly, J. Larsson, A. Lambertsson, H. Handa and D. Gilmour (2003). "NELF and DSIF cause promoter proximal pausing on the hsp70 promoter in Drosophila." *Genes Dev* **17**(11): 1402-1414.
- Xiao, W., S. Adhikari, U. Dahal, Y. S. Chen, Y. J. Hao, B. F. Sun, H. Y. Sun, A. Li, X. L. Ping, W. Y. Lai, X. Wang, H. L. Ma, C. M. Huang, Y. Yang, N. Huang, G. B. Jiang, H. L. Wang, Q. Zhou, X. J. Wang, Y. L. Zhao and Y. G. Yang (2016). "Nuclear m(6)A Reader YTHDC1 Regulates mRNA Splicing." *Mol Cell* **61**(4): 507-519.
- Yamaguchi, H. and M. Miyazaki (2014). "Refolding techniques for recovering biologically active recombinant proteins from inclusion bodies." *Biomolecules* **4**(1): 235-251.
- Yamaguchi, Y., T. Takagi, T. Wada, K. Yano, A. Furuya, S. Sugimoto, J. Hasegawa and H. Handa (1999). "NELF, a Multisubunit Complex Containing RD, Cooperates with DSIF to Repress RNA Polymerase II Elongation." *Cell* **97**(1): 41-51.
- Yang, J., Z. Liu and T. S. Xiao (2017). "Post-translational regulation of inflammasomes." *Cell Mol Immunol* **14**(1): 65-79.
- Yang, S. N. Y., S. C. Atkinson, M. D. Audsley, S. M. Heaton, D. A. Jans and N. A. Borg (2020). "RK-33 Is a Broad-Spectrum Antiviral Agent That Targets DEAD-Box RNA Helicase DDX3X." *Cells* **9**(1).
- Yang, X. D., W. Li, S. Zhang, D. Wu, X. Jiang, R. Tan, X. Niu, Q. Wang, X. Wu, Z. Liu, L. F. Chen, J. Qin and B. Su (2020). "PLK4 deubiquitination by Spata2-CYLD suppresses NEK7-mediated NLRP3 inflammasome activation at the centrosome." *Embo j* **39**(2): e102201.
- Yao, Y., Y. Wang, F. Chen, Y. Huang, S. Zhu, Q. Leng, H. Wang, Y. Shi and Y. Qian (2012). "NLRC5 regulates MHC class I antigen presentation in host defense against intracellular pathogens." *Cell Res* **22**(5): 836-847.
- Ye, Q., Y. F. Hu, H. Zhong, A. C. Nye, A. S. Belmont and R. Li (2001). "BRCA1-induced large-scale chromatin unfolding and allele-specific effects of cancer-predisposing mutations." *J Cell Biol* **155**(6): 911-921.
- Yedavalli, V. S., C. Neuveut, Y. H. Chi, L. Kleiman and K. T. Jeang (2004). "Requirement of DDX3 DEAD box RNA helicase for HIV-1 Rev-RRE export function." *Cell* **119**(3): 381-392.

References

- Yoshihama, S., J. Roszik, I. Downs, T. B. Meissner, S. Vijayan, B. Chapuy, T. Sidiq, M. A. Shipp, G. A. Lizee and K. S. Kobayashi (2016). "NLRC5/MHC class I transactivator is a target for immune evasion in cancer." *Proc Natl Acad Sci U S A* **113**(21): 5999-6004.
- Zatloukal, K., C. Stumptner, A. Fuchsbichler, H. Heid, M. Schnoelzer, L. Kenner, R. Kleinert, M. Prinz, A. Aguzzi and H. Denk (2002). "p62 Is a common component of cytoplasmic inclusions in protein aggregation diseases." *Am J Pathol* **160**(1): 255-263.
- Zebertavage, L. K., A. Alice, M. R. Crittenden and M. J. Gough (2020). "Transcriptional Upregulation of NLRC5 by Radiation Drives STING- and Interferon-Independent MHC-I Expression on Cancer Cells and T Cell Cytotoxicity." *Sci Rep* **10**(1): 7376.
- Zhang, C., G. Shang, X. Gui, X. Zhang, X. C. Bai and Z. J. Chen (2019). "Structural basis of STING binding with and phosphorylation by TBK1." *Nature* **567**(7748): 394-398.
- Zhang, L., S. Chen, J. Ruan, J. Wu, A. B. Tong, Q. Yin, Y. Li, L. David, A. Lu, W. L. Wang, C. Marks, Q. Ouyang, X. Zhang, Y. Mao and H. Wu (2015). "Cryo-EM structure of the activated NAIP2-NLRC4 inflammasome reveals nucleated polymerization." *Science* **350**(6259): 404-409.
- Zhang, L., J. Mo, K. V. Swanson, H. Wen, A. Petrucelli, S. M. Gregory, Z. Zhang, M. Schneider, Y. Jiang, K. A. Fitzgerald, S. Ouyang, Z. J. Liu, B. Damania, H. B. Shu, J. A. Duncan and J. P. Ting (2014). "NLRC3, a member of the NLR family of proteins, is a negative regulator of innate immune signaling induced by the DNA sensor STING." *Immunity* **40**(3): 329-341.
- Zhong, H., J. Zhu, H. Zhang, L. Ding, Y. Sun, C. Huang and Q. Ye (2004). "COBRA1 inhibits AP-1 transcriptional activity in transfected cells." *Biochem Biophys Res Commun* **325**(2): 568-573.
- Zhou, Q. and J. H. N. Yik (2006). "The Yin and Yang of P-TEFb Regulation: Implications for Human Immunodeficiency Virus Gene Expression and Global Control of Cell Growth and Differentiation." *Microbiology and Molecular Biology Reviews* **70**(3): 646-659.
- Zhu, S., S. Ding, P. Wang, Z. Wei, W. Pan, N. W. Palm, Y. Yang, H. Yu, H. B. Li, G. Wang, X. Lei, M. R. de Zoete, J. Zhao, Y. Zheng, H. Chen, Y. Zhao, K. A. Jurado, N. Feng, L. Shan, Y. Kluger, J. Lu, C. Abraham, E. Fikrig, H. B. Greenberg and R. A. Flavell (2017). "Nlrp9b inflammasome restricts rotavirus infection in intestinal epithelial cells." *Nature* **546**(7660): 667-670.
- Zika, E., S. F. Greer, X. S. Zhu and J. P. Ting (2003). "Histone deacetylase 1/mSin3A disrupts gamma interferon-induced CIITA function and major histocompatibility complex class II enhanceosome formation." *Mol Cell Biol* **23**(9): 3091-3102.

Supplement

S. Table I: Proteins specifically identified in GFP co-IPs from HEK293 FlpIn eGFP-NLRC5 cells. #: Experiment number.

Gene symbol	Protein name	Unique peptides	
		#1	#2
ABCF2	ATP-binding cassette sub-family F member 2	2	3
AHSA1	Aha1_N domain-containing protein	4	3
AP3M1	AP-3 complex subunit mu-1	3	4
BAG2	BAG domain-containing protein 2	10	15
BAG5	BAG domain-containing protein 5	11	19
BLVRA	Biliverdin reductase A	2	2
CCT8	T-complex protein 1 subunit theta	5	4
CDKN2A	Cyclin-dependent kinase inhibitor 2A	3	4
CLPTM1L	Cleft lip and palate transmembrane protein 1-like protein	3	2
CTAG2	Cancer/testis antigen 2	2	4
CTBP2	C-terminal-binding protein 2	3	2
DPM1	Dolichol-phosphate mannosyltransferase subunit 1	4	2
DPY30	Protein dpy-30 homolog	2	2
EEF1E1	Eukaryotic translation elongation factor 1 epsilon-1	2	2
FAM120A	Constitutive coactivator of PPAR-gamma-like protein 1	3	3
GAPDH	Glyceraldehyde-3-phosphate dehydrogenase	4	2
HLA-A	HLA class I histocompatibility antigen, A alpha chain	6	10
HSPA4	Heat shock 70 kDa protein 4	28	30
KPNA6	Importin subunit alpha	4	2
LPCAT1	Lysophosphatidylcholine acyltransferase 1	2	2
NUP160	Nuclear pore complex protein Nup160	3	3
NUP188	Nucleoporin NUP188	6	1
PPP1CB	Serine/threonine-protein phosphatase	2	2
PSMC2	26S proteasome AAA-ATPase subunit RPT1	5	3
PSMC6	AAA domain-containing protein; 26S proteasome regulatory subunit 10B	4	6
PSMD1	26S proteasome non-ATPase regulatory subunit 1	4	3
PSMD11	26S proteasome non-ATPase regulatory subunit 11	4	2
PSMD14	26S proteasome non-ATPase regulatory subunit 14	4	4
PSMD2	26S proteasome non-ATPase regulatory subunit 2	11	11
RAB5C	Ras-related protein Rab-5C	3	3
RAD50	Zinc-hook domain-containing protein	4	2
RPS29	40S ribosomal protein S29	2	2
SLC25A22	Mitochondrial glutamate carrier 1	2	2
SMC4	Structural maintenance of chromosomes protein	6	3
STUB1	E3 ubiquitin-protein ligase CHIP	10	4
STXBP3	Syntaxin-binding protein 3	2	1
TRRAP	Transformation/transcription domain-associated protein	12	8
UBR4	E3 ubiquitin-protein ligase UBR4	2	3

Supplement

S. Table II: Proteins specifically identified in GFP co-IPs from HEK293 FlpIn eGFP-NLRC5 isoform 3 cells. #: Experiment number.

Gene symbol	Protein name	Unique peptides	
		#1	#2
ACTN4	Alpha-actinin-4	2	2
ACTR3	Actin-related protein 3	2	2
AP3M1	AP-3 complex subunit mu-1	4	3
BAG2	BAG family molecular chaperone regulator 2	9	11
CAPZB	F-actin-capping protein subunit beta	11	10
DBN1	Drebrin	8	4
FAM129B	PH domain-containing protein	3	3
HSPA4	Heat shock 70 kDa protein 4	9	4
JAK1	Tyrosine-protein kinase JAK1	2	2
PON2	Serum paraoxonase/arylesterase 2	2	3
PRPF38B	Pre-mRNA-splicing factor 38B	2	2
PSMC2	26S proteasome regulatory subunit 7	5	3
PSMC6	26S proteasome regulatory subunit 10B	7	6
PSMD1	26S proteasome non-ATPase regulatory subunit 1	2	3
PSMD11	26S proteasome non-ATPase regulatory subunit 11	2	2
PSMD14	26S proteasome non-ATPase regulatory subunit 14	3	2
PSMD2	26S proteasome non-ATPase regulatory subunit 2	10	3
RAB5C	Ras-related protein Rab-5C	3	3
SLC2A1	Glucose transporter type 1	2	2
STAT1	Signal transducer and activator of transcription	8	4
STXBP3	Syntaxin-binding protein 3	2	3
TRRAP	Transformation/transcription domain-associated protein	37	7

S. Table III: Proteins specifically identified in GFP co-IPs from HEK293 FlpIn eGFP-NLRC5 2xNLS cells. #: Experiment number.

Gene symbol	Protein name	Unique peptides	
		#1	#2
ABCB7	ATP-binding cassette sub-family B member 7	2	3
ABCF2	ATP-binding cassette sub-family F member 2	2	1
ACOT9	Acyl-coenzyme A thioesterase 9	4	2
AP3M1	AP-3 complex subunit mu-1	4	3
BAG2	BAG family molecular chaperone regulator 2	11	12
BAG5	BAG family molecular chaperone regulator 5	3	12
DBN1	Drebrin	7	3
DNAJA3	DnaJ homolog subfamily A member 3	4	4
DPY30	Protein dpy-30 homolog	2	2
EIF2B1	Translation initiation factor eIF-2B subunit alpha	2	2
EIF3D	Eukaryotic translation initiation factor 3 subunit D	3	2
FAM120A	Constitutive coactivator of PPAR-gamma-like protein 1	4	2
HLA-A	HLA class I histocompatibility antigen, A alpha chain	1	7
HSPA4	Heat shock 70 kDa protein 4	15	14
MRPL14	39S ribosomal protein L14	3	2
NUP188	Nucleoporin NUP188	5	2
PCID2	PCI domain-containing protein 2	2	1
PKP3	Plastidial pyruvate kinase 3	3	2
PRSS21	Testisin	2	2
PSMC2	26S proteasome regulatory subunit 7	3	4
PSMC6	26S proteasome regulatory subunit 10B	4	7

Supplement

PUS1	PseudoU_synth_1 domain-containing protein	4	1
RAB2A	Ras-related protein Rab-14	2	4
RAB5C	Ras-related protein Rab-5C	3	6
RAD50	DNA repair protein RAD50	4	2
RBM15	RNA-binding protein 15	2	2
RFC2	Replication factor C subunit 2	2	2
RPL37A	Ribosomal protein L37	3	4
RPS29	40S ribosomal protein S29	2	2
SLC25A22	Mitochondrial glutamate carrier 1	2	2
STXBP3	Syntaxin-binding protein 3	1	1
TFB2M	Dimethyladenosine transferase 2	4	3
TRMT1L	TRMT1-like protein	2	2

S. Table IV: Proteins specifically identified in GFP co-IPs from HEK293 FlpIn eGFP-NLRC5 FL, isoform 3 and 2x NLS cells. #: Experiment number.

Gene symbol	Protein name	Unique peptides					
		Full-length		Isoform 3		2x NLS	
		#1	#2	#1	#2	#1	#2
AP3M1	Adaptor-related protein complex 3, mu 1 subunit	3	4	4	3	4	3
BAG2	BAG family molecular chaperone regulator 2	10	15	9	11	11	12
HSPA4	Heat Shock protein family A member 4	28	30	9	4	15	14
PSMC2	Proteasome 26S subunit, ATPase 2	5	3	5	3	3	4
PSMC6	Proteasome 26S subunit, ATPase 6	4	6	7	6	4	7
RAB5C	Ras-related protein Rab-5C	3	3	3	3	3	6
STXBP3	Syntaxin binding protein 3	2	1	2	3	1	1

S. Table V: Proteins specifically identified in GFP co-IPs from HEK293 FlpIn eGFP-NLRC5 FL and isoform 3 cells. #: Experiment number.

Gene symbol	Protein name	Unique peptides			
		Full-length		Isoform 3	
		#1	#2	#1	#2
PSMD1	26S proteasome non-ATPase regulatory subunit 1	4	3	2	3
PSMD2	26S proteasome non-ATPase regulatory subunit 2	11	11	10	3
PSMD11	26S proteasome non-ATPase regulatory subunit 11	4	2	2	2
PSMD14	26S proteasome non-ATPase regulatory subunit 14	4	4	3	2
TRRAP	Transformation/transcription domain-associated protein	12	8	37	7

Supplement

S. Table VI: Proteins specifically identified in GFP co-IPs from HEK293 FlpIn eGFP-NLRC5 FL and 2xNLS cells. #: Experiment number.

Gene symbol	Protein name	Unique peptides			
		Full-length		2xNLS	
		#1	#2	#1	#2
ABCF2	ATP-binding cassette sub-family F member 2	2	3	2	1
BAG5	BAG family molecular chaperone regulator 5	11	19	3	12
DPY30	Protein dpy-30 homolog	2	2	2	2
FAM120A	Constitutive coactivator of PPAR-gamma-like protein 1	3	3	4	2
HLA-A	HLA class I histocompatibility antigen, A alpha chain	6	10	1	7
NUP188	Nucleoporin NUP188	6	1	5	2
RAD50	DNA repair protein RAD50	4	2	4	2
RPS29	40S ribosomal protein S29	2	2	2	2
SLC25A22	Mitochondrial glutamate carrier 1	2	2	2	2

S. Table VII: Proteins specifically identified in GFP co-IPs from HEK293 FlpIn eGFP-NLRC5 isoform 3 and 2xNLS cells. #: Experiment number.

Gene symbol	Protein name	Unique peptides			
		Isoform 3		2xNLS	
		#1	#2	#1	#2
DBN1	Drebrin	8	4	7	3

S. Table VIII: Proteins identified as interactors of eGFP-NLRC5 2xNLS in the nuclear fraction of HEK293 FlpIn eGFP NLRC5 2xNLS cells. #: Experiment number.

Gene symbol	Protein name	Unique peptides		
		#1	#2	#3
HCFC1	Host cell factor 1	1	2	
ACTL6A	Actin-like protein 6A		2	4
SLC25A6	ADP/ATP translocase 3		10	3
ATP2A2	Sarcoplasmic/endoplasmic reticulum calcium ATPase 2		5	8
ATP5F1A	ATP synthase subunit alpha		5	3
VIM	Vimentin		3	5
MCM5	DNA replication licensing factor MCM5	6	7	
cDNA FLJ60124			5	3
CCT3	T-complex protein 1 subunit gamma		4	5
BAG2	BAG family molecular chaperone regulator 2		5	4
BAG5	BAG family molecular chaperone regulator 5		10	8
STUB1	E3 ubiquitin-protein ligase CHIP		8	8
DSP	Desmoplakin	3	7	
HSD17B12	Very-long-chain 3-oxoacyl-CoA reductase		4	2
GLUD1	Glutamate dehydrogenase 1		3	4
DHX9	ATP-dependent RNA helicase A		2	3
DNAJB11	DnaJ homolog subfamily B member 11		3	2
DNAJA2	DnaJ homolog subfamily A member 2		4	5
DNAJB1	DnaJ homolog subfamily B member 1		5	3
DNAJC7	DnaJ homolog subfamily C member 7		9	8

Supplement

DDX39A	ATP-dependent RNA helicase DDX39A		2	3
NUP155	Nuclear pore complex protein Nup155	2	2	
EEF1G	Elongation factor 1-gamma		2	2
ENO1	Alpha-enolase		2	2
SMARCC2	SWIRM-assoc_2 domain-containing protein		2	3
FKBP8	Peptidyl-prolyl cis-trans isomerase FKBP8		5	5
HNRNPH2	Heterogeneous nuclear ribonucleoprotein H2	2		2
HSPH1	Heat shock 110 kDa protein		2	2
HSP90AA1	Heat shock protein HSP 90-alpha		7	3
HSP90AB1	Heat shock protein HSP 90-beta		6	8
HSPA8	Heat shock cognate 71 kDa protein	3	20	
RPS15A	40S ribosomal protein S15a		2	2
IRS4	Insulin receptor substrate 4		8	5
LYPLA2	Acyl-protein thioesterase 2		2	2
MCM7	DNA replication licensing factor MCM7		6	5
ALDH18A1	Gamma-glutamyl kinase	6	6	
RANBP2	E3 SUMO-protein ligase RanBP2	3	2	
RPS20	30S ribosomal protein S20	4	2	
RUVBL1	RuvB-like 1;		7	8
RUVBL2	RuvB-like 2		10	8
SCO2	Thioredoxin domain-containing protein		2	2
SFPQ	Splicing factor, proline- and glutamine-rich	3		2
SMC3	Structural maintenance of chromosomes protein 3		7	2
SP1	Subtilisin	2		2
TUBB6	Tubulin beta-6 chain		3	3
CCT4	T-complex protein 1 subunit delta		5	4
CCT8	T-complex protein 1 subunit theta		9	5
CCT6A	T-complex protein 1 subunit zeta 1		2	7
TRIM28	RING-type E3 ubiquitin transferase		3	4
TIMM50	Mitochondrial import inner membrane translocase subunit TIM50		5	4

S. Table IX: Proteins identified as interactors of NLRC5 NLS I in the cytosolic fraction of HEK293 FlpIn eGFP NLRC5 NLS I cells. #: Experiment number.

Gene symbol	Protein name	Unique peptides		
		#1	#2	#3
HSPD1	60 kDa heat shock protein	10	23	14
IRS4	Insulin receptor substrate 4	1	23	13
PRKDC	DNA-dependent protein kinase catalytic subunit	0	31	3
BAG2	BAG family molecular chaperone regulator 2	7	11	14
HSP90AA1	Heat shock protein HSP 90-alpha	8	14	8
DNAJC7	DnaJ homolog subfamily C member 7	5	11	12
STUB1	E3 ubiquitin-protein ligase CHIP	3	12	12
HSPA4	Heat shock 70 kDa protein 4	0	18	9
CAD	Aspartate carbamoyltransferase	0	16	8
HSPA9	Stress-70 protein	10	0	13
GLUD1	Glutamate dehydrogenase 1	0	9	13
MCM7	DNA replication licensing factor MCM7	0	14	7
PFKP	ATP-dependent 6-phosphofructokinase, platelet type	0	18	3
CCT8	T-complex protein 1 subunit theta	0	11	10
BAG5	BAG family molecular chaperone regulator 5	3	14	3
ATP2A2	Sarcoplasmic/endoplasmic reticulum calcium ATPase 2	0	14	3

Supplement

HSPA5	Endoplasmic reticulum chaperone BiP	3	0	14
TUBB6	Tubulin beta-6 chain	1	9	6
TIMM50	Mitochondrial import inner membrane translocase subunit TIM50	0	8	8
RUVBL1	RuvB-like 1	0	10	5
SCO2	Protein disulfide-isomerase SCO2	3	7	5
TCP1	T-complex protein 1 subunit alpha	0	6	9
ATP5F1A	ATP synthase F1 subunit alpha	0	10	4
FKBP8	Peptidylprolyl isomerase	0	7	7
CCT7	T-complex protein 1 subunit eta	0	7	7
ACSL3	Long-chain-fatty-acid-CoA ligase 3	0	9	4
RUVBL2	RuvB-like 2	0	7	6
PFKL	ATP-dependent 6-phosphofructokinase liver type	0	8	4
DNAJA2	DnaJ homolog subfamily A member 2	0	5	6
RPS18	40S ribosomal protein S18	4	7	0
CCT6A	T-complex protein 1 subunit zeta 1	1	5	5
ALDH3A2	Aldehyde dehydrogenase family 3 member A2	0	5	5
PSMC2	26S proteasome AAA-ATPase subunit RPT1	0	4	6
HLA-C	HLA class I histocompatibility antigen, C alpha chain	1	2	6
DNAJC10	DnaJ homolog subfamily C member 10	0	5	4
DNAJA1	DnaJ homolog subfamily A member 1	0	4	5
RPS15A	40S ribosomal protein S15a	1	4	4
RPS14	Ribosomal protein S14	0	5	4
RPS20	30S ribosomal protein S20	5	0	4
STIP1	Stress-induced-phosphoprotein 1	0	4	5
CCT4	T-complex protein 1 subunit delta	0	5	4
ASNS	Asparagine-tRNA ligase	0	5	3
GCN1	eIF-2-alpha kinase activator GCN1	0	6	2
HSP90AB1	Heat shock protein HSP 90-beta	3	5	0
NTPCR	Cancer-related nucleoside-triphosphatase	0	4	4
PCNA	Proliferating cellular nuclear antigen 1	0	6	2
RAF1	RAF proto-oncogene serine/threonine-protein kinase	0	3	5
TELO2	Telomere length regulation protein TEL2 homolog	0	4	4
HSD17B12	Very-long-chain 3-oxoacyl-CoA reductase	0	4	3
DNAJB1	DnaJ homolog subfamily B member 1	0	4	3
TUFM	Elongation factor Tu	2	0	5
ILVBL	2-hydroxyacyl-CoA lyase 2	0	5	2
SLC25A11	Mitochondrial 2-oxoglutarate/malate carrier protein	2	5	0
PSMC5	26S proteasome regulatory subunit 8	0	4	3
ARL1	ADP-ribosylation factor-like protein 1	0	3	3
GALK1	Galactokinase	0	4	2
LRRC40	Leucine-rich repeat-containing protein 40	0	3	3
PSMC4	26S proteasome regulatory subunit 6B	0	3	3
PSMD2	26S proteasome non-ATPase regulatory subunit 2	0	3	3
CDK1	Cyclin-dependent kinase 1	0	2	3
ATP5F1C	ATP synthase F1 subunit gamma	0	2	3
H4C12	Histone H4	1	0	4
HSPH1	Heat shock 110 kDa protein	0	3	2
NME2	Nucleoside diphosphate kinase B	0	2	3
SAMHD1	Deoxynucleoside triphosphate triphosphohydrolase SAMHD1	0	3	2
SUGT1	Alpha-crystallin A chain	1	2	2
SLFN11	Schlafen family member 11	0	2	3
BAG6	BAG family molecular chaperone regulator 6	0	2	2

Supplement

AIFM1	Apoptosis-inducing factor 1	0	2	2
MAIP1	m-AAA protease-interacting protein 1	0	2	2
FDFT1	Squalene synthase	1	0	3
MLF2	Myeloid leukemia factor 2	0	2	2
RPL38	60S ribosomal protein L38	0	2	2
SSR4	Translocon-associated protein subunit delta	0	2	2
DARS2	Aspartate-tRNA ligase	2	2	0
TUBA1C	Tubulin alpha-1C chain	1	0	2
RPS10	30S ribosomal protein S10 alpha	1	2	0

S. Table X: Proteins identified as interactors of both eGFP-NLRC5 NLS I and 2xNLS in at least 2 of 3 independent experiments in HEK293 FlpIn eGFP-NLRC5 2xNLS or eGFP-NLRC5 NLSI cells. #: Experiment number.

Gene symbol	Protein name	Unique peptides					
		2xNLS			NLS I		
		#1	#2	#3	#1	#2	#3
ATP2A2	Sarcoplasmic/endoplasmic reticulum calcium ATPase 2	0	5	8	0	14	3
ATP5F1A	ATP synthase subunit alpha, mitochondrial	0	5	3	0	10	4
BAG2	BAG family molecular chaperone regulator 2	0	5	4	7	11	14
BAG5	BAG family molecular chaperone regulator 5	0	10	8	3	14	3
CCT6A	T-complex protein 1 subunit zeta	0	2	7	1	5	5
CCT8	T-complex protein 1 subunit theta	0	9	5	0	11	10
CCT4	T-complex protein 1 subunit delta	0	5	4	0	5	4
DNAJA2	DnaJ homolog subfamily A member 2	0	4	5	0	5	6
DNAJB1	DnaJ homolog subfamily B member 1	0	3	2	0	4	3
DNAJC7	DnaJ homolog subfamily C member 7	0	9	8	5	11	12
FKBP8	Peptidyl-prolyl cis-trans isomerase FKBP8	0	5	5	0	7	7
GLUD1	Glutamate dehydrogenase 1, mitochondrial	0	3	4	0	9	13
HSD17B12	Very-long-chain 3-oxoacyl-CoA reductase	0	4	2	0	4	3
HSP90AA1	Heat shock protein HSP 90-alpha	0	7	3	8	14	8
HSP90AB1	Heat shock protein HSP 90-beta	0	6	8	3	5	0
HSPH1	Heat shock protein 105 kDa	0	2	2	0	3	2
IRS4	Insulin receptor substrate 4	0	8	5	1	23	13
MCM7	DNA replication licensing factor MCM7	0	6	5	0	14	7
RPS15A	40S ribosomal protein S15a	0	2	2	1	4	4
RPS20	40S ribosomal protein S20	4	2	0	5	0	4
RUVBL1	RuvB-like 1	0	7	8	0	10	5
RUVBL2	RuvB-like 2	0	10	8	0	7	6
SCO2	Protein SCO2 homolog, mitochondrial	0	2	2	3	7	5
STUB1	E3 ubiquitin-protein ligase CHIP	0	8	8	3	12	12
TIMM50	Mitochondrial import inner membrane translocase subunit TIM50	0	5	4	0	8	8
TUBB6	Tubulin beta-6 chain	0	3	3	1	9	6

Supplement

S. Table XI: Specifically biotinylated proteins identified by proximal ligation in HEK293T cells transiently transfected with DD-BioID2-HA, or BioID2-HA.

Gene symbol	Protein name	Unique peptides	
		BioID2	DD-BioID2-HA
TCOF1	Treacle protein	0	7
NLRC5	Protein NLRC5	0	5
NONO	Non-POU domain-containing octamer-binding protein	0	4
SART1	U4/U6.U5 tri-snRNP-associated protein 1	0	4
RPL8	60S ribosomal protein L8	0	3
KNOP1	Lysine-rich nucleolar protein 1	0	3
SRSF3	Serine/arginine-rich splicing factor 3	0	2
EEF1A1P5	Putative elongation factor 1-alpha-like 3	0	2
HIST1H2BC	Histone H2B type 1-C/E/F/G/I	0	2
HIST3H3	Histone H3.1	0	2
RBBP6	E3 ubiquitin-protein ligase RBBP6	0	2
PCNP	PEST proteolytic signal-containing nuclear protein	0	2
NOLC1	Nucleolar and coiled-body phosphoprotein 1	0	2

S. Table XII: Specifically biotinylated proteins identified by proximal ligation in HEK293T cells transiently transfected with myc-BioID2-DD, or myc-BioID2.

Gene symbol	Protein name	Unique peptides	
		BioID2	myc-BioID2-DD
TLN1	Talin-1	0	58
FN1	Fibronectin	0	32
MYH9	Myosin-9	0	34
FLNA	Filamin-A	0	16
HSPG2	Basement membrane-specific heparan sulfate proteoglycan core protein	0	6
TUBB	Tubulin beta chain	0	7
TUBA4A	Tubulin alpha-4A chain	0	8
NLRC5	Protein NLRC5	0	6
VCP	Transitional endoplasmic reticulum ATPase	0	5
VCL	Vinculin	0	8
CLTC	Clathrin heavy chain	0	5
FBN2	Fibrillin-2	0	7
ACTB	Actin, cytoplasmic 1	0	6
C3	Complement C3	0	4
KPRP	Keratinocyte proline-rich protein	0	3
HSPA1B	Heat shock 70 kDa protein 1B	0	5
FBLN1	Fibulin-1	0	3
NONO	Non-POU domain-containing octamer-binding protein	0	6
A2M	Alpha-2-macroglobulin	0	3
CALD1	Caldesmon (Fragment)	0	4
FBN1	Fibrillin-	0	4
HMCN1	Hemicentin-1	0	7
NID1	Nidogen-1	0	7
VWF	von Willebrand factor	0	3
GSN	Gelsolin	0	2
ALB	Serum albumin	0	3

Supplement

EEF1A1	Elongation factor 1-alpha 1	0	4
F13A1	Coagulation factor XIII A chain	0	4
LAMA2	Laminin subunit alpha-2	0	3
HBA1	Hemoglobin subunit alpha	0	3
UBB	Polyubiquitin-B	0	3
HIST1H1C	Histone H1.2	0	3
POSTN	Periostin	0	4
COMP	Cartilage oligomeric matrix protein	0	3
FGB	Fibrinogen beta chain	0	3
DSG1	Desmoglein-1	0	4
PCCA	Propionyl-CoA carboxylase alpha chain, mitochondrial (Fragment)	0	2
PRSS3P2	Putative trypsin-6	0	1
TNXB	Tenascin-X	0	4
FLG2	Filaggrin-2	0	4
HMCN2	Hemicentin-2	0	4
PCNP	PEST proteolytic signal-containing nuclear protein	0	4
TCOF1	Treacle protein	0	3
VASP	Vasodilator-stimulated phosphoprotein	0	2
CILP	Cartilage intermediate layer protein 1	0	2
AHSG	Alpha-2-HS-glycoprotein	0	2
NCL	Nucleolin	0	2
TUBB1	Tubulin beta-1 chain	0	2
COL4A1	Collagen alpha-1(IV) chain	0	2
TUBB4B	Tubulin beta-4B chain	0	2
MYL6	Myosin light polypeptide 6	0	2
PLG	Plasminogen	0	1
DSC1	Desmocollin-1	0	2
F2	Prothrombin	0	2
ILK	Integrin-linked protein kinase	0	2
DPYSL2	Dihydropyrimidinase-related protein 2	0	2
LAMC1	Laminin subunit gamma-1	0	2
PKM	Pyruvate kinase	0	2
APOE	Apolipoprotein E	0	2
HIST1H2BA	Histone H2B type 1-A	0	1
HNRNPA1	Heterogeneous nuclear ribonucleoprotein A1	0	2
ITIH2	Inter-alpha-trypsin inhibitor heavy chain H2	0	2
LDHB	L-lactate dehydrogenase B chain	0	2
TUBA1A	Tubulin alpha-1A chain	0	2
RAN	GTP-binding nuclear protein Ran	0	2
LAMB1	Laminin subunit beta-1	0	2
COL2A1	Collagen alpha-1(II) chain	0	2
THBS1	Thrombospondin-1	0	1
TGFBI	Transforming growth factor-beta-induced protein ig-h3	0	1
CLEC11A	C-type lectin domain family 11 member A	0	1
ILF3	Interleukin enhancer-binding factor 3	0	1
PRDX2	Peroxiredoxin-2	0	1
SERPINC1	Antithrombin-III	0	1
TPI1	Triosephosphate isomerase	0	1
LASP1	LIM and SH3 domain protein 1	0	1
COL1A2	Collagen alpha-2(I) chain	0	1
PC	Pyruvate carboxylase, mitochondrial	0	1

Supplement

STAM	Signal transducing adapter molecule 1	0	1
AP2A1	AP-2 complex subunit alpha-1	0	1
ITIH4	ITIH4 protein	0	1
EEF2	Elongation factor 2	0	1
PHGDH	D-3-phosphoglycerate dehydrogenase	0	1
ADAMTSL4	ADAMTS-like protein 4	0	1
SERPINF2	Alpha-2-antiplasmin	0	1
ACACA	Acetyl-CoA carboxylase 1	0	1
RPL10	60S ribosomal protein L10	0	1
PDLIM1	PDZ and LIM domain protein 1	0	1
RBBP6	E3 ubiquitin-protein ligase RBBP6	1	3

S. Table XIII: Specifically biotinylated proteins identified by proximal ligation in K562 DD-BioID2-HA or BioID2-HA cells (experiment 1).

Gene symbol	Protein name	Unique peptides	
		BioID2	DD-BioID2-HA
EIF2S3	Eukaryotic translation initiation factor 2 subunit 3	4	8
PRDX6	Peroxiredoxin-6	2	6
APEX1	DNA-(apurinic or apyrimidinic site) endonuclease	2	6
PAICS	AIR carboxylase	2	5
TALDO1	Transaldolase	1	4
YBX1	Y box-binding protein 1	2	4
UBE2L3	Ubiquitin-conjugating enzyme E2 L3	2	4
ALDH1L2	Formyltetrahydrofolate dehydrogenase	2	4
NASP	Nuclear autoantigenic sperm protein	2	4
PAFAH1B3	Platelet-activating factor acetylhydrolase IB subunit alpha1	2	4
SRSF5	Serine/arginine-rich splicing factor 5	2	4
RPL34	60S ribosomal protein L34	1	3
PDHA1	Pyruvate dehydrogenase E1 component subunit alpha	1	3
PAFAH1B2	Platelet-activating factor acetylhydrolase IB subunit alpha2	1	3
CARS	Cysteinyl-tRNA synthetase	1	3
ASNA1	ATPase ASNA1	1	3
BZW2	Basic leucine zipper and W2 domain-containing protein 2	1	3
VDAC3	Voltage-dependent anion-selective channel protein 3	1	3
ABCF2	ATP-binding cassette sub-family F member 2	1	3
NPEPPS	Puromycin-sensitive aminopeptidase	0	2
GLG1	Golgi apparatus protein 1	0	2
SSRP1	FACT complex subunit SSRP1	0	2
SRSF11	Serine/arginine-rich splicing factor 11	0	2
SRSF2	Serine/arginine-rich splicing factor 2	0	2
NNT	NAD(P) transhydrogenase subunit beta	0	2
SRP72	Signal recognition particle subunit SRP72;	0	2
PITPNB	Phosphatidylinositol transfer protein beta isoform	0	2

Supplement

CELF1	CUGBP Elav-like family member 1	0	2
PGP	Glycerol-3-phosphate phosphatase	0	2
H3F3A	Histone H3	0	2
RAB10	Ras-related protein Rab-10	0	2
TUFM	Elongation factor Tu	0	2
BUB3	Mitotic checkpoint protein BUB3	0	2
MAGED2	Melanoma-associated antigen D2	0	2
HDAC1	Histone deacetylase 1	0	2
ARHGDI1B	Rho GDP-dissociation inhibitor 2	0	2
RDX	Radixin	0	2
DCTN1	Dynactin subunit 1	0	2
PPFIBP1	Liprin-beta-1	0	2
H2AFY	Histone H2A	0	2
VPS26A	Vacuolar protein sorting-associated protein 26A	0	2
DHX15	Pre-mRNA-splicing factor ATP-dependent RNA helicase DHX15	1	2
EZR	Ezrin	1	2
RPS26	40S ribosomal protein S26	1	2
HUWE1	E3 ubiquitin-protein ligase HUWE1	1	2
SDHA	Succinate dehydrogenase [ubiquinone] flavoprotein subunit	1	2
SF3B4	Splicing factor 3B subunit 4	1	2
UBA2	Ubiquitin-activating enzyme E1 2	1	2
PPP2R2A	Serine/threonine-protein phosphatase 2A 55 kDa regulatory subunit B	1	2
PSMD6	26S proteasome non-ATPase regulatory subunit 6	1	2
CSRP1	Cysteine and glycine-rich protein 1	1	2
CHD4	Chromodomain-helicase-DNA-binding protein 4	1	2
MCM3	DNA replication licensing factor MCM3	1	2
HCFC1	Host cell factor 1	1	2
ANXA3	Annexin A3	1	2
RAP1B	Ras-related protein Rap-1b	1	2
TPM4	Tropomyosin alpha-4 chain	1	2
RCC2	Protein RCC2	1	2
PES1	Pescadillo homolog	1	2
GOLPH3	Golgi phosphoprotein 3	1	2
RAP2C	Ras-related protein Rap-2	1	2
ATP5O	ATP synthase peripheral stalk subunit OSCP	1	2
FLII	Protein flightless-1 homolog	1	2
FAM114A1	Protein FAM114A2	1	2
OAT	Ornithine aminotransferase	1	2
PRPF4B	PRP4 pre-mRNA-processing factor 4 homologue	1	2
RAB2A	Ras-related protein Rab-2A	1	2
DYNC1LI1	Cytoplasmic dynein 1 light intermediate chain 1;	1	2
PBDC1	Protein PBDC1	1	2
LUC7L	Putative RNA-binding protein Luc7-like 1	1	2
PPP1R14B	Protein phosphatase 1 regulatory subunit 14B	1	2

Supplement

TMED10	Transmembrane emp24 domain-containing protein 10	1	2
PFDN5	Prefoldin subunit alpha	1	2
UBQLN2	Ubiquilin-2	1	2
FKBP2	Peptidyl-prolyl cis-trans isomerase FKBP2	1	2
FDPS	Farnesyl pyrophosphate synthase	1	2
ADSL	Adenylosuccinate lyase	1	2
BAZ1B	Tyrosine-protein kinase BAZ1B	1	2
HIBADH	3-hydroxyisobutyrate dehydrogenase	1	2
IDI1	Isopentenyl-diphosphate Delta-isomerase 1	1	2
DDX39A	ATP-dependent RNA helicase DDX39A	1	2
DYNLL2	Dynein light chain	0	1
HPCAL1	Hippocalcin-like protein 1	0	1
PHF5A	PHD finger-like domain-containing protein 5A	0	1
EIF4A3	Eukaryotic initiation factor 4A-III	0	1
UBTF	Nucleolar transcription factor 1	0	1
THRAP3	Thyroid hormone receptor-associated protein 3	0	1
SUMO2	Small ubiquitin-related modifier 2	0	1
GSTM1	Glutathione S-transferase Mu 1	0	1
CASP3	Caspase-3	0	1
SNRPN	Small nuclear ribonucleoprotein-associated protein	0	1
MTA3	Metastasis-associated protein MTA3	0	1
METAP1	Methionine aminopeptidase 1	0	1
TPR	Nucleoprotein TPR	0	1
SUCLG2	Succinate-CoA ligase subunit beta	0	1
RALA	Ras-related protein Ral-A	0	1
PCMT1	Protein-L-isoaspartate O-methyltransferase	0	1
MTCH2	Mitochondrial carrier homolog 2	0	1
AHSA1	Aha1 N domain-containing protein	0	1
AP2A2	AP-2 complex subunit alpha	0	1
TOP1	DNA topoisomerase 1	0	1
TBC1D15	TBC1 domain family member 15	0	1
UQCRB	Cytochrome b-c1 complex subunit 7	0	1
PAPSS1	Bifunctional 3'-phosphoadenosine 5'-phosphosulfate synthase 1	0	1
CAPZA1	F-actin-capping protein subunit alpha-1	0	1
ADH5	Alcohol dehydrogenase 5	0	1
TIPRL	TIP41-like protein	0	1
SEC11A	Signal peptidase complex catalytic subunit SEC11	0	1
EPHX1	Epoxide hydrolase	0	1
AIP	AH receptor-interacting protein;	0	1
CUL5	Cullin-5	0	1
TLN2	Talin-2	0	1
ATL3	Atlastin-3	0	1
ATXN2L	Ataxin-2-like protein	0	1
GNPNAT1	Glucosamine 6-phosphate N-acetyltransferase	0	1
ACTL6A	Actin-like protein 6A	0	1
IMMT	MICOS complex subunit MIC60	0	1
NAA10	N-alpha-acetyltransferase 10	0	1

Supplement

P4HA2	Prolyl 4-hydroxylase subunit alpha-2	0	1
DOCK1	Dedicator of cytokinesis protein 1	0	1
PPP3R2	Calcineurin subunit B type 2	0	1
FXN	Frataxin	0	1
CAPN1	Calpain-1 catalytic subunit	0	1
IK	Protein Red	0	1
UBA3	Ubiquitin-activating enzyme E1 3	0	1
WDR61	WD repeat-containing protein 61	0	1
PFDN2	Prefoldin subunit 2	0	1
PNN	Pinin	0	1
RPS21	40S ribosomal protein S21	0	1
RAB5A	Ras-related protein Rab-5A	0	1
RPIA	Ribose-5-phosphate isomerase	0	1
SUGT1	Protein SGT1 homolog	0	1
RBM17	Splicing factor 45	0	1
NDUFS4	NADH dehydrogenase [ubiquinone] iron-sulfur protein 4	0	1
RAVER1	Ribonucleoprotein PTB-binding 1	0	1
CHMP3	Charged multivesicular body protein 3	0	1
NDUFS2	NADH dehydrogenase [ubiquinone] iron-sulfur subunit	0	1
MYO1E	Unconventional myosin-Ie	0	1
HMGA1	High mobility group AT-hook protein 1	0	1
ZYX	Zyxin	0	1
CDC73	Parafibromin	0	1
MTX2	Metaxin-2	0	1
SDHB	Succinate dehydrogenase [ubiquinone] iron-sulfur subunit	0	1
RPA1	Replication protein A subunit	0	1
RAI14	Ankycorbin	0	1
EIF3J	Eukaryotic translation initiation factor 3 subunit J	0	1
UBE2M	NEDD8-conjugating enzyme Ubc12	0	1
EIF2S3	Eukaryotic translation initiation factor 2 subunit 3	4	8

S. Table XIV: Specifically biotinylated proteins identified by proximal ligation in K562 DD-BioID2-HA or BioID2-HA cells (experiment 2).

Gene symbol	Protein name	Unique peptides	
		BioID2	DD-BioID2-HA
TTN	Titin	0	1
SYNE1	Nesprin-1	0	1
TARDBP	TAR DNA-binding protein 43	0	1
ACTBL2	Beta-actin-like protein 2	0	1
RBM39	RNA-binding protein 39	0	1
CBX5	Chromobox protein homolog 5	0	1
DSTN	Destrin	0	1
KHSRP	Far upstream element-binding protein 2	0	1
GSTP1	Glutathione S-transferase P	0	1
PDLIM4	PDZ and LIM domain protein 4	0	1
TXNDC5	Thioredoxin domain-containing protein 5	1	3

Supplement

S. Table XV: Prey fragment analysis of ULTImate Yeast two-hybrid screen. Global PBS: global predicted biological score; IF: in frame; OOF: out of frame; 3P: 3-prime; 5P: 5-prime; Start, Stop: position of the 5-prime and 3-prime prey fragment ends, relative to the ATG start codon.

Gene name	Global PBS	Start	Stop	Type seq.	Frame	Sense
AKAP13	D	No data	941	3p	??	Sense
AKAP13	D	No data	1146	3p	??	Sense
AKAP13	D	177	942	5p 3p	IF	Sense
AKAP13	D	177	942	5p 3p	IF	Sense
AKAP13	D	177	942	5p 3p	IF	Sense
ANKFY1	D	1761	No data	5p	IF	Sense
ARHGEF18	N/A	No data	162	3p	??	Sense
BRPF3	D	1290	1847	5p 3p	IF	Sense
C22orf29	B	69	710	5p 3p	IF	Sense
C22orf29	B	117	845	5p 3p	IF	Sense
C22orf29	B	117	799	5p 3p	IF	Sense
C22orf29	B	177	807	5p 3p	IF	Sense
CCHCR1	B	733	1763	5p 3p	OOF1	Sense
CCHCR1	B	1053	1741	5p 3p	IF	Sense
CCHCR1	B	1083	1804	5p 3p	IF	Sense
CCHCR1	B	1110	1880	5p 3p	IF	Sense
CHFR	N/A	1125	468	5p 3p	??	AntiSense
CHFR	N/A	1125	468	5p 3p	??	AntiSense
COBRA1	B	-85	1373	5p 3p	IF	Sense
COBRA1	B	171	1215	5p 3p	IF	Sense
COBRA1	B	171	1215	5p 3p	IF	Sense
COP9 signalosome subunit 5 variant	N/A	No data	1119	3p	??	Sense
COPS5	F	No data	1169	3p	??	Sense
COPS5	F	105	897	5p 3p	IF	Sense
COPS5	F	108	1209	5p 3p	IF	Sense
COPS5	F	108	1209	5p 3p	IF	Sense
COPS5	F	108	1209	5p 3p	IF	Sense
COPS5	F	108	1209	5p 3p	IF	Sense
COPS5	F	108	1209	5p 3p	IF	Sense
COPS5	F	108	1209	5p 3p	IF	Sense
COPS5	F	108	1209	5p 3p	IF	Sense
COPS5	F	120	821	5p 3p	IF	Sense
COPS5	F	120	821	5p 3p	IF	Sense
COPS5	F	120	821	5p 3p	IF	Sense
COPS5	F	125	825	5p 3p	IF	Sense
CPOX	D	336	1284	5p 3p	IF	Sense
CPOX	D	336	1284	5p 3p	IF	Sense
CPOX	D	336	No data	5p	IF	Sense
CPOX	D	336	1284	5p 3p	IF	Sense
CPOX	D	336	1284	5p 3p	IF	Sense
CPOX	D	336	1284	5p 3p	IF	Sense
CPOX	D	336	1284	5p 3p	IF	Sense
CPOX	D	336	1284	5p 3p	IF	Sense
CPOX	D	336	1284	5p 3p	IF	Sense
CPOX	D	336	1284	5p 3p	IF	Sense
CPOX	D	336	1284	5p 3p	IF	Sense
CPOX	D	336	1284	5p 3p	IF	Sense
DKFZp434K1323	N/A	801	416	5p 3p	??	AntiSense
DNHD1	D	11919	12224	5p 3p	IF	Sense
DYNC1H1	D	8499	9741	5p 3p	IF	Sense

Supplement

DZIP3	N/A	No data	1869	3p	??	Sense
EIF3A	D	1488	No data	5p	IF	Sense
FLNB var1	N/A	1591	1262	5p 3p	??	AntiSense
FOXP1	N/A	-59	289	5p 3p	OOF2	Sense
GANAB	A	No data	3134	3p	??	Sense
GANAB	A	No data	2840	3p	??	Sense
GANAB	A	1878	No data	5p	IF	Sense
GANAB	A	1878	3114	5p 3p	IF	Sense
GANAB	A	1905	3036	5p 3p	IF	Sense
GANAB	A	1905	3036	5p 3p	IF	Sense
GANAB	A	1938	3065	5p 3p	IF	Sense
GANAB	A	1938	3065	5p 3p	IF	Sense
GANAB	A	2016	3071	5p 3p	IF	Sense
GANAB	A	2109	3076	5p 3p	IF	Sense
GLTSCR2	D	603	1163	5p 3p	IF	Sense
GLTSCR2	D	603	1163	5p 3p	IF	Sense
GLTSCR2	D	603	1163	5p 3p	IF	Sense
GW1	N/A	1186	1750	5p 3p	OOF1	Sense
GW1	N/A	1186	1750	5p 3p	OOF1	Sense
HIVEP1	D	1113	1812	5p 3p	IF	Sense
HIVEP2	E	No data	1241	3p	??	Sense
HIVEP2	E	198	1242	5p 3p	IF	Sense
HMMR var3	D	-46	491	5p 3p	IF	Sense
HMMR var3	D	-46	491	5p 3p	IF	Sense
HMMR var3	D	-46	501	3p	IF	Sense
INTS8	N/A	No data	499	3p	??	Sense
INTS8	N/A	No data	501	3p	??	Sense
IQGAP1	E	No data	1243	3p	??	Sense
IQGAP1	E	435	1246	5p 3p	IF	Sense
KDM2A	N/A	3773	3444	5p 3p	??	AntiSense
KDM2A	N/A	3773	3444	5p 3p	??	AntiSense
KPNA1	A	No data	1640	3p	??	Sense
KPNA1	A	315	1540	5p 3p	IF	Sense
KPNA1	A	621	1828	5p 3p	IF	Sense
KPNA1	A	648	1542	5p 3p	IF	Sense
KPNA1	A	656	1535	5p 3p	IF	Sense
KPNA3	D	693	1393	5p 3p	IF	Sense
KPNA3	D	693	1393	5p 3p	IF	Sense
KPNA4	C	-49	No data	5p	IF	Sense
KPNA4	C	531	1372	5p 3p	IF	Sense
KPNA6	B	537	1363	5p 3p	IF	Sense
KPNA6	B	537	1363	5p 3p	IF	Sense
KPNA6	B	546	No data	5p 3p	IF	Sense
LMNB2	N/A	1663	1082	5p 3p	??	AntiSense
LZTS2	D	1794	2237	5p 3p	IF	Sense
MCM7	D	1743	2321	5p 3p	IF	Sense
MYCBP2	D	11766	13027	5p 3p	IF	Sense
NBEA	D	125	617	5p 3p	IF	Sense
NRD1	D	2115	3061	5p 3p	IF	Sense
HMMR var3	D	-46	491	5p 3p	IF	Sense
HMMR var3	D	-46	501	3p	IF	Sense
INTS8	N/A	No data	499	3p	??	Sense
INTS8	N/A	No data	501	3p	??	Sense
IQGAP1	E	No data	1243	3p	??	Sense

Supplement

IQGAP1	E	435	1246	5p 3p	IF	Sense
KDM2A	N/A	3773	3444	5p 3p	??	AntiSense
KDM2A	N/A	3773	3444	5p 3p	??	AntiSense
KPNA1	A	No data	1640	3p	??	Sense
KPNA1	A	315	1540	5p 3p	IF	Sense
KPNA1	A	621	1828	5p 3p	IF	Sense
KPNA1	A	648	1542	5p 3p	IF	Sense
KPNA1	A	656	1535	5p 3p	IF	Sense
KPNA3	D	693	1393	5p 3p	IF	Sense
KPNA3	D	693	1393	5p 3p	IF	Sense
KPNA4	C	-49	No data	5p	IF	Sense
KPNA4	C	531	1372	5p 3p	IF	Sense
KPNA6	B	537	1363	5p 3p	IF	Sense
KPNA6	B	537	1363	5p 3p	IF	Sense
KPNA6	B	546	No data	5p 3p	IF	Sense
LMNB2	N/A	1663	1082	5p 3p	??	AntiSense
LZTS2	D	1794	2237	5p 3p	IF	Sense
MCM7	D	1743	2321	5p 3p	IF	Sense
MYCBP2	D	11766	13027	5p 3p	IF	Sense
NBEA	D	125	617	5p 3p	IF	Sense
NRD1	D	2115	3061	5p 3p	IF	Sense
NRD1	D	2115	3061	5p 3p	IF	Sense
NRD1	D	2115	3061	5p 3p	IF	Sense
ORC3	D	924	1886	5p 3p	IF	Sense
ORC3	D	924	1886	5p 3p	IF	Sense
ORC3	D	924	1886	5p 3p	IF	Sense
PACS1	N/A	No data	1984	3p	??	Sense
PBX3	D	6	776	5p 3p	IF	Sense
PBX3	D	6	No data	5p	IF	Sense
PEX10	N/A	No data	1234	3p	??	AntiSense
PEX10	D	No data	1247	3p	??	Sense
PEX10	D	678	1248	5p 3p	IF	Sense
PEX10	D	678	1248	5p 3p	IF	Sense
PEX10	D	678	1248	5p 3p	IF	Sense
PEX10	D	678	1248	5p 3p	IF	Sense
PEX10	D	678	1248	5p 3p	IF	Sense
PEX10	D	678	1248	5p 3p	IF	Sense
PEX10	D	678	1248	5p 3p	IF	Sense
PEX10	D	678	1248	5p 3p	IF	Sense
PEX10	D	678	1248	5p 3p	IF	Sense
PKP2	D	744	No data	5p	IF	Sense
PLEC	D	3396	4206	5p 3p	IF	Sense
PPP3CB	D	1236	1896	5p 3p	IF	Sense
PPP3CB	D	1236	1896	5p 3p	IF	Sense
PPP3CB	D	1236	1896	5p 3p	IF	Sense
PPP3CB	D	1236	1896	5p 3p	IF	Sense
SDHB	D	144	909	5p 3p	IF	Sense
SIN3A	A	No data	2274	3p	??	Sense
SIN3A	A	No data	2265	3p	??	Sense
SIN3A	A	No data	2289	3p	??	Sense
SIN3A	A	No data	2325	3p	??	Sense
SIN3A	A	1008	2550	5p 3p	IF	Sense
SIN3A	A	1128	2216	5p 3p	IF	Sense

Characterization of the role of the NLR proteins NLRC5 and NLRP11 in the immune response

Supplement

SIN3A	A	1200	No data	5p	IF	Sense
SIN3A	A	1200	2415	5p 3p	IF	Sense
SIN3A	A	1200	2415	5p 3p	IF	Sense
SIN3A	A	1212	2323	5p 3p	IF	Sense
SIN3A	A	1212	2323	5p 3p	IF	Sense
SIN3A	A	1212	2323	5p 3p	IF	Sense
SIN3A	A	1245	2351	5p 3p	IF	Sense
SIN3A	A	1248	2153	5p 3p	IF	Sense
SIN3A	A	1248	No data	5p	IF	Sense
SIN3A	A	1248	2153	5p 3p	IF	Sense
SIN3A	A	1260	2266	5p 3p	IF	Sense
SIN3A	A	1260	2266	5p 3p	IF	Sense
SIN3A	A	1260	2266	5p 3p	IF	Sense
SIN3A	A	1302	2352	5p 3p	IF	Sense
SIN3A	A	1386	2323	5p 3p	IF	Sense
SIN3A	A	1386	2323	5p 3p	IF	Sense
SIN3A	A	1386	2323	5p 3p	IF	Sense
SIN3A	A	1386	2323	5p 3p	IF	Sense
SIN3A	A	1386	No data	5p	IF	Sense
SIN3A	A	1485	2424	5p 3p	IF	Sense
SIN3A	A	1575	2346	5p 3p	IF	Sense
SIN3A	A	1575	2346	5p 3p	IF	Sense
SIN3A	A	1575	2346	5p 3p	IF	Sense
SIN3A	A	1655	2343	5p 3p	IF	Sense
SIN3A	A	1665	2353	5p 3p	IF	Sense
SIN3A	A	1686	2215	5p 3p	IF	Sense
SIN3A	A	1782	2281	5p 3p	IF	Sense
SIN3A	A	1782	2281	5p 3p	IF	Sense
SIN3A	A	1782	2281	5p 3p	IF	Sense
SIN3A	A	1782	2281	5p 3p	IF	Sense
SIN3A	A	1782	2281	5p 3p	IF	Sense
SIN3A	A	1782	2281	5p 3p	IF	Sense
SMARCA4	N/A	No data	2415	3p	??	Sense
SPTAN1	D	No data	4019	3p	??	Sense
SPTAN1	D	3510	No data	5p	IF	Sense
T-cell receptor alpha chain AV17S1 J43AC	B	260	806	3p	OOF2	Sense
T-cell receptor alpha chain AV17S1 J43AC	B	291	771	5p 3p	IF	Sense
T-cell receptor alpha chain AV17S1 J43AC	B	291	771	5p 3p	IF	Sense
T-cell receptor alpha chain AV17S1 J43AC	B	291	771	5p 3p	IF	Sense
T-cell receptor alpha chain AV17S1 J43AC	B	291	771	5p 3p	IF	Sense
T-cell receptor alpha chain AV17S1 J43AC	B	291	771	5p 3p	IF	Sense

Characterization of the role of the NLR proteins NLRC5 and NLRP11 in the immune response

Supplement

T-cell receptor alpha chain AV17S1 J43AC	B	291	771	5p 3p	IF	Sense
T-cell receptor alpha chain AV17S1 J43AC	B	291	771	5p 3p	IF	Sense
T-cell receptor alpha chain AV17S1 J43AC	B	291	771	5p 3p	IF	Sense
T-cell receptor alpha chain AV17S1 J43AC	B	291	771	5p 3p	IF	Sense
TAF1	E	3000	4185	5p 3p	IF	Sense
TAF1	E	3000	4185	5p 3p	IF	Sense
TAF1	E	3060	3939	5p 3p	IF	Sense
TAF1	E	3245	No data	5p	OOF2	Sense
TAF1	E	3245	3943	5p 3p	OOF2	Sense
TAF1	E	3245	3943	5p 3p	OOF2	Sense
TAF1	E	3279	4204	5p 3p	IF	Sense
TAF1	E	3435	3947	5p 3p	IF	Sense
TAF1	E	3435	3947	5p 3p	IF	Sense
TAF1	E	3759	4333	5p 3p	IF	Sense
TAF1B	D	306	720	5p 3p	IF	Sense
TAF1B	D	306	720	5p 3p	IF	Sense
TAF1B	D	306	720	5p 3p	IF	Sense
TIMP2	N/A	No data	561	3p	??	Sense
TIMP2	N/A	No data	561	3p	??	Sense
TNFRSF25	B	-55	918	5p 3p	IF	Sense
TNFRSF25	B	-49	416	5p 3p	IF	Sense
TNFRSF25	B	No data	917	3p	??	Sense
UBE2Q1	N/A	74	253	3p	OOF2	Sense
UBR5	F	3267	4556	5p 3p	IF	Sense
UQCRC2	N/A	1231	609	5p 3p	??	AntiSense
USP9X	N/A	No data	2384	3p	??	Sense
WDR1	D	1116	1426	5p 3p	IF	Sense
ZNF862	N/A	No data	4214	3p	??	Sense
ZNF862	N/A	3603	3908	5p 3p	IF	Sense
ZNF862	N/A	3603	3908	5p 3p	IF	Sense
ZNF862	N/A	3603	3908	5p 3p	IF	Sense
ZNF862	N/A	3603	3908	5p 3p	IF	Sense
ZNF862	N/A	3603	3908	5p 3p	IF	Sense
ZNF862	N/A	3603	3908	5p 3p	IF	Sense
ZNF862	N/A	3603	3908	5p 3p	IF	Sense
ZNF862	N/A	3663	4215	5p 3p	IF	Sense
ZNF862	N/A	3663	4250	3p	IF	Sense
GenMatch	D	-1	1121	5p 3p	IF	Sense
GenMatch	D	-1	1122	5p 3p	IF	Sense
GenMatch	D	-1	776	5p 3p	IF	Sense
GenMatch	N/A	No data	659	3p	??	Sense
GenMatch	D	-1	517	5p 3p	IF	Sense
GenMatch	D	-1	520	5p 3p	IF	Sense
GenMatch	D	-1	No data	5p 3p	IF	Sense
GenMatch	D	-1	675	5p 3p	IF	Sense
GenMatch	D	-1	542	5p 3p	IF	Sense

Characterization of the role of the NLR proteins NLRC5 and NLRP11 in the immune response

Supplement

GenMatch	D	-1	542	5p 3p	IF	Sense
GenMatch	D	-1	542	5p 3p	IF	Sense
GenMatch	D	-1	542	5p 3p	IF	Sense
GenMatch	D	-1	324	5p 3p	IF	Sense
GenMatch	D	-1	392	5p	IF	Sense
GenMatch	N/A	No data	768	3p	??	Sense
GenMatch	N/A	No data	634	3p	??	Sense
GenMatch	D	-1	No data	5p 3p	IF	Sense
GenMatch	N/A	No data	713	3p	??	Sense
GenMatch	D	-1	598	5p 3p	IF	Sense
GenMatch	D	-1	752	5p 3p	IF	Sense

Eidesstattliche Versicherung über die eigenständig erbrachte Leistung

gemäß § 18 Absatz 3 Satz 5 der Promotionsordnung der Universität Hohenheim für die Fakultäten Agrar-, Natur- sowie Wirtschafts- und Sozialwissenschaften

1. Bei der eingereichten Dissertation zum Thema

Characterization of the role of the NLR proteins NLRC5 and NLRP11 in the immune response

handelt es sich um meine eigenständig erbrachte Leistung.

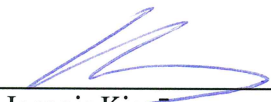
2. Ich habe nur die angegebenen Quellen und Hilfsmittel benutzt und mich keiner unzulässigen Hilfe Dritter bedient. Insbesondere habe ich wörtlich oder sinngemäß aus anderen Werken übernommene Inhalte als solche kenntlich gemacht.

3. Ich habe nicht die Hilfe einer kommerziellen Promotionsvermittlung oder -beratung in Anspruch genommen.

4. Die Bedeutung der eidesstattlichen Versicherung und der strafrechtlichen Folgen einer unrichtigen oder unvollständigen eidesstattlichen Versicherung sind mir bekannt.

Die Richtigkeit der vorstehenden Erklärung bestätige ich. Ich versichere an Eides Statt, dass ich nach bestem Wissen die reine Wahrheit erkläre und nichts verschwiegen habe.

Stuttgart den 19.7.2021
Ort und Datum


Ioannis Kienēs

Danksagung

Mein Dank gilt im Besonderen meinem Doktorvater Prof. Dr. Thomas Kufer für seine allzeit hervorragende Betreuung, für die fachliche Diskussionen und Anregungen und nicht zuletzt auch für seine moralische Unterstützung in herausfordernden Phasen. Ich danke Ihm für die Möglichkeit, meine Doktorarbeit in seiner Arbeitsgruppe durchführen zu können, für sein Vertrauen in meine Arbeit und für sein Engagement, mir einen Einblick in die akademische Welt zu geben.

Vielen Dank an Prof. Dr. Dr. Sascha Venturelli für die Übernahme des Zweitgutachtens meiner Arbeit.

Vielen Dank an Prof. Dr. Jan Frank für die Bereitschaft der Prüfungskommission anzugehören.

Des Weiteren gilt mein Dank Asst. Prof. Dr. Marina Schröder für die hervorragende Zusammenarbeit und die hilfreiche fachliche Unterstützung zum Thema DDX3X.

Ebenfalls will ich mich herzlich bei Assoc. Prof. Dr. Maria Kaparakis-Liaskos und Assoc. Prof. Dr. Begoña Heras für die großartige Möglichkeit, meinen Forschungsaufenthalt in ihren Laboren der La Trobe University Melbourne zu absolvieren bedanken. Vielen Dank für die hervorragende Betreuung vor Ort und auch für die persönliche Unterstützung während der pandemiebedingten plötzlichen und vorzeitigen Abreise.

Mein Dank gilt auch allen Kollegen der AG Kufer. Vielen Dank für eure Unterstützung und eure Hilfsbereitschaft und das angenehme Arbeitsklima. Petra, vielen Dank für die großartige Organisation. Yvonne, vielen Dank für die hilfreiche Unterstützung im Labor.

Mein Dank gilt natürlich auch meiner Familie, ohne deren Unterstützung mein Studium der Biologie nicht möglich gewesen wäre. Vielen Dank für die Kraft, die ihr mir in der Zeit meiner Promotion gegeben habt. Vielen Dank auch an meine Freunde, die auch in schwierigen Zeiten immer für mich da waren. Und natürlich auch besonderer Dank an dich Hannah, dafür, dass du immer hinter mir stehst, immer an mich glaubst und dass du jederzeit Geduld und Verständnis für mich hast.

Publikationen

Teile dieser Arbeit wurden in folgenden Artikeln publiziert:

Ellwanger, K., E. Becker, **I. Kienes**, A. Sowa, Y. Postma, Y. Cardona Gloria, A. N. R. Weber and T. A. Kufer (2018). "The NLR family pyrin domain-containing 11 protein contributes to the regulation of inflammatory signaling." J Biol Chem **293**(8): 2701-2710.

Kienes, I., T. Weidl, N. Mirza, M. Chamaillard and T. A. Kufer (2021). "Role of NLRs in the Regulation of Type I Interferon Signaling, Host Defense and Tolerance to Inflammation." Int J Mol Sci **22**(3).

Kienes, I., S. Bauer, C. Gottschild, N. Mirza, J. Pfannstiel, M. Schröder and T. A. Kufer (2021). "DDX3X Links NLRP11 to the Regulation of Type I Interferon Responses and NLRP3 Inflammasome Activation." Front Immunol **12**: 653883.

Curriculum Vitae

Curriculum Vitae

Personal information:

Name	Ioannis Kienēs
Address	Sauerampferweg 24 70599 Stuttgart Germany
Telephone	+49 711 38924756
E-Mail	ioannis.kienes@uni-hohenheim.de
Date of birth	July 10 th 1992, Munich

Education

Since 12/2016

PhD Thesis

Further characterization of the role of NLRC5 and NLRP11 in the immune response

Prof. Dr. Kufer, Thomas; Institute of Nutritional Medicine, Department of immunology at the University of Hohenheim

10/2013 – 09/2016

Master of Science Biology (Final grade 1,6)

Technical University of Munich

Major: Medical Biology

Minors: Biochemistry and Cellular Biology; Microbiology

Master's Thesis

The Role of Adenoviral Proteins in PML-mediated Differentiation of Hepatocytes

PD. Dr. Schreiner, Sabrina; Institute of Virology at the Technical University of Munich (Prof. Protzer, Ulrike M.D.)

10/2015 – 12/2015

Internship at the Institute of Virology at the Technical University of Munich

PD. Dr. Schreiner, Sabrina; Institute of Virology at the Technical University of Munich (Prof. Protzer, Ulrike M.D.)

06/2013

Participation in a seminar about **Working under GLP** (Good laboratory praxis) – Technical University of Munich

08/2012

Internship at the Institute of Microbiology and Laboratory Diagnostics at the Asklepios Clinic in Gauting; Hoffmann, Harald M.D.

10/2010 – 08/2013

Bachelor of Science Biology (Final grade 2,2)

Technical University of Munich

Bachelor's Thesis

Establishment and Application of qPCR Systems for the Detection of pathogenic Bacteria

Curriculum Vitae

Prof. Dr. Schloter, Michael; Department of Environmental Genomics at the Helmholtz Center Munich

07/2010 – 09/2010

Language trip: Greece

06/2010

Abitur (Final grade 1,7); Josef-Effner-Gymnasium Dachau, Bavaria, Germany

Conferences and Poster-Presentations

- 09/2021 Scheduled participation and Short Talk at the virtual 6th European Congress of Immunology
- 04/2021 Participation short talk and Co-Chair of the session: **Inflammasomes** at the Keystone eSymposium Innate Immunity: Mechanisms and Modulation 2021
- 09/2018 Participation and Short Talk at the 5th European Congress of Immunology; Amsterdam, Netherlands
- 08/2017 Participation and Poster-presentation at the Autumn School Current Concepts in Immunology; German Society of Immunology (DGfI), Merseburg, Germany
- 03/2017 Participation at the Conference Novel Concepts in Innate, Tübingen, Germany

Invited Talks

- 09/2021 Scheduled oral presentation at the virtual 6th European Congress of Immunology; title **DDX3X Links NLRP11 to the Regulation of Type I Interferon Responses and NLRP3 Inflammasome Activation** in the workshop: Immune Regulation and Signaling
- 04/2021 Oral Presentation at the Keystone Symposium Innate Immunity: Mechanisms and Modulation 2021; title **DDX3X Links NLRP11 to the Regulation of Type I Interferon Responses and NLRP3 Inflammasome Activation** in the session: Inflammasomes
- 09/2017 Oral presentation at the 5th European Congress of Immunology; title ***NLRP11 negatively regulates NF- κ B and type I interferon responses*** in the workshop: Responses to mucosal microbial pathogens.

Session Chair

- 04/2021 Session Co-Chair of the: **Inflammasomes** at the Keystone Symposium Innate Immunity: Mechanisms and Modulation 2021

Curriculum Vitae

Scholarships

09/2021	EFIS-EJI Waved Registration Grant to attend the 6 th European Congress of Immunology (ECI 2021)
02/2020 – 04/2020	DAAD – Exchange Scholarship in collaboration with Assoc. Prof. Maria Kaparakis-Liaskos, PhD; La Trobe University, Melbourne, Australia
09/2018	EFIS-EJI Travel Grant to attend the 5th European Congress of Immunology (ECI 2018)
04/2018 – 03/2020	Landesgraduiertenförderung of the Ministry of Science, Research and Arts in Baden-Württemberg, Germany

Further Qualifications

Course in **Basics of Laboratory Animal Science** according to FELASA Category B Guidelines

Course about **MALDI-TOF** at the Core Facility Hohenheim

Experience working in biosafety levels S2 and S3

Participation in a seminar about **Working under GLP** (Good laboratory praxis) – Technical University of Munich

Sound knowledge in the use of MS Office and Adobe Illustrator

Languages

German, native speaker

English, highly proficient

Greek, good command

Memberships and Voluntary work

MinD (Mensa in Deutschland e.V.; German national group of the Mensa International Society)

MHN (MinD-Hochschul-Netzwerk; Interdisciplinary academic project of MinD, focussing on (PhD) students and young professionals in academic research)

DGfI (German Society for Immunology)

Voluntary work at the animal shelter in Dachau (2016)

Supporting member of the Voluntary Firefighters Dachau

References

- Prof. Dr. rer. nat. Kufer, Thomas Institute of Nutritional Medicine, Department of Immunology at the University of Hohenheim
Tel: +49711 459 24850
- PD. Dr. rer. nat. Schreiner, Sabrina Institute of Virology – Technical University of Munich
Tel: +4989 3187 3466

Publications:

Steinle, H., K. Ellwanger, N. Mirza, S. Brise, **I. Kienes**, J. Pfannstiel and T. A. Kufer (2021). "14-3-3 and Erlin proteins differentially interact with RIPK2 complexes." J Cell Sci.

Kienes, I., S. Bauer, C. Gottschild, N. Mirza, J. Pfannstiel, M. Schröder and T. A. Kufer (2021). "DDX3X Links NLRP11 to the Regulation of Type I Interferon Responses and NLRP3 Inflammasome Activation." Front Immunol **12**: 653883.

Kienes, I., T. Weidl, N. Mirza, M. Chamailard and T. A. Kufer (2021). "Role of NLRs in the Regulation of Type I Interferon Signaling, Host Defense and Tolerance to Inflammation." Int J Mol Sci **22**(3).

Ellwanger, K., S. Briese, C. Arnold, **I. Kienes**, V. Heim, U. Nachbur and T. A. Kufer (2019). "XIAP controls RIPK2 signaling by preventing its deposition in speck-like structures." Life Sci Alliance **2**(4).

Ellwanger, K., E. Becker, **I. Kienes**, A. Sowa, Y. Postma, Y. Cardona Gloria, A. N. R. Weber and T. A. Kufer (2018). "The NLR family pyrin domain-containing 11 protein contributes to the regulation of inflammatory signaling." J Biol Chem **293**(8): 2701-2710.

Arnold, C., **I. Kienes**, A. S. Sowa and T. A. Kufer NOD-Like Receptors. eLS: 1-16.

Stuttgart, den 19.07.2021

Ort, Datum


Ioannis Kienes